ROLE OF P2X7-MEDIATED INFLAMMASOME ACTIVATION IN GLOMERULONEPHRITIS

A thesis submitted to Imperial College London in candidature for the degree of Doctor of Philosophy by:

SIMONA DEPLANO

Imperial College London, Renal Section, Department of Medicine

Commonwealth Building, Hammersmith Campus, Du Cane Road

London, W12 0NN

ABSTRACT

Glomerulonephritis is a major cause of kidney failure and current treatment is based on nonspecific immunosuppressive therapies. The purinergic P2X7 receptor (P2X7R) is usually not detectable in renal tissue. However, previous studies have demonstrated an increased glomerular P2X7R expression in animal models of glomerulonephritis. Furthermore, P2X7R knock-out mice have been shown to be significantly protected from antibody-mediated glomerulonephritis. P2X7R activation represents a fundamental step for the activation of the NLRP3 inflammasome which leads to the processing and release of IL-1β and IL-18. The role of the inflammasome activation in glomerulonephritis is not clear yet. The work presented in this thesis describes three aspects of P2X7R activation: cytokine production, signalling cascade following ATP stimulation and inflammasome activation. My data show that macrophages from wild type mice produce higher levels of IL-1β and IL-18 compared to macrophages from P2X7 deficient mice. ATP stimulation activates several signalling pathways in macrophages. Among them, the ribosomal pathway appears to be strictly regulated by P2X7R. To investigate the role of the inflammasome activation in glomerulonephritis I have compared macrophages from the susceptible rat strain Wistar-Kyoto with macrophages from the resistant strain Lewis. WKY macrophages express higher P2X7 mRNA and protein levels, release higher levels of IL-1β and IL-18 and exhibit a greater caspase-1 activity. Similarly, WKY nephritic glomeruli show higher P2X7, IL-1β, IL-18 and caspase-1 levels compared to Lewis glomeruli. Finally, in the attempt to identify genes responsible for the inflammasome regulation, I have examined macrophages and nephritic glomeruli from congenic rats. My data seem to indicate that the susceptibility locus Crgn2 contains one or more genes that control IL-1β and IL-18 release in macrophages. Further studies are certainly required to verify the relevance of these data. The results are important in understanding the

pathogenesis of glomerulonephritis and identification of new potential therapeutic targets.

ACKNOWLEDGEMENTS

First and foremost, I would like to express my deep and sincere gratitude to my supervisor, Dr Frederick W. Tam, for his continuous support, enthusiasm, motivation and expertise. He has been an excellent adviser to me throughout my PhD and at the same time he has always given me great freedom to pursue independent work. A special thanks goes out to Dr Jacques Behmoaras for his continuous help and guidance throughout my research. I would like also to thank Professor Terry Cook for the precious intellectual stimulation and Miss Jenny Smith who has provided a great contribution to the work presented in this thesis. Finally, I cannot forget all the other members of the Renal lab who have always supported me during these years.

Contents

FIGURES

LIST OF TABLES

ABBREVIATIONS

ATP	adenosine triphosphate
BMDMs	bone marrow derived macrophages
CAPS	cryopyrin-associated periodic syndromes
CLRs	C-type lectin receptors
Crgn	Crescentic glomerulonephritis
DMEM	Dulbecco's Modified Eagle Medium
FCAS	Familial cold autoinflammatory syndrome
FMF	Familial Mediterranean fever
GPCRs	G protein-coupled receptors
HBSS	Hank's balanced buffer solution
HRP	Horseradish peroxidase
IFN	Interferon
l; ml, µl	Litre; millilitre, microlitre
LEW	Lewis rat
LPS	Lipopolysaccharide
LW16	Congenic rat strain where the quantitative trait locus Crgn2 from a WKY rat was introgressed onto Lew genetic background
M; mM, µM, nM, pM	Molar; millimolar, micromolar, nanomolar, picomolar
MAPK	Mitogen-activated protein kinase
MMPs	Matrix metalloproteinases
MWS	Muckle–Wells syndrome

NaCl	Sodium chloride
NF-κB	Nuclear factor kappa-light-chain enhancer of activated B cells
NLRP3	NLR family, pyrin domain containing 3
NLRs	Nod-like receptors
(NOMID/CINCA)	neonatal onset multi-systemic inflammatory disease/chronic infantile neurological cutaneous articular syndrome
NTN	Nephrotoxic nephritis
NTS	Nephrotoxic serum
P2X7R	P2X7 receptor
P2X7RA	P2X7 receptor antagonist
PAMP	Pathogen-associated molecular pattern
PAPA	Pyogenic arthritis, pyoderma gangrenosum and acne
PBS	Phosphate-buffered saline
PCR	Polymerase chain reaction
PLCβ	Phospholipase C beta
PLD	Phospholipase D
PRRs	Pattern recognition receptors
qRT-PCR	Quantitative reverse transcription polymerase chain reaction
QTL	Quantitative trait locus
RIG-I	Retinoic acid inducible gene-I
RNA	Ribonucleic acid
siRNA	Small interfering RNA
SNPs	Single-nucleotide polymorphisms

TLR	Toll-like receptor
WKY	Wistar-Kyoto rat
WL16	Congenic rat strain where the quantitative trait locus Crgn2 from the LEW rat was introgressed onto WKY rat background.
YVAD	Caspase-1 inhibitor Ac-YVAD-CHO

PUBLISHED AND PRESENTED WORK

Published abstracts and oral presentations

Simona Deplano, Reiko Hewitt, Robert J. Unwin, and Frederick W.K. Tam

Activation of ERK and mTOR signalling pathways via the purinergic receptors in macrophages (poster presentation)

American Society of Nephrology Annual Meeting, Denver, USA, November 2010

Simona Deplano, Frederick W. Tam, Terry Cook, Charles D Pusey, Robert Unwin and Jacques Behmoaras

Genetically Determined Regulation of the P2X7 receptor-inflammasome pathway in macrophages of glomerulonephritis-susceptible WKY rat (poster presentation)

American Society of Nephrology Annual Meeting, Denver, USA, November 2010

Simona Deplano, Frederick W. Tam, Terry Cook, Charles D Pusey, Robert Unwin and Jacques Behmoaras

Genetically determined regulation of the P2X7 receptor- inflammasome pathway in macrophages of glomerulonephritis-susceptible WKY rat (oral presentation)

41st Renal Research Forum, London, UK, March 2011

Simona Deplano, Reiko Hewitt, Robert J. Unwin, and Frederick W.K. Tam

Activation of ERK and mTOR signalling pathways via the purinergic receptors in macrophages (poster presentation)

BRS/RA Annual Conference, Birmingham, UK, June 2011

Simona Deplano, Frederick W. Tam, Terry Cook, Charles D Pusey, Robert Unwin and Jacques Behmoaras

Genetically determined regulation of the inflammasome pathway in macrophages of glomerulonephritis susceptible WKY rat (oral presentation)

BRS/RA Annual Conference, Birmingham, UK, June 2011

Simona Deplano, Jennifer Smith, Charles D. Pusey, Frederick W.K. Tam, H. Terence Cook and Jacques Behmoaras

Inflammasome activation and processing of IL-1β and IL-18 in experimental crescentic glomerulonephritis in the rat (poster presentation at the American Society of Nephrology annual meeting (Philadelphia, USA, November 2011)

Simona Deplano, Richard Hull, Terence Cook, Timothy Aitman, Frederick Tam, Jacques Behmoaras

Genetic determinants of inflammasome activation in macrophage-mediated crescentic glomerulonephritis in the Rat (abstract selected for oral presentation at the Rat Genomics & Models 2011 meeting, New York, USA, December 2011).

STATEMENT OF CONTRIBUTION

This thesis is composed of my original work, and contains no material previously published or written by another person except where due reference has been made in the text. I would like to acknowledge the following people for the collaborative support they have given to me during my research: Dr Pedro Cutillas from Barts Cancer Institute, University of London carried out the phosphoproteomic analysis of primary bone marrow derived macrophages from WT and P2X7 deficient mice and Dr Annalisa Vilasi from University College of London helped me with data analysis. Ms Jennifer Smith from the Renal Section, Imperial College has performed the injection of nephrotoxic serum in rats. Mrs Reiko Hewitt from the Renal Medicine Department carried out the genotyping of WT and P2X7 deficient mice. Gelatin zymography for MMP-9 enzymatic activity study was performed by Dr Jacques Behmoaras, Centre for Complement and Inflammation Research. Miss Zelpha D'Souza of the Physiological Genomics and Medicine Group (PGM) provided L929 cells supernatant for macrophages differentiation and has collected the kidneys and bones from rats for isolation of glomeruli and bone marrow cells respectively.

CHAPTER ONE-GENERAL INTRODUCTION

1.1 INTRODUCTION

The work described in this thesis is a study of the role of P2X7R-mediated inflammasome activation in glomerulonephritis. Previously in my lab, using experimental models of glomerulonephritis, it has been shown that P2X7 deficiency is significantly renoprotective compared to the wild-type controls, supporting a pro-inflammatory role for P2X7R in immune-mediated renal injury and suggesting P2X7R as a potential therapeutic target (Taylor et al., 2009). P2X7R activation is known to be a key step for the assembly and function of the NLRP3 (NLR family, pyrin domain containing 3) inflammasome which leads to the maturation and release of the pro-inflammatory cytokines IL-1β and IL-18. The role of these cytokines in glomerulonephritis is well established and in particular, treatment with interleukin-1 receptor antagonist has been demonstrated to be effective in reducing the severity of disease in anti-glomerular basement membrane antibody-induced glomerulonephritis (Tang et al., 1998). However, a clear role of the NLRP3 inflammasome in the pathogenesis of glomerulonephritis has not been recognized yet. Therefore, the aim of this work was to establish a correlation between the P2X7R-mediated inflammasome activation and renal injury using in vitro studies and in vivo experimental models of glomerulonephritis. The thesis includes the subsequent chapters: Chapter 1, the general introduction, where mainly P2X7R structure and function as well as the inflammasome machinery are described, followed by a chapter of methods and materials (Chapter 2), then 3 chapters of results and finally a discussion chapter with conclusions and future directions. Chapter 3 describes the differences between bone marrow derived macrophages from wild-type and two different lines of P2X7R deficient mice in the release of the inflammasome-dependent cytokines IL-1β and IL-18 in response to different stimuli and the

effects on their secretion of P2X7 selective inhibition. In Chapter 4, the cell signalling cascade following P2X7R activation is explored in bone marrow derived macrophages from wild-type and P2X7 deficient mice stimulated with ATP at different time points. Both a Western blotting and a mass-spectrometry phosphoproteomics approach have been used to carry on this analysis. In Chapter 5, the role of inflammasome activation in glomerulonephritis has been investigated using the rat model of nephrotoxic nephritis and examining the expression of several inflammasome-related genes and the secretion of IL-1β and IL-18 in bone marrow derived macrophages from Wistar-Kyoto (WKY) and Lewis rats. The analysis has then been extended to macrophages from single and double congenic rat strains. Additionally, glomeruli isolated from kidneys of WKY, Lewis and congenic rats at day 4 from the injection of nephrotoxic serum, an important time point that corresponds with the maximal P2X7R expression and macrophage infiltration as well as onset of proteinuria as previously described (Turner et al., 2007), were examined. Finally, Chapter 6 contains the general discussion of all the work presented in this thesis and the potential implications for the treatment of glomerulonephritis and outlines the key future work directions.

1.2 RECOGNITION OF ATP AS AN IMPORTANT INTERCELLULAR SIGNAL

The first studies to indicate that purine nucleotides and nucleosides might have an additional role outside cells as signalling molecules were conducted by Drury and Szent-Györgyi in 1929 when, injecting cardiac extracts intravenously in whole animals, they noticed an alteration of the cardiac rhythm and demonstrated that the biologically active compound responsible for this effect was an "adenine compound" (Drury & Szent-Gyorgyi, 1929). Many other studies followed confirming the biological activity of purines in different systems, including the uterus and the intestine (Burnstock, Fredholm, North, & Verkhratsky, 2010). Then, in 1970, evidence was presented for ATP as a neurotransmitter in so-called nonadrenergic, noncholinergic neurotransmission (NANC) in the gut (Burnstock, Campbell, Satchell, & Smythe, 1970) and in 1972 the word "purinergic" was used for the first time (Burnstock, 1972). In 1978, Burnstock classified the purinergic receptors into P1 and P2 receptors: adenosine acts on P1 receptors, whereas ATP and its breakdown products, ADP and AMP, act on P2 receptors (Burnstock, 2006b). Later, in 1985, Burnstock and Kennedy proposed a sub-classification of the P2 receptors, based on pharmacological criteria, dividing them into P2X and P2Y receptors (Burnstock & Kennedy, 1985). In 1994, Abbracchio and Burnstock described the P2X receptors as ionotropic ligand-gated ion channel receptors and P2Y metabotropic as G protein-coupled receptors (Abbracchio & Burnstock, 1994). Seven subtypes of P2X receptors and eight subtypes of P2Y receptors are currently recognized (Burnstock, 2006a). The seven P2X receptors subtypes are named as $P2X_{1-7}$, the eight P2Y receptors subtypes include P2Y1, P2Y2, P2Y4, P2Y6, P2Y11, P2Y12, P2Y13 and P2Y14. The P2Y receptors are G protein-coupled receptors (GPCRs) belonging to the rhodopsin family of G protein-coupled receptors also called Class A GPCRs characterized by seven transmembrane domains (Costanzi, Siegel,

Tikhonova, & Jacobson, 2009). The N-terminus locates on the extracellular side and the C-terminus on the cytoplasmic side of the plasma membrane (figure 1.1). The P2Y receptors can be further sub-divided into two groups based on their coupling to specific G proteins (Abbracchio et al., 2006). The P2Y1, P2Y2, P2Y4, P2Y6, and P2Y11 receptors couple to G_q, to activate Phospholipase C beta (PLCβ), and the P2Y12, P2Y13, and P2Y14 receptors couple to G_i to inhibit adenylyl cyclase (Jacobson & Boeynaems, 2010). The P2Y11 receptor has the unique property to couple through both G_q and G_s. The different P2Y subtypes with their agonists and associated G proteins are summarized in table 1.1.

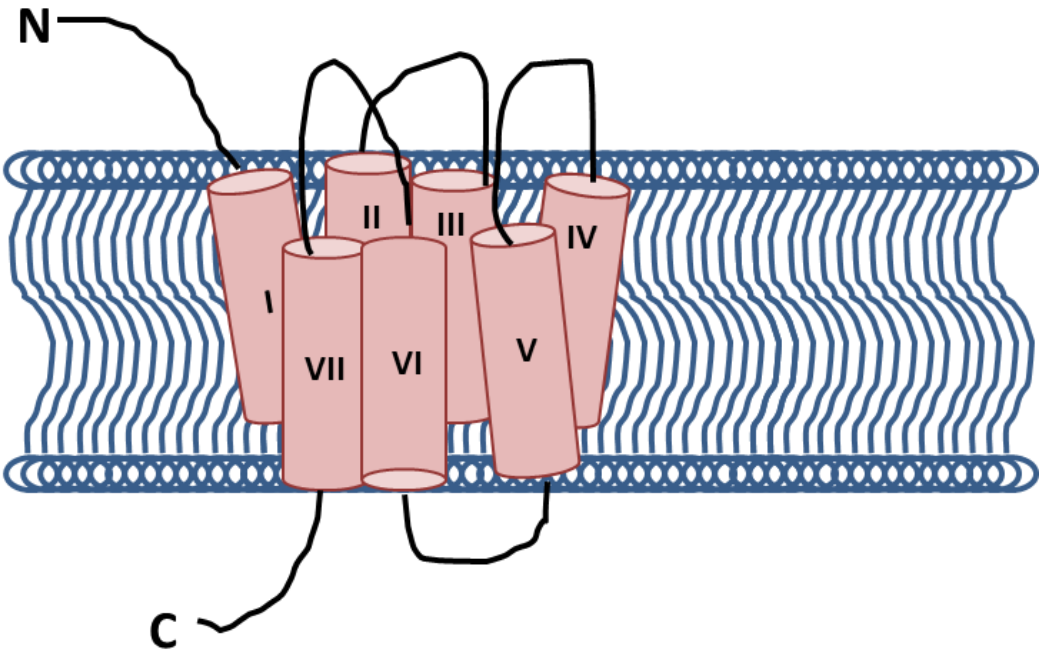

Figure 1.1 P2Y receptors structure

P2Y receptors consist of a single polypeptide chain which crosses the plasma membrane seven times, forming seven trans-membrane domains. The amino terminal region is located outside the cell, while the carboxyl terminal region is located in the cytoplasm where the G proteins are activated. Figure adapted from the following article: “Purinergic signalling in neuron–glia interactions” (Fields & Burnstock, 2006).

Receptor	Primary endogenous agonist	Associated G proteins
P2Y1	ADP (ATP)	G_q
P2Y2	ATP, UTP	G_q and $G_{i/0}$
P2Y4	UTP (ATP)	G_q and $G_{i/0}$
P2Y6	UDP	G_q
P2Y11	ATP	G_s and G_q
P2Y12	ADP (ATP)	$G_{i/0}$
P2Y13	ADP	G_s and $G_{i/0}$
P2Y14	UDP glucose	$G_{i/0}$

Table 1.1 Properties of P2Y purinergic receptors.

The P2Y family is composed of eight members activated by different nucleotides. The subtypes $P2Y_1$, $P2Y_2$, $P2Y_4$, $P2Y_6$, and $P2Y_{11}$ receptors couple to G_q, to activate Phospholipase C beta, while the $P2Y_{12}$, $P2Y_{13}$, and $P2Y_{14}$ receptors couple to G_i to inhibit adenylyl cyclase. The $P2Y_{11}$ receptor couples through both G_s and G_q. Adapted from (Jacobson & Boeynaems, 2010).

1.3 THE P2X RECEPTORS FAMILY

P2X receptors (P2XRs) are membrane ion channels that open, within milliseconds, in response to the binding of extracellular adenosine triphosphate (ATP) (Di Virgilio, 1995). The first cDNAs encoding P2X receptor subunits were isolated in 1994 (North, 2002). There are seven genes for P2X receptor subunits. Their chromosomal locations in humans are summarized in table 1.2. P2X2, P2X3 and P2X6 receptor genes are all on different chromosomes. P2X1 and P2X5 subunit genes are located close on the short arm of chromosome 13. P2X4 and P2X7 subunit genes are also both located on the long arm of chromosome 12 (North, 2002). The full-length of seven P2X receptors have 11-13 exons, and they all share a common structure, with well conserved amino acids in the outer loop and trans-membrane regions (Li, Liang, & Chen, 2008). These seven genes are considerable different in size. The P2X subunit proteins are 384 (P2X4) to 595 (P2X7) amino acids long (North, 2002). A significant progress in the understanding of the P2X receptors structure has been achieved in 2009 when Kawate and colleagues reported the crystal structure of a truncated mutant of the zebrafish P2X4.1 receptor (DzfP2X4.1) (Kawate, Michel, Birdsong, & Gouaux, 2009). This study has revealed that P2XRs form homomeric or heteromeric trimers and each subunit consists of two trans-membrane domains separated by a large extracellular loop and N- and C-terminal residues both on the cytoplasmic side of the plasma membrane (Nicke et al., 1998) (figure 1.2). All mammalian P2X receptors contain ten conserved cysteine residues in their extracellular domains, which are thought to form disulfide bond pairs (Young, 2010). The most fully characterized complexes are: homomeric P2X1, P2X2, P2X3, P2X4, P2X5, and P2X7 channels and heteromeric P2X2/3 and P2X1/5 channels (Dubyak, 2007). Initially it was thought that all P2XR subtypes, apart from P2X7R, were implicated in the assembly of heteromeric complexes. Then a study from Guo et al. has demonstrated the existence of heteromers P2X4/P2X7

which show properties in common with both of the parent homomeric receptors (Guo, Masin, Qureshi, & Murrell-Lagnado, 2007) (figure 1.3). However, there is still controversy whether structural heteromers of P2X4/P2X7 really exist (Nicke, 2008; Skaper, Debetto, & Giusti, 2010).

Subunit	Chromosome
P2X1	17p13.2
P2X2	12q24.33
P2X3	11q12
P2X4	12q24.31
P2X5	17p13.3
P2X6	22q11
P2X7	12q24.31

Table 1.2 Chromosomal localization of human P2X receptors.

Chromosomal localizations are from the National Center for Biotechnology Information, NCBI (http://www.ncbi.nlm.nih.gov/).

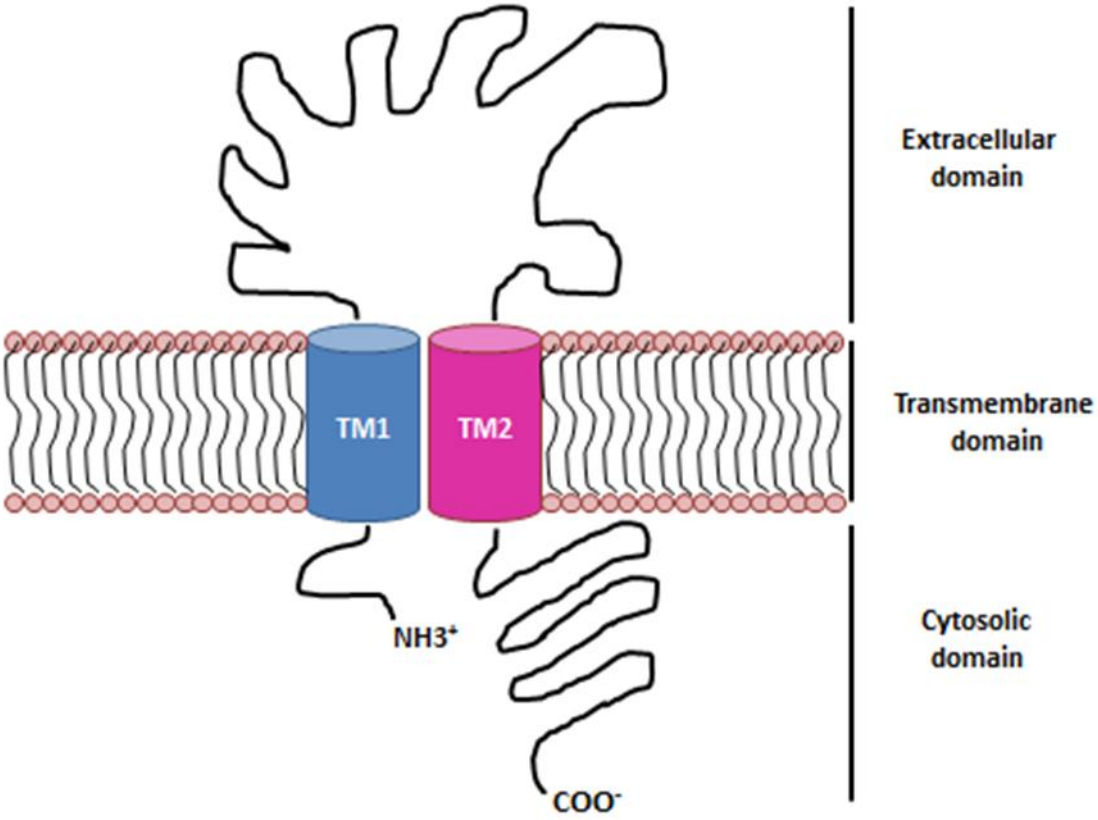

Figure 1.2 Schematic representation of the P2X subunits structure.

Schematic representation showing the membrane topology of a typical P2X receptor subunit characterized by two trans-membrane domains, indicated as TM1 and TM2, separated by a large extracellular loop and intracellular NH3+ and COO- termini. Figure adapted from the following article: "P2X receptors as cell-surface ATP sensors in health and disease" (Khakh & North, 2006).

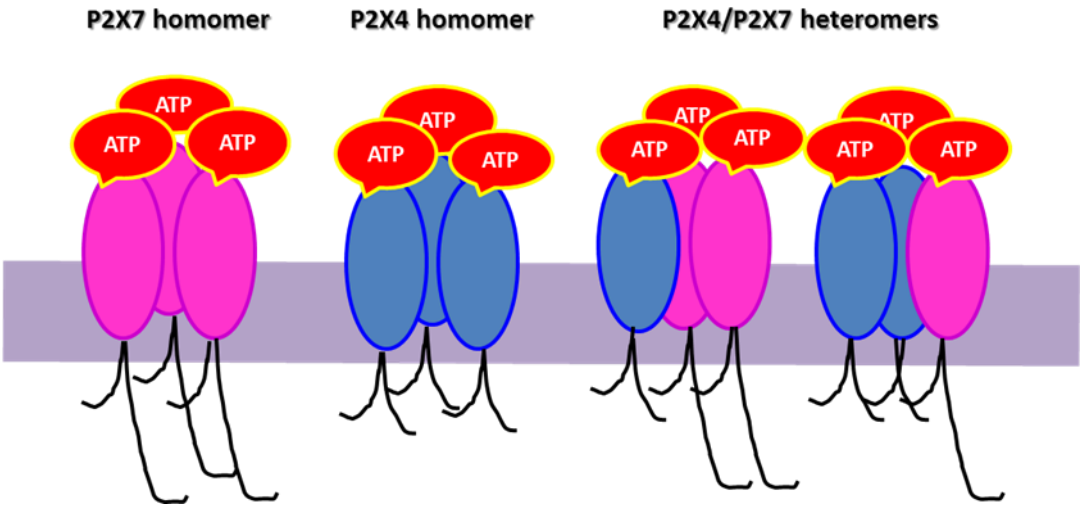

Figure 1.3 Trimeric structure of P2X7R homomers, P2X4R homomers and P2X4R/P2X7R heteromers.

P2X receptors form trimeric complexes composed of protein subunits. P2X7 receptor can form homomeric trimers or heteromeric trimers in association with P2X4 receptor. Figure adapted from the following article: “Go it alone no more: P2X7 joins the society of heteromeric ATP-gated receptor channels” (Dubyak, 2007).

1.4 THE UNIQUE PROPERTIES OF P2X7 RECEPTOR

The P2X7 subunit, previously termed as the 'P2Z receptor' (Surprenant, Rassendren, Kawashima, North, & Buell, 1996), was initially cloned from rat and then from human brain (Collo et al., 1997) and human macrophages (Rassendren et al., 1997). The sequence identity with other P2X receptors is of approximately 40–50 % (Erb, Liao, Seye, & Weisman, 2006). At the beginning, P2X7R was thought to be selectively expressed on cells of hematopoietic lineage such as mast cells, lymphocytes, erythrocytes, fibroblasts, peripheral macrophages and epidermal Langerhans cells (Surprenant et al., 1996). More recent studies have demonstrated that P2X7R is also widely expressed in epithelial cells including salivary glands epithelial cells (Hwang et al., 2009), bronchial epithelial cells (Denlinger et al., 2009) and cervical epithelial cells (Wang et al., 2004). Within the central nervous system, functional P2X7Rs have been localized on microglia and Schwann cells as well as on astrocytes (Ferrari et al., 1996). Among all the P2XRs, the P2X7 subtype presents some peculiar characteristics: it has a low sensitivity for ATP (mM range), while it appears to be much more sensitive to the synthetic ATP analog 3'-O-(4-benzoyl) benzoyl ATP (BzATP), so that BzATP is often used experimentally to induce P2X7R activation (Bianchi et al., 1999); it shows a long intracellular C-terminus with an extra 200 amino acid residues compared with the other receptors and it is characterized by two different states of permeability (Klapperstuck, Buttner, Schmalzing, & Markwardt, 2001): brief agonist stimulation induces a non-selective, cation-carrying pore, permitting the permeation of monovalent and divalent cations such as sodium, potassium and calcium and leading to depolarization of the plasma membrane, whereas prolonged and repetitive agonist application leads to an increased membrane permeability to larger cations such as N-methyl-D-glucamine (NMDG), (MW 195) (Pelegrin, 2011). Membrane permeability increases further under prolonged agonist stimulation allowing cellular uptake of

higher MW fluorescent dyes such as Yo-Pro-1 (MW 629) or ethidium bromide (MW 394) (Cankurtaran-Sayar, Sayar, & Ugur, 2009; Cankurtaran-Sayar et al., 2009). Recent studies have reported that the dilatation of the pore in the plasma membrane following prolonged agonist stimulation is not a unique feature of P2X7 receptors but also occurs in cells expressing P2X2 or P2X4 receptors (Chaumont & Khakh, 2008).

Mechanisms of pore formation

Despite the large amount of attention that has been paid to understanding the mechanisms underlying this time-dependent increase in permeability associated with P2X7R activation, the exact mechanisms and the physiological role of the permeabilization response are not fully understood yet. At the beginning, it was thought that P2X7R itself was able to dilate allowing the passage of large molecules (Khakh, Bao, Labarca, & Lester, 1999). More recent studies have suggested instead that the permeation of large molecules was mediated by a gap-junction protein, pannexin-1, which is also known to form functional hemichannels (Pelegrin & Surprenant, 2009). Several studies have indeed demonstrated that Panx1 gene silencing by small interfering RNA could inhibit some functions of P2X7R, including pore formation (Locovei, Scemes, Qiu, Spray, & Dahl, 2007). A recent study from Marques-da Silva et al. has shown that colchicine, which is known to induce microtubule disruption, potently inhibits both P2X2 and P2X7R-dependent dye uptake without affecting receptor channel ionic currents, supporting the hypothesis of a distinct permeation pathway for high MW dyes (Marques-da-Silva, Chaves, Castro, Coutinho-Silva, & Guimaraes, 2011).

The C and N termini of P2X7R

The C terminus of the P2X7R has attracted a lot of interest because of its bigger length compared to the other P2X C-termini and it is thought to be involved in the majority of functions related to P2X7R including signaling pathway activation, cellular localization, protein–protein interactions, and post-translational modification (Costa-Junior, Sarmento, & Coutinho-Silva, 2011). In 2001, Denlinger et al. demonstrated that the murine P2X7 C-terminus contains several protein-protein and protein-lipid interaction motifs with potential importance to macrophage signaling and LPS action (Denlinger et al., 2001). Among them, a putative Src homology (SH3)-binding domain has been described within residues 441–460, suggesting the involvement of the C terminus in regulating phospholipase D (PLD) activity by interacting with SH3 proteins that control Rho or other small G proteins. Residues 436–531 also have been shown to contain a conserved death domain, which may contribute to P2X7 receptor-mediated caspase activity and apoptosis (Denlinger et al., 2001). In their study, Denlinger et al. also described a LPS-binding region and demonstrated that two basic residues (Arg 578, Lys 579) within this motif are essential for LPS binding to P2X7 in vitro. In a later study, they also showed that a mutation in these amino acid residues resulted in trafficking defects and impaired pore formation and channel activity (Denlinger et al., 2003). The P2X7R C terminus contains 12 cysteine residues that are thought to participate in membrane localization (Gonnord et al., 2009). Mutations on these twelve cysteine residues have been shown to compromise the presence of P2X7R on the cell surface and to induce receptor expression on the endoplasmic reticulum and lysosomes (Gonnord et al., 2009). The N-terminal part of the P2X receptors is a very short region consisting of between 22 and 34 amino acids and there is a small amount of similarity in the N-termini of different P2X receptors (Soto, Garcia-Guzman, & Stuhmer, 1997). The N-terminus of the receptor has been linked to the activation of extracellular signal- regulated kinases ERK 1 and ERK2 (Amstrup &

Novak, 2003). Amstrup et al., using C- and N-terminal P2X7-receptor mutants demonstrated that the N-terminus is important in activation of ERKs, whereas deletion of the last 230 amino acids in the C-terminus did not affect ERK activation. On the other hand, Ca2+ entry was impaired in C-terminal but not in N-terminal mutants (Amstrup & Novak, 2003). The extracellular loop contains several conserved amino acid residues, including 10 cysteines that form a series of disulphide bridges, 13 glycines and 2–6 asparagines that may serve as N-linked glycosylation sites (Brake, Wagenbach, & Julius, 1994).

1.5 P2X7 DEFICIENT MOUSE LINES AND P2X7 SPLICE VARIANTS

Mice lacking the P2X7R are healthy and fertile and demonstrate no overt phenotype upon gross examination. However, a study conducted by Ke et al. has demonstrated that P2X7 deficient mice have a unique skeletal phenotype, exhibiting smaller bone diameter and lower cortical mass, associated with a striking reduction in the rate of periosteal bone formation (Ke et al., 2003). In addition, mice lacking the P2X7R show higher trabecular bone resorption indicating a key role for this receptor in periosteal bone formation and trabecular bone remodelling (Ke et al., 2003). There are two strains of mice in which the P2X7 gene has been disrupted. One mouse line has been generated by the pharmaceutical company GlaxoSmithKline (GSK) by insertion of a lacZ transgene into exon 1 (Sim, Young, Sung, North, & Surprenant, 2004) (Figure 1.4). In the mouse line generated by Pfizer, a neomycin cassette was inserted into exon 13, replacing a region that encodes Cys-506¬-Pro-532 of the intracellular C-terminus of the receptor (Fig 1.4). The P2X7 deficient mouse line generated by Pfizer has demonstrated a clear role of this receptor in bone formation and resorption (Ke et al., 2003) as well as in cytokine production and in inflammation (Labasi et al., 2002), while the knock-out mice generated by

GlaxoSmithKine have shown an important role of P2X7R in chronic inflammatory and neuropathic pain (Chessell et al., 2005). Experiments conducted on primary cells from the two P2X7 deficient mouse lines have demonstrated important differences between the two strains. One example is the difference in IL-6 production following ATP stimulation in macrophages. Pfizer macrophages show a significant reduction in IL-6 production compared to macrophages from WT mice (Solle et al., 2001), while macrophages from GSK knock-out mice exhibited a significant increase in IL-6 secretion (Chessell et al., 2005). In experimental autoimmune encephalomyelitis, a mouse model of multiple sclerosis, the Pfizer knock-out mice showed exacerbation of disease (Chen & Brosnan, 2006), while GSK mice had a reduction in the incidence of disease (Sharp et al., 2008).

P2X7 splice variants

Several splice variants have been described for both the human and mouse isoforms of P2X7R, which differ in their functional properties from the full length P2X7A receptor (Feng, Li, Wang, Zhou, & Gorodeski, 2006a; Cheewatrakoolpong, Gilchrest, Anthes, & Greenfeder, 2005). In particular, nine variants of human P2X7 resulting from alternative splicing named P2X7A–J, have been identified, P2X7A being the well-characterized full-length P2X7 receptor (Cheewatrakoolpong et al., 2005). Of the 9 splice variants, 4, P2X7B, P2X7E, P2X7G, and P2X7J, lack the C terminus. One of these variants (P2X7B) is characterized by a large C-terminal deletion and it has been shown to be able to mediate calcium influx and membrane depolarization but it can no longer trigger membrane permeabilization to larger molecules (Adinolfi et al., 2010). This variant has also been shown to have a growth promoting activity (Feng, Li, Zeng, & Gorodeski, 2006). Another splice variant of human P2X7 containing a larger deletion at the C-terminus and lacking the second transmembrane domain was found in cervical cancer cells (Feng, Li, Wang, Zhou, & Gorodeski, 2006). This

truncated P2X7 isoform seems to interact with the full length receptor in a dominant negative fashion promoting uncontrolled growth of cells (Feng, Li, Zeng, & Gorodeski, 2006b). For the mouse P2X7R, a splice variant characterized by an alternative exon 1 encoding the N-terminus and part of the first trans-membrane domain has been described. This variant, called P2X7K, showed much higher sensitivity to agonists such as BzATP than the original P2X7A, rapidly triggers membrane permeabilization and seems to be selectively expressed in spleen lymphocytes (Nicke et al., 2009). Being characterized by an alternative exon 1 and a different translation start point, this variant can escape gene inactivation in the Glaxo P2X7 knock-out mice. A recent study has described two further P2X7 variants in the mouse characterized by alternative exon 13's which encode much shorter C-termini than the original exon 13 and are able to escape gene inactivation in the Pfizer knock-out mouse strain (Masin et al., 2011). These two variants are identical with P2X7A between residues 1-430, one of the variants then terminates at T431 (P2X7 13B) and the other has an additional 11 amino acids at the C-terminus (P2X7 13C). Although they appear to form stable homotrimers, it has been demonstrated that the efficiency with which these trimers traffic out of the endoplasmic reticulum to reach the plasma membrane is considerably reduced compared to the full-length variant leading to a decreased amplitude of the whole cell currents compared to the P2X7A variant (Masin et al., 2011). In their study, Masin et al. have reported that the variant P2X7 13B, when co-expressed with the full-length P2X7R, acts in a dominant negative fashion reducing the surface expression of P2X7A and the amplitude of agonist-evoked whole cell currents. The identification of these splice variants can explain the diversity of P2X7 mediated responses in different tissues and leads to the conclusion that both the Glaxo and the Pfizer mouse strains are not null for P2X7R expression in all tissues.

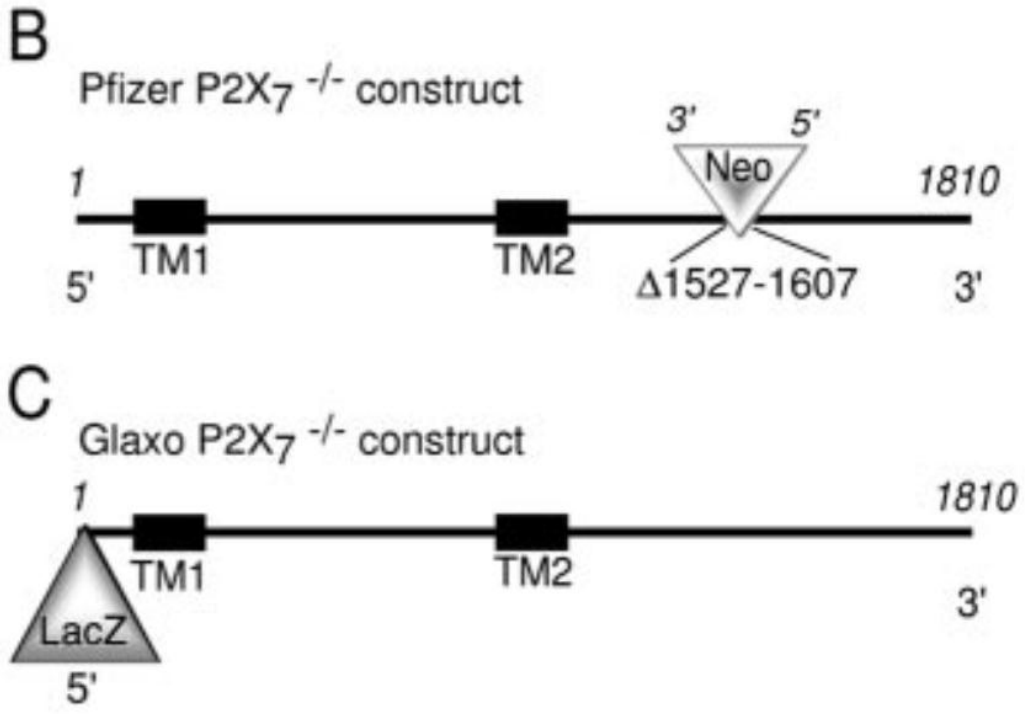

Figure 1.4 Simplified representation of the Pfizer and GlaxoSmithKline P2X7 knock-out constructs.

The construct of the Pfizer P2X7 knock-out has nucleotides 1527-1607 deleted and a neomycin cassette inserted 5' to 3', whereas the construct of the Glaxo P2X7 knock-out mice (C) had a LacZ gene inserted after ATG at the 5' end. Figure adapted from the following article: "Reanalysis of P2X7 receptor expression in rodent brain" (Sim, Young, Sung, North, & Surprenant, 2004).

1.6 GENETICS OF THE P2X7 RECEPTOR IN HUMAN DISEASE

Single-nucleotide polymorphisms (SNPs) are the most common genetic variation in the human genome and are now widely used to identify susceptibility genes in human diseases. The P2RX7 gene contains 13 exons and has been mapped to the 12q24.31 chromosomal region (Buell et al., 1998). The P2RX7 gene is highly polymorphic and to date 32 non-synonymous, amino acid-altering SNPs have been identified (Fuller, Stokes, Skarratt, Gu, & Wiley, 2009). The majority of identified SNPs in P2RX7 confer a loss-of-function phenotype to various P2X7-dependent downstream events (Gu et al., 2001), while one ectodomain SNP (His-155 to Tyr) confers a gain of-function effect (Cabrini et al., 2005). The first SNP to be functionally described was 1513A>C that changes glutamic acid to alanine at residue 496 (Glu496 to Ala) in the carboxyl terminus of the receptor. This amino acid substitution in native or transfected cells leads to an impairment of the pore formation activity, while the cation selective channel activity is not affected (Boldt et al., 2003). The polymorphism (489C>T) changes amino acid 155 from histidine to tyrosine (His155 to Tyr) in the extra-cellular portion of the receptor and has an allele frequency of 0.455 in Caucasians (Cabrini et al., 2005). Functional analysis in recombinant HEK293 cells expressing the P2X7 489T mutant revealed that the His155 to Tyr substitution produces a gain-of-function effect leading to an increased ethidium uptake and calcium influx. Several genetic association case–control studies using synonymous and non-synonymous SNPs have revealed a role for P2RX7 as a susceptibility gene in bipolar disorder and major depression (Roger et al., 2010) and in susceptibility to infections with intracellular pathogens such as tuberculosis (Fernando et al., 2007). Three independent case-control studies from Canada, Germany and the UK have identified a SNP at nucleotide 1405 A>G in the gene which is strongly associated with both bipolar and major depressive disorders. This SNP is present in about 15% of the Caucasian population and changes Glutamine-460 to

Arginine in the long carboxyl tail of the receptor but the functional effect of this SNP on P2X7R is yet to be determined (Barden et al., 2006). P2X7R has also been shown to play an important role in the killing of phagocytosed Mycobacterium tuberculosis by extracellular ATP (Fairbairn, Stober, Kumararatne, & Lammas, 2001a). Several epidemiological studies have confirmed the role of P2X7R in the control of tuberculosis. A study conducted on individuals from Southeast Asia revealed that the inheritance of the 1513A>C loss-of-function polymorphic variant of P2RX7 was associated with reduced killing of Mycobacterium Tuberculosis and with extrapulmonary tuberculosis (Fernando et al., 2007). Other conditions linked to P2RX7 gene polymorphisms include resistance to infection with Chlamydia (Coutinho-Silva, Perfettini, Persechini, Dautry-Varsat, & Ojcius, 2001), increased fracture risk in post-menopausal women (Ohlendorff et al., 2007) and multiple sclerosis (Oyanguren-Desez et al., 2011).

1.7 P2X7 RECEPTOR ANTAGONISTS

Several P2X7R antagonists have been discovered so far and some of them have also been recently used in Phase I and Phase II clinical trials (Guile et al., 2009). The molecular structure of the main P2X7R antagonists is illustrated in figure 1.5. The currently available P2X7 receptor antagonists can be classified into five main groups (North, 2002). The first group contains ions, such as calcium, copper, magnesium, zinc and protons which all inhibit ATP-evoked currents at the rat P2X7R (Friedle, Curet, & Watters, 2010; North, 2002). P2X7 receptors are distinct from other ATP-gated P2X receptors in that they are potently inhibited by submicromolar concentrations of zinc and copper (Liu et al., 2008). Similar concentrations seem instead to potentiate the current activity of the other members of the P2X family (North, 2002). The second group is represented by non-selective P2X7R antagonists such as suramin, pyridoxal-phosphate-6-azophenyl-2',4'-disulfonate (PPADS), Brilliant Blue G (BBG) and oxidized ATP. Suramin and PPADS were among the first antagonists identified. They both block P2X7 receptors with low affinity and typically show non-competitive antagonism and a low specificity (Jacobson, Jarvis, & Williams, 2002). Brilliant Blue G (BBG) is a more potent and selective antagonist with a 30- to 50-fold greater selectivity for rat versus human P2X7 receptors (Jiang, Mackenzie, North, & Surprenant, 2000). Oxidized-ATP is an irreversible inhibitor of P2X7R but requires one-two hours incubation to completely block P2X7 function and furthermore is not selective leading also to the blockade of P2X1 and P2X2 receptors and to the inhibition of nuclear factor k-B (NF-kB) (Murgia, Hanau, Pizzo, Rippa, & Di Virgilio, 1993). The third group includes compounds that contain two large organic cations, such as the isoquinoline KN-62 (1-(N,O-bis[5-isoquinolinesulfonyl]-N-methyl-L-tyrosyl)-4-phenylpiperazine) and the imidazole calmidazolium. The isoquinoline KN-62 potently blocks P2X7 receptor function in a non-competitive fashion (Gargett & Wiley, 1997). It has been shown that KN-

62 blocks currents in cells expressing the human P2X7R but has little effect at the rat P2X7R (Humphreys, Virginio, Surprenant, Rice, & Dubyak, 1998). The fourth class of P2X7 antagonists described is represented by 17β-estradiol (Cario-Toumaniantz, Loirand, Ferrier, & Pacaud, 1998). In 1998, Cario-Toumaniantz et al. have demonstrated that 2.17 β-Oestradiol rapidly and reversibly inhibited the ATP and BzATP evoked currents in COS cells expressing the human P2X7R and in the human monocytic cell line U937 (Cario-Toumaniantz et al., 1998). Finally, a monocolonal antibody specific for the human P2X7R was generated in mice (Buell et al., 1998). In 2003, two novel series of P2X7R antagonists, composed of cyclic imides (Alcaraz et al., 2003) and adamantane amides (Baxter et al., 2003), were shown to be effective P2X7R antagonists. These compounds however show a preferential affinity for the human versus the rat P2X7R. In 2006 two novel series of P2X7R antagonists have been discovered by Abbott Laboratories: disubstituted tetrazoles such as A-438079 (Nelson et al., 2006) and cyanoguanidines (Honore et al., 2006). These new compounds demonstrated enhanced potency and selectivity as antagonists at rat and human P2X7 receptors compared to previous antagonists and their action was reversible (Donnelly-Roberts & Jarvis, 2007). Another P2X7R antagonist that belongs to the family of cyanoguanidines is A-740003 ((N-(1- 2,2-dimethylpropyl)-2-(3,4-dimethoxyphenyl)acetamide). (Honore et al., 2006). This compound shows similar properties as A-438079 but it has been shown to be more potent in blocking BzATP-evoked IL-1β release and pore formation in differentiated human THP-1 cells (Honore et al., 2006). Several Phase I and Phase II clinical trials investigating the safety and the efficacy of the P2X7R antagonists have been conducted (Arulkumaran, Unwin, & Tam, 2011). Current P2X7R antagonists have proven to be safe and well tolerated. Phase II clinical trials have investigated the use of P2X7R antagonists in rheumatoid arthritis, inflammatory bowel disease and chronic obstructive airway disease

(Arulkumaran et al., 2011). The main reported side effects were gastrointestinal symptoms such as nausea and diarrhoea, dizziness and headaches.

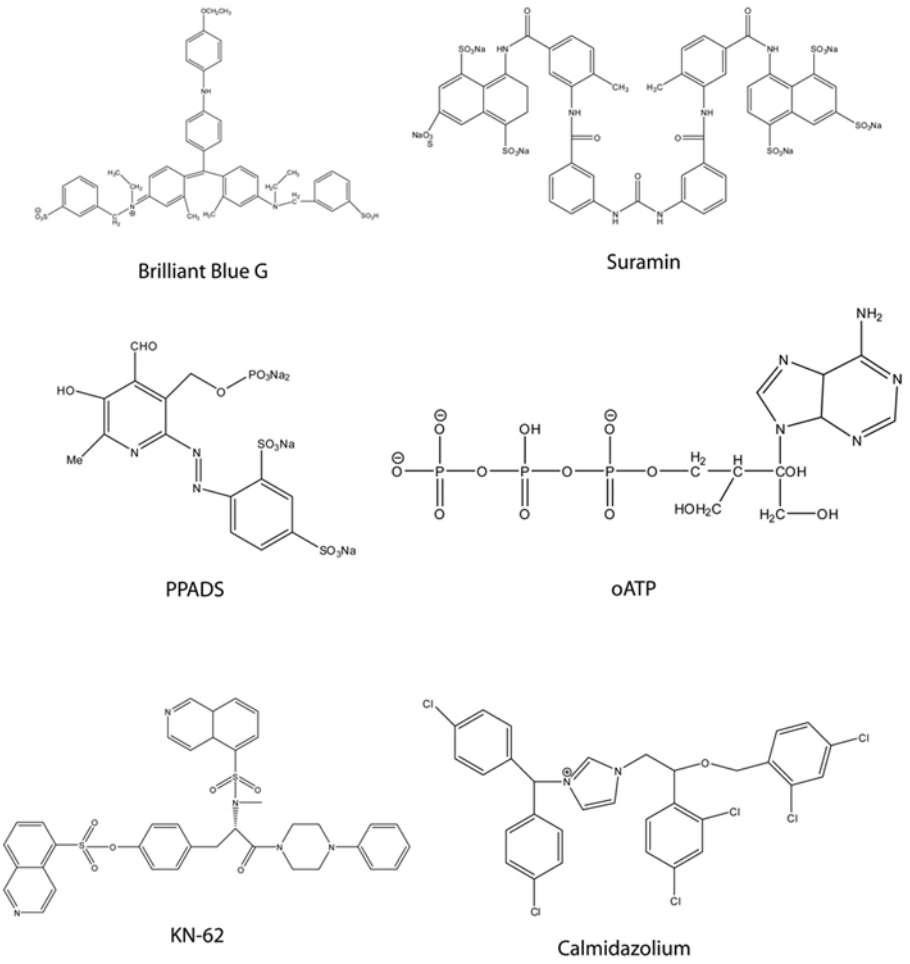

Figure 1.5 Molecular structure of P2X7 receptor antagonists.

Pyridoxal-phosphate-6-azophenyl-2',4'-disulfonate (PPADS), oxidized ATP, suramin and Brilliant Blue are non-selective antagonists. Brilliant Blue G shows a higher potency for rat versus human P2X7 receptors, while KN62 appears to be more effective in blocking the human versus the rat P2X7 receptor. Figure adapted from the following article: “Recent patents on novel P2X(7) receptor antagonists and their potential for reducing central nervous system inflammation” (Friedle, Curet, & Watters, 2010).

1.8 FUNCTIONAL CONSEQUENCES OF P2X7 RECEPTOR ACTIVATION

P2X7R activation has been associated with many important cellular functions, including: pore-formation activity (Aga et al., 2002), maturation and release of pro-inflammatory cytokines (Pelegrin, Barroso-Gutierrez, & Surprenant, 2008), killing of pathogens (Fairbairn, Stober, Kumararatne, & Lammas, 2001), membrane blebbing formation (Pfeiffer et al., 2004), cell cycle regulation (Bianco et al., 2006), activation of phospholipases A2 and D (Alzola et al., 1998), activation of mitogen-activated protein kinase (MAPK) and nuclear factor-κB (NF-κB) and many others (Armstrong, Brust, Lewis, & MacVicar, 2002; Di Virgilio, 1995; Ferrari, Stroh, & Schulze-Osthoff, 1999). One of the first studied cellular responses to P2X7R activation is represented by pore formation and rapid changes in ionic fluxes (Virginio, Mackenzie, Rassendren, North, & Surprenant, 1999). Prolonged stimulation of the pore activity has been shown to have a cytotoxic effect (Le Feuvre, Brough, Iwakura, Takeda, & Rothwell, 2002) and lead to membrane blebbing and apoptosis, so that P2X7R has been historically defined “the suicide receptor (Chiozzi et al., 1997). More recent studies however, have shown that basal levels of ATP, naturally present in the extracellular milieu, cause a tonic activation of P2X7R which increases calcium influx in the mitochondria and this, in turn, induces ATP synthesis promoting cell survival and proliferation in the absence of serum (Adinolfi et al., 2005). In their study, Adinolfi et al. have demonstrated that this growth promoting function of the P2X7R is dependent on pore formation, since it does not occur in cells transfected with a truncated form that cannot form a pore. Consistent with these findings is also the observation that P2X7R is expressed at high levels in several malignancies (Adinolfi et al., 2002; Jelassi et al., 2011). P2X7R activation induces not only pore formation in the plasma membrane but activates a wide range of membrane trafficking responses such as shedding of plasma membrane

surface proteins, phagosome maturation and fusion with lysosomes, exocytosis of secretory lysosomes, that can modulate the direct interactions between P2X7R expressing cells and other cell types in sites of immune and inflammatory activation (Mackenzie, Young, Adinolfi, & Surprenant, 2005; Qu & Dubyak, 2009). Several studies have reported that P2X7R activation is associated with the activation of the MAPK signalling pathway. These enzymes are a highly conserved family of protein serine/threonine kinases and include the extracellular signal-regulated kinases ERK1/2, the c-Jun NH2-terminal kinases JNK1/2, and the p38 stress-activated protein kinases (Dong, Davis, & Flavell, 2002). These kinases can trigger the nuclear accumulation and activity of various transcription factors, such as NF-κB, and c-Jun, which can modulate cytokine and inflammatory mediator expression (Bhat, Zhang, & Bhat, 1999). Work by Bradford et al. has shown that P2X7R activation induced by ATP or BzATP, promotes an increase in both the activity and autophosphorylation of Protein Kinase D (PKD) in rat parotid acinar cells and this effect was also associated with an increased phosphorylation of ERK1 and ERK 2 (Bradford & Soltoff, 2002a). Studies conducted on primary astrocyte cultures have also demonstrated that activation of the purinergic P2X7R increases Monocyte Chemoattractant Protein-1 (MCP-1) expression via activation of the MAPK pathway (Panenka et al., 2001a). The activation of P2X7R has been also linked to the production of reactive oxygen species (ROS) in macrophages through the MAPKs ERK1/2 signalling pathway and the nicotinamide adenine dinucleotide phosphate oxidase complex (NADPH) (Lenertz, Gavala, Hill, & Bertics, 2009). Transcription factors such as nuclear factor κB (NF-κB), nuclear factor of activated T cells (NFAT), cyclic AMP response element-binding (CREB) protein, and activator protein 1 (AP-1), whose activation and nuclear translocation are associated with the expression of inflammatory genes have been shown to be activated by P2X7R in microglia (Ferrari, Stroh, & Schulze-Osthoff, 1999; Potucek, Crain, & Watters, 2006). Studies from Korcok et al. have also revealed that P2X7R

directly activates NF-kB in osteoclasts (Korcok, Raimundo, Ke, Sims, & Dixon, 2004). P2X7R activation has also been associated with activation of different phospholipases including phospholipase A2 (Alzola et al., 1998) and phospholipase D (Coutinho-Silva et al., 2003). A study conducted on microglial cells has also shown that P2X7R promotes cell proliferation positively regulating cell cycle progression (Bianco et al., 2006). Proteomic analysis performed on human embryonic kidney cells (HEK) revealed the existence of a P2X7R signalling complex formed by 11 proteins that interact directly with the rat P2X7R (Kim, Jiang, Wilson, North, & Surprenant, 2001). The majority of these proteins are involved in the cytoskeleton organization and include: the extracellular matrix protein laminin α3, the membrane spanning proteins integrin β2 and receptor protein tyrosine phosphatase β and eight intracellular proteins. In their study Kim et al also showed that P2X7R becomes dephosphorylated at Tyr 343 upon activation and the effects of this dephosphorylation are a delay in membrane blebbing and an inhibition of membrane currents (Kim et al., 2001).

1.9 P2X7 RECEPTOR AND MACROPHAGE FUNCTION

Macrophages are cells that function as a first line of defence against invading microorganisms thanks to their ability to recognize and directly kill pathogens while recruiting and activating other inflammatory cells through the secretion of cytokines that act as danger signals (Zhang & Mosser, 2008). The ability of exogenous pathogen-associated molecular patterns (PAMPS) such as bacterial lipopolysaccharide (LPS) to induce the processing and the release of IL-1β by monocytes/macrophages was well established since the discovery of IL-1β as an endogenous pyrogen (Murphy, Simon, & Willoughby, 1980). It was observed, however, that LPS was a very efficient stimulus in inducing accumulation of pro-IL-1β in the cytosol, while it was only a weak stimulator of IL-1β processing and release (Dinarello, 2004). This observation has led investigators to postulate a second stimulus to induce efficient IL-1β conversion and release. The first studies showing ATP as a strong IL-1β releasing molecule were conducted by Perregaux et al. who indicated the massive efflux of intracellular potassium following ATP stimulation as the underlying mechanism of IL-1β activation and release (Perregaux & Gabel, 1994). At that time the identity of the plasma membrane receptor involved in this process was unknown. Later studies performed in vitro and in vivo in P2X7 deficient mice conclusively recognised P2X7 as the receptor responsible for ATP-dependent IL-1β release (Ferrari et al., 1997; Labasi et al., 2002). During inflammation, circulating blood monocytes migrate from the vasculature to the extravascular compartments where they mature into tissue macrophages (Takashiba et al., 1999). Several studies have reported that synthesis and release of IL-1β differ between monocytes and macrophages (Netea et al., 2009). Monocytes indeed, have constitutively activated caspase-1, leading to release of active IL-1β after a single stimulation event with bacterial ligands such as LPS, whereas in macrophages, the process of IL-1β secretion is thought to require two different steps (Ward et al., 2010)

(figure 1.6). The first signal is triggered by the so-called PAMPs such as LPS, which, through the interaction with Toll-Like-Receptors activate several intracellular signal transduction pathways including MAPK and NF-κB cascades leading to the increased production of pro-IL-1β within the cell (Bauernfeind et al., 2009). This LPS priming stimulus is necessary as ATP stimulation alone will not induce the release of active IL-1β (Mehta, Hart, & Wewers, 2001). The exact function of the LPS priming step however remains still unclear. It was thought that LPS priming was necessary to increase the levels of pro-IL-1β within the cells in order to generate enough substrate for caspase-1 activity. However, studies conducted on the other well recognized caspase-1 dependent cytokine IL-18 have demonstrated that substrate generation is not the only function of LPS priming (Gu et al., 1997). Indeed, macrophages contain already high levels of pre-formed pro-IL18 even under basal conditions but they release no mature IL-18 unless primed with LPS (Wewers & Sarkar, 2009). The second step required for IL-1β maturation and release can be triggered by different stimuli such as extracellular ATP, crystals (monosodium urate crystals), or pathogenic dusts (asbestos or silica) which induce the assembly of the multiprotein complex inflammasome with activation of caspase-1, ultimately responsible for the cleavage and secretion of the active cytokine (Martinon, Petrilli, Mayor, Tardivel, & Tschopp, 2006), (Dostert & Petrilli, 2008). P2X7R activation by ATP represents therefore a crucial event for the processing and release of active IL-1β (Hogquist, Unanue, & Chaplin, 1991). The exact mechanism by which P2X7R activation by ATP leads to the assembly of the NLRP3 inflammasome and the consequent activation of caspase-1 is not completely understood yet. It is known that ATP leads to a rapid efflux of potassium from the cell and triggers gradual recruitment and pore formation by the pannexin-1 hemichannel (Petrilli et al., 2007; Kanneganti et al., 2007). It has been suggested that NLRP3 senses either low intracellular potassium or a breakdown in membrane integrity or that hemichannel pore formation allows extracellular NLRP3 agonists to access the

cytosol, to activate NLRP3 directly (Schroder, Zhou, & Tschopp, 2010). Blocking the potassium efflux by exogenous potassium, inhibits the ability of ATP to induce the release of active IL-1β and IL-18 suggesting that the formation of pores that allows potassium escape is a key step for the release of these caspase-1 dependent cytokines (Perregaux & Gabel, 1994). The constitutive caspase-1 activation in monocytes has been related to their ability to release ATP (Piccini et al., 2008). Endogenous ATP from monocytes can in turn activate the NLRP3 inflammasome and induce IL-1β secretion through P2X7R. In contrast, macrophages completely lack the capacity to release ATP, therefore they require a second stimulus to generate active IL-1β and IL-18 (Ferrari, Chiozzi, Falzoni, Hanau, & Di Virgilio, 1997).

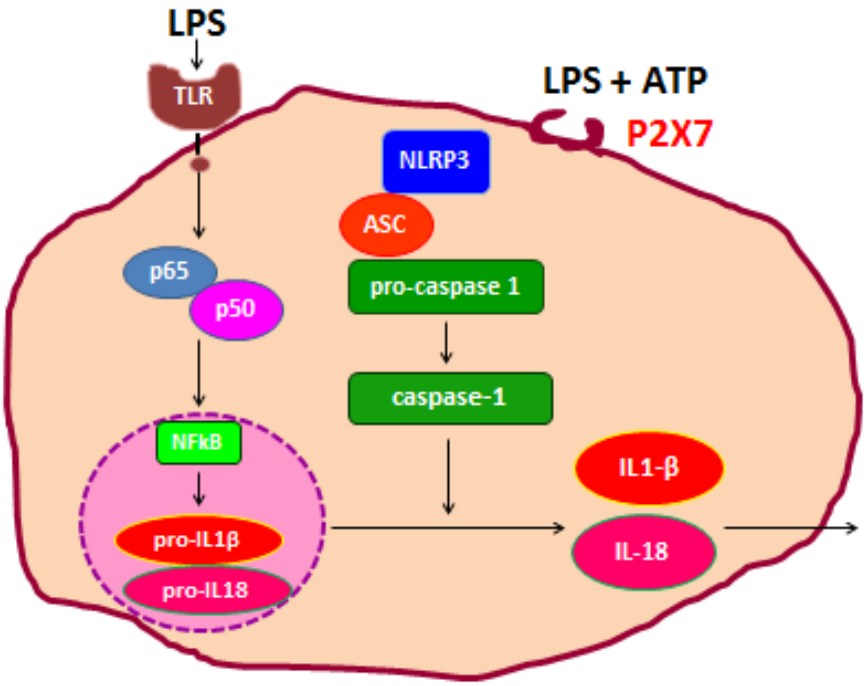

Figure 1.6 Schematic representation of the processing and release of IL-1 beta and IL-18 in macrophages.

Two different steps are required for the generation of active IL-1β and IL-18 in macrophages: the first stimulus is triggered by LPS which through the activation of the Toll-like receptor 4 (TLR4) activates the NF-kB signalling cascade leading to an increased synthesis of pro-IL-1β and pro-IL-18 within the cells. The second step is represented by P2X7 receptor activation by ATP, necessary for the NLRP3 inflammasome assembly and activation of pro-caspase 1 which is now able to cleave pro-IL-1β and pro-IL-18 into their mature forms and these are immediately secreted outside the cells. Figure adapted from: http://www.invivogen.com/review-nlrp3-inflammasome.

1.10 IDENTIFICATION OF THE CATHELICIDIN PEPTIDE LL-37 AS A NOVEL P2X7R AGONIST

LL-37 is the only human member of a family of antimicrobial peptides called cathelicidins. It is an 18 KDa molecule, mainly expressed in neutrophils and epithelial cells (Larrick et al., 1996). LL-37 is synthesized as an inactive precursor and in neutrophils is stored within the peroxidase-negative granules (Elssner, Duncan, Gavrilin, & Wewers, 2004a). The precursor is then converted into its active form by serine proteases contained in the azurophil granules of neutrophils (Oren, Lerman, Gudmundsson, Agerberth, & Shai, 1999). LL-37 has been shown to exert antimicrobial activity toward both Gram-negative and Gram-positive bacteria and to directly mediate chemotaxis of neutrophils, monocytes and T cells through a member of the formyl peptide receptor family, formyl peptide receptor-like 1 (FPRL1) (De et al., 2000). The antibacterial function of LL-37 has been attributed to its membrane pore-forming activity (Johansson, Gudmundsson, Rottenberg, Berndt, & Agerberth, 1998). Perregaux et al. have documented that protegrins, a group of antimicrobial peptides derived by proteolytic cleavage of a porcine cathelicidin precursor, can induce IL-1β processing and release in LPS-primed monocytes through a P2X7 independent way (Perregaux, Bhavsar, Contillo, Shi, & Gabel, 2002). The mechanism by which protegrins were able to generate active IL-1β was related to their membrane-permeabilizing activity leading to a rapid efflux of potassium from the cells. The results of this study suggested that other antimicrobial peptides, such as LL-37 might promote IL-1β secretion in a similar manner. However, a study conducted by Elssner et al. has shown that LL-37 stimulation of LPS-primed monocytes led to maturation and release of IL-1β but this effect was completely abolished when monocytes were pretreated with P2X7R inhibitors such as oxidised ATP, KN04 and KN62, indicating that LL-37 acts via P2X7R (Elssner, Duncan, Gavrilin, & Wewers, 2004). However, the interaction between

LL-37 and P2X7R remains controversial since the antagonists used may have non-selective effects. Therefore, studies to investigate the effects of LL-37 in macrophages from WT mice and comparison with macrophages with P2X7R deficient mice will be informative to clarify this controversy.

1.11 GENERATION OF ACTIVE IL-1β VIA CASPASE-1 INDEPENDENT PATHWAYS

In 1988, Black et al. demonstrated that Chymotrypsin and Staphylococcus aureus protease were able to generate active IL-1β (Black et al., 1988). Further studies from Kapur et al. also showed that a cysteine protease derived from Streptococcus pyogenes was able to induce the cleavage of IL-1β precursor to produce active IL-1β (Kapur, Majesky, Li, Black, & Musser, 1993). Similarly, neutrophil-derived serine proteases such as cathepsin G, neutrophil elastase and proteinase 3 as well as mast cell derived serine proteases including granzyme A and chymase have been also shown to cleave the IL-1β precursor at distinct sites into a secreted biologically active form (Mizutani, Schechter, Lazarus, Black, & Kupper, 1991; Irmler et al., 1995). In vivo experiments conducted by Fantuzzi et al. on caspase-1 deficient mice to investigate their response to local inflammation, revealed that there were no differences between WT and caspase-1 knock-out mice in the development of the systemic acute phase response and that the levels of mature IL-1β were similar in the two mouse strains (Fantuzzi et al., 1997). Work from Schonbeck et al. demonstrated that several components of the family of matrix metalloproteinases (MMPs) including stromelysin-1 (MMP-3), gelatinases A (MMP-2) and B (MMP-9), process recombinant human IL-1β precursor into biologically active forms (Schonbeck, Mach, & Libby, 1998). MMPs are known to play an important role in extracellular matrix degradation and have been also shown to be markedly upregulated in macrophages at sites of inflammation (Lemjabbar et al., 1999).

Interestingly, IL-1β itself has been shown to regulate the expression of MMPs in different cell types (Mountain, Singh, Menon, & Singh, 2007; Yokoo & Kitamura, 1996), indicating an important cross-regulation among these two classes of effectors of inflammation.

1.12 THE INFLAMMASOMES

The innate immune system is an evolutionarily conserved system that represents the first line of protection against invading microbial pathogens through different processes such as phagocytosis and the induction of inflammation (Khare, Luc, Dorfleutner, & Stehlik, 2010). Host cells, in particular cells of the myeloid lineage, express germline encoded pattern recognition receptors (PRRs) for the detection of various microbial components (Taylor et al., 2005). PRRs belong to different classes of receptors such as trans-membrane toll-like receptors (TLRs), C-type lectin receptors (CLRs), the retinoic acid inducible gene-I (RIG-I) receptors which belong to the RNA helicases family that specifically detects RNA species derived from viruses in the cytoplasm, cytosolic Nod-like receptors (NLRs), and the recently identified HIN-200 family members (O'Neill & Bowie, 2010; Takeuchi & Akira, 2010; Skeldon & Saleh, 2011). These receptors are also able to sense and to respond to endogenous, host-derived, danger signals that are released in response to cell death, tissue injury or stress (Bianchi & Manfredi, 2009). Following the recognition of microbial components or danger stimuli, these receptors activate a signalling cascade that leads to the generation of the appropriate immune response. The inflammasome was first described in 2002 as a molecular platform activating pro-inflammatory caspases leading to the maturation and release of the pro-inflammatory cytokines IL-1β and IL-18 (Martinon, Burns, & Tschopp, 2002). Since, the interest for this complex has constantly increased and several inflammasome complexes with different specificities have been identified. To date, five cytoplasmic receptors have been described that form an inflammasome complex: NLR family, pyrin domain containing 1 (NLRP1; also called NALP1), NLRP3 (also called NALP3 or cryopyrin), NLR family, caspase recruitment domain (CARD) containing 4 (NLRC4; also called IPAF) and the more recent absent in melanoma 2 (AIM2) and retinoic acid inducible gene 1 (RIG-1) (Guarda & So, 2010). NLRP1, NLRP3 and NLRC4

belong to the NLR family of receptors, AIM2 is a member of the haematopoietic interferon inducible nuclear protein (HIN) family of proteins while RIG-1 is an RNA helicase that recognises viral RNA (Poeck et al., 2010). The NLRs are intracellular receptors characterized by a tripartite structure, consisting of an N-terminal protein–protein interaction domain, a central NACHT [NAIP (NLR family, apoptosis inhibitory protein), CIITA (class II, major histocompatibility complex, transactivator), HET-E (plant het gene product involved in vegetative incompatibility) and TP-1 (telomerase-associated protein 1)] domain and a C-terminal tail which in NLRs is a series of leucine-rich repeats (LRRs), as found in TLRs (Skeldon & Saleh, 2011). These receptors can be divided in three subfamilies according to the characteristics of their N-terminal domain: the NOD receptors, the NLRPs and the NLRC4/NAIP clade (Figure 1.7). In basal conditions, the NLRs are present in the cytoplasm in an inactive form. Upon stimulation, they undergo a conformational change to expose their NACHT domain, they bind and recruit the adaptor protein apoptosis speck protein with CARD (ASC) via a PYD–PYD interaction (Kufer, Fritz, & Philpott, 2005). The ASC protein is composed of an N-terminal PYD and a C-terminal CARD. Through its CARD, ASC interacts with the CARD of caspase-1, as shown in figure 1.6 (Srinivasula et al., 2002). On the other hand, both NLRP1 and NLRC4 contain a CARD themselves, and are potentially able to directly recruit caspase-1. The exact role of ASC in these two inflammasomes is not fully understood yet, although experimental evidence indicates that ASC could increase the stability of the overall structure (Faustin et al., 2007). In the case of NLRP3 and AIM2, however, which do not possess a CARD, ASC is strictly required for the formation of their respective inflammasomes. AIM2 receptors probably oligomerize and initiate inflammasome formation directly around the bound DNA strand (Schroder, Muruve, & Tschopp, 2009; Burckstummer et al., 2009). Several agonists have been identified that activate the inflammasomes, some of them showing a high specificity for a particular NLR. Among them, ATP appears to be a very effective

stimulus for the assembly and activation of the NLRP3 inflammasome (Schroder, Zhou, & Tschopp, 2010b). Elevated concentrations of ATP activate P2X7R, inducing potassium efflux and causing the recruitment of the pannexin-1 channel which amplifies this response (Pelegrin & Surprenant, 2009). NLRP3 inflammasome can also be activated by a variety of different stimuli including pore forming toxins such as the antimicrobial peptide LL-37, monosodium urate crystals (Martinon, Petrilli, Mayor, Tardivel, & Tschopp, 2006), haemozoin and pathogens such as Candida albicans (Hise et al., 2009). Due to the heterogeneous nature of the stimuli activating the NLRP3 inflammasome, it has been hypothesized that other receptors, specific to the individual stimuli, are activated and proceed to induce NLRP3 inflammasome formation or that a secondary messenger molecule, which is induced by the different activators, in turn directly activates NLRP3 (Bryant & Fitzgerald, 2009). Caspases are a large family of cysteine proteases that cleave their substrates after an aspartic acid residue. The majority of them are known to be involved in the apoptotic process; only a few of them, in particular caspase-1, -4, -5 and -12 in humans and caspase-1, -11 and -12 in the mouse and in the rat (Kersse, Vanden Berghe, Lamkanfi, & Vandenabeele, 2007), have an inflammatory activity playing a key role in the maturation and releasing of pro-inflammatory cytokines. Under basal conditions, caspase-1 is present in the cells in an inactive form. Once recruited within an inflammasome complex, caspase-1 undergo an autoproteolytic process, leading to the formation of two subunits of 10 (p10) and 20 (p20) kilodaltons (KDa) respectively. Caspase-1 once activated, converts pro-IL-1β, which has a molecular weight of approximately 31 KDa, into its active 17 KDa form. Caspase-5 and caspase-11 are thought to increase caspase-1 autoproteolytic activity (Wang et al., 1998). Apart from IL-1β, caspase-1 cleaves other substrates such as the inflammatory cytokine IL-18 which is converted from the pro-IL-18 of about 24 KDa into its active 18 KDa form or the apoptotic caspase-7 (Gu et al., 1997).

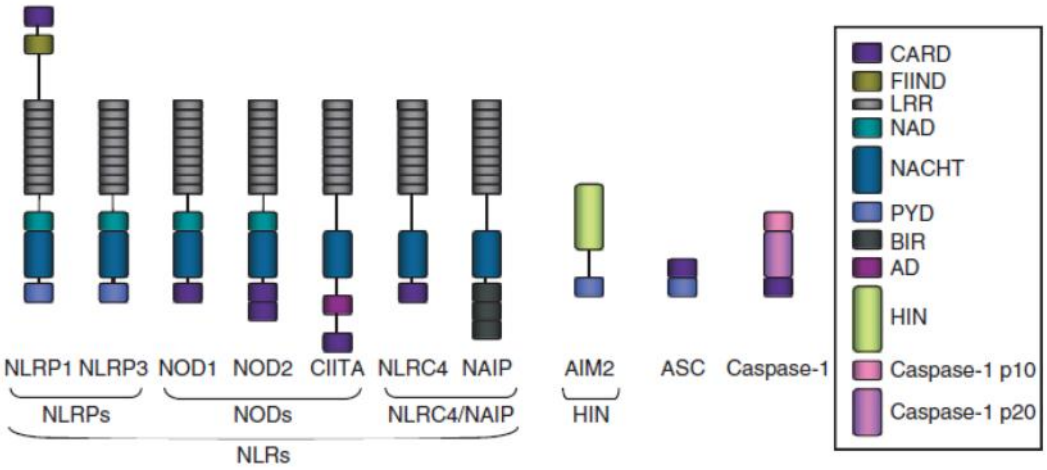

Figure 1.7 Schematic representation of the NLR and HIN families of receptors.

The NLRs can be divided into three subgroups: NLRPs, NODs and NLRC4/NAIP. They share a typical tripartite structure with an effector domain, which can be either a pyrin domain (PYD), a caspase recruitment domain (CARD) or a baculovirus IAP repeat (BIR) domain], the central NACHT [NAIP (NLR family, apoptosis inhibitory protein), CIITA (class II, major histocompatibility complex, transactivator), HET-E (plant het gene product involved in vegetative incompatibility) and TP-1 (telomerase-associated protein 1)] domain and the C-terminal LRR. The majority of the NLRs also contain a NACHT-associated domain (NAD). Absent in melanoma 2 (AIM2), which belongs to the haematopoietic interferon-inducible nuclear protein (HIN) family of proteins, is characterized by an N-terminal PYD and a C-terminal HIN domain. The adaptor protein apoptosis speck protein with CARD (ASC) is also represented and consists of a PYD and a CARD domain, the further being fundamental for homotypic CARD–CARD interactions with caspase-1. Figure adapted from (Skeldon & Saleh, 2011).

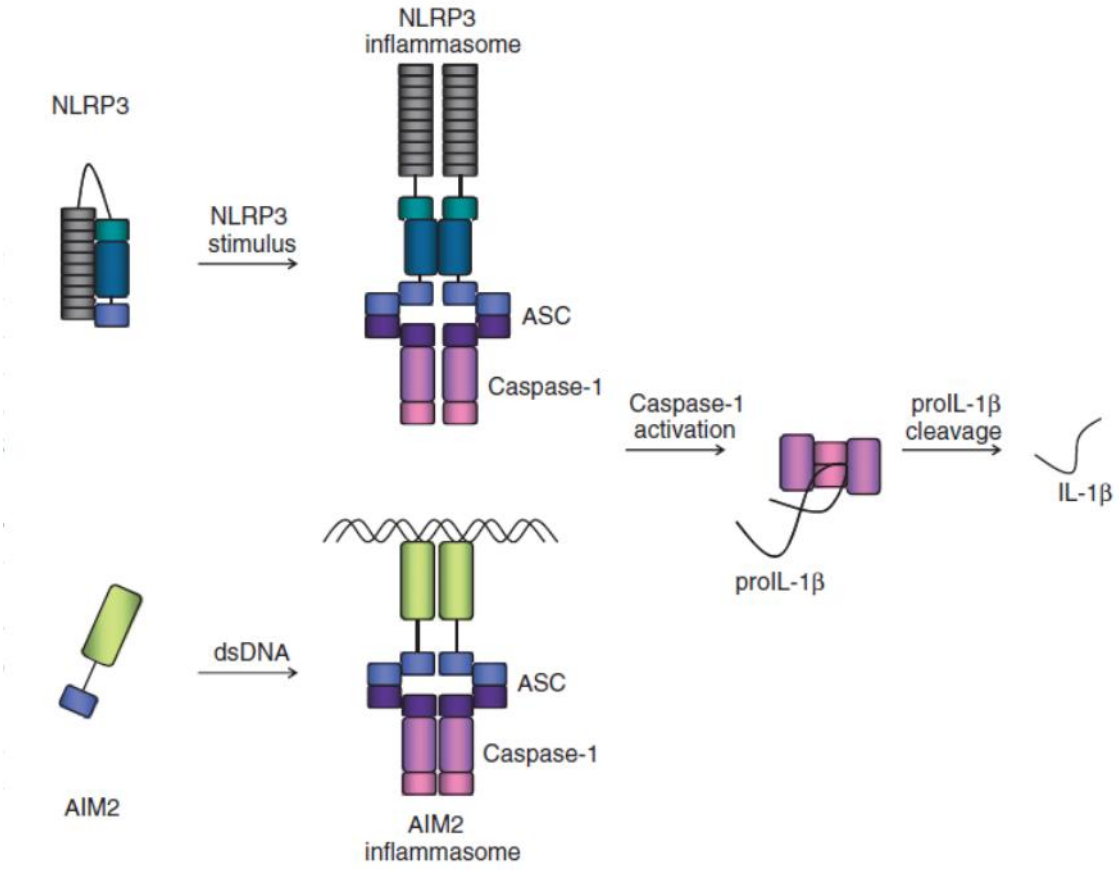

Figure 1.8 Schematic representation of the NLRP3 and AIM2 inflammasome complexes.

In response to a stimulus, NLRP3 changes conformation to expose its NACHT domain, recruits and binds the adaptor protein apoptosis speck protein with CARD (ASC) via a PYD–PYD interaction. ASC, in turn, interacts with caspase1 through its CARD domain. AIM2 is thought to oligomerize and form its complex around its ligand double-stranded (ds) DNA directly. Once recruited within the inflammasome complex, caspase-1 is activated through autoproteolytic cleavage and can then process its substrates, such as IL-1β. Figure adapted from (Skeldon & Saleh, 2011).

1.13 ROLE OF THE NLRP3 INFLAMMASOME IN HUMAN DISEASES

The NLRP3 inflammasome has been implicated in the pathogenesis of several human inflammatory diseases (Schroder & Tschopp, 2010). Point mutations targeting the NACHT domain of the NLRP3 protein have been identified as the cause of a group of inflammatory disorders known as the cryopyrin-associated periodic syndromes (CAPS) (Conforti-Andreoni, Ricciardi-Castagnoli, & Mortellaro, 2011). These include: the familial cold autoinflammatory syndrome (FCAS), the Muckle–Wells syndrome (MWS) and the neonatal onset multi-systemic inflammatory disease/chronic infantile neurological cutaneous articular syndrome (NOMID/CINCA) (Aganna et al., 2002). These cryopyrinopathies were once thought to be distinct conditions but now are used to describe different grades of disease severity (Yu & Leslie, 2011). Clinically, they are characterized by recurrent fevers, urticarial-like skin rashes, joint and ocular symptoms, amyloidosis and, in the case of NOMID/CINCA, severe neurological complications (Hoffman, 2009). In all three phenotypes of CAPS, there is a gain-of-function mutation of the NLRP3 gene which results in a constitutive activation of the NLRP3 inflammasome and overproduction of IL-1β (Agostini et al., 2004). This was also confirmed in in vitro studies that have demonstrated that monocytes and macrophages isolated from patients with MWS were able to spontaneously release high levels of IL-1β in the absence of any stimuli (Agostini et al., 2004). These observations provided a convincing rationale for the use of the recombinant form of the naturally occurring IL-1 receptor antagonist (IL-1Ra), Anakinra, which has been proved to be extremely successful in the treatment of these patients resulting in a complete cessation of clinical symptoms and biochemical changes within hours of administration (Hawkins, Lachmann, & McDermott, 2003). The NLRP3 inflammasome has been implicated in the pathogenesis of several additional autoinflammatory syndromes aside from CAPS incliding: Familial Mediterranean fever (FMF), pyogenic arthritis, pyoderma

gangrenosum and acne (PAPA) syndrome (Masters, Simon, Aksentijevich, & Kastner, 2009). FMF and and pyogenic arthritis are caused by mutations in the gene encoding for pyrin, while PAPA syndrome is due to a mutation in the gene that encodes for PSTPIP1 (proline-serine-threonine phosphatase interacting protein 1), a protein that directly interacts with pyrin. The interaction between PSTPIP1 and pyrin has been suggested to be very important for the regulation of the NLRP3 activation (Waite et al., 2009). FMF is an autosomal recessive disease characterized by recurrent episodes of fever associated with severe abdominal pain, pleuritic chest pain, arthritis and a skin rash (Wise, Bennett, Pascual, Gillum, & Bowcock, 2000). The PAPA syndrome is inherited in a dominant manner, and characterized by painful flares of recurrent sterile arthritis coupled to skin manifestations such as pyoderma gangrenosum and acne (Lindor, Arsenault, Solomon, Seidman, & McEvoy, 1997). IL-1 antagonism has proved to be an effective treatment for both conditions as in CAPS (Brenner, Ruzicka, Plewig, Thomas, & Herzer, 2009; Belkhir et al., 2007). More recently, the NLRP3 inflammasome has been implicated in the development of major diseases such as gout, type 2 diabetes and obesity-induced insulin resistance (Kingsbury, Conaghan, & McDermott, 2011; Choi & Nakahira, 2011) and many other studies are currently exploring the role of this complex system in several human diseases.

Table 1.3 Clinical characteristics of cryopyrinopathies.

Feature	FCAS	MWS	CINCA (NOMID)
Inheritance	Autosomal-dominant	Autosomal-dominant (typical) Or de novo (rare)	De novo (typical) Or autosomal-dominant (rare)
Severity	Low	Medium	High
Frequency of fever and/ or rash	Usually daily symptoms with circadian rhythm	Variable: rare to daily symptoms with circadian rhythm	Variable: usually rare fever with daily rash
Joint involvement	Arthralgia	Arthralgia, arthritis	Arthralgia, arthritis, overgrowth arthropathy
Neurological involvement	none	none	Chronic aseptic meningitis (headache, possible mental delay)
Eye involvement	Conjunctivitis	Conjunctivitis, uveitis	Uveitis, papillary edema, possible optic neuritis
Deafness	No	Frequent (60-70%)	Frequent (>60%)
Amyloidosis	No	Frequent (~25%)	Frequent (~25%)

Cryopyrinopathies are a group of rare autoinflammatory diseases characterized by a mutation in the gene that encodes for NLRP3. They include: the familial cold autoinflammatory syndrome (FCAS), the Muckle–Wells syndrome (MWS) and the chronic infantile neurologic cutaneous articular syndrome (also termed neonatal-onset multisystemic inflammatory disease) (CINCA/NOMID). They were initially considered different disease entities but are now recognized as different phenotypes of the same disease. Table adapted from the following article:"Cryopyrinopathies: update on pathogenesis and treatment" (Neven, Prieur, & Quartier dit, 2008).

1.14 ROLE OF P2X7R IN EXPERIMENTAL AND HUMAN GLOMERULONEPHRITIS

Glomerulonephritis (GN) represents still a leading cause of end-stage renal disease and its current treatment relies on non-specific and toxic immunosuppression which may lead to severe side effects, including life-threatening sepsis and reduced fertility (Tam, 2006). GN is characterised by inflammation and cell proliferation in the glomerulus, although injury typically extends to the renal tubules, interstitium and vasculature (Hricik, Chung-Park, & Sedor, 1998). Animal models of glomerulonephritis have been extremely useful to understand the pathogenesis of this disease. It is now well established that most cases of glomerulonephritis are secondary to an immunological response to a variety of endogenous and exogenous antigens. Deposition of antibodies against these antigens, in turn, activates a number of biological responses such as complement activation, leukocytes recruitment, cytokine release that result in glomerular inflammation and injury (Couser, 1999). The involvement of proinflammatory cytokines such as IL-1β, MCP-1 and TNF-α in the pathogenesis of most forms of glomerulonephritis is well documented in literature and treatments with either IL-1β receptor antagonist or TNF-α inhibitor have been found to be effective in reducing the severity of the disease in animal models of GN (Lan, Nikolic-Paterson, Zarama, Vannice, & Atkins, 1993; Karkar, Smith, & Pusey, 2001). P2X7R is not expressed or expressed at a very low level in normal kidney tissue (Hillman, Burnstock, & Unwin, 2005); cultured mesangial cells express the receptor when stimulated with TNF-α (Harada, Chan, Loesch, Unwin, & Burnstock, 2000) while in podocytes and in renal tubular cells an upregulation of the receptor has been shown under diseased conditions (Vonend et al., 2004; Turner et al., 2007). P2X7R expression in renal diseases was first described in a rat model of hypertension and diabete mellitus (Vonend et al., 2004). In their study, Vonend et al. showed that P2X7R was poorly expressed in normal rat

glomeruli, while a significant increase in P2X7R expression was detectable at 12 weeks in a rat transgenic model of renin-dependent hypertension. A significant increase of glomerular P2X7R expression was also observed at 6 and 9 weeks in rats with streptozotocin-induced diabetes. The role of P2X7R and TGF-β in fibrosis was investigated in a mouse model of unilateral ureteral obstruction (UUO) (Goncalves et al., 2006). Goncalves et al. demonstrated that both the myofibroblast accumulation and collagen deposition were markedly reduced in P2X7 deficient mice compared with the WT ones in the UUO model. In this model, P2X7R was expressed only in tubular epithelial cells at day 7 of UUO WT mice. P2X7R expression appears to be significantly increased in both rat and mouse glomeruli in the animal model of accelerated nephrotoxic nephritis as well as in patients with lupus glomerulonephritis (Turner et al., 2007) suggesting an important role of this receptor in the pathogenesis of this disease. Furthermore, it has been reported that P2X7 deficient mice develop a much less severe glomerulonephritis when injected with nephrotoxic globulin compared to the wild type mice in terms of a reduced glomerular macrophage infiltration, glomerular thrombosis, proteinuria and improved renal function (Taylor et al., 2009). Similarly, pharmacologic inhibition of P2X7R using the antagonist A-438079 has been shown to prevent the development of NTN in rats injected with nephrotoxic serum (Taylor et al., 2009). These studies demonstrated that there is increased renal P2X7R expression in glomerulonephritis and that P2X7R has a role in mediating renal inflammation representing therefore a potential target for the treatment of glomerulonephritis.

1.15 THE RAT MODEL OF NEPHROTOXIC NEPHRITIS

The first animal model of glomerulonephritis has been established in 1900 by Lindeman who injected rabbits with heterologous antiserum to rabbit kidney raised in guinea pigs (Hoedemaeker & Weening, 1989). Since then, several animal models of glomerulonephritis have been developed. A reproducible model of crescentic glomerulonephritis characterized by acute glomerular inflammation and subsequent glomerulosclerosis and tubule-interstitial scarring leading to renal failure has been described by several research groups (Fujinaka et al., 1997; Tam et al., 1999). The principal method to induce crescentic glomerulonephritis (CRGN) in animals is the injection of a heterologous antibody raised against a preparation of glomerular antigen (Tam et al., 1999). The binding of the heterologous antibody to the glomerular basement membrane generates an acute injury which is followed by a second phase of injury in which there is an autologous immune response against the heterologous antibody (Sheerin, Springall, Abe, & Sacks, 2001). In the accelerated model of nephrotoxic nephritis this second phase is accelerated by preimmunization of animals with heterologous immunoglobulin (Sato et al., 1993). In the rat model of NTN described by Tam et al., glomerulonephritis is induced in Wistar Kyoto rats by a single intravenous injection of 0.1 ml rabbit antiglomerular basement membrane antiserum. At day four from the injection of nephrotoxic serum, rats develop albuminuria and glomerular fibrinoid necrosis can be seen in kidney histology preparations. By day eleven at least 60% of glomeruli show the presence of cellular crescents. By six weeks, rats develop renal failure with more than 90% of glomeruli showing glomerulosclerosis.

Strain susceptibility to nephrotoxic nephritis

One of the most interesting features of the rat NTN model is that WKY rats are uniquely susceptible to NTN, developing progressive proteinuria and proliferative necrotising crescentic glomerulonephritis at doses of NTS that are sub-nephritogenic in the other rat strains such as Lewis, Wistar and Brown Norway (Kawasaki, Yaoita, Yamamoto, & Kihara, 1992). The unique susceptibility demonstrated by the WKY rat compared to the Lewis rat, with which it shares the same MHC haplotype, along with the highly reproducible nature of the NTN model led to the study of its underlying genetic determinants (Aitman et al., 2006). The F1 cross performed between the WKY and Lewis rats had intermediate phenotypes for Crgn disease including crescent formation, proteinuria and macrophage infiltration whilst the F2 generation demonstrated phenotypes that spanned the whole range of the phenotypes observed in the WKY and Lewis parental strains (Aitman et al., 2006). Analysis in the F2 rats demonstrated that crescent formation was highly correlated with proteinuria and macrophage infiltration and all the phenotypes were highly heritable (Behmoaras et al., 2010). The genome screen performed for NTN susceptibility loci in the F2 generation found two major quantitative trait loci (QTL) on chromosomes 13 and 16 which were designated as crescentic glomerulonephritis 1 (Crgn1) and 2 (Crgn2) (Behmoaras et al., 2010). Both loci were linked to crescent formation and proteinuria (with highly significant logarithm of odds (LOD) scores 7.4-9.1) and infiltration of macrophages was linked to Crgn1. A further 5 loci (Crgn3-7) were also identified with LOD scores > 3. Haplotype mapping was used to positionally clone Fcgr3 as the candidate gene for Crgn1. In the WKY rat, deletion of the rat-specific Fcgr3 paralogue, Fcgr3-related sequence (Fcgr3-rs) was identified as the molecular basis for the QTL whilst in humans, low copy number of FCGR3B, an orthologue of rat Fcgr3, was associated with glomerulonephritis (Aitman et al., 2006). In order to map candidate genes responsible for the phenotype controlled by the QTL and to

characterize the biology of the QTL genes, Behmoaras et al have generated congenic strains. Congenic strains are new inbred strains generated by backcrossing one strain onto another to produce a rat with a particular genomic region from one strain whilst the remainder of its genome is from the other (Markel et al., 1997). The congenic lines for Crgn2 were generated by backcrossing (WKYxLEW) F1 rats onto the recipient WKY or LEW parental strains for nine generations (Behmoaras et al., 2010). As shown in figure 1.10, induction of nephrotoxic nephritis in WKY.LCrgn1 and WKY.LCrgn2 rats, generated by introgression of Crgn1 or Crgn2 respectively from the non-susceptible Lewis strain onto the WKY background produced markedly fewer glomerular crescents compared to control animals. Bone marrow transplant experiments demonstrated that susceptibility to crescent formation can be transferred by bone marrow cells. Indeed, Lewis rats that receive WKY bone marrow develop crescents but fewer compared to WKY rats receiving isologous bone marrow (Smith et al., 2007). It has been also shown however that not only circulating cells but also intrinsic renal cells contribute to this susceptibility as demonstrated by kidney transplant experiments. When kidneys were transplanted from WKY to LEW rats and vice versa, acute rejection occurred despite the shared MHC haplotype between the strains. F1 rats derived from crossing WKY with LEW exhibit an intermediate susceptibility phenotype to NTN and transplants from the parental strains into the F1 rat were successful with no rejection seen (Smith et al., 2007). In the analysis of these transplants, the severity of disease in the transplanted kidney was compared with the native kidney to mitigate the effects of the transplantation process. These results found that following the injection of NTS, LEW kidneys developed Crgn when transplanted into the F1 rats. However the severity relative to native kidneys was less than that of transplanted WKY kidneys indicating that the kidney itself contributed to susceptibility to Crgn (Smith et al., 2007). If susceptibility was mediated just by circulating cells, the degree of disease should have been the

same whether a LEW or WKY kidney was transplanted into the F1 rats. The data therefore showed that whilst bone marrow derived cells do make the major contributions to disease; the susceptibility to Crgn is not solely dependent upon them (Smith et al., 2007).

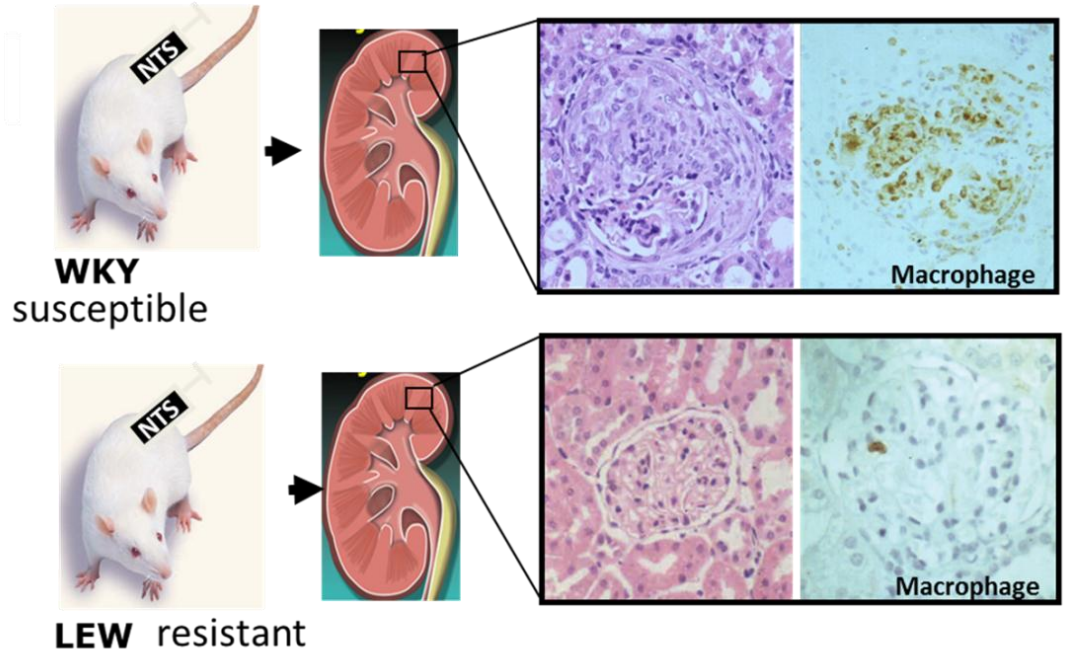

Figure 1.9 Renal histology in WKY and LEW rats at day 10 from NTS injection.

Injection of a small dose of nephrotoxic serum in WKY rats induces a rapid onset of nephrotoxic nephritis with presence of crescents in 80% of glomeruli at day 10. The same dose of NTS induces only mild glomerular hypercellularity with no crescents in Lewis rats. Macrophages infiltration is shown by immunohistochemistry using ED-1 monoclonal antibody.

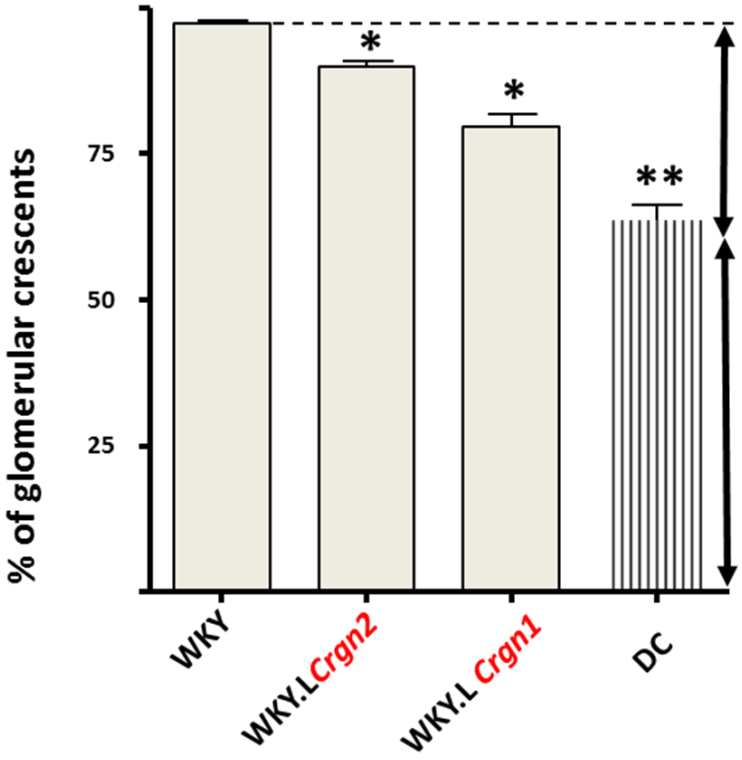

Figure 1.10 Percentage of glomerular crescents in single and double congenic strains in comparison with parental WKY rats.

Introgression of Lew Crgn2 into the WKY recipients reduces by 8% the number of crescents; introgression of Crgn1 leads to a reduction of 18%, while the introgression of both Crgn1 and Crgn2 has a synergistic effect with a reduction by 34% of glomerular crescents. Figure adapted from the following article: ”Genetic Loci Modulate Macrophage Activity and Glomerular Damage in Experimental Glomerulonephritis” (Behmoaras et al., 2010).

1.16 ROLE OF BONE MARROW DERIVED MACROPHAGES IN CRESCENTIC GLOMERULONEPHRITIS

Macrophages are known to play a central role in the pathophysiology of crescentic glomerulonephritis (Cook et al., 1999). Indeed, monocytes/macrophages represent the major cell type in the glomerular infiltrate and macrophage depletion studies have shown that the accumulation correlates with the degree of histological and functional injury (Nikolic-Paterson & Atkins, 2001). As previously discussed, bone marrow transplant experiments have demonstrated that the susceptibility to crescent formation can be transferred, so that the glomerulonephritis resistant rats Lewis that receive WKY bone marrow develop crescents but fewer compared to WKY rats receiving autologous bone marrow (Smith et al., 2007). Macrophages migrate into the inflamed glomerulus and once activated, release proinflammatory cytokines, reactive oxygen species and proteases that disrupt the integrity of the glomerular basement membrane and finally lead to fibrin deposition (Lai et al., 2001). Macrophages display different phenotypes that can switch in response to their micro-environment (Stout et al., 2005). It has been proposed by many researchers that macrophages develop into two major functional subsets that display inflammatory versus anti-inflammatory patterns of function in association with Th1 or Th2 driven responses respectively (Goerdt et al., 1999). This finding is very important because it means that is not only the number of macrophages influences the progression of the disease but also their phenotypic properties. Defining these phenotypic variants and how they may be induced could be extremely important in altering the outcome of experimental and human glomerulonephritis (Chavele et al., 2010).

1.17 PROJECT AIMS

Given that P2X7R is thought to play an important role in glomerulonephritis, understanding the cell signalling cascade following P2X7R activation and the role of P2X7-mediated inflammasome activation in the pathogenesis of the disease can be relevant to identify new mechanisms of disease progression and new potential therapeutic targets. Thus, my key hypothesis is that P2X7R and the NLRP3 inflammasome activation are critical in the pathogenesis of glomerulonephritis. The study of the P2X7R mediated cytokine production and cell signalling cascade will provide a deeper understanding of the mechanisms relevant to the hypothesis.

Specific project aims:

1. To study and compare the processing and release of IL-1β and IL-18 in response to P2X7R agonists in macrophages from WT and P2X7 deficient mice.
2. To characterize the cell signalling pathways that are switched on in response to ATP stimulation in macrophages from WT and P2X7 deficient mice.
3. To analyse and compare the expression of inflammasome genes and downstream activities in macrophages from glomerulonephritis-susceptible (WKY) and glomerulonephritis-resistant (LEW) rats.
4. To identify a genetic link between inflammasome activation and disease severity in the rat model of nephrotoxic nephritis.

CHAPTER TWO-MATHERIALS AND METHODS

2.1 P2X7 DEFICIENT AND CONTROL MICE

Mice used in the experiments described in this thesis were housed in the Biological Services Unit at Hammersmith Hospital. Mice were kept in a standard animal house environment and experiments were performed according to institutional and Home Office guidelines. Experimental groups were matched for age, gender and strain. Two to three-month old male wild-type (WT) and P2X7 receptor knockout mice (P2X7−/−) both from GlaxoSmithKline (GSK) and from Pfizer were sacrificed by CO_2 asphyxiation in accordance with local institutional guidelines. Homozygous P2X7 receptor deficient mice were bred on a background of C57BL/6 for at least 7 generations. The Pfizer P2X7 knock out line was purchased from the Jackson laboratory, while the GSK line was a kind gift from the company (Chessell et al., 2005b). Genomic DNA was isolated from the tails of WT and P2X7−/− animals, and the genotypes were confirmed by PCR analysis.

2.2 WKY, SINGLE CONGENIC, DOUBLE CONGENIC AND LEWIS RAT STRAINS

Wistar Kyoto (WKY) and Lewis (LEW) rats were purchased from Charles River (Margate, UK). Congenic strains are new inbred strains generated by backcrossing one strain onto another to produce a rat with a particular genomic region from one strain whilst the remainder of its genome is from the other. The double-congenic line, a single strain in which both Crgn1 and Crgn2 were introgressed from Lewis rats on the WKY genetic background, was previously

constructed by Dr Behmoaras et al. as follows: WKY.LCrgn1 and WKY.LCrgn2 strains were crossed to produce an F1 generation. The F1 rats were backcrossed with WKY.LCrgn1. The F2 rats heterozygous for Crgn2 and homozygous for Crgn1 were crossed by brother–sister mating to obtain an F3 generation double congenic for LEW Crgn1 and LEW Crgn2 on a WKY background. The single congenic line WL16 was generated by introgression of Crgn2 from Lewis rats onto a WKY genetic background, while the single congenic strain LW16 was created by introgression of Crgn2 from WKY rats onto a Lewis background (Behmoaras et al., 2008; Behmoaras et al., 2010).

2.3 PREPARATION OF MURINE AND RAT BONE MARROW DERIVED MACROPHAGES

After sacrifice, whole mice or rats were soaked in 100% ethanol and taken to the tissue culture hood. Femurs and tibiae were isolated and cleaned from hair and soft tissues, both ends of the cleaned bones were then cut and bone marrow cells were flushed out with a 20 gauge needle using 10 mL of cold Hanks buffer and collected into a 50 mL centrifuge tube. Cells were then spinned down at 1500 rpm (300 x g) for five minutes at 4^0C and resuspended in 10 mL Hanks buffer. The 50 mL centrifuge tube was then placed in the CO_2 incubator in a horizontal position for 10 minutes to hypotonically lyse the red blood cells. After that, cells were centrifuged again at 1500 rpm (300 x g) for 5 minutes, the supernatant was aspirated and the cell pellet was resuspended in DMEM (Invitrogen, UK) culture medium containing 25 mM Hepes, 25% L929 cell line conditioned medium, 25% FBS, 2 mM L-glutamine, 100 IU/mL penicillin and 100 µg/mL streptomycin. The L929 conditioned medium, rich in Macrophage Colony Stimulating Factor (M-CSF) was prepared by culturing the L929 cell line, a murine fibroblast cell line available in the lab, in DMEM supplemented with 10% FBS, 2

mM L-glutamine, 100 IU penicillin and 100 µg/mL streptomycin. The bone marrow cells were then cultured in T150 tissue culture flasks for 5 days. At day 5, cells were removed from the flasks after 30 minutes- one hour incubation with cell dissociation buffer, counted with a hemocytometer and $1x10^6$ cells were plated into each well of a 6 well plate containing 2 mL of pre-warmed full culture medium. Cells were left to adhere overnight and on day 6 the full culture medium was replaced with serum free DMEM prior to any stimulations.

2.4 STIMULATION OF BONE MARROW DERIVED MACROPHAGES

In order to analyse the secretion of IL-1β and IL-18, both murine and rat bone marrow derived macrophages after five days of differentiation in L929 medium, were non-enzymatically detached by cell dissociation buffer (Invitrogen, UK) and counted on a haemocytometer. Macrophages were then plated into six-well plates at a density of 1×10^6 cells per well in complete L929 conditioned medium (3 ml per well) and incubated at 37^0 C overnight to let them adhere. On day 6 of differentiation, the medium was aspirated and macrophages were primed for five hours, unless differently specified, with Lipopolysaccharides from Escherichia Coli purified by phenol extraction (LPS) (Sigma, UK) used at a concentration of 1 µg/mL in serum free DMEM supplemented with 100 IU of penicillin and 100 µg/mL of streptomycin. After LPS priming, the medium was aspirated, cells were washed with HBSS and fresh serum free medium containing ATP at a concentration of 5 mM was added. After thirty minutes of ATP stimulation, both culture medium and cell layers were collected by scraping and samples were then stored at -20^0C. To evaluate the effects of ATP stimulation on the phosphorylation of proteins, macrophages at day 5 of differentiation, were

detached by cell dissociation buffer and counted using a haemocytometer. For Western blotting detection of phosphorylated proteins, about one million cells per well were seeded into six-well plates in complete L929 conditioned medium and incubated at 37^0C for 24 hours. The day before the stimulation with ATP, macrophages were serum starved overnight using DMEM supplemented with 100 IU of penicillin and 100 µg/mL of streptomycin. Prior to ATP stimulation, the medium was aspirated, cells were washed once with 1 ml of pre-warmed HBSS and 1 ml of serum free medium containing ATP at a concentration of 5 mM was added. At the end of ATP stimulation cell lysates were prepared as described in the Western blotting section. When P2X7R antagonist was used, it was added in the medium together with ATP at a concentration of 3 µM.

2.5 ISOLATION AND CULTURE OF RAT NEPHRITIC GLOMERULI

Glomeruli were isolated sequentially using stainless steel meshes of the following pore sizes: 250, 150 and 75 µm. A wash solution of cold 1 x PBS was used. With this process, connective tissue and tubular fragments are retained by the first two sieves, whereas glomeruli are retained by the final sieve. Using a Pasteur pipette and small amounts of buffered saline, glomeruli were collected from the final sieve by repeated rinsing and aspiration, followed by centrifugation at 1500 rpm for 5 minutes, and suspension of the glomerular pellet in DMEM supplemented with penicillin and streptomycin. Glomerular yield was determined by counting the number of glomeruli in three separate 10 µl samples of each preparation under the light microscope at × 100 power. A number of 1 x 10^4 glomeruli were seeded into each well of a six-well plate using one ml of DMEM per well. After 48 hours of incubation at 37^0C, supernatants and cell layers were collected and stored at -20^0C for future analysis.

2.6 INDUCTION OF NEPHROTOXIC NEPHRITIS IN RATS

Nephrotoxic nephritis (NTN) was induced in male rats weighing 200-250 g by a single intravenous injection of 0.1 ml of nephrotoxic serum (rabbit anti-rat GBM anti-serum). Four days after nephrotoxic serum injection, rats were sacrificed and kidneys were removed for glomeruli isolation. The nephrotoxic serum injection is known to cause a rapid influx of monocytes/macrophages into glomeruli within hours of administration, followed by segmental fibrinoid necrosis by day 4. This is a well-chatacterized model with the onset of detectable proteinuria and maximal macrophage infiltration of glomeruli occurring 4 days after the nephrotoxic serum injection (Tam et al., 1999).

2.7 RNA EXTRACTION AND qRT-PCR

2.7.1 Extraction of RNA

Precautions against contaminating samples with RNAses were observed. The bench working area was wiped with RNAse Zap (Ambion Ltd., UK), disposable gloves were worn at all times and sterile disposable plasticwear and pipettes reserved for RNA work only were used. Total RNA was extracted from macrophages or isolated glomeruli using Trizol/chloroform extraction and isopropyl alcohol precipitation. After the required time of incubation in the presence or absence of a stimulus, cell culture medium was removed by aspiration and about 1 x 10^6 cells were resuspended in 1 ml of Trizol (Invitrogen Ltd., Renfrew, UK) and passed through a pipette several times to ensure a homogeneous suspension. Two hundred microliters of chloroform were added

and the samples were mixed thoroughly, incubated for 3 minutes at room temperature and then centrifuged at 12000 x g for 15 minutes at 4^0C. After centrifugation, the upper aqueous phase containing the RNA was removed to a separate clean tube and the lower organic phase was discarded. RNA was precipitated from the aqueous phase by addition of 500 µl of isopropyl alcohol (Sigma-Aldrich Co., Ltd., Poole, UK), incubated at room temperature for 10 minutes and then centrifuged at 12000 x g for 10 minutes (4^0C). The resulting RNA pellet was washed with 75% ethanol and centrifuged at 7500 x g for 5 minutes (4^0C). The final pellet was air dried and resuspended in RNAse free distilled water (Promega UK Ltd., Southampton, UK). RNA concentration and purity were determined by measuring the absorbance of RNA in water at 260 nm using a spectrophotometer (Beckman DU 650 Spectrophotometer, High Wickam, Bucks, UK). RNA concentration was calculated using the formula A_{260} * 40 = µg RNA/ml. In distilled water, the RNA had an $A_{260/280}$ ratio of 1.9-2.1 indicating RNA free of contamination. RNA samples were stored at -80^0C until further use.

2.7.2 Synthesis of copy DNA (cDNA)

One µg of total RNA was reverse transcribed with 0.5 µg oligo(dt) 12-18 primer and a first strand cDNA synthesis kit, Superscript II RNase H^- reverse transcriptase (Invitrogen Ltd., Renfrew, UK). The reaction buffer contained 20 mM Tris-HCl (pH 8.4), 50 mM KCl, 500 µM each of dATP, dCTP, dGTP, dTTP, 5 mM Dithiothreitol, 40 units of RNaseOUT™ Recombinant Ribonuclease Inhibitor and 50 units of superscript™ reverse transcriptase in a 20 µl reaction volume. The reaction was incubated for 50 minutes at 42^0C in a Hybaid sprint thermocycler (Thermo Electron Molecular Biology, USA). To inactivate the RT enzyme, samples were heated to 70^0C for 10 minutes, storage was at -20^0C.

2.7.3 Real-time PCR amplification

The resulting cDNA transcripts were used for PCR amplification using the Roche Lightcycler (Roche diagnostics, Penzberg, Germany) and QuantiTect SYBR Green PCR kit (Qiagen, Crawley, UK). QuantiTect SYBR Green I PCR master mix contains SYBR Green I, HotStarTaq DNA Polymerase and a dNTP mix (including dUTP). SYBR Green I, present in the PCR mix, only emits light when bound to double-stranded DNA and once bound, it is excited at 494 nm and emits light at 521 nm. The lightcycler fluorimeter monitors emissions at 521 nm and values are recorded by a computer (Dell Computers, Bracknell, UK). Each PCR reaction mix contained 1 µl cDNA template, 5 pmol forward and 5 pmol reverse primers, 10 µl of 2x QuantiTect SYBR Green I PCR master mix and distilled water to a final volume of 20 µl. Primer sequences are indicated in Table 2. The PCR cycling conditions were initial denaturation at 95^0C for 15 minutes, denaturation at 94^0C for 15 seconds, annealing at 60^0C for 20 seconds and extension at 72^0C for 30 seconds. The temperature of fluorescence acquisition was set at 78^0C for 5 seconds, 20^0C below the product melting temperature. The product melting temperature was determined in a test run by examining the melting curve. All experiments were performed in duplicate and for each sample the gene of interest and the control gene were run in parallel. A ratio of relative abundance of the gene of interest to the constitutively expressed gene hypoxanthine phosphoribosyl transferase (HPRT) was calculated by the Lightcycler Relative Quantification Software version 1.0 (RelQuant) (Roche Diagnostics, Penzberg, Germany). HPRT was chosen as a control gene for the quantification of P2X7 mRNA levels because its expression level is similar to P2X7 gene. In other reactions the house keeping gene glyceraldehyde-3-phosphate dehydrogenase (GAPDH) was used as control gene. After completion of the PCR amplification cycles, a melting curve was determined for each PCR product. Each double-stranded DNA has its own melting temperature (Tm) based on the strand length

and the G-C content. Therefore melting curve analysis can be used to identify unwanted by-products of the PCR reaction such as primer dimers. A melting curve is produced by plotting fluorescence against temperature. The PCR products were heated to 65^0C and then the temperature was increased slowly (0.5^0C per second) whilst fluorescence was continually monitored. At low temperatures all DNA is double-stranded, SYBR Green I is binding and fluorescence is maximal. As the temperature increases, DNA products are denaturated and the fluorescence decreases. Primer dimers and other short non-specific products can be distinguished because they usually melt at lower temperatures than the desired product.

2.74 Agarose gel electrophoresis

Agarose gel electrophoresis of PCR amplified DNA samples was performed in electrophoresis tanks with 1xTAE buffer used as the gel and running buffer. Gels were prepared by heating 100ml of 1xTAE buffer with 1.5-2% agarose added until the agarose was dissolved. Following cooling in running water, 1ìl of ethidium bromide was added to the agarose-1xTAE buffer mix and the mixture poured into a gel mould. DNA samples were mixed using 2ìl Orange G per 10ìl PCR product and loaded into the agarose gel. A 2-log ladder (New England Biolabs) was used as a DNA size standard. The samples were electrophoresed at 120V for 1 hour and the gels visualised on an ultra-violet transilluminator (Bio-Rad, Hemel Hempstead, Hertfordshire, UK) and photographed using the gel doc system (Bio-Rad).

Table 2 Primer sequences used for qPCR.

Gene	Forward primer	Reverse primer
IL-1b	CTTTTCTGTGTGATGCCCCT	GTGAAGATGGTGTTTGGGCT
IL-18	ACCGCAGTAATACGGAGCAT	TAGGGTCACAGCCAGTCCTC
IL-18 bp	ATGAGACACTGTGGCTGTGC	ACTGCTGGAGACCAGGAAGA
Pyrin (ASC)	GCAATGTGCTGACTGAAGGA	TGTTCCAGGTCTGTCACCAA
Caspase-1	GGAGGGAATATGTGGGATCA	CCCTCTTCGGAGTTCCCTAC
P2RX7	GTGCCATTCTGACCAGGGTTGTATAAA	GCCACCTCTGTAAAGTTCTCTCCGATT
MMP-9	TTATTGTGAGCATCCCTAGGG	AGTGTCCGAGGAAGATACTTG
HPRT	GCTACCTGCTGGATTACATTA	CCACTTTCGCTGATGACACAA
GAPDH	GCCATCAATGACCCCTTCAT	GAGGGGGCAGAGATGATGAC

2.8 WESTERN BLOTTING

2.8.1 Cell lysate preparation

Lysis buffer was prepared as follows: 10 mM Tris-HCl pH 7.6, 5mM EDTA, 50 mM NaCl, 30 mM sodium pyrophosphate, 50 mM NaF, 100 µM Na3VO4, 1% Triton-X100, 1 mM phenylmethylsulfonyl fluoride. Immediately before use, 1 µg/ml pepstatin, 2 µg/ml aprotinin, 5 µg/ml leupeptin and 5 µg/ml antipain were added. The cell monolayer was then washed once with cold 1xPBS and lysis buffer was added; cells were scraped and transferred to an eppendorf tube and left on ice for twenty minutes to ensure complete lysis of the cells. Lysates were then clarified by centrifugation (13,500 g, 20 minutes) and the supernatants were transferred to fresh tubes and stored at -20^{0}C. To analyse excreted proteins, cells were scraped and both cells and supernatant were collected and stored at -20 ^{0}C. The supernatant containing the cells was then filtered using Amicon ultra centrifugal filters for protein purification and concentration (Millipore) and the concentrated sample was collected and stored at -20^{0}C. The concentration of protein in cell lysates was measured using the BCA TM Protein assay kit (Pierce) following the manufacturer's instructions.

2.8.2 Electrophoresis, transfer and developing

Cell lysates were diluted with 5x sample buffer containing 200 mM Tris-HCl, 6% SDS, 2mM EDTA, 4% 2- Mercaptoethanol, 10% glycerol and boiled for 10 minutes. The samples were then resolved by SDS polyacrylamide gel electrophoresis (PAGE). Seven percent resolving gels were prepared to detect proteins with a high molecular weight, such as mTOR. Fifteen percent resolving

gels were used to detect proteins with a low molecular weight, such as cleaved IL-1β and cleaved caspase 1. On the basis of the percentage of the running gel selected, gels were prepared using varying volumes of the following components: distilled water, 1.5M Tris-HCl solution, pH 8.8, 30% acrylamide/bisacrylamide solution, 10% Sodium dodecyl sulphate (SDS), 10% APS and tetramethylethylenediamine (TEMED). When the resolving gel had polymerized, the stacking gel (5%) was prepared using the following components: distilled water, 1 M Tris-HCl solution, pH 6.8, 30% acrylamide/bisacrylamide solution, 10% Sodium dodecyl sulphate (SDS), 10% APS and tetramethylethylenediamine (TEMED). SDS-PAGE electrophoresis was carried out at 100V using the following running buffer: (0.025M Tris, 0.192 M glycine, 0.1% SDS). Transfer of protein from SDS- PAGE gel onto polyvinylidene difluoride (PVDF) membrane was carried out using cold 1x transfer buffer (48 mM Tris, 412 µM Glycine, 0.03% SDS and 0.1% Methanol) at 100 V for 1 hour. Membranes were then blocked for 1 hour with 5% skimmed dry milk prepared in TBS containing 0.1% Tween-20 (TBST, pH 7.6) and membranes were then incubated with primary antibody diluted by 1:1000 with 5% Bovine Serum Albumin (BSA) in TBS/1% Tween 20 overnight. Immunoreactive proteins were identified using polyclonal goat anti-mouse or anti rabbit antibodies horseradish peroxidase (HRP) (Dako). Secondary antibodies were diluted 1:3000 with 5% dry milk in TBST. The incubation period for secondary antibodies was one hour. Visualization of these immunoreactive proteins was achieved with the ECL (enzyme-linked chemiluminescence) system (Amersham). Films were exposed and developed using a CanoScan 8000F scanner.

2.8.3 Removal of bound antibodies from membranes

Membranes previously immunoprobed were incubated in stripping buffer (62mm Tris ph 6.8, 2% SDS, 100 mM 2-Mercaptoethanol) for 15 minutes twice at 60°C, then washed twice with TBST for 10 minutes and blocked for 30 minutes with 5% dry milk prior to reprobe them.

2.84 Densitometry

For some of the most relevant Western blot results, including caspase-1 expression in macrophages from WT and P2X7 deficient mice, phospho-S6, phospho-mTOR and phospho-ERK levels in response to ATP stimulation in macrophages from WT and P2X7 deficient mice, densitometry was performed on scanned immunoblot images using the ImageJ software. The gel analysis tool was used to obtain the absolute intensity for each experimental band and corresponding actin band used as control. Relative intensity for each experimental band was calculated by normalizing the experimental absolute intensity to the corresponding control absolute intensity.

2.9 ENZYME-LYNKED IMMUNOSORBENT ASSAY (ELISA)

To quantify cytokines secreted by macrophages, supernatants were analysed by sandwich ELISA using kits from R&D Systems. A 96 well microplate was coated with the appropriate dilution of the capture antibody and incubated overnight. The wells were then washed with the appropriate wash buffer and blocked for one hour with reagent diluent containing 1% BSA. After further washing, serial dilutions of the standard and the samples were loaded into the wells in duplicate

and incubated at room temperature for two hours. The plates were then washed and detection antibody in the appropriate dilution was added to the wells and incubated for two hours at room temperature. The plates were then washed again and working dilution of Streptavidin-HRP was added. After 20 minutes incubation and further washing substrate solution was added to the plates for 20 minutes. The colorimetric reaction was then stopped with the addition of stop solution and the optical density of each well was determined using a microplate reader set to 450 nm.

2.10 TRANSFECTION OF MACROPHAGES WITH SMALL INTERFERING RNA (siRNA)

siRNA knockdown was carried out to silence JUND expression in BMDMs from WKY rats. The siRNA used was siGENOME SMARTpool, rat JUND (24518) M-092127-00-0010, 10nmol (Dharmacon, Lafayette, CO, USA) and the scrambled control siRNA was siGENOME Non-targeting siRNA Pool #1 D-001206-13-20, 20nmol (Dharmacon, Lafayette, CO, USA). siRNA was resuspended as per manufacturer's instructions by adding RNase-free water to achieve a working concentration of 20 nmol and then incubated at room temperature on an orbital mixer for 30 minutes. Aliquots were made to ensure minimisation of freeze thaw events on the siRNA. Transfection with siRNA was performed on day 6 of culture. To prepare the transfection mixture, 2.64 ml Optimem (Invitrogen) was incubated with 60 µl Dharmafect 1 (Dharmacon) for 5 minutes at room temperature. At the same time 240µl of Optimem was incubated with 60µl siRNA (20µM) for 5 minutes at room temperature. The two preparations were then mixed and incubated at room temperature for 20 minutes with frequent mixing by tube inversion to allow the integration of siRNA particles into the

liposomal particles contained within Dharmafect transfection reagent. Meanwhile the media in the 6 well culture plates was aspirated, the cells washed with pre-warmed DMEM and then 1.5 ml DMEM with no supplementation was added to each well. Five hundred microlitres of the transfection mixture was then added to each well and mixed resulting in a final siRNA concentration of 100nM. The cells were incubated for 48 hours in a 5% CO2 incubator at 37^{o}C. On day 8 the cells were primed with LPS 1 μg/ml for 1 hour and then stimulated with ATP 5 mM for 30 minutes.

2.11 MASS SPECTROMETRY-BASED QUANTITATIVE PHOSPHOPROTEOMICS

Phosphorylation of proteins is a very important post translational modification that regulates multiple effects including translocation, protein–protein interactions, and activation or inactivation (Pawson & Nash, 2000). In many cases, a protein can be phosphorylated on multiple sites, which can either act independently or synergistically when phosphorylated simultaneously (Han et al., 2009). It is therefore important to investigate not only the level of phosphorylation for individual sites on a given protein but also the overall level of protein phosphorylation. The main difficulties in the detection of phosphorylation sites are due to the fact that phosphorylation usually occurs at low stoichiometry or can occur on a protein with low expression level (Schmelzle & White, 2006). In the past few years, several advances in mass spectrometry (MS) based approaches have enabled the analysis of thousands of phosphorylation sites so that MS combined with enrichment strategies for phosphorylated proteins and peptides is nowadays the tool of choice for the identification of novel phosphorylation sites (Larsen, Thingholm, Jensen, Roepstorff, & Jorgensen, 2005).

2.11.1 Cell lysis and protein digestion

Cell pellets were resuspended in an appropriate volume (1 ml per 10 x 10^6 cells) of Lysis Buffer with the following composition: 8M Urea in 20 mM Hepes (pH 8). Cell suspension was then sonicated at 50% intensity 3 times for 15 seconds and centrifuged at 20000 x g for 10 minutes at 4^0C. Supernatants were collected and transferred into a protein low-bind tube. (Montoya et al., 2011).

2.11.2 Protein denaturation and digestion

For Disulphide bridges reduction, 10 µl of 1M Dithiothreitol (DTT) were added to each sample. Samples were then vortexed vigorously and incubated at room temperature in the dark for 15 minutes. Cysteines alkylation was obtained by addition of 40 µl of 415 mM Iodoacetamide (IAM) to each sample followed by a further 15 minutes incubation at room temperature in the dark. Protein digestion was achieved with the use of immobilized Trypsin beads. About 80 µl (centrifuged volume) of Trypsin beads were required for digestion of 500 µg of proteins. Before addition to the samples, trypsin beads were resuspended in an equal volume of 20 mM Hepes and samples were then incubated at 37^0C for 16 hours with shaking. Digestion was stopped by addition of TFA at a final concentration of 1%. (Montoya et al., 2011).

2.11.3 Desalting of Tryptic protein digests

The resultant peptide solutions were desalted by solid phase extraction (SPE) using Oasis HLB extraction cartridges (Waters UK Ltd., Manchester, UK) according to manufacturer instructions with some modifications. Briefly, cartridges were activated with 1 mL of 100% ACN and equilibrated with 1.5 mL

of wash solution (2% ACN, 0.1% TFA in water). After the cartridges were loaded with peptide solution, they were washed with 1 mL of wash solution. Peptides were eluted with 0.5 mL of glycolic acid solution (1 M Glycolic acid in 80% ACN and 5% TFA). All the steps were done in a vacuum manifold set at 5 mm Hg. (Montoya et al., 2011).

2.11.4 Phosphopeptide enrichment with TiO_2 beads

Titanium dioxide at acidic pH has a positively charged surface that selectively adsorbs phosphorylated compounds and is currently the most popular metal oxide resin used to capture phosphopeptides (Pinkse, Uitto, Hilhorst, Ooms, & Heck, 2004). Briefly, eluates from Oasis cartridges were normalized to 1 mL with glycolic acid solution and incubated for 5 minutes at room temperature with varying volumes of TiO2 solution (50% slurry, GL Sciences Inc., Japan). TiO2 beads were then packed by centrifugation in equilibrated C-18 spin columns (PepClean C-18 Spin Columns, Thermo Scientific, Rockford, IL). Beads were sequentially washed with 300 µL of glycolic acid solution, 50% ACN and ammonium acetate solution (20 mM ammonium acetate pH 6.8 in 50% ACN). An extra 50% ACN wash can be also added after the ammonium acetate solution. For phosphopeptide elution, beads were incubated three times with 50 µL 5% NH4OH for 1 min at room temperature and centrifuged. The three eluates of each fraction were pooled and acidified by addition of formic acid (FA) to a final concentration of 10%. Samples were then dried using a SpeedVac and pellets were stored at −80 °C. (Montoya et al., 2011).

2.11.5 Nanoflow-liquid chromatography tandem mass spectrometry (LC–MS/MS)

Phosphopeptide pellets were dissolved in 10–20 µl of 0.1% TFA and run in a LTQ-Orbitrap XL mass spectrometer (Thermo Fisher Scientific, Hemel Hempstead, UK) coupled online to a nanoflow ultra-high pressure liquid chromatography (UPLC, nanoAcquity, Waters). (Montoya et al., 2011).

2.11.6 Mass-spectrometry data analysis

For phosphorylated peptides identification, mass-spectrometry data were analysed using the software Mascot Daemon (v2.2.2; Matrix Science, London, UK). This software takes the mass spectrometry data and searches it against molecular sequence databases to identify the constituent proteins and to characterize post-translational modifications. For phosphorylated peptide quantification, a program in Visual Basic created by Dr Pedro Cutillas called Pescal (Peak Statistic Calculator) was used and incorporated it into an Excel macro (Cutillas & Vanhaesebroeck, 2007). This program uses m/z and retention time (tR) values for each identified peptide ion to generate extracted ion chromatograms (XICs) and uses them to calculate the peak heights and areas. The resulting quantitative data were parsed into Excel files for normalization and statistical analysis. Peptide intensities were normalized to the total chromatogram intensity and further expressed as a percentage relative to the largest intensity value across samples (Montoya et al., 2011).

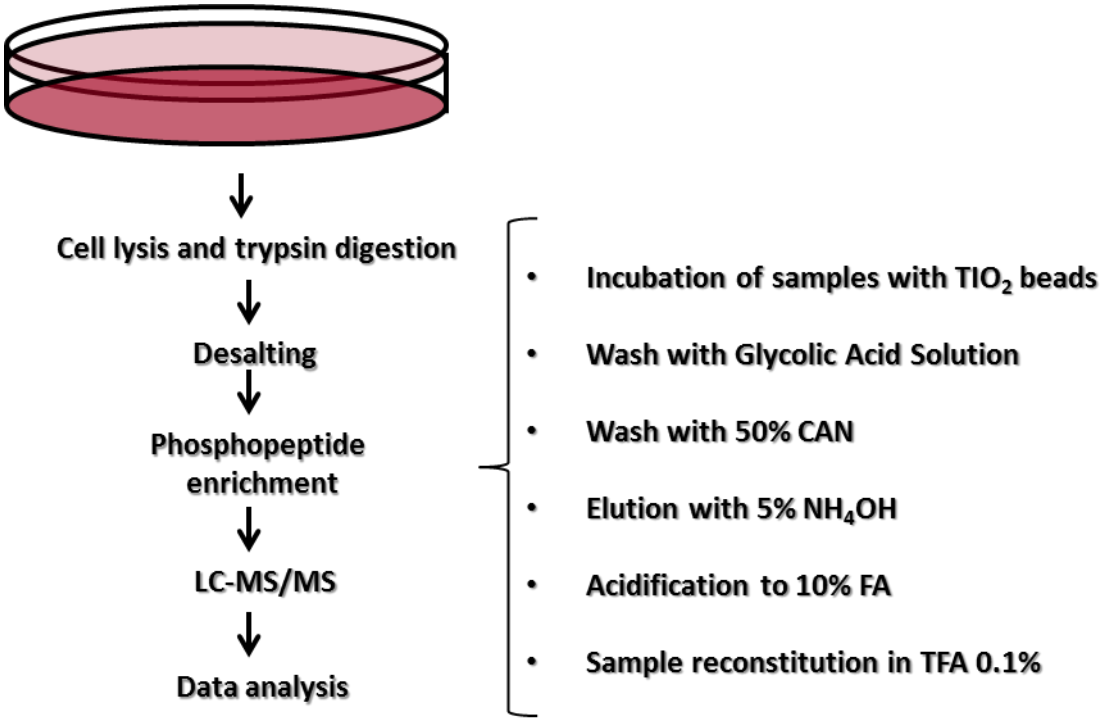

Figure 2.1 Workflow of TiO2 based phosphopeptide enrichment technique.

Cell pellets are lyzed, reduced, alkylated, digested with trypsin and desalted. The protocol for TiO_2 enrichment includes the binding of peptides to TiO_2 beads followed by the removal of unphosphorylated peptides by sequential washing with glycolic acid solution. Phosphopeptides are then eluted using NH4OH, acidified and reconstituted in TFA prior to LC–MS/MS analysis. Figure adapted from the following article:"Characterization of a TiO_2 enrichment method for label-free quantitative phosphoproteomics" (Montoya et al., 2011).

2.12 Gelatin zymography

Twenty µg of total protein, measured using the Micro BCA™ Protein Assay kit (Thermo Scientific/Pierce, Rockford, IL), was mixed with an equal volume of Novex® Tris-glycine SDS native sample buffer (Invitrogen™ Carlsbad, CA, USA) and the mixture was loaded into wells of pre-cast 10% Novex® zymogram gelatin gels (Invitrogen™). Pre-stained molecular weight standards were also run on the gels. The gels were electrophoresed at a constant voltage of 100 V for approximately 2 h. Following electrophoresis, the gels were rinsed in distilled water and then gently shaken in a renaturing solution of 2.7% Triton X-100 (Novex® zymogram renaturing buffer, Invitrogen™) for 1 h at 37°C to reactivate MMPs. The gels were then incubated on a rotary shaker in a developing buffer (Novex® zymogram developing buffer, Invitrogen™) for 24 h at 37°C to allow denatured MMPs to digest the gelatin substrate. After the digestion phase, the gels were rinsed and stained by incubation with Coomassie Blue Rapid stain (Diversified Biotech, Boston, MA, USA) for 1 h. Gels were destained with a solution of acetic acid, methanol and water (10: 50: 40) to maximize contrast between proteolytic areas and non-digested areas. Proteolytic activity was visualized as areas of clear bands against a dark blue background.

2.13 STATISTICAL ANALYSES

Each experiment was performed in triplicate and repeated 3 independent times, unless stated otherwise. Results were then expressed as mean ± SEM, with n being the number of independent observations. Statistical significance of differences between means was evaluated using computer-based software (Prism, Graphpad, San Diego, CA, version 4.0). Either a paired student t test, two

tailed or two-way ANOVA with Bonferroni correction for multi-comparison test were performed. A P value of $P \leq 0.05$ was regarded a statistically significant.

CHAPTER THREE-INVESTIGATION OF PRO-INFLAMMATORY CYTOKINES PRODUCTION IN PRIMARY BONE MARROW DERIVED MACROPHAGES FROM WILD TYPE AND P2X7R KNOCK OUT MICE

3.1 INTRODUCTION

3.2 EXPRESSION OF P2X7R IN BONE MARROW DERIVED MACROPHAGES FROM WILD TYPE AND P2X7 DEFICIENT MICE

Aims and experimental design

Results

3.3 IL-1 BETA SECRETION IN RESPONSE TO BZATP, ATP OR LL37 IN BMDM FROM WT AND P2X7 DEFICIENT MICE

Aims and experimental design

Results

3.4 IL-18 SECRETION IN RESPONSE TO ATP IN LPS PRIMED BMDM FROM WT AND P2X7 DEFICIENT MICE

Aims and experimental design

Results

3.5 EFFECTS OF P2X7R INHIBITION ON THE SECRETION OF IL-1BETA IN BMDM FROM WT AND P2X7 DEFICIENT MICE

Aims and experimental design

Results

3.6 CASPASE-1 ACTIVATION IN RESPONSE TO ATP IN BMDM FROM WT AND P2X7 DEFICIENT MICE

Aims and experimental design

Results

3.7 DISCUSSION

3.1 INTRODUCTION

As previously described, both IL-1β and IL-18 are synthesized as intracellular precursors and they need to be enzymatically cleaved in order to become biologically active. In macrophages the process of IL-1β and IL-18 secretion requires two different steps: a primary pro-inflammatory stimulus, which can be experimentally reproduced by LPS, is needed to induce high levels of pro-IL1-β and pro-IL-18 synthesis within the cells, but, applied alone, results in minimal IL-1β and IL-18 secretion. A second stimulus is then required to activate caspase-1 and ATP, acting on the P2X7R, is widely recognized as having this role. The function of caspase-1 in the release of mature IL-1β has been demonstrated in several in vitro and in vivo studies which have shown that cells that do not express caspase-1 such as fibroblasts and keratinocytes (Young, Hazuda, & Simon, 1988; Cerretti et al., 1992), as well as caspase-1 knock- out mice (Kuida et al., 1995), lack the capacity to release active IL-1β. Although the caspase-1 dependent IL-1β secretion is the most well established, other proteases have been identified that are also able to generate active IL-1β from its precursor in a caspase-1 independent manner including bacterial enzymes and several components of the family of metalloproteinases, particularly gelatinase A (MMP-2) and B (MMP-9). Furthermore, studies from Maelfait et al. have demonstrated that also caspase-8 is able to induce IL-1β maturation in response to TLR3 and TLR4 stimulation (Maelfait et al., 2008). ATP's effect on P2X7R is maximum at concentrations of 1-5 mM range and induces a rapid efflux of potassium from the cells which is necessary for the assembly and activation of the NLRP3 inflammasome (Kahlenberg & Dubyak, 2004). The importance of the rapid potassium efflux in inducing the NLRP3 inflammasome activation is also confirmed by the observation that molecules capable of inducing pores in the plasma membrane, such as the antibiotic nigericin or antimicrobial peptides such as protegrins can activate caspase- 1 in a P2X7R independent manner

(Perregaux, Bhavsar, Contillo, Shi, & Gabel, 2002). Macrophages are known to express high levels of P2X7R and therefore represent a good model to investigate the functions of this receptor. Since macrophages can express at the same time multiple P2X and P2Y receptors, the use of primary macrophages from WT and P2X7 deficient mice is extremely important to differentiate the responses that might involve other purinergic receptors from the ones that are selectively mediated by P2X7R. Furthermore, I have used primary macrophages from two different P2X7 deficient mouse lines for my experiments, which have been shown to behave differently in several in vivo models of disease. The comparison between the two P2X7 deficient lines could also contribute to a better understanding of P2X7R functions, particularly in view of the recent findings that both of them might express P2X7 splice variants.

3.2 EXPRESSION OF P2X7R IN BONE MARROW DERIVED MACROPHAGES FROM WILD TYPE AND P2X7 DEFICIENT MICE

Aims and experimental design

There is a growing literature that describes new splice variants for both the mouse and the human P2X7. Nicke et al. have described a P2X7 splice variant (P2X7k) characterized by an alternative N terminus and trans-membrane domain 1 which, due to a different exon 1 and translation start, escapes gene inactivation in the GSK P2X7 knock-out mice (Nicke et al. 2009). In this study the P2X7k variant is shown to be expressed in the spleen of the GSK P2X7 knock-out mice. Two further P2X7 variants have been more recently described in the mouse which are characterized by alternative exon 13's encoding much shorter C-termini than the original exon 13 and that are able to escape gene inactivation in the Pfizer knock out mouse strain (Masin et al. 2011). I therefore examined the expression of the full length P2X7R and P2X7K splice variant in WT, GSK and Pfizer BMDMs through PCR and Western blotting.

Results

As shown in figure 3.2A, a band of the predicted size of 75 KDa was detected in both WT and GSK BMDMs under basal conditions while no band was detected in the Pfizer BMDMs. Compared to WT, BMDMs from GSK mice show much lower levels of the protein. The primary antibody used for P2X7 protein detection is a rabbit polyclonal antibody from Alomone Labs (Israel) that recognizes the peptide (C)KIRK EFPKT QGQYS GFKYP Y, corresponding to amino acid residues 576-595 of rat P2X7 which has an identical homology of 18/20 amino acid residues in the mouse. Among the functional mouse P2X7 variants described so

far, the only one that could be detected by the Alomone Labs antibody is the variant P2X7k, since the isoforms 13B and 13C, as shown in figure 3.2B, are characterized by much shorter C termini. In the P2X7k variant, the alternative exon 1 encodes 39 amino acid residues instead of the 42 amino acid residues of the P2X7a subunit, so that the molecular masses of the proteins are similar. Furthermore, in their study Nicke et al., after transfecting X. Laevis oocytes with both a and k isoforms, have shown that upon separation by SDS-PAGE and immunoblotting the two subunits revealed a similar band of 77 KDa using the same anti P2X7 antibody from Alomone Labs that I used. To assess whether the band detected in the GSK BMDMs corresponded to the P2X7k variant, I have performed a PCR using specific forward primers for the exon 1 of P2X7a and exon 1' of P2X7k isoforms (5'-CACATGATCGTCTTTTCCTAC-3' AND 5'-GCCCGTGAGCCACTTATGC-3' respectively) and a common antisense primer in exon 4 (5'-GGTCAGAAGAGCACTGTGC-3'). As shown in figure 3.2C, using primers specific to exon 1, I could detect a band in both the WT and the Pfizer BMDMs, while no band was seen in the GSK BMDMs. However, using primers specific to the alternative exon 1 I could not detect any bands in BMDMs from all of the three mouse strains.

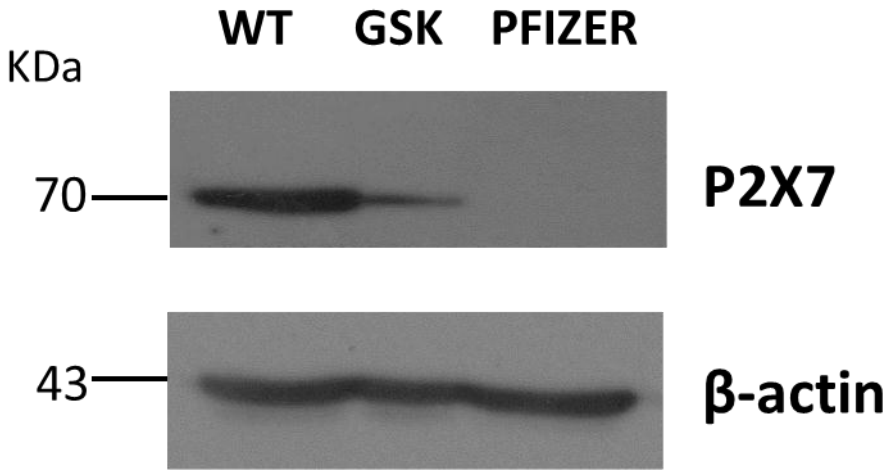

Figure 3.2A P2X7R expression in WT and P2X7 deficient BMDMs.

Aliquots of protein (20 µg) from cell lysates of primary BMDM from WT, GSK and Pfizer knock-out mice under basal conditions were separated by gel electrophoresis and transblotted to PVDF membrane. Detection of P2X7 was performed by Western blotting using a rabbit polyclonal anti-P2X7 antibody from Alomone Labs (APR-004). Beta actin was used as loading control.

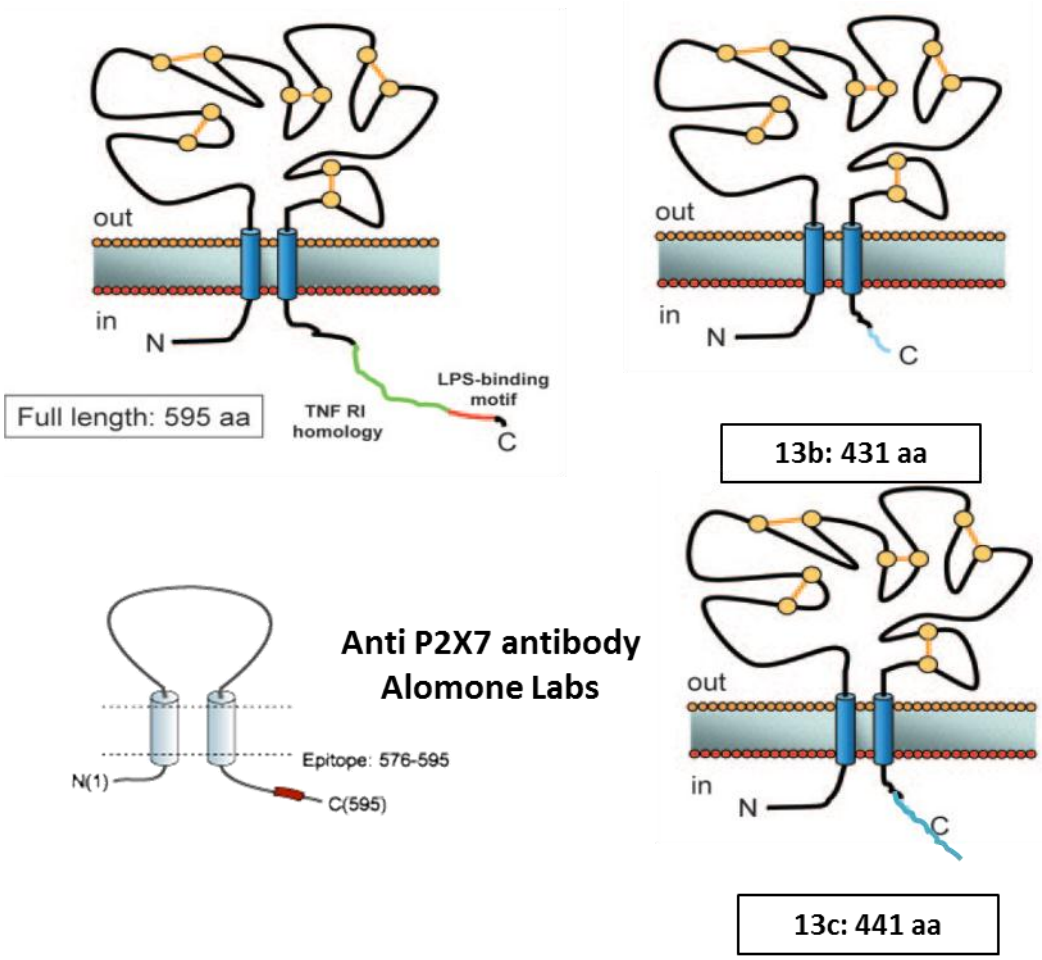

Figure 3.2B Schematic representation of the P2X7 full length receptor and the C-truncated P2X7 isoforms 13b and 13c.

The full length receptor is 595 amino acids long, while the splice variants 13b and 13 c contain 431 and 441 amino acid residues respectively. The epitope corresponding to the amino acids 576-595 recognized by the anti-P2X7 antibody from Alomone Labs (APR-004) is also represented. Figure adapted from the following article: The P2X7 Receptor: "A Key Player in IL-1β Processing and Release" (Ferrari et al., 2006).

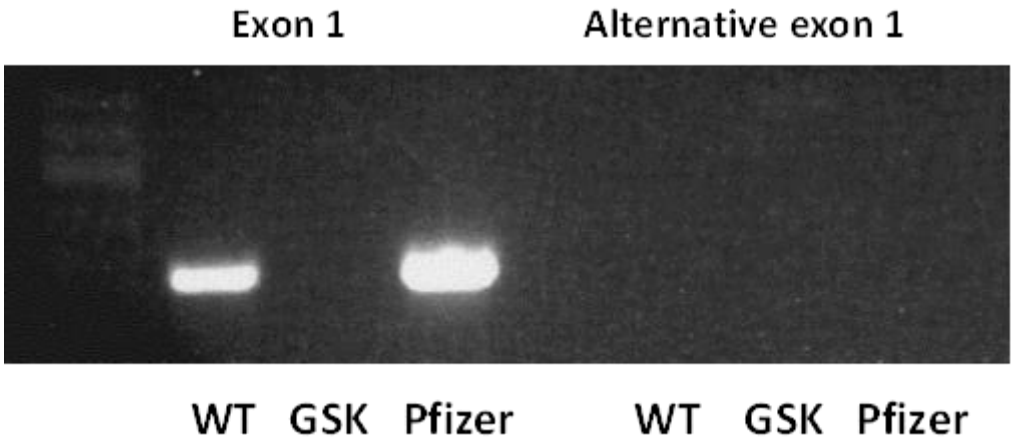

Figure 3.2C Analysis of P2X7k variant expression in BMDMs from WT, GSK and Pfizer P2X7 deficient mice by PCR.

Exon 1 and alternative exon 1 specific forward primers were combined with reverse primers in exon 4. Exon 1 was expressed in both WT and Pfizer BMDMs, but not in BMDMs from GSK mice. The alternative exon 1 of the P2X7 k variant was expressed by none of them.

3.3 IL-1BETA SECRETION IN RESPONSE TO BZATP, ATP OR LL37 IN BMDM FROM WT AND P2X7 DEFICIENT MICE

Aims and experimental design

Previous work from Pelegrin et al. has analysed patterns of ATP-mediated release of IL-1β and IL-18 from different macrophage types. In their study, they used peritoneal macrophages from the GSK P2X7R deficient mouse line and found that release of IL-1β and IL-18 by ATP was completely abolished in P2X7 knock-out peritoneal macrophages even when supramaximal concentration of LPS were used to prime the cells (Pelegrin, Barroso-Gutierrez, & Surprenant, 2008). Due to the discovery of distinct release mechanisms of IL-1β and due to the presence of discordant data in the literature, probably secondary to the different techniques used to detect the mature forms of IL-1β and IL-18, I have investigated the secretion of both IL-1β and IL-18 by both Western blotting and ELISA methods in response to several P2X7R agonists in LPS primed bone marrow derived macrophages from wild type mice and from the two P2X7 deficient mouse lines, the GSK and Pfizer respectively. BzATP and ATP are well known P2X7R agonists and more recently, the antimicrobial peptide LL-37 has been shown to induce caspase-1 activation and release of active IL-1β in LPS-primed monocytes through P2X7R activation (Elssner, Duncan, Gavrilin, & Wewers, 2004). In order to evaluate and to compare the levels of IL-1β secreted by BMDMs from WT, GSK and Pfizer P2X7 deficient mice in response to these stimuli, I have primed the macrophages with LPS used at a concentration of 1 µg/mL for 5 hours and I have then stimulated them with either BzATP (final concentration in the medium 150 µM), ATP (final concentration in the medium 5 mM) or LL-37 (final concentration in the medium 10 µM) for 30 minutes. Supernatants were then collected and analysed by sandwich ELISA. To optimize the conditions for this experiment, I have tried two different concentrations of

LPS (100 ng/ml and 1μg/ml) and I have used different time points for the priming step, starting from 1 hour incubation up to an overnight incubation. I have also used two different media for LPS priming and ATP stimulation: serum free DMEM and complete L929 conditioned medium. Of the two LPS concentrations used, 1μg/ml resulted much more efficient compared to the lower one leading to much higher levels of both IL-1β and IL-18. Although the current view is that the priming step is necessary to increase the precursors synthesis, I could detect active IL-1β and IL-18 even after one hour LPS priming, which clearly is not a sufficient time for new protein synthesis. On the other hand, an overnight incubation with LPS followed by 30 minutes stimulation with ATP did not induce any active IL-1β or IL-18 secretion probably as a consequence of the LPS-tolerance phenomenon described in literature, characterized by a downregulation of proinflammatory genes after prolonged exposure to LPS (West & Heagy, 2002). The levels of active IL-1β and IL-18 in response to ATP stimulation were significantly lower when L929 medium was used instead of serum free DMEM. I could not establish however, whether it was the presence of serum or other components of the L929 conditioned medium to affect IL-1β and IL-18 processing. I have also tried two different concentrations of ATP (3 mM and 5 mM) and the highest concentration appeared to be the most effective one, while there was no difference in cytokine production when the stimulation was prolonged for 30 minutes or 1 hour. I did not try any longer stimulation with ATP because of the known cytotoxic effect which was already visible under the microscope after 30 minutes when the cells started showing a round-shape morphology. A dose-dependent effect was also observed with BzATP and LL-37 and the concentrations of 150 μM and 10 μM respectively were the most effective ones.

Results

As illustrated in figure 3.3 A, BMDMs from WT mice produce significant higher levels of IL-1β compared to both GSK and Pfizer BMDMs in response to BzATP and ATP. After stimulation with the anti-microbial peptide LL-37, macrophages from WT mice produce higher levels of IL-1β compared to GSK and Pfizer BMDMs, although the difference between WT and GSK BMDMs was not statistically significant. GSK BMDMs exhibit significant higher levels of IL-1β in response to all the agonists tested compared to Pfizer P2X7 deficient mice. ATP stimulation appears to be the most effective stimulus, leading to the highest levels of IL-1β compared to BzATP and LL-37 in WT mice. However, much higher concentrations of ATP, in the millimolar range were required for this effect in comparison with BzATP and LL-37 for which concentrations within the micromolar range were used. ATP also seems to be the most selective agonist compared to BzATP and LL-37 leading to the highest production of IL-1β in BMDMs from WT mice and to the lowest in BMDMs from the Pfizer Knock-out mice. To confirm the ELISA data, I have examined the secretion of IL-1β in response to ATP in LPS-primed BMDMs from WT and P2X7 knock-out mice by Western blotting. As shown in figure 3.3 B, in response to ATP, a band of the predicted size of 17 KDa, corresponding to the active form of IL-1β was detectable in BMDMs from WT and GSK mice but not in BMDMs from Pfizer mice. BMDMs from WT mice, in accordance with the ELISA results show higher levels of active IL-1β compared to macrophages from GSK mice.

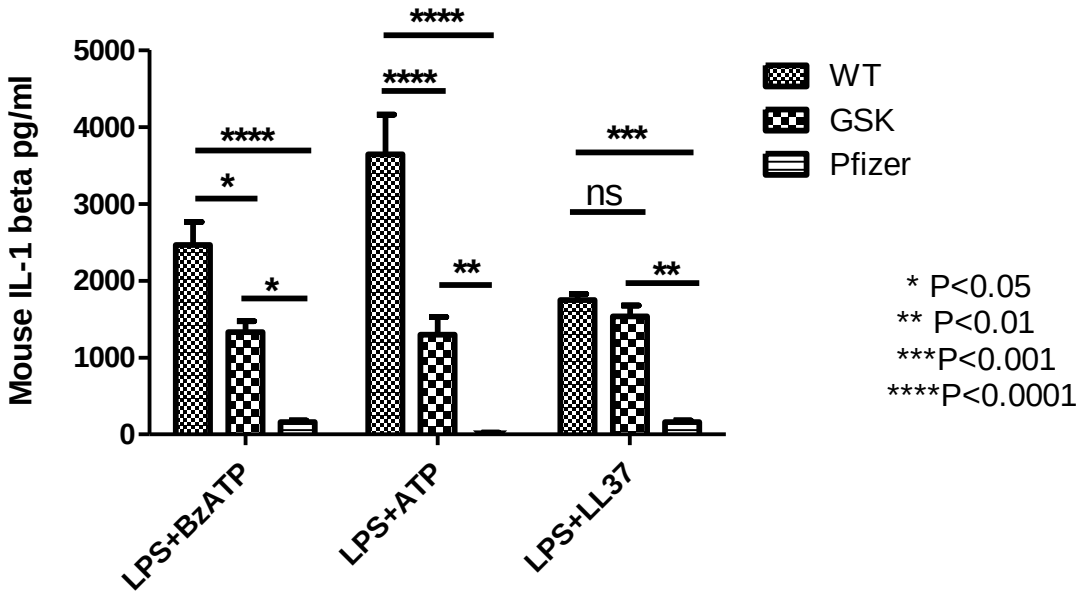

Figure 3.3A IL-1β release in BMDMs cultured from WT, GSK and Pfizer P2X7 deficient mice in response to BzATP, ATP and LL-37.

BMDM from WT, GSK and Pfizer P2X7 deficient mice were plated in six-well plates at a density of 1 x 10^6 cells per well, primed with LPS 1µg/mL for 5 hours and then stimulated with either BzATP 150 µM, ATP 5mM or LL37 10 µM for 30 minutes. Supernatants were then collected and analysed by sandwich ELISA using the mouse IL-1β Duoset ELISA Kit from R&D Systems. Data are representative of three independent experiments.

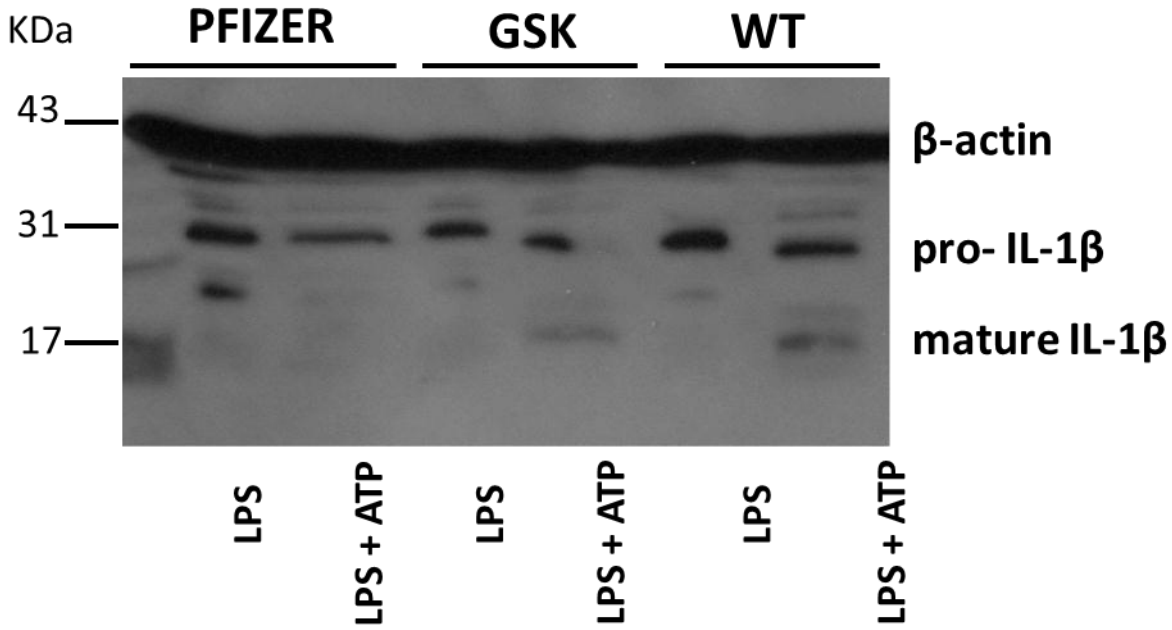

Figure 3.3B IL-1β secretion in BMDMs from WT and P2X7 deficient mice in response to ATP.

BMDMs from WT, GSK and Pfizer P2X7 deficient mice were plated in six-well plates at a density of 1 x 10^6 cells per well, primed with LPS 1 μg/ml for 5 hours and then stimulated with or without ATP 5 mM for 30 minutes. Supernatants and cell layers were collected, filtered using Amicon ultra centrifugal filters (Millipore) and analysed by Western blotting. Detection of pro- and mature IL-1β was performed using a specific anti IL-1β antibody from New England Biolabs (UK).

3.4 IL-18 SECRETION IN RESPONSE TO ATP IN LPS PRIMED BMDM FROM WT AND P2X7 DEFICIENT MICE

Aims and experimental design

To evaluate and compare IL-18 production in BMDMs cultured from WT, GSK and Pfizer P2X7 KO mice, I have primed these cells with LPS 1µg/mL for five hours and then stimulated them with ATP used at a concentration of 5 mM for 30 minutes. Both supernatants and cell layers were then collected, filtered using Amicon ultra centrifugal filters for protein concentration and purification (Millipore) and analysed by Western blotting. Unfortunately, I could not find a reliable ELISA kit for mouse IL-18 detection, therefore a quantitative analysis was not possible. The active form of the cytokine was detectable only when supernatants and cell layers where analysed together, while in the cell lysates I could only detect the precursor.

Results

As shown in figure 3.4, in response to ATP, BMDMs from WT and GSK mice produce similar levels of active IL-18. Macrophages from Pfizer mice show only a faint band of the predicted size of 18 KDa when stimulated with ATP. Macrophages from WT and GSK mice also release active IL-18 after stimulation with LPS alone. The levels of active IL-18 produced by WT and GSK BMDMs in response to LPS alone are similar to the levels of active IL-18 secreted by macrophages from Pfizer mice in response to ATP.

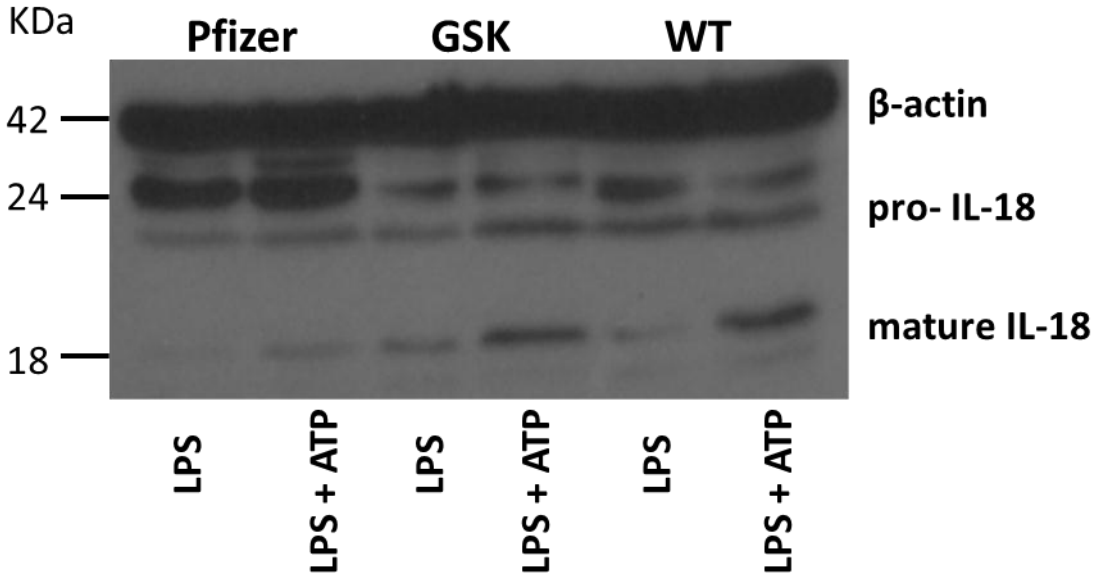

Figure 3.4 IL-18 secretion in response to ATP in BMDMs from WT and P2X7 deficient mice.

BMDMs from Pfizer, GSK and WT mice were seeded into six-well plates at a density of 1 x 10^6 cells per well, primed with LPS 1 µg/ml for 5 hours and then stimulated with or without ATP 5 mM for 30 minutes. Supernatants and cell layers were then collected, filtered using Amicon ultra centrifugal filters (Millipore) and analysed by Western blotting. Detection of pro- and mature IL-18 was performed using a specific anti IL-18 antibody from Santa Cruz Biotechnology.

3.5 EFFECTS OF P2X7R INHIBITION ON THE SECRETION OF IL-1 BETA IN BMDMs FROM WT AND P2X7 DEFICIENT MICE

Aims and experimental design

Previous studies from Grahames et al. have shown that the use of the non-selective P2X7 antagonists KN-62, PPADS and oxidized ATP significantly inhibited 5mM ATP-induced IL-1β release in human monocytic cells THP-1 (Grahames, Michel, Chessell, & Humphrey, 1999). Later studies from Honore' et al. demonstrated that the selective P2X7 antagonist A-740003 potently blocks the BzATP-evoked IL-1β release in THP-1 cells (Honore et al., 2006). To assess whether P2X7R inhibition by A-740003 affects also ATP-evoked IL-1β secretion, I have primed BMDMs from WT, GSK and Pfizer mice with LPS 1 μg/mL for 5 hours, cells were then incubated for 30 minutes with either the inhibitor or serum free DMEM and then stimulated with ATP 5 mM in the presence or absence of the P2X7 receptor antagonist A-740003 used at a final concentration in the medium of 3 μM. Although A-740003 is a selective P2X7R antagonist and BMDM from GSK and Pfizer mice for definition should not express the full length receptor, in order to evaluate the specificity of the inhibitor I have analysed its effects on IL-1β release also in BMDM from the two P2X7 deficient lines GSK and Pfizer. Supernatants and cell layers were then collected, filtered using Amicon ultra centrifugal filters for protein concentration and purification (Millipore) and analysed by Western blotting.

Results

As shown in figure 3.5A, the use of the P2X7R antagonist A-740003 dramatically decreases IL-1β secretion in WT BMDM. Surprisingly, in the GSK BMDM, the use

of the P2X7RA seems to slightly increase the production of IL-1β. No effects were seen in the Pfizer BMDMs.

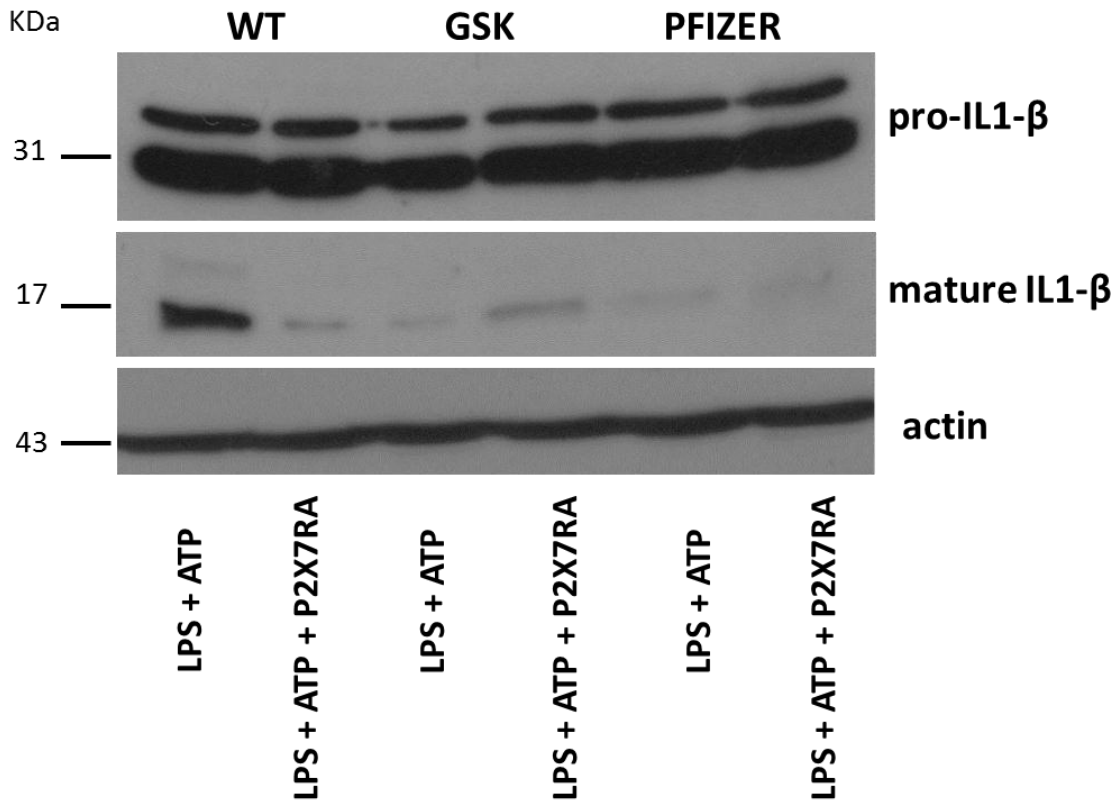

Figure 3.5 Effects of P2X7RA on IL-1 β secretion in response to ATP in LPS primed macrophages from WT and P2X7 deficient mice.

BMDMs from WT, GSK and Pfizer knock-out mice were plated into six-well plates at a density of 1 x 10^6 cell per well, primed with LPS 1 μg/ml for 5 hours and then stimulated with ATP for 30 minutes in the presence or absence of the P2X7R antagonist A-740003 used at a final concentration in the medium of 3 μM. Supernatants and cell layers were collected, filtered using Amicon ultra centrifugal filters (Millipore) and analysed by Western blotting.

3.6 CASPASE-1 ACTIVATION IN RESPONSE TO ATP IN BMDM FROM WT AND P2X7 DEFICIENT MICE

Aims and experimental design

As previously described, both IL-1β and IL-18 require to be enzymatically cleaved in order to become biological active and this process is mediated by the IL-1β converting enzyme, caspase-1. Caspase-1 is synthesized as an inactive, monomeric zymogen (pro-caspase-1) that is thought to be activated by dimerization and autoproteolytic processing (Martinon, Mayor, & Tschopp, 2009) which leads to the generation of two subunits of 20 and 10 KDa respectively, termed p20 and p10. Although the function of caspase-1 in the release of mature IL-1β and IL-18 is well established, some studies have demonstrated that, aside from caspase-1, other proteases such as the metalloproteinases MMP-9 and MMP-12 are capable of generating active IL-1β. Therefore, to establish whether the secretion of mature IL-1β and IL-18 involved caspase-1 activity, I have assessed the expression of the active fragment p10 in BMDMs from WT and P2X7 deficient mice after priming with LPS 1 μg/ml and stimulation with ATP 5 mM. The antibody used for caspase-1 detection by Western blotting was from Santa Cruz Biotechnology and recognized both the precursor and the active p10 fragment. I could detect the active p10 fragment only analysing cell layers and supernatants together, while I could not detect any active form in the cell lysates indicating that caspase-1 is released from the cells soon after the conversion as demonstrated by several studies (Laliberte, Eggler, & Gabel, 1999).

Results

As shown in figure 3.6, in response to ATP, the p10 subunit was detectable only in BMDMs from WT mice, whereas macrophages from GSK and Pfizer KO expressed only the precursor. BMDMs from WT and GSK mice exhibit similar levels of the precursor, while Pfizer macrophages showed much lower levels.

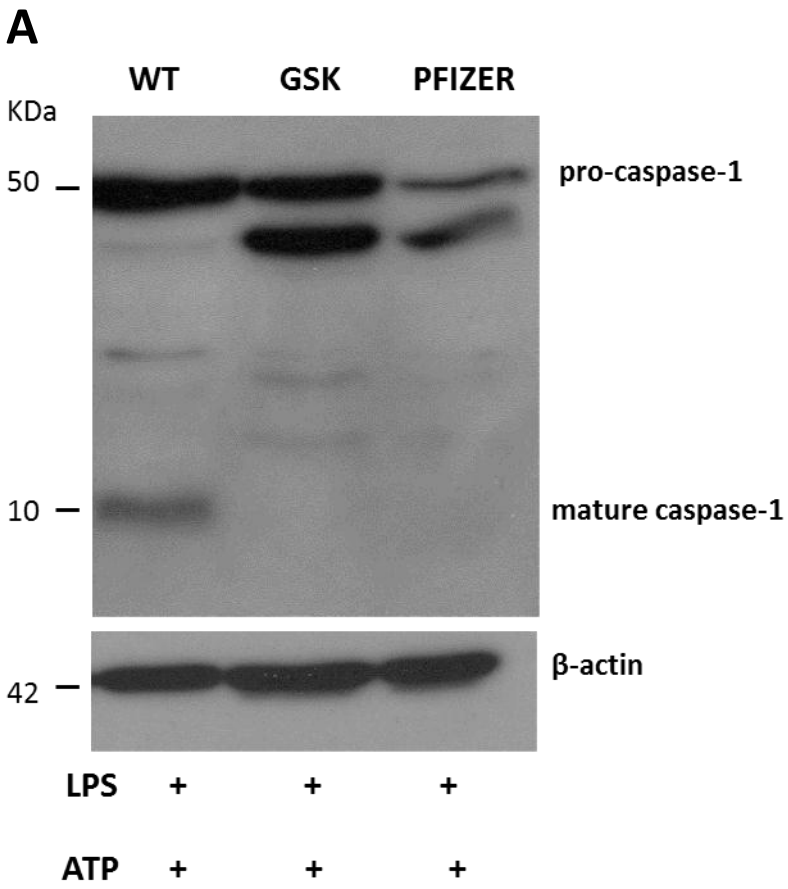
A
WT
GSK
PFIZER
KDa
50
pro-caspase-1
10
mature caspase-1
42
β-actin
LPS + + +
ATP + + +

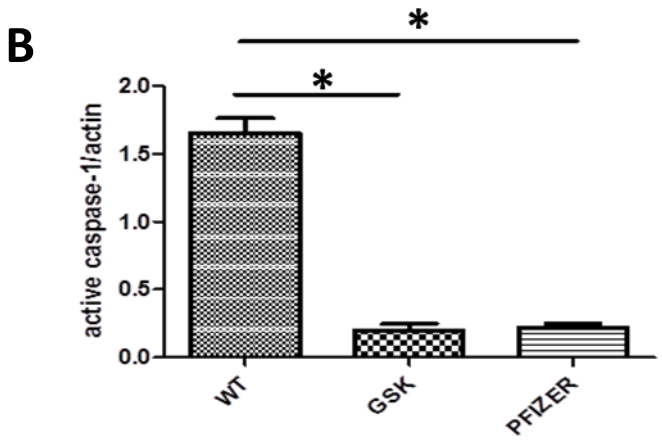

Figure 3.6 A and B. Caspase-1 activation in response to ATP in BMDMs from WT and P2X7 deficient mice.

BMDMs from WT, GSK and Pfizer BMDM were seeded into six-well plates at a density of 1 x 10^6 cells per well, primed with LPS 1 µg/ml for 5 hours and then stimulated with ATP 5 mM for 30 minutes. Supernatants and cell layers were collected, filtered using Amicon ultra centrifugal filters for protein purification and concentration and analysed by Western blotting. Detection of pro-caspase 1 and its active subunit p10 **(A)** was performed using a specific anti-caspase 1 p10 antibody from Santa Cruz Biotechnology (sc-514). **(B)** Quantification by Western blot densitometry for active caspase-1 as indicated. *P<0.05 Student paired T test for indicated comparisons. The blots are representative of at least n=3 independent experiments.

3.7 DISCUSSION

My studies lead me to the following conclusions:

1. Western blotting analysis of P2X7 protein expression in macrophages from WT and P2X7 deficient mice revealed the presence of a band of the predicted size of the full length P2X7R (75 KDa) in both WT and GSK macrophages, while no band was detectable in the Pfizer ones. The band intensity in GSK macrophages was however much lower compared to the one detected in WT macrophages.

2. BMDMs from WT produce higher levels of active IL-1β compared to BMDM from GSK and Pfizer P2X7 deficient mice in response to all the agonists tested (BzATP, ATP and the human cathelicidine LL-37).

3. Among all the agonists tested, ATP appears to be the most efficient and selective agonist leading to the highest levels of active IL-1β in BMDM from WT mice and the lowest in BMDM from Pfizer knock-out mice.

4. BMDMs from GSK knock-out mice show an intermediate phenotype between WT and Pfizer macrophages, releasing much higher levels of active IL-1β compared to macrophages from Pfizer KO mice in response to all the agonists tested.

5. The use of the selective P2X7 inhibitor A-740003 dramatically affects IL-1β secretion in response to ATP in BMDMs from WT mice.

6. Only BMDMs from WT mice are able to generate active caspase-1 in response to ATP.

Analysis of P2X7R expression in BMDM from WT and P2X7 deficient mice

As previously described, 12 splice variants of mouse P2X7 have been identified so far, although only three are thought to be functional. The variant P2X7k, which appears to be strongly expressed in the liver and spleen, is characterised by an alternative exon 1 and escapes gene deletion in the GSK mouse strain. The alternative exon 1 of P2X7k encodes 39 amino acid residues which replace the first 42 amino acid residues of the P2X7a subunit. This includes the intracellular N-terminus and about 80% of the first transmembrane domain. In their study, Nicke et al. have transfected Xenopus Laevis oocytes with both isoforms P2X7a and P2X7k and have shown that, upon separation by SDS-PAGE and immunoblotting, both P2X7a and P2X7k revealed bands of a similar size of about 77 KDa. The two other splice variants identified are characterized by alternative exon 13 which encode much shorter C-termini than the original exon 13a. As illustrated in figure 3.2B, the variant 13b has a C-terminus truncated at position 430, while the variant 13c has an alternative C-terminus with specific 11 amino acid residues beyond the common residue 430. When I examined the expression of P2X7R protein in WT, GSK and Pfizer mice by Western blotting, I could detect a band of the predicted size of about 75 KDa in both WT and GSK BMDM under basal conditions. The antibody that I used for the detection of P2X7 protein is a

highly specific antibody from Alomone Laboratories, Israel, directed against an antigenic epitope, corresponding to residues 576-595 of rat P2X7 (18/20 residues identical in mouse sequence). Since the variant 13b terminates at residue 431 and the variant 13c has an additional 11 amino acids at the C-terminus, both these variants should not be detected by the Alomone Labs antibody which can instead bind to the C-terminus of the P2X7k variant. To verify whether macrophages from GSK mice effectively expressed the variant P2X7k, I have performed a PCR analysis using forward primers specific to the normal and alternative exon 1 combined with reverse primers in exon 4. As expected, the normal exon 1 was expressed only by BMDMs from WT and Pfizer mice and not by GSK BMDMs. However, unfortunately I could not demonstrate the expression of the alternative exon 1 of the P2X7k variant in none of the three mouse strains BMDMs. The impossibility to demonstrate by PCR the expression of the alternative exon 1 in GSK macrophages could be due to a technical issue or might indicate that GSK BMDMs express instead another P2X7 variant with an alternative exon 1 different from the one expressed by the variant P2X7k. Further studies are certainly needed to investigate the latter hypothesis.

IL-1β secretion in response to BzATP, ATP and LL-37 in BMDM from WT and P2X7 deficient mice.

BzATP, ATP and the human cathelicidine LL-37 are all known to be powerful P2X7R agonists. It is well established that one unique property of P2X7R is its low sensitivity to ATP, so that concentrations within the millimolar range are usually used in vitro to activate the receptor. The antimicrobial peptide LL-37 has emerged only recently as a molecule able to generate biologically active IL-1β, although the exact mechanisms by which LL-37 activates P2X7R is not fully

understood yet. In order to evaluate the efficiency of these agonists in activating P2X7R and also their specificity, I have analysed the effects of these compounds on IL-1β secretion in LPS-primed BMDMs from WT and P2X7 deficient mice. Sandwich ELISA was used as quantitative analysis. As shown in figure 3.3 A, whatever agonist I used, BMDMs from WT mice always release more IL-1β compared to BMDM from the two P2X7 deficient mouse lines. When stimulated with BzATP or ATP, BMDMs from WT mice produce significant higher levels of IL-1β compared to both GSK and Pfizer macrophages. However, when LL-37 was used to activate P2X7R, the difference in IL-1β levels between WT and GSK macrophages was not statistical significant. Interestingly, BMDMs from GSK mice produce significant higher levels of IL-1β compared to BMDMs from Pfizer mice in response to all the agonists tested. These results would be in agreement with the hypothesis that GSK BMDMs express P2X7k or another P2X7 splice variant. In their study Nicke et al. have shown that the isoform P2X7k has 8-fold higher BzATP sensitivity and a slower deactivation compared to the P2X7a variant. My data however seem to be not in accordance with these findings. BMDMs from WT mice produce significant higher levels of IL-1β (up to 2500 pg/ml) in response to ATP compared to BzATP or LL-37 (less than 1000 pg/ml). It is true that mM rather than μM concentrations have been used for ATP stimulation, due to the low sensitivity of the receptor to the compound; however, higher concentrations in the mM range could not be used for BzATP or LL-37 because they would have induced cell death rather than an increased secretion of IL-1β. Among the agonists tested, ATP appears to be also the most selective one, leading to the highest IL-1β secretion in WT BMDM and to the lowest in the Pfizer BMDM. These data were reproduced in at least three independent experiments. Given that ATP stimulation seems to be the most effective and the most specific, I have used ATP as the main P2X7 agonists in all the following experiments to induce P2X7R activation.

Analysis of IL-1β and IL-18 secretion in response to ATP by Western blotting

The ELISA technique is generally a reliable and rapid method to quantify cytokines released in the supernatant. To be sure that by ELISA I was effectively measuring only the active form of IL-1β and not also the pro-form, I decided to analyse both IL-1β and IL-18 secretion in response to ATP in BMDM from WT and P2X7 deficient mice by western blotting. The anti-IL-1β and anti-IL-18 antibodies that I used were able to recognize both the precursors and the cleaved forms. As shown in figure 3.3B, a band of the predicted size of 17 KDa, corresponding to the active form of the molecule was detected both in WT and GSK BMDMs but not in macrophages from Pfizer mice. In accordance with the ELISA data WT BMDMs show higher levels compared to the GSK ones although the difference does not seem to be significant as shown by ELISA. Western blotting indeed is not a quantitative method, therefore only when the differences are dramatic as between WT and Pfizer macrophages can be easily evaluated by the presence or absence of the band of interest. This might explain why when I analysed by Western blotting IL-18 secretion in response to ATP I could not see any differences between the WT and the GSK BMDMs (Figure 3.4), while it was clear that Pfizer BMDMs produce much lower levels of IL-18. In figure 3.4 it is also shown that in response to LPS alone, both WT and GSK macrophages but not the Pfizer BMDMs are able to generate active IL-18 although the levels are much lower than the ones secreted after ATP stimulation. It is well known that LPS alone induces the release of a small amount of both IL-1β and IL-18 particularly after a prolonged stimulation of five hours. Before adding ATP to the cells, the medium containing LPS was aspirated and replaced by fresh medium with ATP. This means that the levels of both IL-1β and IL-18 produced in response of ATP have been released in only 30 minutes which is a very short time compared to five hours stimulation with LPS alone. When quantified by ELISA, the levels of IL-1β released after 30 minutes of ATP stimulation were about 10 fold higher

compared to the levels of IL-1β secreted in response to 5 hours stimulation with LPS alone (data not shown).

Effects of the P2X7R antagonist A-740003 on IL-1β secretion in response to ATP

As previously described, A-740003 is a highly selective P2X7R inhibitor and previous studies from Honore et al. have already shown that it potently blocks agonist-evoked IL-1β release in human monocytes. To confirm these data, I have analysed the effects of A-740003 on IL-1β secretion in BMDMs from WT, GSK and Pfizer mice. Being a highly selective P2X7R inhibitor, it should not affect IL-1β secretion in the GSK and Pfizer BMDM, which, for definition, should not express the receptor. However, due to the potential expression of other P2X7 splice variants in BMDMs from GSK and Pfizer mice, I decided to analyse the effects of the inhibitor also in the knock-out macrophages. As shown in figure 3.5A, treatment of WT BMDM with A-740003 dramatically affects IL-1β secretion in response to ATP. In the GSK BMDM surprisingly, the use of the inhibitor seems to slightly increase the production of IL-1β, although it seems to be more a loading issue rather than a real effect, while no effect at all was observed in Pfizer BMDMs.

Caspase-1 activation in response to ATP in WT and P2X7 deficient BMDM

A condition necessary for the release of the biologically active forms of IL-1β and IL-18 is the activation of caspase-1 which is thought to occur through an autocatalytic activity. The cleavage of the precursor leads to the generation of fragments of 20 and 10 KDa. To evaluate whether IL-1β secretion was caspase-1

dependent in WT BMDMs, I have analysed the expression of both the precursor and the active forms by Western blotting. The antibody used was able to recognise the precursor of about 50 KDa and a fragment of 10 KDa (p10). As shown in figure 3.6, a band of the predicted size of 10 KDa, corresponding to the active form of caspase-1 was detectable only in BMDMs from WT mice. WT and GSK BMDMs exhibit similar levels of pro-caspase-1, while Pfizer BMDMs show lower levels of the precursor compared to WT and GSK BMDMs. The expression of the full length P2X7R appears to be therefore required for caspase-1 activation.

Key discoveries in this chapter

To my knowledge, this is the first study in which P2X7R mediated cytokine release is analysed comparing macrophages from WT mice with the ones from two different P2X7 deficient mouse lines. ATP stimulated LPS primed BMDMs from both lines of P2X7R deficient mice release lower concentration of both IL-1β and IL-18 in comparison to macrophages from WT mice. BMDMs from GSK P2X7 deficient mice behave very differently compared to macrophages from the Pfizer ones releasing much higher levels of both IL-1β and IL-18 in response to ATP. Interestingly, when stimulated with LL-37, LPS-primed BMDMs from GSK mice release similar levels of IL-1β as macrophages from WT mice. In addition, Western blotting analysis of lysates from GSK BMDMs revealed the expression of a band of about 75 kDa using a specific anti-P2X7R antibody, which might represent a novel P2X7 splice variant with functional activity and would explain the more active phenotype of GSK macrophages compared to the Pfizer ones.

CHAPTER FOUR-INVESTIGATION OF THE SIGNALLING CASCADE FOLLOWING P2X7R ACTIVATION IN RESPONSE TO ATP

4.1 INTRODUCTION

4.2 EFFECTS OF ATP STIMULATION ON THE PHOSPHORYLATION OF ERK IN BMDM FROM WT AND P2X7 DEFICIENT MICE

Aims and experimental design

Results

4.3 EFFECTS OF ATP STIMULATION ON THE PHOSPHORYLATION OF MTOR AND S6 RIBOSOMAL PROTEIN IN BMDM FROM WT AND P2X7 DEFICIENT MICE

Aims and experimental design

Results

4.4 PHOSPHOPROTEOMIC ANALYSIS OF THE CELL SIGNALLING CASCADE FOLLOWING ATP STIMULATION IN MACROPHAGES FROM WT AND P2X7 DEFICIENT MICE

Aims and experimental design

Results

4.5 DISCUSSION

4.1 INTRODUCTION

Extracellular nucleotides such as adenosine triphosphate (ATP) have been recognised as important intercellular signals in many biological processes, including neurotransmission, muscle contraction, pain sensation and different immune responses (Bours, Swennen, Di, Cronstein, & Dagnelie, 2006). ATP represents the physiologic P2X7R agonist and many questions still remain concerning P2X7 signalling and the regulation of its activity via intracellular trafficking. It has been reported that P2X7 promotes ROS production in human monocytes through the activation of the MEK/ERK cascade (Lenertz, Gavala, Hill, & Bertics, 2009). In other studies conducted on astrocytes, application of the P2X7 agonist BzATP led to the activation of the MAP kinases ERK1, ERK2 and p38 and this effect was prevented by the use of a selective P2X7 antagonist (Panenka et al., 2001b). Historically P2X7 has been linked with apoptosis, due to the observation that prolonged application of ATP led to cell death (Schulze-Lohoff et al., 1998). However, there is now a growing literature regarding a growth promoting activity of this receptor but the exact mechanisms by which in certain condition P2X7 promotes cell proliferation are not fully understood yet (Baricordi et al., 1999). The regulation of cell proliferation is a complex process, which is primarily regulated by external growth factors provided by surrounding cells (Zhang & Liu, 2002). Two signalling pathways which have been closely linked to cell proliferation and survival are the ERK/MAPK and the mTOR pathways (Roux & Blenis, 2004; Fingar et al., 2004). The mitogen-associated protein kinases (MAPKs) are an evolutionarily conserved family of enzymes that phosphorylate target proteins both in the cytoplasm and nucleus (Kondoh, Torii, & Nishida, 2005). Four conventional MAPK pathways have been characterized: the extracellular signal-regulated kinases 1/2 (ERK1/2), the c-JUN N-terminal kinases 1-3 (JNK1-3) or stress-activated protein kinases (SAPKα, β and γ), the p38 MAPKs (p38α, β, γ and δ), and the big MAPK (BMK1/ERK5) modules (Kostenko,

Dumitriu, Laegreid, & Moens, 2011). The MAPK cascade includes many proteins which are sequencially phosphorylated such as MAPKKK (also known as Raf) and MAPKK (also known as MEK1/2) which ultimately phosphorylates p44 MAPK and p42 MAPK, also known as ERK1 and ERK2 (figure 4.1). Then the activated ERKs translocate to the nucleus and activate transcription factors such as Elk-1(E-twenty six-like transcription factor 1) and Myc, changing gene expression to promote growth, differentiation or mitosis (Costa et al., 2006). Activated ERKs can also phosphorylate cytoplasmic and nuclear kinases, for example MNK1, MNK2, MAPKAP-2, RSK, and MSK1,2 (Junttila, Li, & Westermarck, 2008). Most of the signals activating the ERK pathway are initiated through receptor-mediated activation of the small G-protein Ras, a membrane-bound protein activated through the exchange of bound GDP to GTP (McKay & Morrison, 2007). Activated Ras then recruits cytoplasmic Raf (MAPKKK) to the cell membrane for activation. The role of the MAPK signalling pathway in the regulation of cell proliferation and cell survival has been demonstrated in many in vitro and in vivo studies (Zhang & Liu, 2002). Chemical inhibition of ERK1/2 has been shown to be effective in suppressing tumor growth in a mouse model of colon cancer and ERK pathway inhibition is still considered a powerful tool in anticancer therapy (Sebolt-Leopold, 2000) (Roberts & Der, 2007). The mTOR signalling pathway was originally discovered about 15 years ago studying the mechanisms of action of the immunosuppressive agent rapamycin (Hwang, Perez, Moretti, & Lu, 2008). This highly conserved pathway represents a key regulator of cell growth and proliferation in response to environmental stimuli (Ramirez-Valle, Braunstein, Zavadil, Formenti, & Schneider, 2008). MTOR is a relatively large protein of 289-kDa that contains a catalytic domain with homology to the phosphatidylinositol-3-kinase enzymes but, instead of phosphoinositide kinase activity, mTOR is a protein kinase (Chiang & Abraham, 2004). MTOR exists in two distinct multi-protein complexes termed mTOR complex 1 (mTORC1) and mTOR complex 2 (mTORC2) (Huang & Manning, 2009). MTOR integrates stimuli from a

number of sources. These include nutrients such as glucose and aminoacids, metabolic status and growth factor-mediated signal transduction pathways (Tato, Bartrons, Ventura, & Rosa, 2011). Growth factors such as insulin, activate the PI3K class I PI3K enzymes that phosphorylate phosphatidylinositol-4,5-bisphosphate (PIP2) to produce phosphatidylinositol-3,4,5-triphosphate (PIP3) (Hietakangas & Cohen, 2007). PIP3 binds and translocates pleckstrin homology (PH) domain-bearing proteins such the phosphoinositide dependent kinase (PDK) family members and Akt. PDK1 and Akt are recruited to the membrane where PDK1 phosphorylates and activates Akt (Scheid, Parsons, & Woodgett, 2005). In turn, Akt phosphorylates the tuberous sclerosis complex 2 (TSC2) which forms a complex with tuberous sclerosis 1 (TSC1/TSC2). AKT-mediated phosphorylation of tuberous sclerosis TSC2 inhibits the TSC complex (Coleman, Marshall, & Olson, 2004). Signalling through the RAF–MEK–ERK/MAPK pathway also leads to phosphorylation and inhibition of the TSC complex (Ma, Chen, Erdjument-Bromage, Tempst, & Pandolfi, 2005). The GTPase-activating protein domain of TSC2 would otherwise drive the small GTPase Rheb into the inactive GDP-bound state (Inoki, Li, Xu, & Guan, 2003). Therefore, inhibition of the TSC complex results in Rheb activation, which signals to target of rapamycin (TOR), which, in turn, phosphorylates several proteins including S6 kinase and ribosomal protein S6 (figure 4.2).

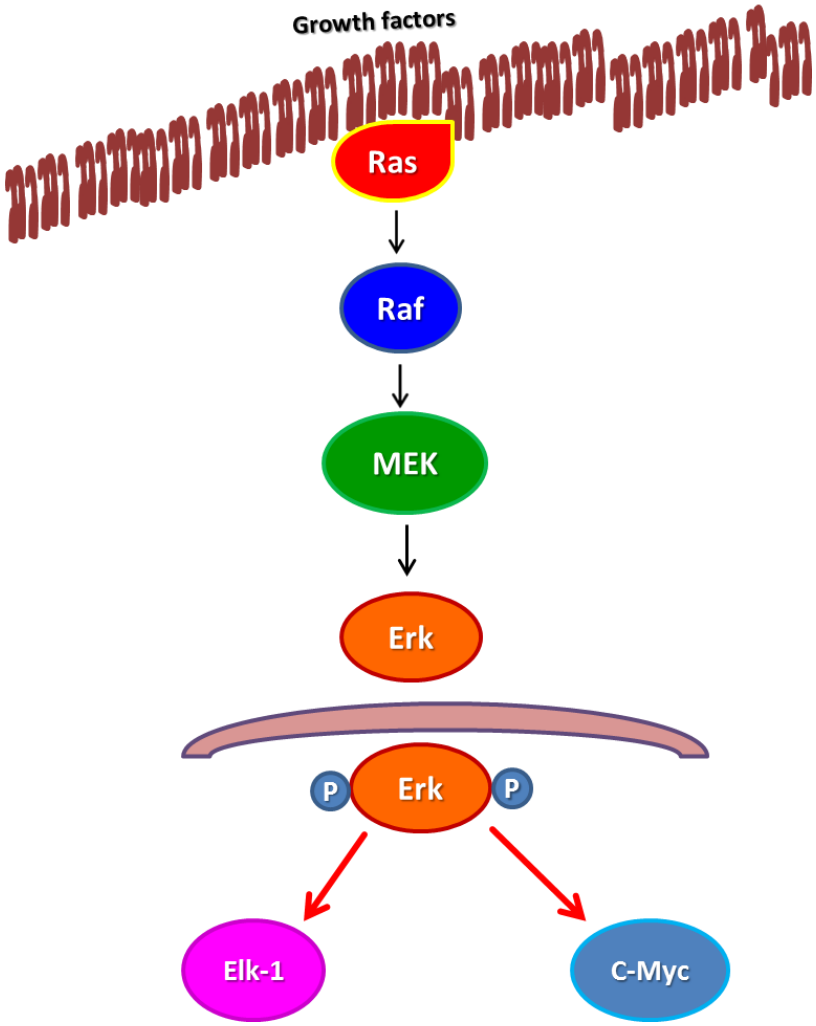

Figure 4.1A Schematic representation of the MAPK cascade.

Growth factors activate the MAPK cascade in a multistep process. The first kinase to be activated is Raf, which is activated by the GTP-binding protein Ras and in turn phosphorylates MAPKK including MEK 1 and MEK 2. Finally, the MEKs activate through phosphorylation ERK 1 and 2 which translocate to the nucleus activating transcription factors such as Elk-1 and c-myc that regulate cell cycle progression and proliferation. Figure adapted from the following article:" ERK Inhibitors as a Potential New Therapy for Rheumatoid Arthritis" (Ohori, 2008).

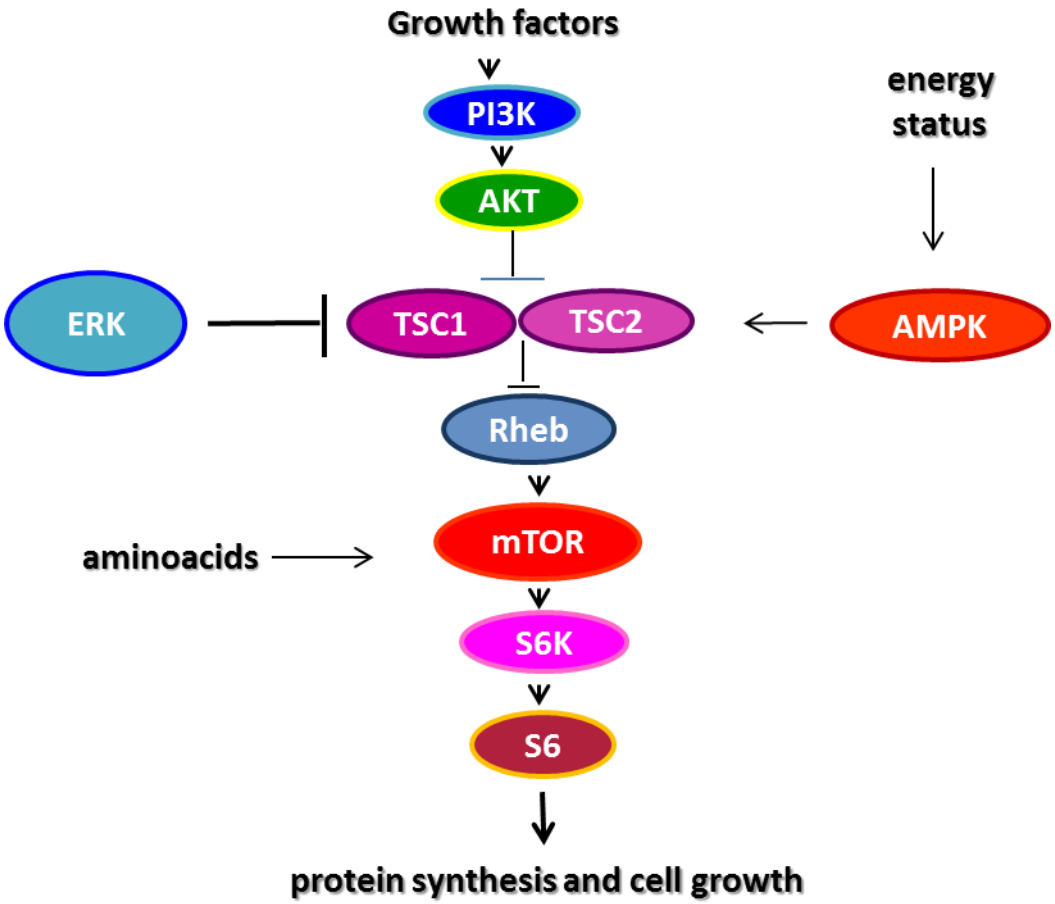

Figure 4.1B Schematic representation of the mTOR signalling pathway.

mTOR is activated by different stimuli including growth factors, hormones, amino acids and cellular energy levels. MTOR also integrates stimuli from upstream signalling pathways such as the PI3K/Akt pathway. Once activated, mTOR phosphorylates and activates downstream effectors such as S6 kinase and the ribosomal protein S6 regulating protein synthesis and cell growth. Figure adapted from the following article:" The phosphatidylinositol 3-Kinase/Akt/Mammalian target of rapamycin signaling network as a new target for acute myelogenous leukemia therapy" (Martelli et al., 2011).

4.2 EFFECTS OF ATP STIMULATION ON THE PHOSPHORYLATION OF ERK IN BMDM FROM WT AND P2X7 DEFICIENT MICE

Aim and experimental design

Activation of P2X7R has been demonstrated to induce ERK1/2 activation in microglia, monocytes and macrophages (Hide et al., 2000). Previous studies from Papp et al. have shown that ATP stimulation significantly increases p38 MAPK phosphorylation in hippocampal slices of WT mice while these effects were absent in hippocampal slices from P2X7 knock-out mice (Papp, Vizi, & Sperlagh, 2007). To confirm the role of P2X7 in the activation of ERK signalling pathway, I have stimulated primary bone marrow derived macrophages from WT, GSK and Pfizer P2X7 knock-out mice with ATP 5 mM for different times (5, 15 and 30 minutes). After 5 days of differentiation in L929 conditioned medium, macrophages were plated into six-well plates at a density of 1 x 10^6 and incubated at 37^0C for 24 hours to let them adhere. The cells were then serum starved overnight before the stimulation with ATP. Intentionally, macrophages were not primed with LPS prior to ATP treatment because it has been already reported that LPS itself increases the phosphorylation of ERK1/2 (Durando, Meier, & Cook, 1998). Furthermore, the aim of this experiment was to evaluate the effects of P2X7R activation on the phosphorylation of proteins, therefore the priming step was not required. At the end of the stimulation, the medium was aspirated and cell lysates were prepared as described in Materials and methods.

Results

As shown in figure 4.3, ATP induces a rapid and time-dependent increased phosphorylation of ERK1/2 in BMDMs from wild type mice, while no effects were seen in macrophages from both the GSK and the Pfizer P2X7 knock-out mouse lines. The highest levels of phosphorylation were seen after 15 minutes of ATP stimulation, while they start to decrease at 30 minutes.

4.3 EFFECTS OF ATP STIMULATION ON THE PHOSPHORYLATION OF MTOR AND S6 RIBOSOMAL PROTEIN IN BMDM FROM WT AND P2X7 DEFICIENT MICE

Aim and experimental design

Due to the more recent findings that P2X7R might also promote cell growth and proliferation I have also investigated the effects of ATP stimulation on the activation of another important pro-survival pathway: the mTOR signalling pathway. Many studies have documented that MTOR activity is regulated by nutrient/energy status and some studies have also proposed that mTOR directly senses ATP levels in the cell (Dennis et al., 2001). As markers of mTOR activation I have used mTOR and one of its downstream effector, the ribosomal protein S6. To date, 4 different mTOR phosphorylation sites have been described, however, a functional role for site-specific mTOR phosphorylation has not been demonstrated (Acosta-Jaquez et al., 2009). The antibody that I used for the detection of phosphorylated mTOR recognizes the phosphorylation site Serine 2448. Chiang et al. have shown that phosphorylation of mTOR at Ser 2448 is mediated by p70S6 kinase which is a downstream effector of mTOR and is in turn activated through phosphorylation by mTOR itself representing therefore a feedback signal to mTOR from its downstream target (Chiang & Abraham, 2005). Serine 2448 is also considered a nutrient regulated phosphorylation: in response to insulin becomes phosphorylated via Akt, while phosphorylation at this site is attenuated with amino acid starvation (Cheng, Fryer, Carling, & Shepherd, 2004). S6 is a protein of the 40S ribosomal subunit which plays a key role in protein synthesis (Dufner & Thomas, 1999). Phosphorylation of S6 ribosomal protein correlates with an increase in translation of mRNA transcripts that contain an oligopyrimidine tract in their 5' untranslated regions (Meyuhas & Dreazen, 2009). These particular mRNA transcripts (5'TOP) encode proteins involved in

cell cycle progression as well as ribosomal proteins and elongation factors necessary for translation (Ferrari, Bandi, Hofsteenge, Bussian, & Thomas, 1991). S6 ribosomal protein can be phosphorylated at 4 different sites: Serine 235, Serine 236, Serine 240 and Serine 241. All these phosphorylation sites are located within a small, carboxy-terminal region of the S6 protein (Flotow & Thomas, 1992). The antibody I used for detection of phosphorylated S6 recognizes Serine 235 and Serine 236 phosphorylation sites.

Results

As shown in figure 4.3, ATP stimulation leads to a time dependent increased phosphorylation of mTOR in macrophages from WT mice, while only a mild increase was seen after prolonged exposure in macrophages from the two P2X7 deficient mouse lines. ATP also induces a time dependent increased phosphorylation of S6 both in macrophages from WT and P2X7 deficient mice, however the levels of phosphorylation were much higher in the wild tipe macrophages compared to macrophages from P2X7 knock-out mice. The macrophages from the GSK knock-out mouse line show higher levels of phosphorylated S6 compared to macrophages from the Pfizer P2X7 deficient mice.

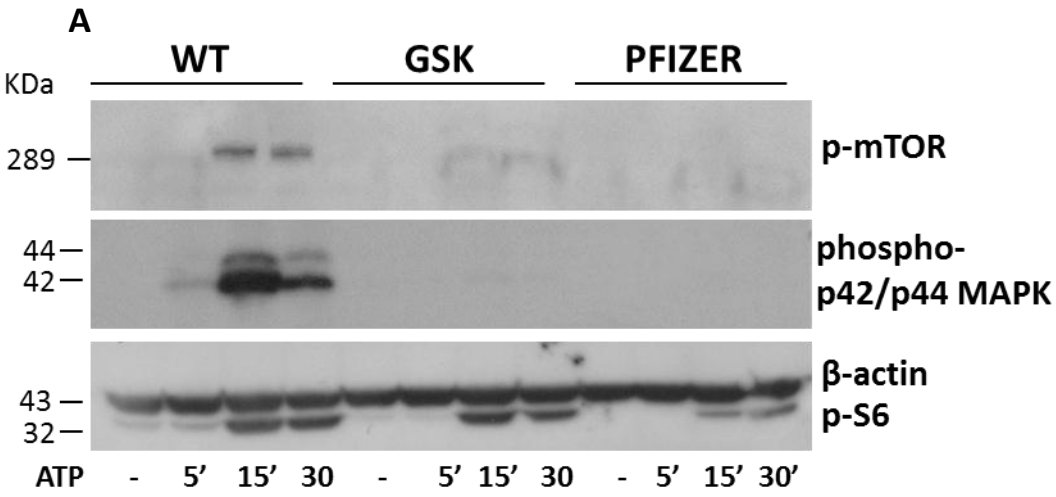
A
WT
GSK
PFIZER
KDa
289
p-mTOR
44
42
phospho-
p42/p44 MAPK
43
32
β-actin
p-S6
ATP - 5' 15' 30 - 5' 15' 30 - 5' 15' 30'

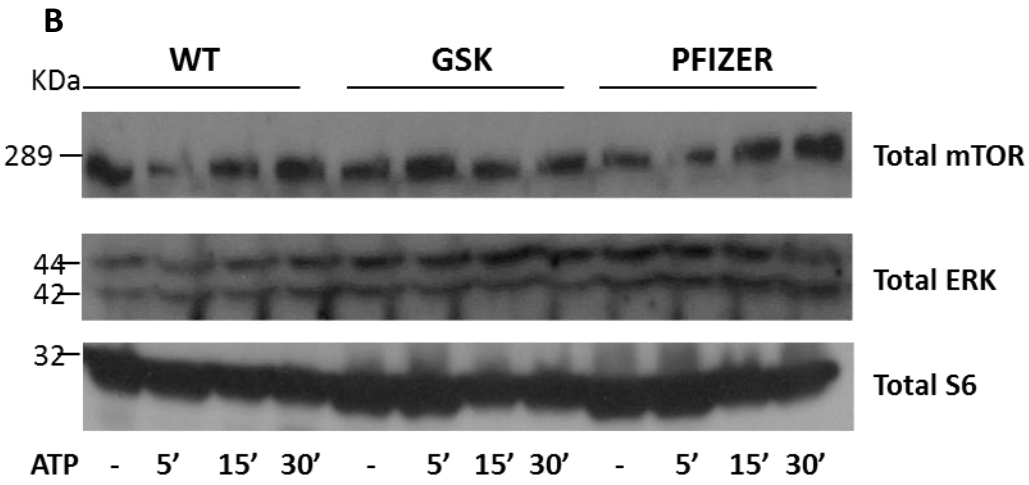
B
WT
GSK
PFIZER
KDa
289
Total mTOR
44
42
Total ERK
32
Total S6
ATP - 5' 15' 30' - 5' 15' 30' - 5' 15' 30'

C

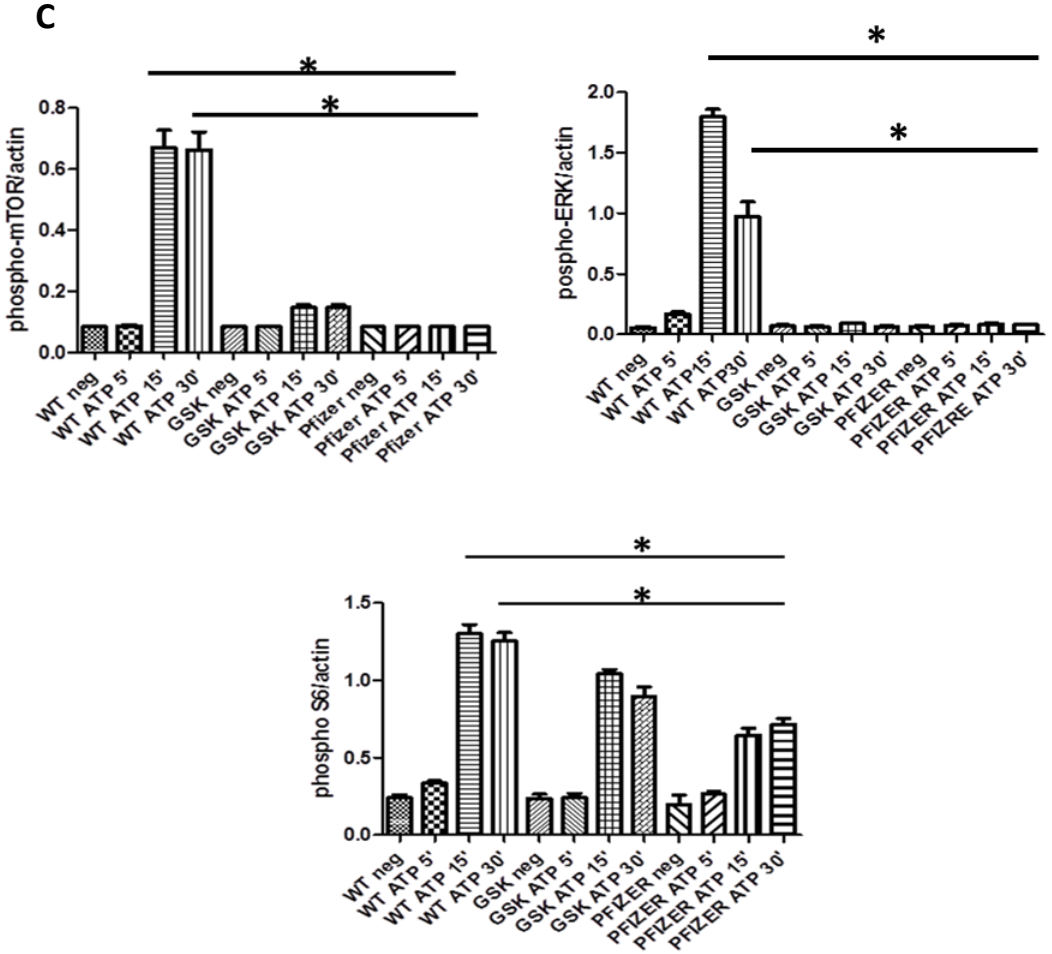
phospho-mTOR/actin
0.0
0.2
0.4
0.6
0.8
*
*
WT neg
WT ATP 5'
WT ATP 15'
WT ATP 30'
GSK neg
GSK ATP 5'
GSK ATP 15'
GSK ATP 30'
Pfizer neg
Pfizer ATP 5'
Pfizer ATP 15'
Pfizer ATP 30'
pospho-ERK/actin
0.0
0.5
1.0
1.5
2.0
*
*
WT neg
WT ATP 5'
WT ATP15'
WT ATP30'
GSK neg
GSK ATP 5'
GSK ATP 15'
GSK ATP 30'
PFIZER neg
PFIZER ATP 5'
PFIZER ATP 15'
PFIZRE ATP 30'
phospho S6/actin
0.0
0.5
1.0
1.5
*
*
WT neg
WT ATP 5'
WT ATP 15'
WT ATP 30'
GSK neg
GSK ATP 5'
GSK ATP 15'
GSK ATP 30'
PFIZER neg
PFIZER ATP 5'
PFIZER ATP 15'
PFIZER ATP 30'

Figure 4.3 A, B and C. Effects of ATP stimulation on the phosphorylation of mTOR, p42/p44 MAPK and S6 ribosomal protein.

BMDMs from WT and P2X7 knock-out mice (GSK and Pfizer) were plated into six-well plates at a density of 1x 10^6 cells per well, serum starved overnight and stimulated with or without ATP 5 mM at the indicated time points. Aliquots of protein (20 μg) from cell lysates were separated by gel electrophoresis and transblotted to PVDF membrane. Detection of phospho-mTOR (Ser 2448), phospho-p42/p44 MAPK and phospho-S6 (Ser 235-236) **(A)** and of their correspondent total forms **(B)** was performed by Western blotting using specific antibodies from New England Biolabs (UK). The blots are representative of at least n=3 independent experiments. **(C)** Quantification by Western blot densitometry for p-mTOR, pERK and pS6 as indicated. *P<0.05 Student paired T test for indicated comparisons.

4.4 PHOSPHOPROTEOMIC ANALYSIS OF THE CELL SIGNALING CASCADE FOLLOWING ATP STIMULATION IN MACROPHAGES FROM WT AND P2X7 DEFICIENT MICE

Aim and experimental design

Protein phosphorylation controls many basic cellular processes, such as cell growth, differentiation, migration, metabolism, and cell death, and its study can provide key insights into the signal transduction pathways that are activated in cells in response to different stimuli (Cohen, 2002). This post-translational modification is controlled by two families of proteins: kinases and phosphatases, which add or remove the phosphate group, respectively (Montoya et al., 2011). Recently, quantitative proteomics has emerged as a powerful tool to study cell signalling on a proteome-wide scale (de la Fuente van Bentem, Mentzen, de la Fuente, & Hirt, 2008). Compared to western blotting which typically focus on one protein at a time, the phosphoproteomic approach has the advantage of studying many phosphoproteins and phosphorylation sites at once (Jensen, 2006). Furthermore, the phosphoproteomic approach provides a quantitative analysis of the proteins that are phosphorylated and on the level of phosphorylation, compared to western blotting which is a semiquantitative technique (Schmelzle & White, 2006). The questions I wanted to answer using the mass-spectrometry based phosphoproteomic approach were two: 1) which are the signalling pathways that are activated in response to ATP stimulation and 2) which are the pathways that are regulated selectively by P2X7R. To answer these important questions, I stimulated BMDMs from WT and from the two P2X7 deficient mouse strains GSK and Pfizer with or without ATP 5 mM using three different time points: 5, 15 and 30 minutes. In order to reduce as much as possible the basal levels of protein phosphorylation and to syncronize the cells, I have serum starved them for 12 hours. Due to the high protein concentration

required (500 μg) for mass spectrometry analysis, I collected bone marrow cells from three different mice per strain. After five days of differentiation in L929 medium, cells were counted and seeded into 100 mm culture dishes at a density of 5 x 10^6 cells per condition. At the end of the stimulation, I aspirated the medium and washed the cell layers with cold PBS. I then collected the cells by scraping and centrifuge them at 4 ^{0}C for five minutes at 15000 x g. Cell pellets were then stored in -80^0 C until further analysis.

Results

The number of phosphoserine- or phosphothreonine-containing peptides detected by mass-spectrometry was 1271. The level of phosphorylation of these peptides was mostly low under basal conditions and increased after stimulation with ATP. The phosphorylation levels at time zero were generally similar between macrophages from the three mouse strains. However, some peptides showed high basal phosphorylation levels in WT BMDMs and low in the P2X7 deficient ones and vice versa. In many cases more than one peptide within the same protein were phosphorylated. To compare the levels of phosphorylation of peptides at different time points and between macrophages from the 3 mouse strains a heat map has been generated (figure 4.4A) in which the colour intensity correlates with the level of phosphorylation of each protein or peptide. To investigate P2X7R involvement in the phosphorylation of these peptides, I have analyzed and compared the phosphorylation levels between macrophages from the three mouse strains both under basal conditions and after ATP treatment. The analysis of the phosphorylation levels under basal conditions of the 1271 phospho-peptides detected by mass-spectrometry, revealed that 31 were significantly different between WT and P2X7 KO BMDMs. Interstingly, 16 peptides were much more highly phosphorylated in both GSK and Pfizer

macrophages (table 4.2), while 15 resulted more phosphorylated in the WT ones (table 4.1). Among the peptides that showed higher basal phosphorylation levels in WT compared to P2X7 KO macrophages, several of them belong to proteins that play an important role in translation such as the eukaryotic translation initiation factors 4 gamma and beta, Pre-mRNA 3' end processing factor Fip1, High mobility group protein HMG-I/HMG-Y and Heterogeneous nuclear ribonuclear proteins C1/C2 (Khaleghpour, Pyronnet, Gingras, & Sonenberg, 1999), (Du & Maniatis, 1994). Other peptides that exhibit higher phosphorylation levels in macrophages from WT mice compared to the ones from P2X7 deficient mice belong to proteins involved in cytoskeleton organization and cell migration including, Microfibrillar associated protein 1 and Marcks related protein 1 (Finlayson & Freeman, 2009). The peptides that were more phosphorylated in P2X7 deficient macrophages belong to proteins with very different biological functions. These include proteins involved in the translation process such as the La-related protein 1 (LARP-1) and Pumilio homolog 2 (Burrows et al., 2010). The latter is a sequence-specific RNA-binding protein that regulates translation and mRNA stability by binding the 3'-UTR of mRNA targets (Burrows et al., 2010), (Jenkins, Baker-Wilding, & Edwards, 2009). Some peptides belong to proteins that regulate cell cycle progression such as E3 ubiquitin protein ligase Rbbp6 also called Retinoblastoma binding protein 6. This protein interacts with both p53 and pRb, and has been identified as an E3 ubiquitin ligase due to the presence of a RING finger domain. It has been shown that RBBP6 promotes the degradation of p53, thereby increasing cell proliferation (Motadi, Bhoola, & Dlamini, 2011). Another protein that appears to be more phosphorylated in P2X7 KO macrophages under basal conditions is the regulator of G protein signalling 14 (RGS 14), a member of the G protein signalling family, which has been shown to act as accelerator of Gα-mediated GTP hydrolysis but it has also been reported that RGS14 facilitates the formation of a selective Ras-GTP-Raf-MEK-ERK multiprotein complex to promote sustained

ERK activation which is critical for neuronal cell differentiation (Willard et al., 2009). Serine/threonine-protein kinase ULK1 is also highly phosphorylated in P2X7 KO macrophages. This kinase is involved in autophagy, a homeostatic process by which cells adapt to nutrient starvation breaking down their own components (Levine, Mizushima, & Virgin, 2011). Ulk1 has been shown to act both as a downstream effector and negative regulator of mammalian target of rapamycin complex 1 (mTORC1) (Kim, Kundu, Viollet, & Guan, 2011). More than 30 different signalling pathways were activated in response to ATP, the most activated ones are summarized in table 4.3. Among them, the MAPK pathway appears to be the most important one with a total of 20 proteins involved. The phosphorylated proteins that belong to the MAPK signalling pathway are listed in table 4.4. To establish the relative contribution of P2X7R in the activation of the MAPK pathway, I have compared the phosphorylation levels of proteins involved in this pathway in WT and P2X7 deficient BMDMs both under basal conditions and after stimulation with ATP. As shown in figure 4.4.D, ATP stimulation leads to an increase phosphorylation of Protein phosphatase 3, Stathmin and Tao kinase 3 only in WT BMDMs, while in macrophages from both GSK and Pfizer knock-out mice the phosphorylation levels of these proteins remained the same as when unstimulated. These results indicate that P2X7R is playing a key role in this process. Protein phosphatase 3, also called calcineurin, is a key signaling molecule which has been shown to be involved in diverse types of physiological processes (Bandyopadhyay et al., 2002). It is a calcium dependent serine/threonine phosphatase which is known to regulate the transcription of the T-cell growth factor and interleukin-2 as well as to mediate the dephosphorylation of the transcription factor NF-ATp (nuclear factor–activated T cells), an important step necessary for the translocation of NF-AT from the cytoplasm to the nucleus, where it induces the transcription of various immune response genes in T lymphocytes as well as genes with diverse functions in other cell types (Sanna, Bueno, Dai, Wilkins, & Molkentin, 2005).

Stathmin is a ubiquitous, highly conserved 18-kDa cytoplasmic protein which triggers the depolymerization of microtubules into short tubulin oligomers and has been shown to be a critical regulator of cell migration and cell cycle progression through its control of interphase microtubule dynamics and the assembly of the mitotic spindle (Ng, Zhao, Yeap, Ngoei, & Bogoyevitch, 2010). Tao (Thousand and one amino acids) kinase 3 is known to act upstream of MAPKs activating p38 MAPK in response to DNA damage. TAO kinases have been implicated in regulation of cytoskeleton stability, G protein-coupled receptor signaling to p38, and cell survival (Hutchison, Berman, & Cobb, 1998), (Chen et al., 2003). Other proteins such as Fas death domain associated protein, Mitogen associated kinase 8, and Phospholipase A2 showed higher phosphorylation levels in WT BMDMS compared to the GSK and Pfizer ones, however also macrophages from P2X7 deficient mice exhibit an increased phosphorylation in response to ATP suggesting that other purinergic receptors might contribute to the phosphorylation of these proteins (figure 4.4.E). Interestingly, JunD appeared to be more phosphorylated in the knock-out BMDMs compared to the WT ones following ATP stimulation, which might suggest that P2X7R negatively regulates JunD phosphorylation in response to ATP (figure 4.4 E). However, it is important to consider that phosphorylation does not necessarily mean activation. Many proteins, indeed, become inactivated when phosphorylated. Among the signalling pathways that appear to be more activated in response to ATP stimulation is the mTOR signalling pathway. Nine peptides within this pathway showed an increased phosphorylation after treatment with ATP in macrophages from WT and P2X7 deficient mice (figure 4.4F). Apart from AKT1 and Ribosomal protein S6 kinase which shows higher phosphorylation levels in response to ATP in WT BMDMs, all the other peptides surprisingly were more phosphorylated in macrophages from P2X7 deficient mice (figures 4.4F and 4.4G). One other important signalling pathway that appears to be activated by ATP is the ribosome pathway with 15

phosphorylated peptides. Interestingly, all these peptides showed an increased phosphorylation following ATP stimulation only in macrophages from WT mice and not in the P2X7 deficient ones (figures 4.4H and 4.4J). This is a very important finding which clearly demonstrates a fundamental role of P2X7R in the regulation of the translation process. Many other proteins showed an increased phosphorylation only in macrophages from WT mice after treatment with ATP. Some of these proteins are implicated in endocytic membrane trafficking such as intersectin 1 which is known to regulate the formation of clathrin-coated vesicles (Pechstein et al., 2010). As shown in figure 4.4K intersectin 1 appears to be phosphorylated in two different sites in response to ATP and in both of them an increased phosphorylation occurred only in WT BMDMs. Two other proteins that participate in vesicular transport from the endoplasmic reticulum to the Golgi complex, Bet 1 and COG3, showed an increased phosphorylation in response to ATP stimulation only in WT BMDMs confirming the important role of P2X7R in the regulation of vesicle transport (Zhang & Hong, 2001) (figure 4.4L).

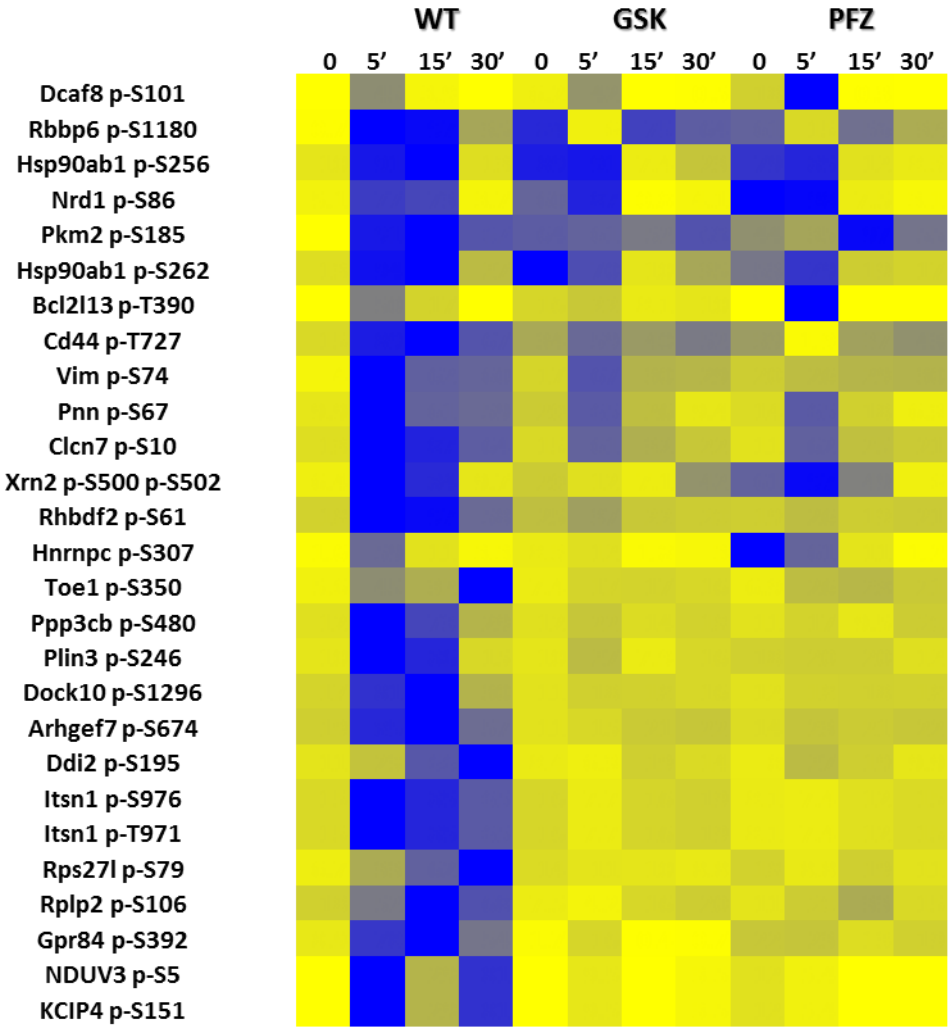

Figure 4.4A Heat map of phosphorylated peptides in BMDMs from WT and P2X7 deficient mice treated with or without ATP.

The phosphorylation data obtained by mass spectrometry analysis were used to generate a heat map. Each column of the heat map represents one time point of the time course experiment and the colour intensity correlates to the intensity (log ratio) of the phosphorylation of each peptide at the specified time point, with blue representing the highest level of phosphorylation and yellow the lowest one.

Peptide/protein	Phosphorylation site
Osteopontin 1	S263
Marcks related protein 1	T86
Eukaryotic translation initiation factor 4 gamma	S1190
Heterogeneous nuclear ribonuclear proteins C1/C2	S233
Heat Shock Protein 105 KDa	S811
Eukaryotic initiation translation factor 4b	S407
Pre-mRNA 3' end processing factor Fip1	S281
High mobility group protein HMG-I/HMG-Y	S100
Pleckstrin	S118
Calpastatin	S445
Hepatoma derived growth factor related protein 2	S367-S368
Myosin regulatory light chain RLC-a	T20-T21
Microfibrillar associated protein 1	S117-S119
Probable ATP dependent RNA helicase Ddx46	S805
Histone deacetylase 1	S422-S424

Table 4.1 List of peptides/proteins showing higher basal phosphorylation levels in WT macrophages compared to the P2X7 deficient ones.

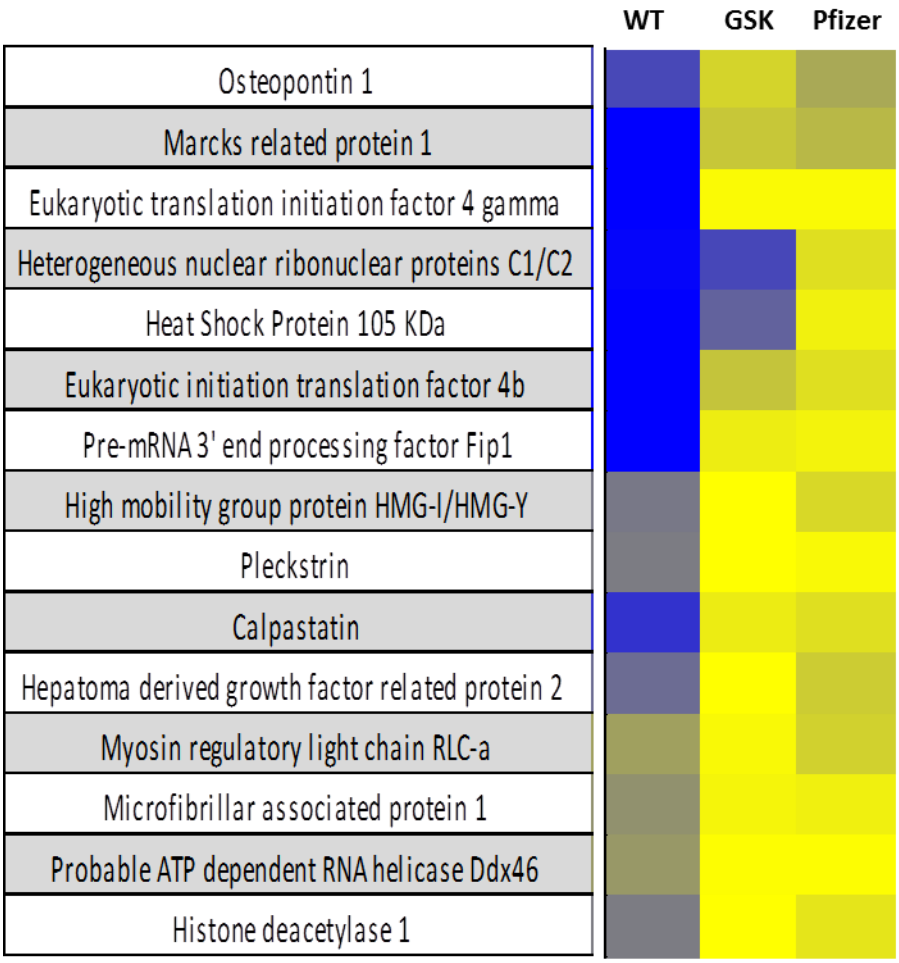

Figure 4.4B Heat map representing the differences in basal phosphorylation levels of peptides between WT and P2X7 deficient macrophages.

Peptide/protein	Phosphorylation site
Pyruvate dehydrogenase E1 component subunit alpha	S233
Protein transport protein Sec61 subunit beta	S18
Cullin 4a	S11
Myosin9	S1944
Phosphoacetylglucosamine mutase3	T63
Heat shock protein HSP 90 beta	S256
E3 ubiquitin protein ligase Rbbp6	S1180
Nardilysin 1	S86
Pumilio homolog 2	S137
La related protein1	S69
NAD kinase	S65
DNA Ligase 1	S52
Regulator of G protein signalling 14	S290
Receptor expression enhancing protein 4	S153
Proteasome subunit alpha type 3	S251
Serine-threonine protein kinase Ulk1	S638

Table 4.2 List of peptides showing higher basal phosphorylation levels in P2X7 deficient macrophages compared to the WT ones.

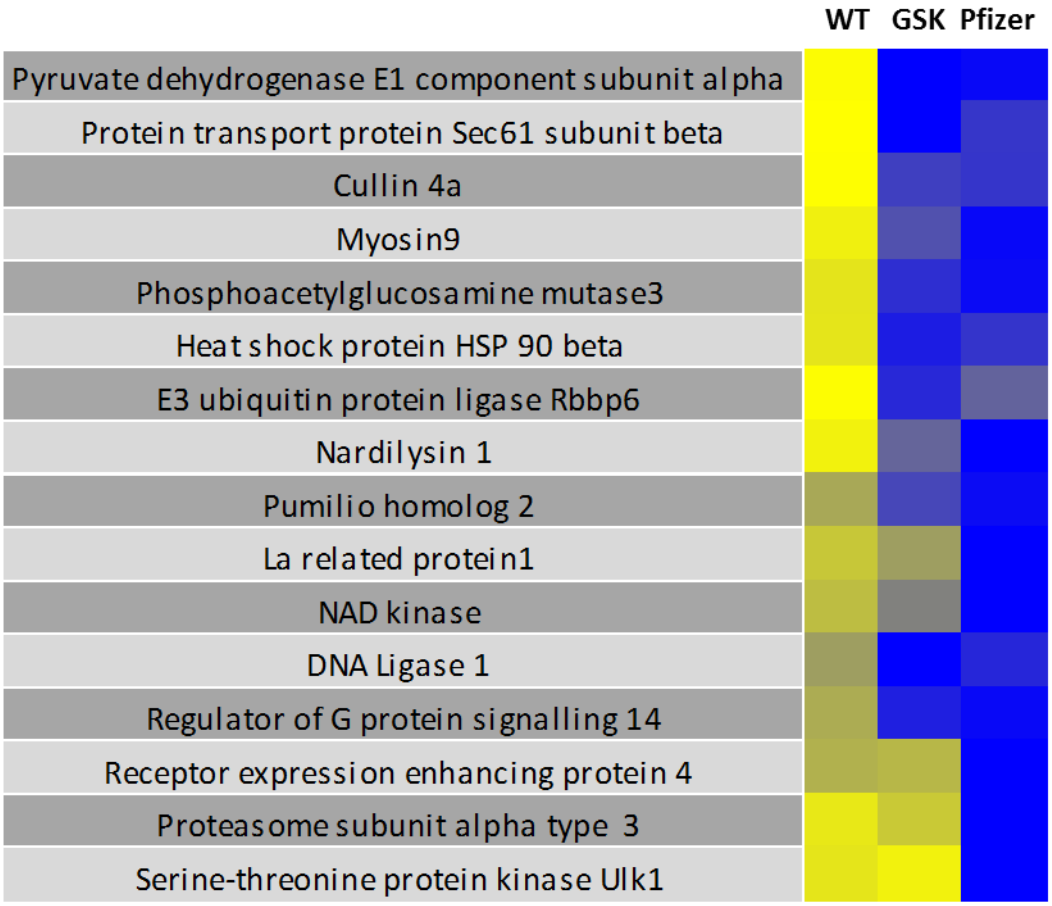

Figure 4.4C Heat map representing the differences in basal phosphorylation levels of peptides between WT and P2X7 deficient macrophages.

Pathway	Number of phosphorylated peptides/proteins
MAPK signalling pathway	20
Fc-gamma receptor mediated phagocytosis	18
Insulin signalling pathway	16
Chemokine signalling pathway	16
Endocytosis	16
Ribosome	15
Regulation of actin cytoskeleton	15
B cell receptor signalling pathway	10
Apoptosis	10
Toll-like receptor signalling pathway	10
T cell receptor signalling pathway	10
mTOR signalling pathway	9
Phosphatidylinositol signalling system	9

Table 4.3 Signalling pathways activated in BMDMs from WT and P2X7 deficient mice in response to ATP.

Mass spectrometry analysis of BMDMs from WT and P2X7 deficient mice revealed that in response to ATP stimulation 35 signalling pathways were activated. Here are represented the most activated ones with the number of phosphorylated peptides within each pathway.

DAXX_MOUSE	Fas death domain-associated protein
JUND_MOUSE	Jun proto-oncogene related gene d
TAOK3_MOUSE	TAO kinase 3
FLNA_MOUSE	filamin, alpha
GBG12_MOUSE	guanine nucleotide binding protein (G protein), gamma 12
NEMO_MOUSE	inhibitor of kappaB kinase gamma
M3K1_MOUSE	mitogen-activated protein kinase kinase kinase 1
M3K2_MOUSE	mitogen-activated protein kinase kinase kinase 2
M3K7_MOUSE	mitogen-activated protein kinase kinase kinase 7; predicted gene 8188
M3K8_MOUSE	mitogen-activated protein kinase kinase kinase 8
NFAC2_MOUSE	nuclear factor of activated T-cells, cytoplasmic, calcineurin-dependent 2
NFKB1_MOUSE	nuclear factor of kappa light polypeptide gene enhancer in B-cells 1, p105
PAK2_MOUSE	p21 protein (Cdc42/Rac)-activated kinase 2
PA24A_MOUSE	phospholipase A2, group IVA (cytosolic, calcium-dependent)
KPCB_MOUSE	protein kinase C, beta
PP2BB_MOUSE	protein phosphatase 3, catalytic subunit, beta isoform
KS6A1_MOUSE	ribosomal protein S6 kinase polypeptide 1
KS6A3_MOUSE	ribosomal protein S6 kinase polypeptide 3
STMN1_MOUSE	stathmin 1; predicted gene 11223; predicted gene 6393
AKT1_MOUSE	thymoma viral proto-oncogene 1; similar to serine/threonine protein kinase

Table 4.4 List of peptides/proteins belonging to the MAPK signalling pathway that show an increased phosphorylation in response to ATP in macrophages from WT and P2X7 deficient mice.

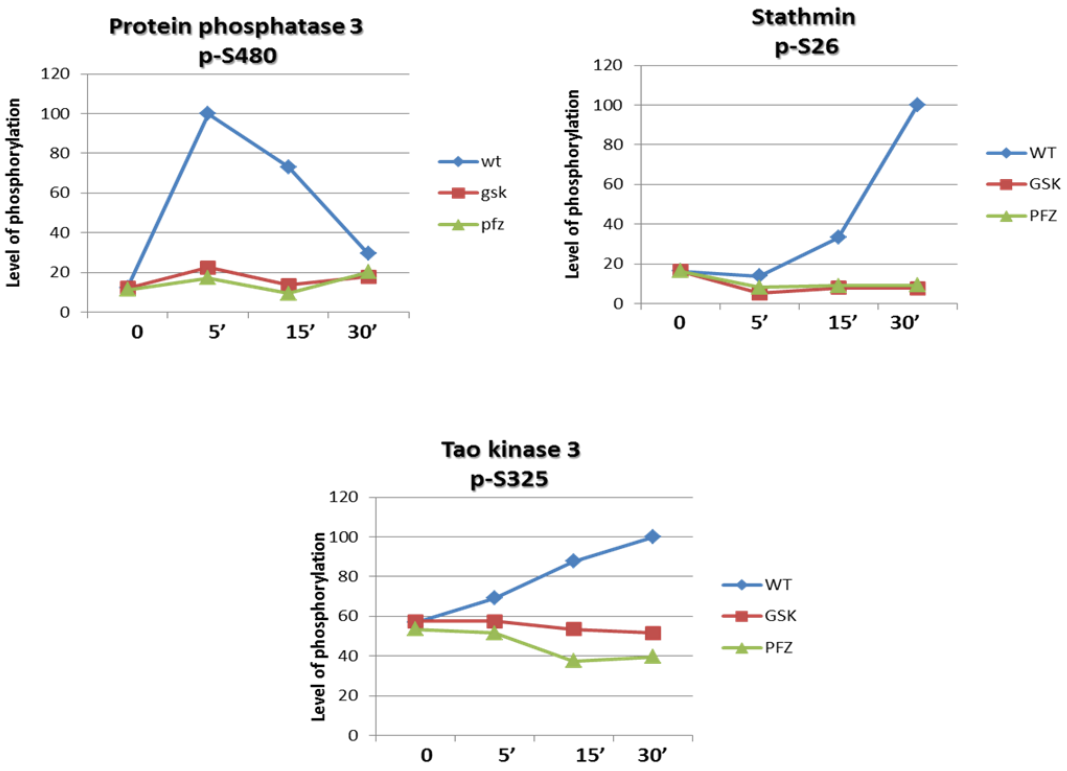

Figure 4.4D Phosphorylation of Protein phosphatase 3, Stathmin and Tao kinase 3 (members of the MAPK pathway) in response to ATP in macrophages from WT and P2X7 deficient mice.

ATP stimulation led to an increased phosphorylation of Protein phosphatase 3, Stathmin and Tao kinase 3 in WT BMDMs, while both GSK and Pfizer P2X7R deficient macrophages showed similar levels of phosphorylation as under basal conditions.

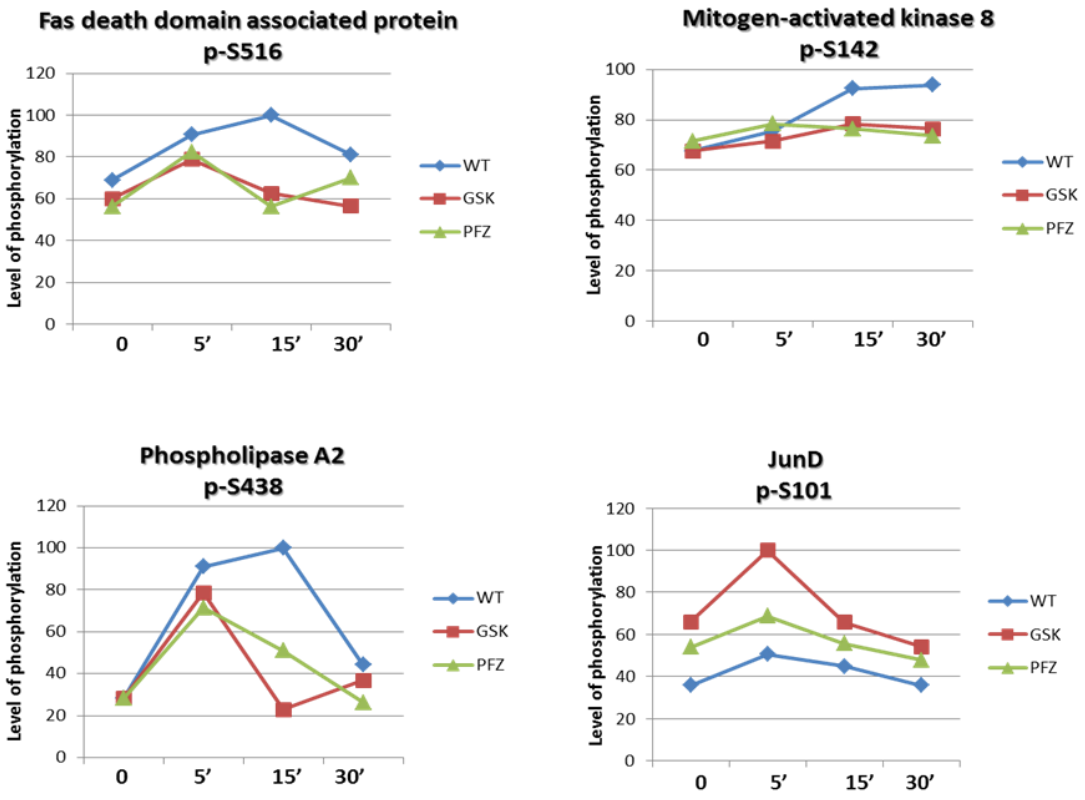

Figure 4.4E Phosphorylation of Fas death domain associated protein, Mitogen-activated kinase 8, Phospholipase A2 and Jun D proteins in response to ATP in BMDMs from WT and P2X7 deficient mice.

In response to ATP, WT BMDMs showed higher phosphorylation levels of Fas death domain associated protein, Mitogen-activated kinase 8 and Phospholipase A2 compared to GSK and Pfizer BMDMs. JunD was more phosphorylated in GSK and Pfizer macrophages compared to the WT ones.

GENE ID	PHOSPHORYLATED PEPTIDES/PROTEINS
PDPK1_MOUSE	3-phosphoinositide dependent protein kinase-1
ULK1_MOUSE	Unc 51- like kinase 1 (C.elegans)
IF4B_MOUSE	Eukaryotic translation initiation factor 4B
PI3R5_MOUSE	Phosphoinositide- 3-kinase, regulatory subunit 5, p101
RS6_MOUSE	Ribosomal protein S6
RPTOR_MOUSE	Regulatory associated protein of mTOR, complex 1
KS6A1_MOUSE	Ribosomal protein S6 kinase, polypeptide 1
KS6A3_MOUSE	Ribosomal protein S6 kinase, polypeptide 3
AKT1_MOUSE	Thymoma viral proto-oncogene 1; similar to serine/threonine protein kinase

Table 4.5 List of peptides/proteins belonging to the mTOR signalling pathway that show an increased phosphorylation in response to ATP in macrophages from WT and P2X7 deficient mice.

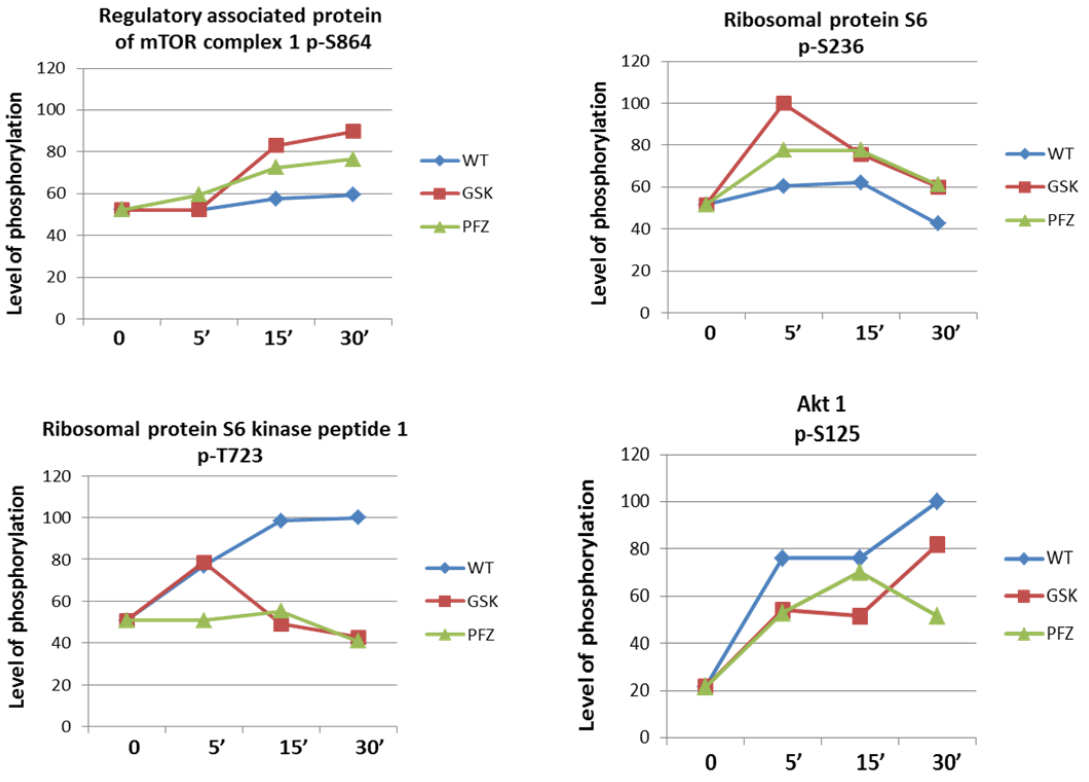

Figure 4.4F Levels of phosphorylation of different peptides belonging to the mTOR signalling pathway in response to ATP in WT and P2X7 deficient BMDMs.

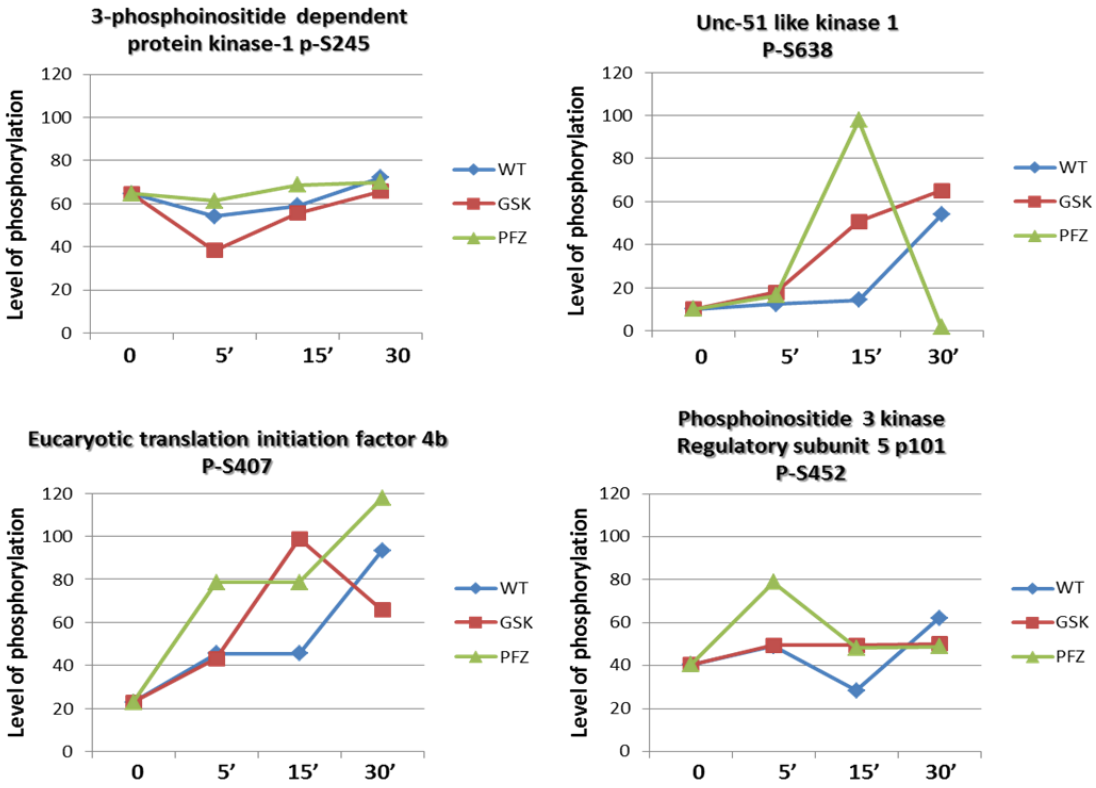

Figure 4.4G Phosphorylation levels of different peptides belonging to the mTOR signalling pathway in response to ATP in WT and P2X7 deficient BMDMs.

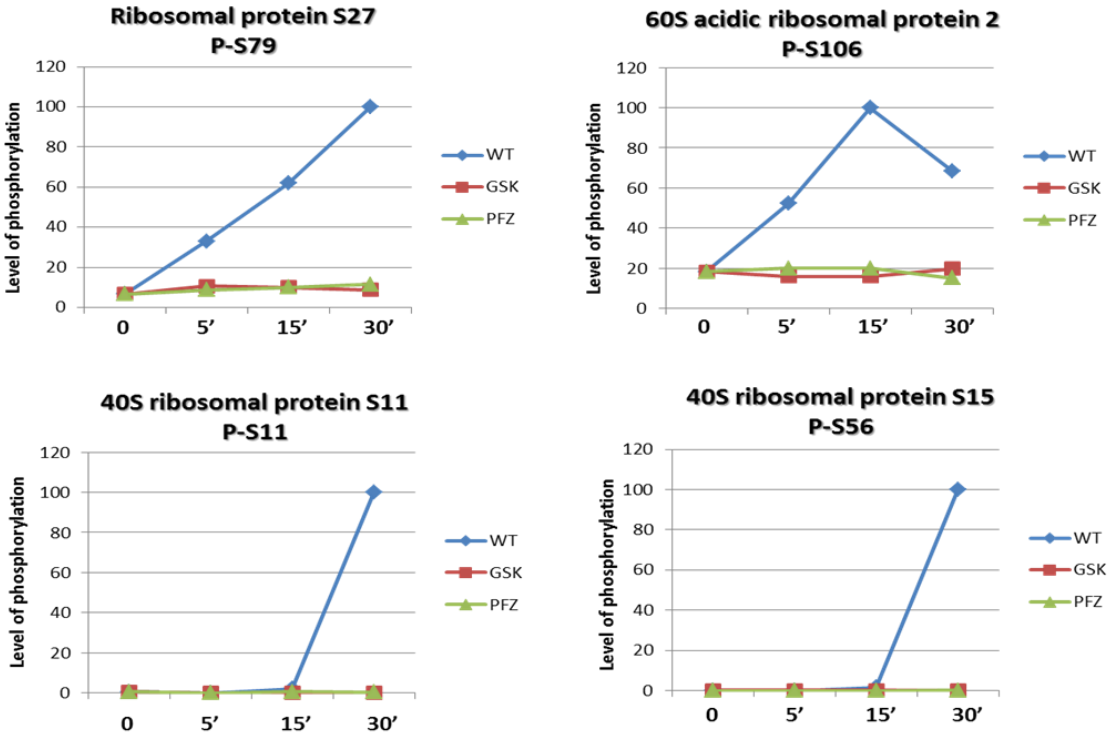

Figure 4.4H Phosphorylation levels of ribosomal proteins in WT and P2X7 deficient BMDMs in response to ATP.

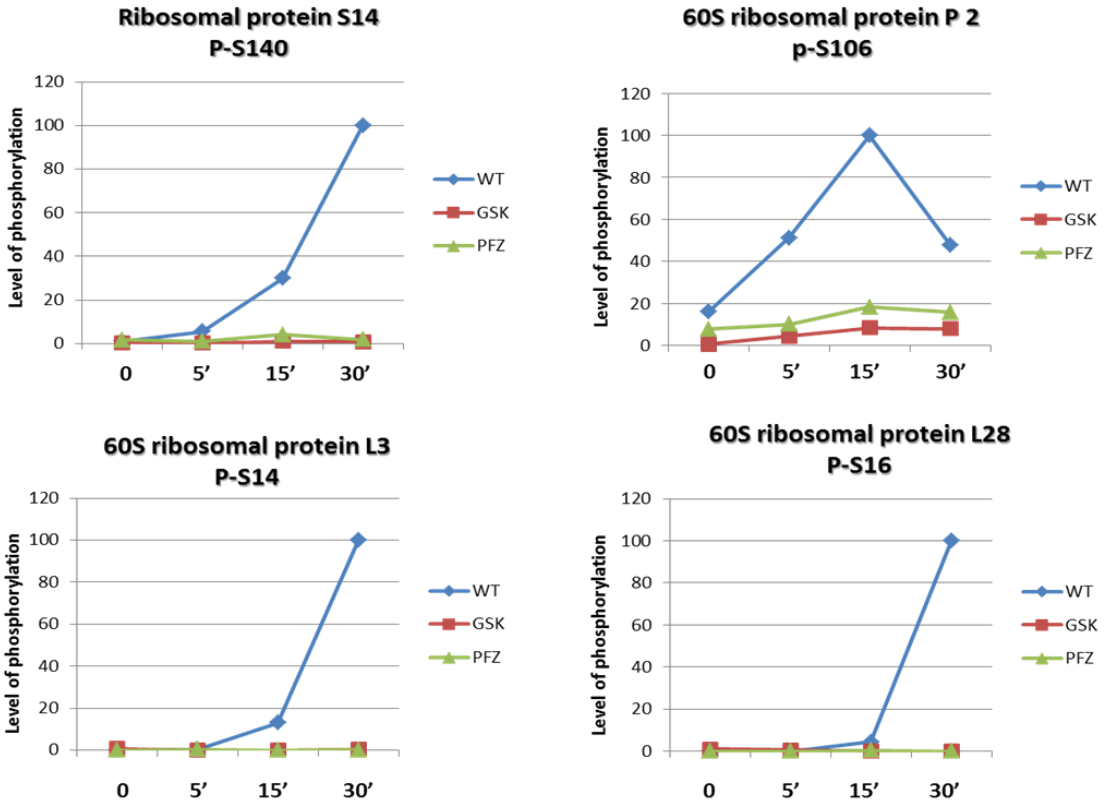

Figure 4.4J Phosphorylation levels of ribosomal proteins following ATP stimulation in macrophages from WT and P2X7 deficient mice.

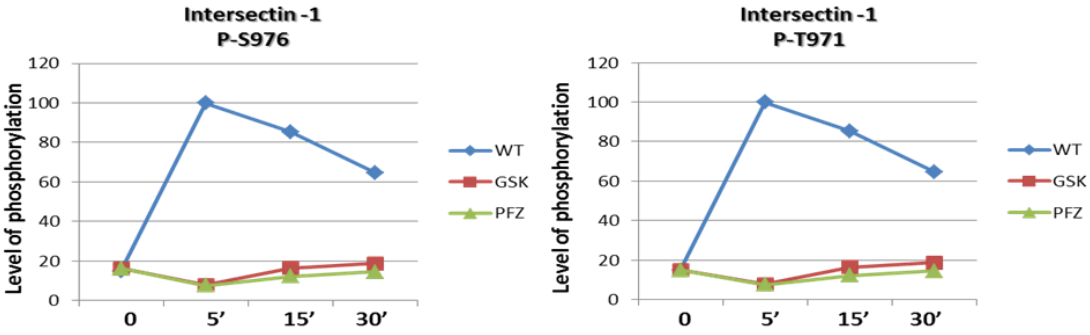

Figure 4.4K Intersectin-1 phosphorylation levels in response to ATP stimulation in BMDMs from WT and P2X7 deficient mice.

ATP stimulation leads to an increased phosphorylation of intersectin-1 at two different sites only in BMDMs from WT mice. GSK and Pfizer macrophages exhibit similar levels of phosphorylation as when unstimulated.

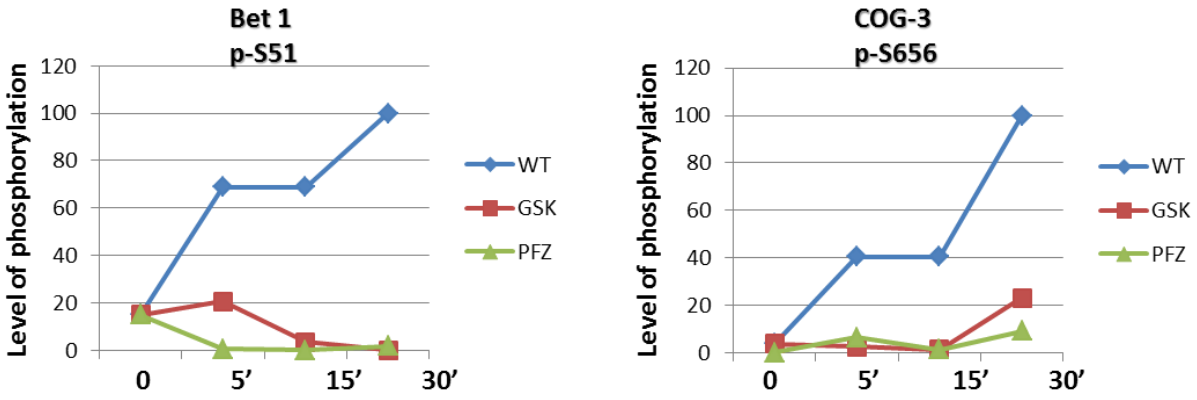

Figure 4.4L Bet-1 and COG-3 phosphorylation levels in response to ATP in BMDMs from WT and P2X7 deficient mice.

4.5 DISCUSSION

My studies led me to the following conclusions:

According to the Western blotting results

1. ATP stimulation leads to a time dependent increased phosphorylation of ERK1/2 in macrophages from WT mice, while no increase was seen in macrophages from both GSK and Pfizer P2X7 deficient mice.
2. ATP induces a greater time dependent increased phosphorylation of mTOR (Ser 2448) in BMDMs from WT mice compared to macrophages from P2X7 knock-out mice.
3. ATP increases the phosphorylation of S6 ribosomal protein (Ser 235-236) in macrophages from WT and P2X7 deficient mice in a time dependent manner, however the levels of phosphorylation were much higher in macrophages from the WT mice compared to the P2X7 knock-out ones.

According to the mass spectrometry analysis

1. A thousand two hundred and 71 peptides were phosphorylated in macrophages from WT and P2X7 deficient mice both under basal conditions and after treatment with ATP.
2. Under basal conditions, the majority of peptides exhibited low phosphorylation levels which were similar in macrophages from the three mouse strains.
3. Among the 1271 phosphorylated peptides, 31 showed significantly different basal phosphorylation levels between WT and P2X7 KO macrophages: 16 appeared to be much more phosphorylated in P2X7 KO macrophages, whereas 15 showed higher basal phosphorylation levels in the WT ones.
4. Thirty five distinct signalling pathways were activated in macrophages from WT and P2X7 deficient mice.

5. The signalling pathway that appears to be the most activated one with 20 different phosphorylated peptides involved is the MAPK pathway.

6. Among the phosphorylated proteins belonging to the MAPK pathway, Protein phosphates 3, Stathmin and Tao kinase 3 showed an increased phosphorylation following ATP treatment only in macrophages from WT mice, while BMDMs from both GSK and Pfizer KO mice exhibited similar levels as when unstimulated.

7. Other proteins within the MAPK signalling pathway such as Fas death domain associated protein, Phospholipase A2 and Mitogen activated kinase 8 showed an increased ATP dependent phosphorylation both in macrophages from WT mice and in the ones from P2X7 deficient mice, however the levels of phosphorylation were higher in WT BMDMs compared to the KO ones.

8. JunD (Ser101) showed higher levels of phosphorylation after treatment with ATP in macrophages from P2X7 deficient mice, compared to the ones from WT mice.

9. ATP stimulation induced the activation of the mTOR signalling pathway, leading to an increased phosphorylation of nine peptides. Among them, only S6 kinase and Akt showed higher levels of phosphorylation in macrophages from WT mice compared to the ones from P2X7KO mice. All the other peptides appeared to be more phosphorylated in macrophages from the P2X7 deficient mice.

10. ATP strongly activated the ribosome pathway, leading to an increased phosphorylation of 15 different peptides.

11. All the peptides belonging to the ribosome pathway exhibited an ATP dependent increased phosphorylation only in macrophages from WT mice and not in BMDMs from the two P2X7 deficient mouse strains.

12. Several proteins involved in the regulation of vesicle transport and actin cytoskeleton organization, such as Bet1 and COG3 showed an increased

phosphorylation following ATP treatment only in macrophages from WT and not P2X7 KO mice.

Analysis of the cell signalling cascade following P2X7R activation by ATP

My Western blotting results clearly demonstrate an important role of P2X7R in the activation of the MAPK signalling pathway. Indeed, only macrophages from WT mice show an increased phosphorylation of ERK1/2 in response to ATP, while no effects at all were seen in both GSK and Pfizer macrophages. Several studies have established that extracellular nucleotides acting via P2X7R can induce the activation of the MAPK signalling pathway. Papp et al. have shown that ATP treatment significantly increases p38 MAPK phosphorylation in hippocampal cells from WT mice, and these effects were absent in the hippocampal cells of P2X7R KO mice (Papp et al., 2007). Another study from Noguchi et al. also revealed that ATP induces an increased phosphorylation of p38 MAPK in Raw 264.7 cells and that this effect is completely abolished by the use of a selective P2X7 antagonist (Noguchi et al., 2008). Further studies from Bradford et al. also showed that exposure of parotid acinar cells to ATP and the P2X7 agonist BzATP produced time-dependent increases in ERK1/2 activity (Bradford & Soltoff, 2002). My Western blotting results appear to be therefore in accordance with these studies.

Phosphoproteomic analysis

The data obtained by mass spectrometry analysis confirm the ability of ATP to activate the MAPK signalling pathway and more importantly reveal that among the 35 different signalling pathways activated in response to ATP the MAPK pathway was the most activated one with 20 different proteins showing an increased phosphorylation in response to the treatment. However, surprisingly nor p38 MAPK nor p42/p44 were among the phosphorylated proteins detected.

One possible explanation could be that the instrument settings for mass-spectrometry analysis were not appropriate for the detection of these phosphorylated proteins. The instrument was set to select the five most abundant multiply charged ions present in the survey spectrum, therefore it is possible that both p38 and p42/p44 were not included in this selection. In this case, additional runs of the samples extending the spectrum of analysis are necessary to detect phospho-ERK and phospho-p44/42. Furthermore, among the 20 phosphorylated proteins belonging to the MAPK pathway, three of them (Calcineurin or Protein phosphates 3, Stathmin and Tao kinase 3) showed an increase phosphorylation following ATP treatment only in macrophages from WT mice. This clearly indicates that P2X7R is playing an important role in this process and its expression is needed for the increased phosphorylation to occur. Interestingly, the family of Tao kinases have been shown to activate p38 MAPK in response to DNA damage and other stimuli (Raman et al., 2007). Other proteins within the MAPK signalling pathway such as Phospholipase A2 showed an increased phosphorylation in response to ATP in macrophages from both WT and P2X7 deficient mice. However, macrophages from WT mice exhibited higher levels of phosphorylation suggesting that P2X7 is playing a role but other purinergic receptors expressed by macrophages from P2X7 KO mice might also contribute to this process. Several studies have previously shown that ATP induces phospholipase A2 activation. One study conducted on ductal cells of rat submandibular gland, showed that ATP activates phospholipases A2 in these cells and that the response to ATP was inhibited by the nonselective P2X purinergic antagonist suramin (Alzola et al., 1998). My results appear to be in accordance with these studies and demonstrate that P2X7R is certainly involved in this process, however it is very likely that other purinergic receptors are also contributing to Phospholipase A2 activation. In their study Alzola et al. indeed, showed that Phospholipase A2 activation was blocked by the use of suramin, which is known to inhibit not only P2X7R but all purinergic receptors. My

Western blotting results also reveal that ATP activates the mTOR signalling pathway leading to an increased phosphorylation of mTOR (Ser 2448) and ribosomal protein S6 (Ser 235-236). Both mTOR and S6 showed higher levels of phosphorylation in macrophages from WT mice compared to macrophages from P2X7 deficient mice. The data obtained by mass spectrometry analysis confirm that the mTOR signalling pathway is activated in response to ATP and nine peptides within the pathway resulted phosphorylated. Among them, only S6 kinase and Akt showed higher levels of phosphorylation in macrophages from WT mice compared to the ones from P2X7KO mice. All the other peptides appeared to be more phosphorylated in macrophages from the P2X7 deficient mice. Surprisingly also S6 ribosomal protein, differently from what shown by Western blotting, exhibited higher levels of phosphorylation in macrophages from both GSK and Pfizer KO mice compared to the WT ones. Taken together these findings seem to indicate that either P2X7R contribution to the activation of the mTOR signalling pathway is marginal compared to the role of other purinergic receptors or that P2X7R might in some circumstances act as a negative regulator of this pathway. However, the interpretation of these data is not so straight forward. Indeed, phosphorylation does not necessarily mean activation. Furthermore, the mTOR signalling pathway, regulating very important cellular processes such as proliferation, migration and translation, is a very complex pathway with many proteins involved and in response to different stimuli, some branches of the pathway will be upregulated while others downregulated. Therefore it is possible that P2X7R might play a central role in some of the mTOR biological functions and at the same time being a negative regulator of others. Another important signalling pathway activated by ATP is represented by the ribosomal pathway. Fifteen peptides within the ribosomal pathway showed an increased phosphorylation following ATP stimulation. All of these peptides interestingly, showed an increased phosphorylation in response to ATP treatment only in macrophages from WT mice suggesting that P2X7R

plays a key role in the regulation of this pathway. P2X7R appear to have a fundamental role also in vesicle transport as the majority of the phosphorylated proteins involved in this process were selectively upregulated in macrophages from WT mice compared to the ones from P2X7 KO mice. Several studies have previously shown that P2X7 regulates vesicle formation and trafficking (Solini et al., 1999; Gutierrez-Martin et al., 2011). An extensive study on P2X7R-mediated effects on membrane composition and trafficking in the plasma membrane has been conducted by Qu et al. who have demonstrated that P2X7R regulates multiple types of membrane trafficking responses including transfer of Phosphatidyl serine to the extracellular leaflet of the plasma membrane, shedding of plasma membrane surface proteins, plasma membrane microvesicle release and transfer of endosomal contents to the cytosolic compartment (Qu & Dubyak, 2009). Furthermore, several proteins involved in actin cytoskeleton organization such as vimentin, plastin 2, stathmin and phostensin showed much higher levels of phosphorylation in macrophages from WT mice compared to BMDMs from P2X7 deficient mice suggesting that P2X7R is also having an important role in this process.

Limitations of the phosphoproteomic analysis

Despite the great progress that mass spectrometry-based phosphoproteomics has made in the analysis of protein phosphorylation and molecular signaling in cells, it is still a considerable challenge due to the low stoichiometry of protein phosphorylation and the resulting low abundance of phosphopeptides. The isolation of phosphopeptides represents a key step in the entire phosphoproteome analysis and current isolation methods cannot always guarantee a high efficiency, selectivity, sensitivity and reproducibility due to the nature of the heterogeneous environment and nonlinear binding dynamics when dealing with extremely low abundant phosphopeptides. This important

limitation of the phosphoproteomic approach needs to be taken into account when interpreting the results of a study and might explain the inconsistency of some results from one run to the next. The results of the phosphoproteomic analysis presented in this thesis in some cases show a poor consistency. Some peptides for example show an increased phosphorylation after 5 minutes stimulation with ATP, then the phosphorylation levels go back to basal levels after 15 minutes to finally go up again after 30 minutes stimulation. Other peptides have very high basal phosphorylation levels, then the phosphorylation levels dramatically drop after 5 minutes stimulation with ATP, go up again after 15 minutes to finally drop after 30 minutes. On the other hand, when the effect of ATP stimulation on the phosphorylation of peptides within the ribosomal pathway was analysed, all the peptides showed the same pattern of phosphorylation, revealing low basal phosphorylation levels and a progressive time-dependent increase in macrophages from WT mice while macrophages from the two P2X7 deficient lines, starting from similar basal levels of phosphorylation, did not show any increase after ATP stimulation. The inconsistency of some of the findings clearly indicates that in order to guarantee data's accuracy and reproducibility, the same sample should be run several times and a single experiment cannot therefore lead to unequivocal conclusions.

Key discoveries in this chapter

To my knowledge, this is the first time quantitative phosphoproteomics has been used to analyse the cell signalling cascade following P2X7R activation by ATP. Furthermore, the specific P2X7R contribution to the activation of the different signalling pathways has been investigated comparing macrophages from WT mice with the ones from two different P2X7 deficient lines. Taken

together my data appear to demonstrate for the first time a crucial role for P2X7R in the regulation of ribosomal activity as well as in vesicle transport and cytoskeleton organization. In addition, my data show that P2X7R contributes to the activation of other important signalling pathways, including MAPK and mTOR, indicating also an important role for this receptor in the regulation of cell growth and proliferation.

CHAPTER FIVE-ACTIVATION OF THE INFLAMMASOME PATHWAY IN BMDM FROM WKY AND LEWIS RATS

5.1 INTRODUCTION

5.2 BMDM FROM WKY RATS SHOW AN UPREGULATION OF THE MAJORITY OF THE INFLAMMASOME-RELATED GENES COMPARED TO THE LEWIS BMDM

Aim and experimental design

Results

5.3 BMDM FROM WKY RATS EXHIBIT HIGHER LEVELS OF P2X7 PROTEIN AND RELEASE SIGNIFICANT HIGHER LEVELS OF ACTIVE IL-1 BETA, IL-18 AND CASPASE-1 IN RESPONSE TO ATP COMPARED TO LEWIS RATS

Aim and experimental design

Results

5.4 CASPASE-1 INHIBITION DRAMATICALLY AFFECTS BOTH IL-1B AND IL-18 SECRETION IN BMDM FROM WKY RATS

Aim and experimental design

Results

5.5 NEPHRITIC GLOMERULI FROM WKY RATS SHOW HIGHER LEVELS OF P2X7 PROTEIN AND ACTIVE IL-1 BETA, IL-18 AND CASPASE 1 COMPARED TO LEWIS GLOMERULI

Aim and experimental design

Results

5.6 ANALYSIS OF THE INFLAMMASOME ACTIVATION IN BMDM FROM CONGENIC RAT STRAINS

Aims an experimental design

Results

5.7 ROLE OF JUND IN THE REGULATION OF THE INFLAMMASOME ACTIVATION

Aims an experimental design

Results

5.8 DISCUSSION

5.1 INTRODUCTION

Several studies have shown that, in the rat model of nephrotoxic nephritis (NTN), the Wistar-Kyoto (WKY) rat is markedly susceptible to crescentic glomerulonephritis (CRGN), as injection of a small dose of nephrotoxic serum, that is subnephritogenic in many other strains tested, leads to rapid onset of nephrotoxic nephritis, characterised by the development of albuminuria by day 4, crescent formation in at least 80% of glomeruli by day 11 and progression to severe scarring, leading to renal failure within 6 weeks (Tam et al., 1999; Smith et al., 2007; Maratou et al., 2011). In contrast Lewis (LEW) rats, which share the same MHC haplotype (RT1-l), when injected with the same dose of nephrotoxic serum, develop only mild glomerular hypercellularity with no crescents at all (Smith et al., 2007). Isome et al. have demonstrated the predominant role of macrophages in inducing glomerular injury in CRGN, representing the major cell type in the glomerular infiltrate and their accumulation correlating with the degree of histological and functional injury (Isome et al., 2004). Several phenotypic differences have been identified between BMDM from WKY rats and those from LEW rats including enhanced antibody-dependent cytotoxicity, Fc receptor-mediated phagocytosis and Fc-receptor-dependent oxidative burst, as well as increased inducible nitric oxide synthase gene (Nos2) expression upon LPS stimulation (Behmoaras et al., 2008). Further studies from Smith et al. (Smith et al., 2007) have shown that the susceptibility to crescent formation can be transferred through bone marrow transplants so that Lewis rats that receive bone marrow from WKY rats develop crescents but fewer compared to WKY rats unmanipulated or receiving isologous bone marrow. Aitman et al. have conducted a genome-wide linkage analysis of an F2 population derived from WKY and LEW rats and mapped seven CRGN quantitative trait loci (QTL) indicated as Crgn1-7 linked to crescent formation, proteinuria or macrophage infiltration (Aitman et al., 2006). The two most significant linkage peaks were

identified on chromosomes 13 (Crgn1) and 16 (Crgn2) respectively. Within the CRgn1 region, deletion of an Fc receptor gene, Fcgr3-rs, has been recognised as a cause of macrophage over-activity and CRGN susceptibility (Behmoaras et al., 2010), while the CRgn2 region contains the AP-1 transcription factor JunD which is markedly upregulated in the WKY rat which explains the enhanced macrophage oxygen burst activity as well as increased iNOS synthesis and WKY susceptibility to CRGN (Behmoaras et al., 2008). Single and double congenic rat strains have been then generated by Behmoaras et al. introgressing either Crgn1 or Crgn2 or both congenic intervals together, from Lew rats onto a WKY genetic background. After injection of nephrotoxic serum, introgression of LEW Crgn2 into the WKY recipients reduced glomerular crescents by 8%, and the single phenotypic effect of LEWCrgn1 corresponded to a reduction of 18%. Introgression of both LEW Crgn1 and Crgn2 into the WKY genetic background reduced glomerular crescents by 34%, demonstrating a synergistic effect of both Crgn loci on glomerular crescent formation (Behmoaras et al., 2010). The identification of the quantitative trait loci Crgn1 and Crgn2 however, only partly explained the susceptibility of WKY rats to CRGN. Indeed, the double-congenic strain still exhibits significant glomerular crescent formation, indicating that other genetic loci are playing a role. Therefore, in view of the already demonstrated role of P2X7R in glomerulonephritis and due to the high reproducibility of the rat model of nephrotoxic nephritis, I decided to investigate the P2X7-mediated inflammasome activation in bone marrow derived macrophages from WKY and LEW rats.

5.2 BMDM FROM WKY RATS SHOW AN UPREGULATION OF THE MAJORITY OF THE INFLAMMASOME-RELATED GENES COMPARED TO THE LEWIS BMDM

Aim and experimental design

To assess whether there was any differences in the P2X7-mediated inflammasome activation between BMDMs from WKY and LEW rats, I have initially examined by Real-Time PCR the expression in these cells, under basal conditions, of several genes involved in the inflammasome pathway including P2X7, pro-IL-1β and its physiological inhibitor IL-1RN (IL-1β receptor antagonist), pycard (ASC), pro-caspase-1, pro-IL-18 and its inhibitor IL-18 binding protein (IL-18 bp). BMDMs from double congenic (DC) rats were also included in the analysis.

Results

As shown in figure 5.2 A and B, under basal conditions, BMDMs from WKY and DC rats exhibit a marked upregulation of the majority of the inflammasome-related genes analysed compared to BMDMs from LEW rats. In particular, the most significant differences in genes expression between WKY and LEW BMDMs were related to P2X7, IL-18, IL-18 binding protein and IL1 receptor antagonist. No differences were seen in the expression of pro-IL-1β between the three rat strains. BMDMs from DC rats show similar IL-18, IL-18 bp and pro-caspase-1 mRNA levels compared to WKY BMDMs. Interestingly, DC BMDMs express higher P2X7 and IL1RN mRNA levels compared to WKY BMDM, although the

difference was not statistically significant. Macrophages from LEW rats express higher NLRP3 mRNA levels compared to WKY and DC ones.

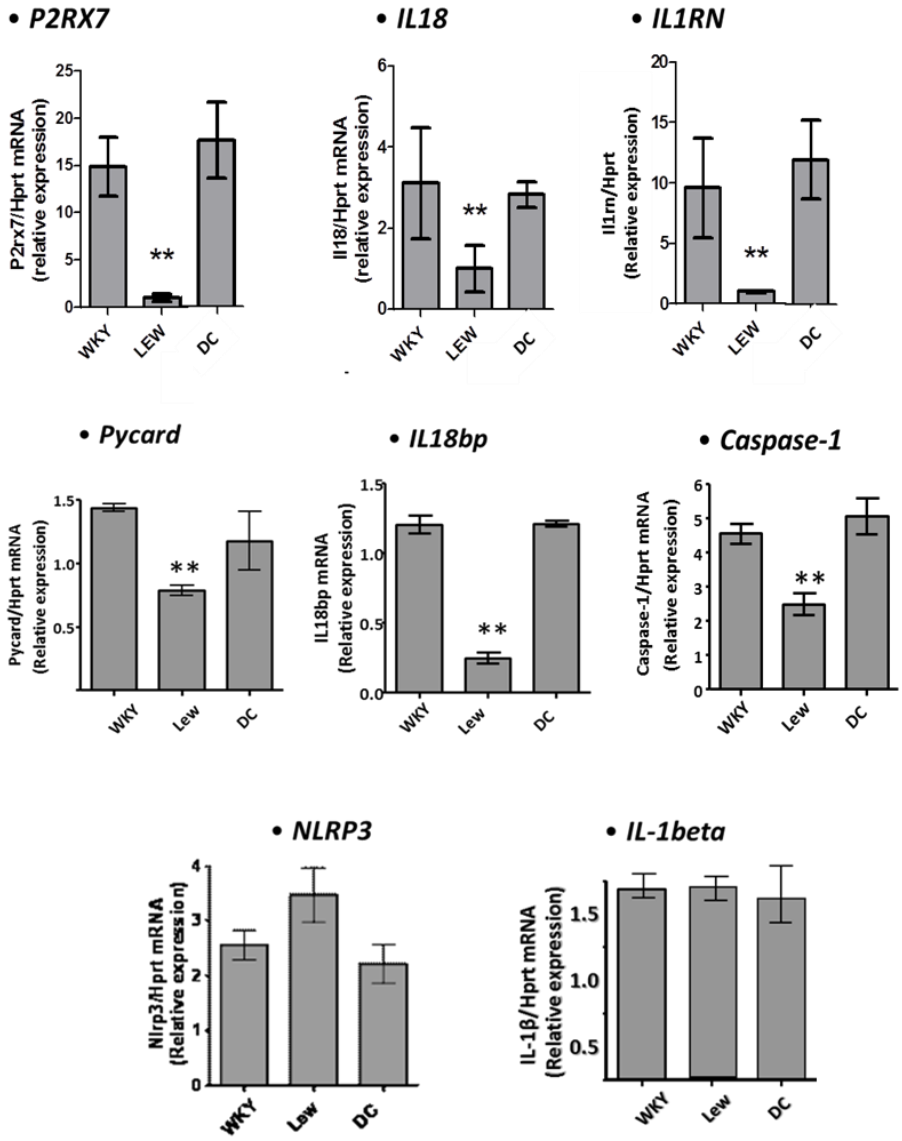

Figure 5.2A Inflammasome-related genes expression in BMDMs from WKY, DC and LEW rats.

Expression of mRNA encoding P2X7R, IL-18, IL-1β receptor antagonist, pycard, IL-18 binding protein, caspase 1, NLRP3 and IL-1β in BMDMs from WKY, DC and LEW rats under basal conditions. Mean expression at each time point is expressed as a ratio to that of the housekeeping gene HPRT.

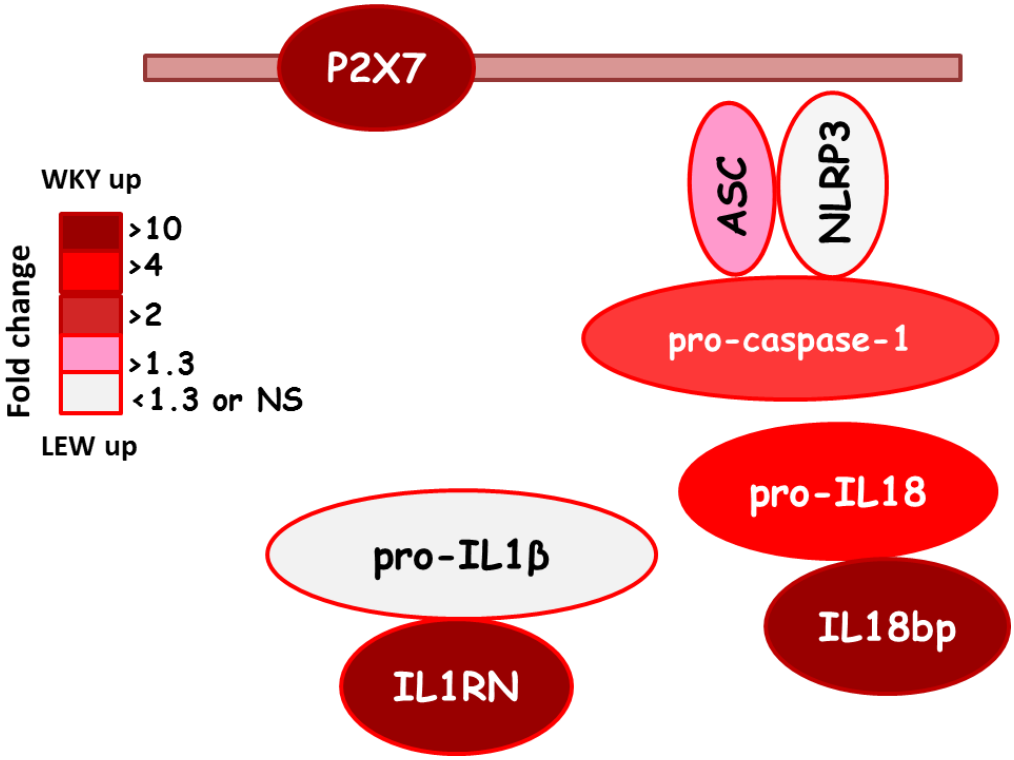

Figure 5.2B Schematic diagram showing the differences in inflammasome-related genes expression under basal conditions between WKY and LEW BMDMs.

5.3 BMDM FROM WKY RATS EXHIBIT HIGHER LEVELS OF P2X7 PROTEIN AND RELEASE SIGNIFICANT HIGHER LEVELS OF ACTIVE IL-1 BETA, IL-18 AND CASPASE-1 IN RESPONSE TO ATP COMPARED TO LEWIS RATS

Aim and experimental design

In view of the RT-PCR results which reveal a marked upregulation of P2X7 gene in WKY and DC BMDM compared to the LEW ones, I have first analysed P2X7 protein expression in these cells both under basal conditions and after 5 hours stimulation with LPS 1μg/ml. P2X7 protein expression was also examined in glomeruli isolated 4 days after the injection of nephrotoxic serum which were then cultured for 72 hours in serum free medium. Previous studies have shown that day four from the injection of nephrotoxic serum is the day of maximal macrophage accumulation and also maximal P2X7R expression (Turner et al., 2007). In order to quantitatively examine and compare the levels of IL-1β released by BMDM from WKY and LEW rats in response to ATP, I have primed these cells with LPS for 5 hours using two different concentrations: a lower concentration of 100 ng/ml and a higher one of 1 μg/ml. The priming step was followed by stimulation with ATP 5 mM for 30 minutes. Supernatants were then collected and analysed by sandwich ELISA (RatIL-1β DuoSet ELISA kit R&D systems). Given the results of this experiment, which will be discussed in details in the results paragraph, all the other experiments were conducted using a concentration of LPS of 1 μg/ml as priming stimulus. Western blotting was used to detect both the precursors and the active forms of IL-1β, IL-18 and caspase-1. Furthermore, to establish whether the increased IL-1β and IL-18 secretion observed in WKY BMDM were due to an increase production of the precursors pro-IL-1β and pro-IL-18 in response to LPS priming, process that is controlled by the NF-κB pathway, I have examined the levels of both pro-IL-1β and pro-IL-18 in

the cell extracts from WKY, DC and LEW BMDM after treatment with LPS alone and LPS + ATP.

Results

As shown in figure 5.3 (A and B), under basal conditions WKY and DC BMDMs show similar levels of P2X7 receptor, while no band of the predicted size of 75 KDa was detected in LEW BMDMs. After 5 hours stimulation with LPS 1 μg/ml, the WKY macrophages exhibit higher levels of P2X7 protein compared to DC BMDMs, while again no band was detected in the LEW ones. Quantitavive analysis by ELISA of IL-1β secretion in response to ATP in BMDMs from WKY and LEW rats which were primed with either LPS 100ng/ml or LPS 1 μg/ml revealed that in both conditions WKY macrophages produce significant higher levels of IL-1β compared to LEW BMDMs (5.3C). The difference appears to be even greater when I used the lowest concentration of LPS. Interestingly, when primed with LPS 100 ng/ml, LEW BMDMs produce similar levels of IL-1β in response to ATP as when treated with LPS alone, while in WKY macrophages ATP stimulation leads to a tenfold increase in IL-1β levels compared to the levels observed when stimulated with LPS alone. Western blotting analysis of supernatants from WKY, DC and LEW macrophages shows that in response to ATP, LPS primed BMDMs from WKY rats show higher levels of active IL-1β, IL-18 and caspase-1 compared to both DC and LEW BMDMs (figure 5.3 D, E and F). Macrophages from DC rats release higher levels of active IL-1β, IL-18 and caspase-1 compared to LEW BMDMS but lower than WKY ones. The analysis of the expression of pro-IL-1β and pro-IL-18 in the cell extracts revealed no differences between BMDMs from WKY, DC and LEW rats (figure 5.3G and 5.3H), indicating that the increased

secretion of mature IL-1β and IL-18 in WKY BMDMs is not due to an increase synthesis of the precursors within the cell.

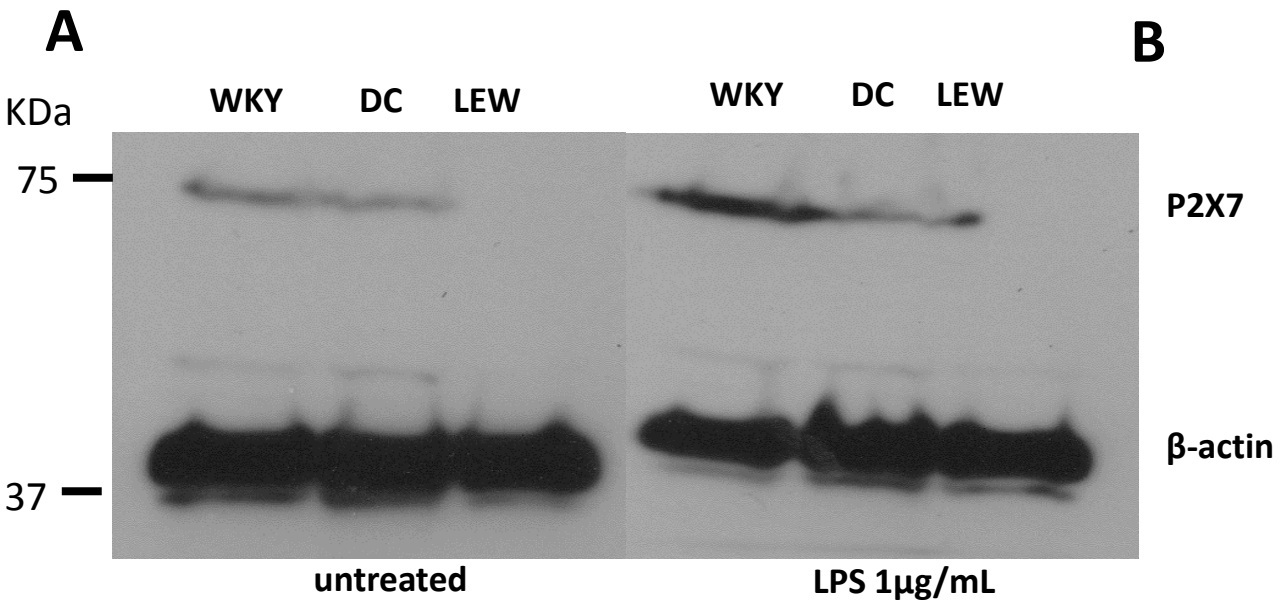

Figure 5.3A and B: P2X7R expression in untreated and LPS stimulated BMDMs from WKY, DC and LEW rats.

BMDMs from WKY, DC and LEW rats were plated in six-well plates at a density of 1 x 10^6 cells per well and stimulated with or without LPS 1 µg/ml for 5 hours. Aliquots of protein (20 µg) from cell lysates were separated by SDS-PAGE electrophoresis and transblotted to PVDF membrane. Detection of P2X7 was performed by Western blotting using anti-P2X7 specific antibody from Alomone Labs (Israel). β-actin was used as loading control.

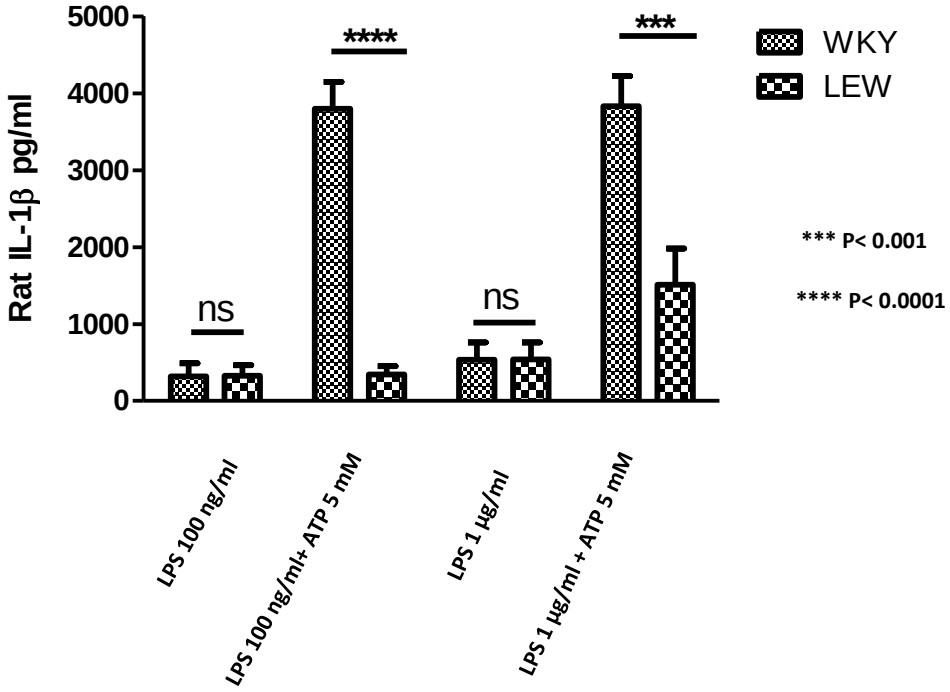

Figure 5.3C BMDMs from WKY rats show a lower threshold for the activation of the inflammasome compared to BMDMs from LEW rats.

BMDMs from WKY and LEW rats were plated into six-well plates at a density of 1 x 10^6 cells per well and primed with either LPS 100 ng/ml or LPS 1 µg/ml for five hours. Macrophages were then stimulated with ATP 5 mM for 30 minutes. Supernatants were then collected and examined by sandwich ELISA for quantification of IL-1β using the Rat IL-1β DuoSet kit (R&D Systems). Data are representative of three independent experiments.

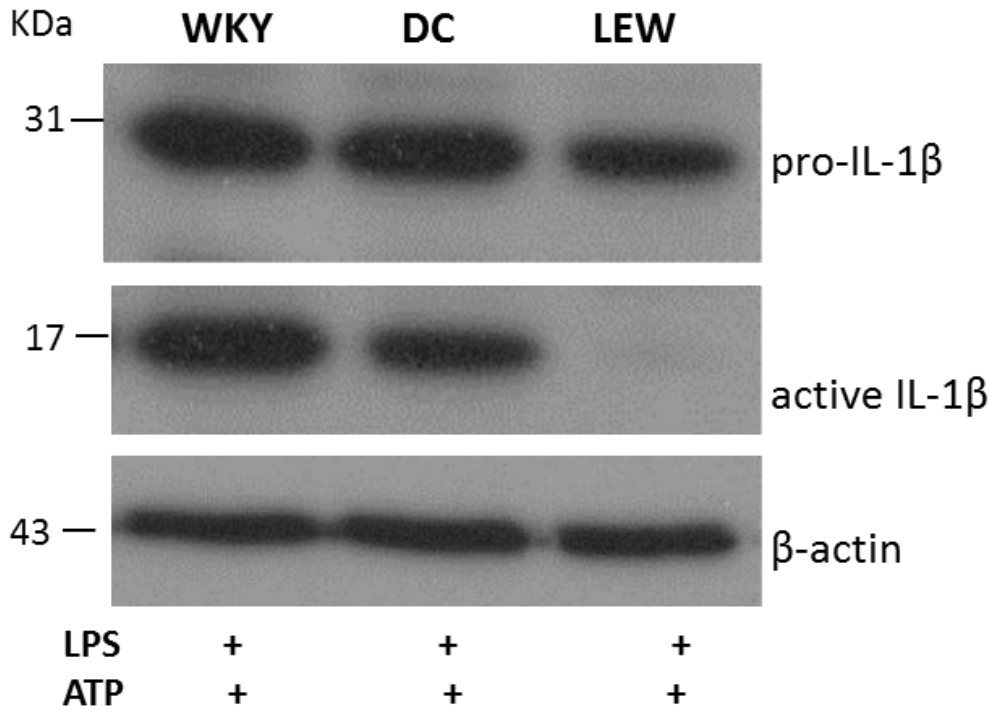

Figure 5.3D IL-1 β secretion in WKY, DC and LEW BMDMs in response to ATP.

BMDMs from WKY, DC and LEW rats were primed with LPS 1 µg/ml for 5 hours and then stimulated with or without ATP 5 mM for 30 minutes. Supernatant and cell layers were then collected and analysed by Western blotting. Pro- and active IL-1β were detected using a specific anti-IL-1β antibody from New England Biolabs (UK).

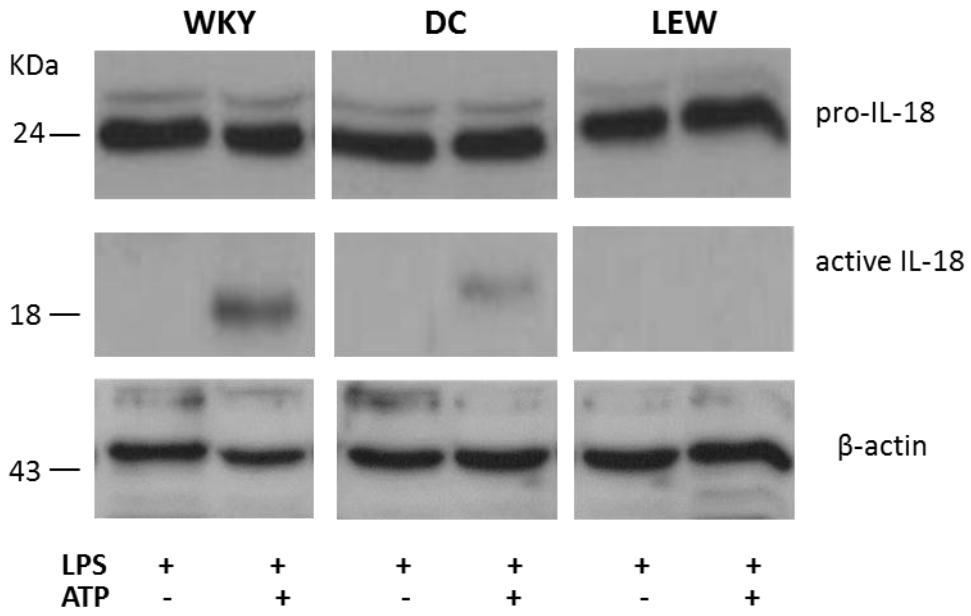

Figure 5.3E IL-18 secretion in WKY, DC and LEW BMDMs in response to ATP.

BMDMs from WKY, DC and LEW rats were plated in six-well plates at a density of 1 x 10^6 cells per well, primed with LPS 1 μg/ml for 5 hours and then stimulated with or without ATP 5 mM for 30 minutes. Supernatants and cell layers were then collected and analysed by Western blotting. Pro- and active IL-18 were detected using a specific anti IL-18 antibody from Santa Cruz Biotechnology (USA). These data are representative of at least three independent experiments.

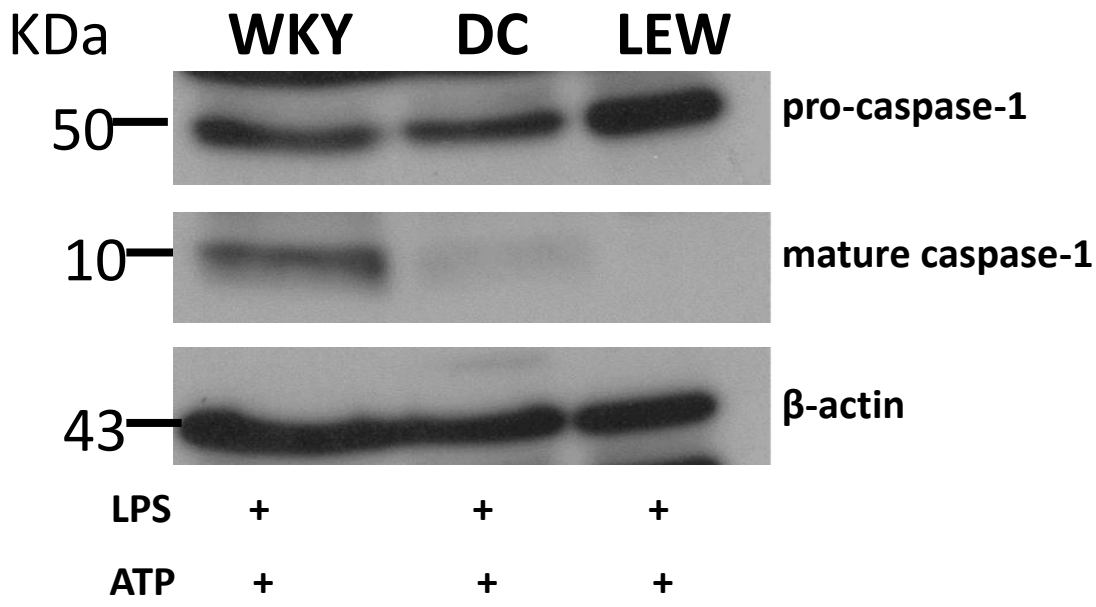

Figure 5.3F Caspase-1 activation in response to ATP in LPS primed macrophages from WKY, DC and LEW rats.

BMDMs from WKY, DC and LEW rats were plated in six-well plates at a density of 1 x 10^6 cells per well, primed with LPS 1 µg/ml for 5 hours and then stimulated with ATP 5 mM for 30 minutes. Supernatants and cell layers were then collected, filtered using Amicon ultra centrifugal filters for protein concentration and purification (Millipore) and analysed by Western blotting. Pro- and active caspase-1 were detected using a specific anti caspase-1 antibody from Santa Cruz Biotechnology (USA). These data are representative of at least three independent experiments.

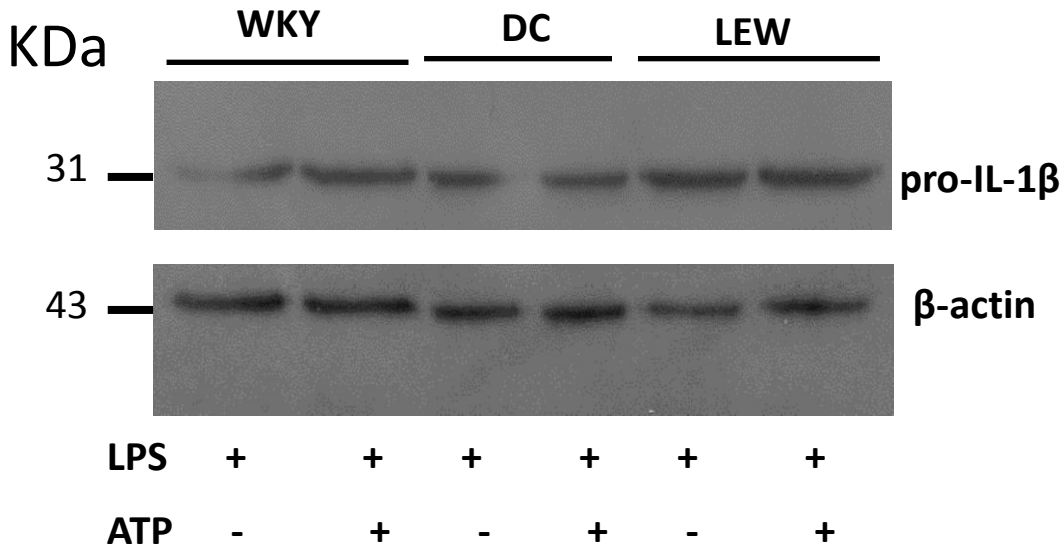

Figure 5.3G WKY, DC and LEW BMDMs show similar pro-IL-1 beta levels in response to LPS.

BMDMs from WKY, DC and LEW rats were plated in six-well plates at a density of 1 x 10^6 cells per well, primed with LPS 1 μg/ml for 5 hours and stimulated with or without ATP 5 mM for 30 minutes. Aliquots of protein (20 μg) from cell lysates were analysed by western blotting. Pro-IL-1β was detected using a specific anti-IL-1β antibody from New England Biolabs (UK).

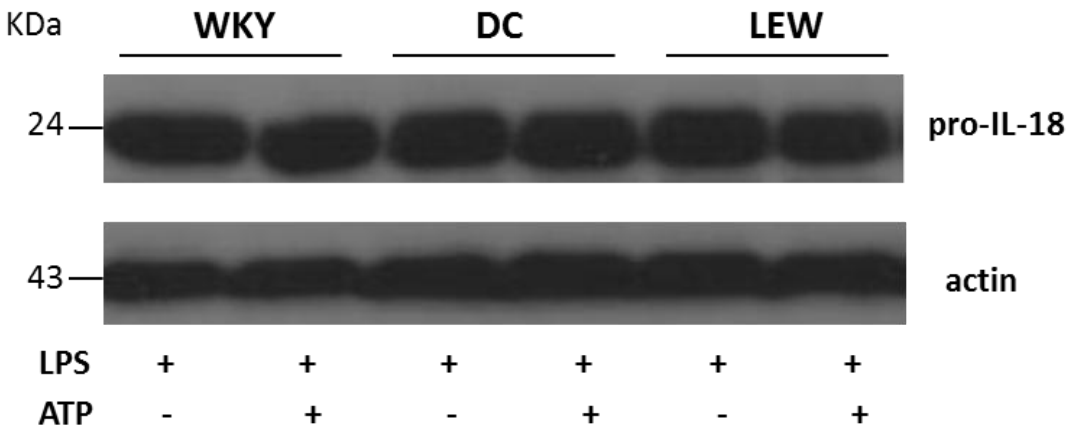

Figure 5.3H WKY, DC and LEW BMDMs show similar pro-IL-18 levels in response to LPS.

BMDMs from WKY, DC and LEW rats were plated in six-well plates at a density of 1 x 10^6 cells per well, primed with LPS 1 μg/ml for 5 hours and stimulated with or without ATP 5 mM for 30 minutes. Aliquots of protein (20 μg) from cell lysates were analysed by Western blotting. Pro-IL-18 was detected using a specific anti-IL-18 antibody from Santa Cruz Biotechnology, (USA).

5.4 CASPASE-1 INHIBITION DRAMATICALLY AFFECTS BOTH IL-1B AND IL-18 SECRETION IN BMDM FROM WKY RATS

Aim and experimental design

As discussed in the introduction, other proteases, such as the metalloproteinases MMP-9 and MMP-12, are able to generate active IL-1β in a caspase-independent manner. To establish whether the increase secretion of mature IL-1β in WKY BMDM was caspase-1 dependent, I have examined the effects of a selective caspase-1 inhibitor, Y-VAD, on the production of IL-1β and IL-18 in response to ATP in primed BMDM from WKY and LEW rats. I have then analysed by RT-PCR the expression of MMP-9 gene in BMDMs from WKY and LEW rats under basal conditions. MMP-9 enzymatic activity was assessed by SDS-PAGE gelatin zymography.

Results

As illustrated in figures 5.4 A and B, the use of the selective caspase-1 inhibitor Y-VAD dramatically affected the secretion of both mature IL-1β and IL-18 in WKY and LEW BMDMs, suggesting that the secretion of these cytokines in WKY BMDMs is mainly caspase-1 dependent. However, since the secretion of active IL-1β is not completely abolished in WKY macrophages, as shown in figure 5.4A, it is possible that other caspase-1 independent pathways contribute to the increased IL-1β production in these cells. Indeed, as shown in figure 5.4D MMP-9 gene is markedly upregulated in WKY BMDMs compared to the LEW ones and is associated with an increased enzymatic activity as revealed by gelatin zymography (figure 5.4D and C).

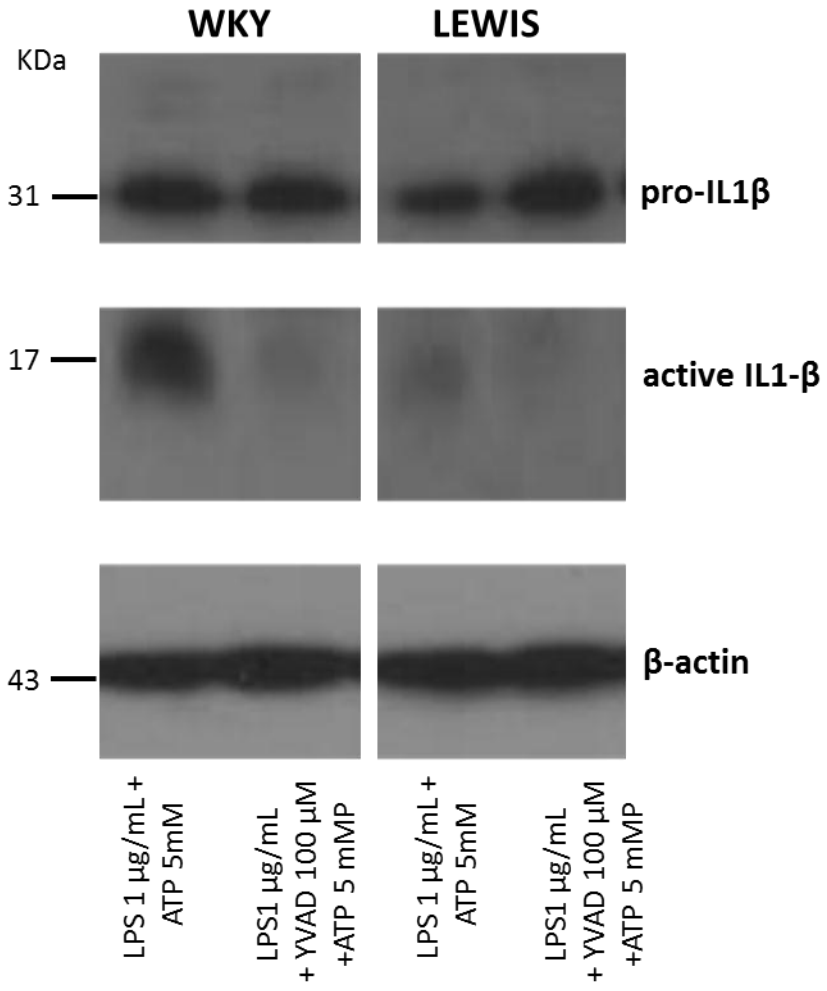

Figure 5.4A Caspase-1 inhibition affects IL-1β secretion in WKY BMDMs.

WKY and LEW BMDM were primed with LPS 1 µg/ml for 5 hours and then stimulated with ATP 5 mM for 30 minutes in the presence or absence of the selective caspase-1 unhibitor Y-VAD used at a final concentration in the medium of 100 µM. Supernatants and cell layers were then collected, filtered and analysed by Western blotting.

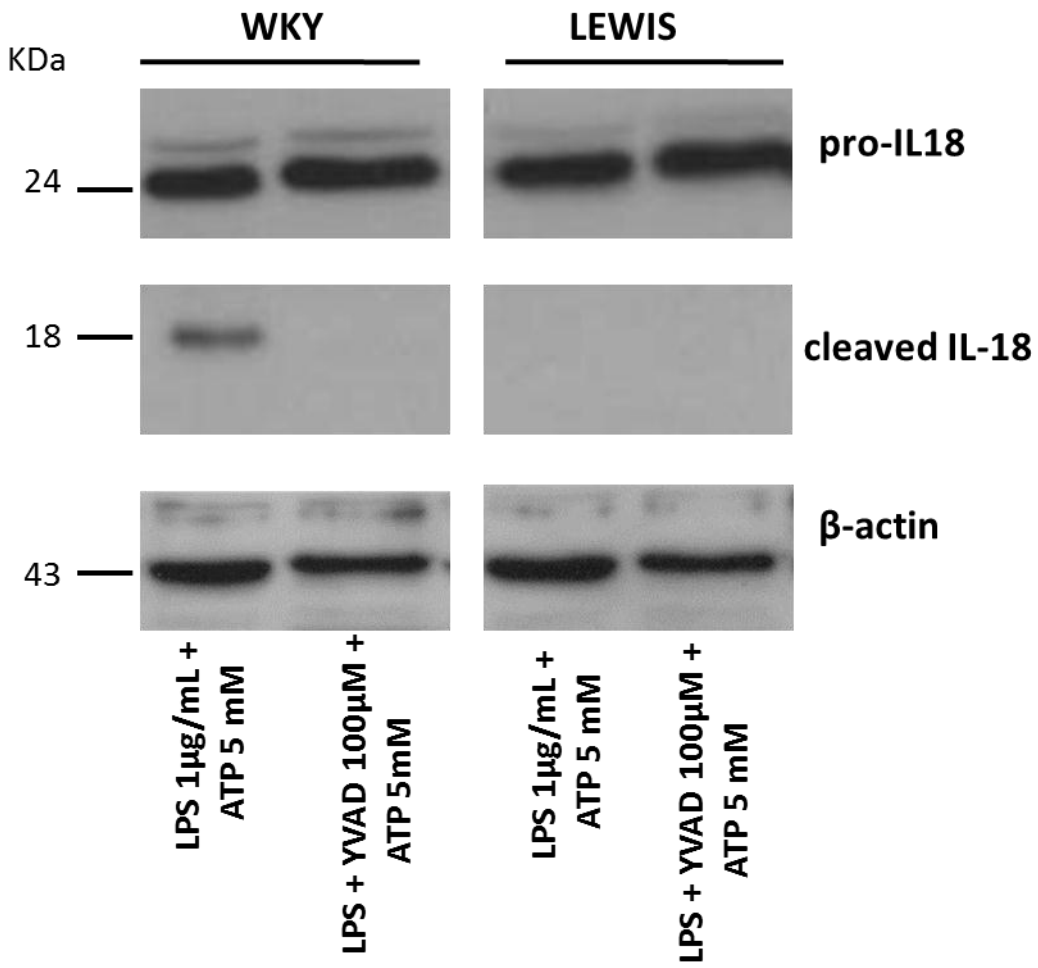

Figure 5.4B Caspase-1 inhibition dramatically affects IL-18 secretion in WKY BMDMs.

WKY and LEW BMDMs were primed with LPS 1 µg/ml for 5 hours and then stimulated with ATP 5 mM for 30 minutes in the presence or absence of the selective caspase-1 unhibitor Y-VAD used at a final concentration in the medium of 100 µM. Supernatants and cell layers were then collected, filtered and analysed by Western blotting.

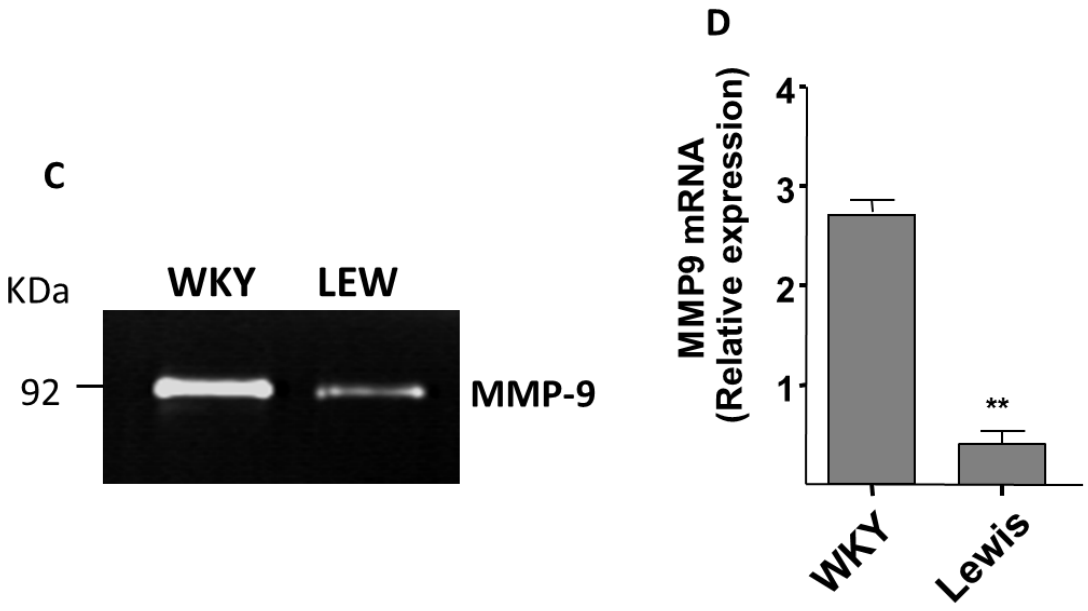

Figure 5.4C and D: MMP-9 enzymatic activity and gene expression are increased in WKY BMDMs.

Detection of MMP-9 by gelatin zymography in BMDMs from WKY and LEW rats under basal conditions(C). Expression of mRNA encoding MMP-9 in untreated BMDMs from WKY and LEW rats (D). Mean expression at each time point is expressed as a ratio to that of the housekeeping gene HPRT.

5.5 NEPHRITIC GLOMERULI FROM WKY RATS SHOW HIGHER LEVELS OF P2X7 PROTEIN AND ACTIVE IL-1 BETA, IL-18 AND CASPASE 1 COMPARED TO LEWIS GLOMERULI

Aim and experimental design

To correlate the in vitro data with the in vivo model of NTN and to establish whether there was a correlation between the inflammasome activation and the severity of disease, I have examined the expression of IL-1β, IL-18 and caspase-1 in glomeruli isolated from the renal cortex of WKY, DC and LEW rats four days after the injection of nephrotoxic serum. Glomeruli were isolated by sieving and cultured for 72 hours in serum free medium. No additional stimulus such as LPS or ATP was added to the medium. The decision to collect the glomeruli on day 4 from the injection of nephrotoxic serum was suggested by the documented evidence that this time-point corresponds to the maximal macrophage accumulation and to the maximal P2X7R expression. After 72 hours of culture, supernatants and cell layers were collected, filtered using Amicon ultra centrifugal filters for protein purification and concentration and analysed by western blotting.

Results

WKY nephritic glomeruli show higher levels of P2X7 protein compared to DC and LEW glomeruli (figure 5.5 A). As shown in figures 5.5 B, C and D, glomeruli from WKY rats exhibit much higher levels of active IL-1β, IL-18 and caspase-1 compared to glomeruli from Lew rats. Glomeruli from DC rats show higher levels of active IL-1β, IL-18 and caspase-1 compared to LEW glomeruli, but lower

compared to the WKY glomeruli resembling the grade of histological injury observed in vivo in these rat strains (figure 5.5E,F,G).

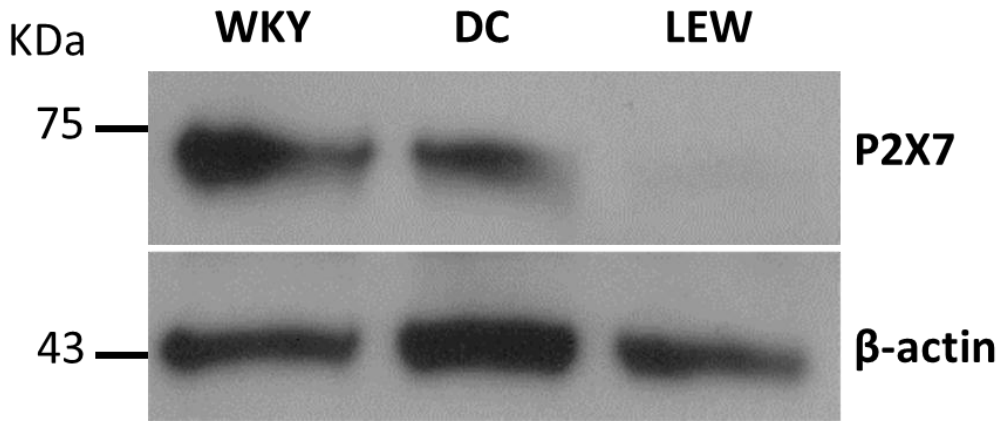

Figure 5.5A P2X7 protein expression in cultured nephritic glomeruli from WKY, DC and LEW rats.

At day 4 after NTS injection, glomeruli from WKY, DC and LEW rats were isolated from the renal cortex by sieving and cultured in serum free conditions for 72 hours. Supernatants and cell layers were then collected, filtered using Amicon ultra centrifugal filters (Millipore) and analysed by western blotting. Detection of P2X7 was performed using an anti-P2X7 antibody from Alomone Labs (Israel). Beta-actin was used as loading control.

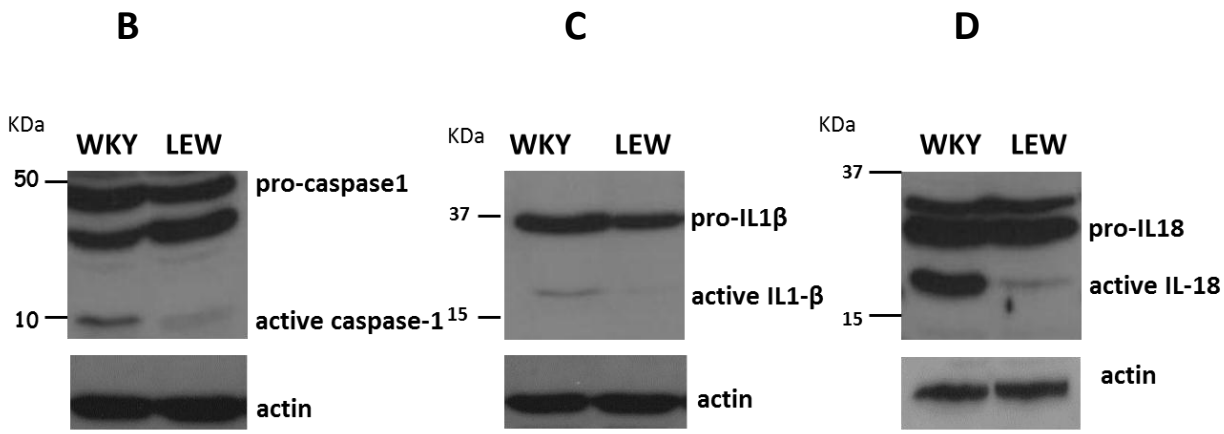

Figure 5.5B, C and D: WKY nephritic glomeruli exhibit higher IL-1 beta, IL-18 and caspase-1 levels compared to LEW glomeruli.

Nephritic glomeruli from WKY and LEW rats were isolated at day 4 from NTS injection and cultured for 72 hours in serum free medium. Supernatants and cell layers were then analysed by Western blotting.

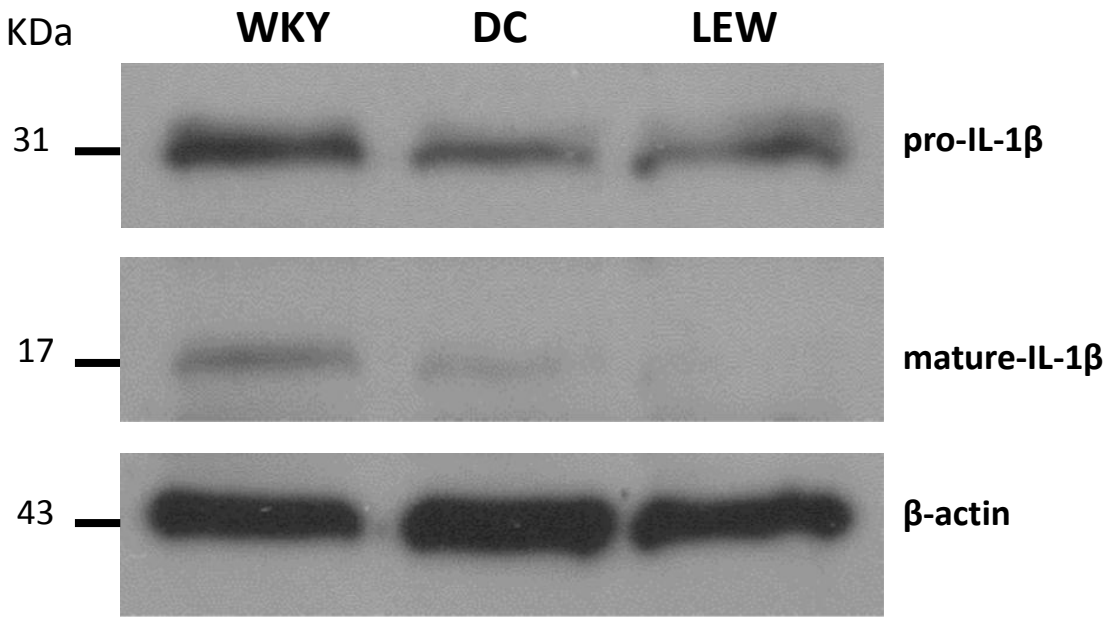

Figure 5.5 E IL-1 β secretion in nephritic glomeruli from WKY, DC and LEW rats.

Glomeruli from WKY, DC and LEW rats were isolated by sievieng at day 4 from NTS injection. Glomeruli were then cultured in serum free medium for 72 hours and supernatants and cell layers were collected and analysed by Western blotting.

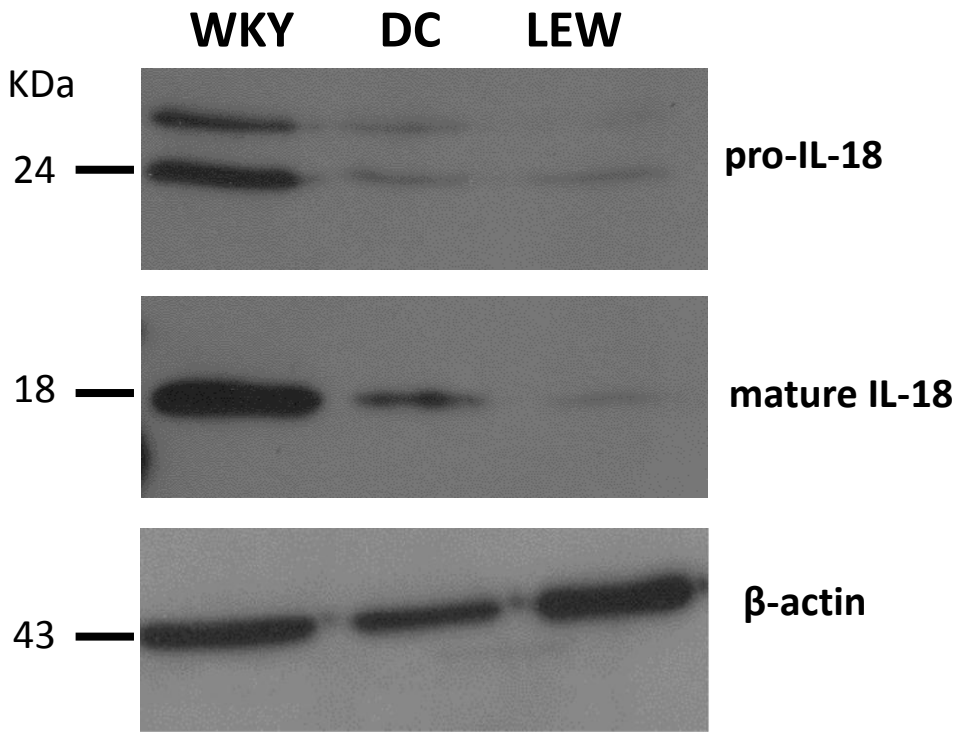

Figure 5.5F IL-18 secretion in cultured nephritic glomeruli isolated from WKY, DC and LEW rats.

Glomeruli from WKY, DC and LEW rats were isolated by sievieng at day 4 from NTS injection. Glomeruli were then cultured in serum free medium for 72 hours and supernatants and cell layers were collected and analysed by Western blotting.

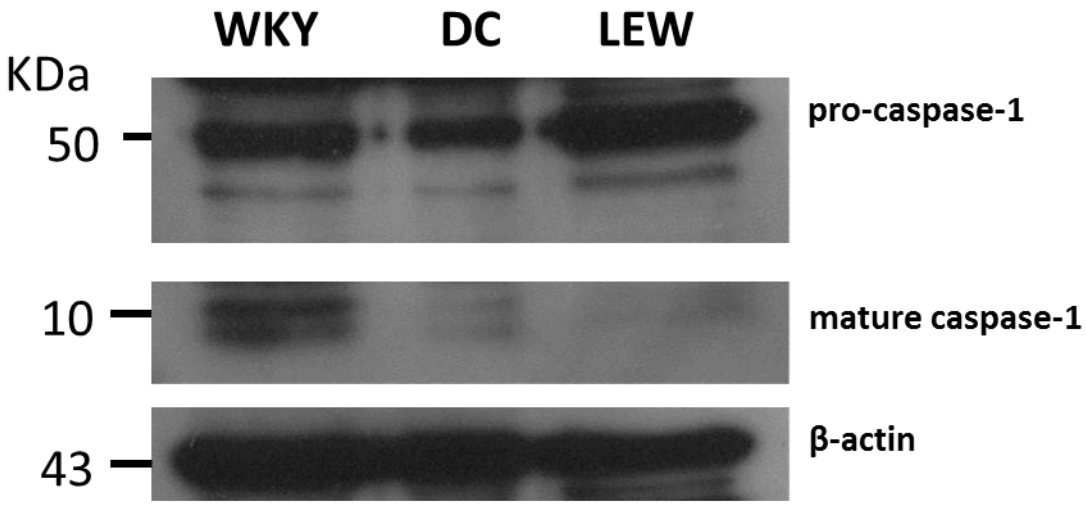

Figure 5.5G Caspase-1 activation in cultured nephritic glomeruli from WKY, DC and LEW rats.

Glomeruli from WKY, DC and LEW rats were isolated by sievieng at day 4 from NTS injection. Glomeruli were then cultured in serum free medium for 72 hours and supernatants and cell layers were collected and analysed by Western blotting. A specific anti-caspase-1 antibody from Santa Cruz Biotechnology was used for the detection of pro- and cleaved caspase-1. β-actin was used as loading control.

5.6 ANALYSIS OF THE INFLAMMASOME ACTIVATION IN BMDM FROM CONGENIC RAT STRAINS

Aims and experimental design

My previous data have shown that BMDMs and nephritic glomeruli from DC rats have lower levels of P2X7 protein and reduced active IL-1β, IL-18 and caspase-1 compared to WKY BMDMs and glomeruli. When compared with LEW BMDMs and glomeruli, DC exhibit higher levels of P2X7 protein and active IL-1β, IL-18 and caspase-1. Since in the NTN model, DC rats show a reduction by 40% in the number of crescents, there seems to be a correlation between the severity of the disease and the grade of inflammasome activation in both BMDMs and nephritic glomeruli. As previously described, the DC strain is characterized by the introgression of both the CRGN1 and the CRGN2 intervals from Lew rats onto a WKY genetic background. In order to examine the relative contribution of CRGN1 and CRGN2 in the regulation of P2X7R expression and inflammasome activation, I have analysed the inflammasome-dependent cytokine production in BMDMs and nephritic glomeruli from single congenic rats generated by either the introgression of CRGN2 from LEW rats onto a WKY genetic background (WL16) or by the introgression of CRGN2 from WKY rats onto a LEW background (LW16). Unfortunately, the single congenic rats with introgression of the CRGN1 interval were not available. In the NTN model, WL16 rats show significantly reduced glomerular crescent formation, fibrin deposition and macrophage infiltration compared to WKY rats, whereas LW16 rats exhibit significantly more proteinuria and macrophage infiltration than the background strain (Behmoaras et al., 2010).

Results

BMDMs from WL16 rats show lower levels of P2X7 protein compared to WKY BMDMs (figure 5.6 A). The levels of P2X7 protein in WL16 macrophages are similar to the levels expressed by DC BMDMs. LW16 macrophages resemble LEW BMDMs exhibiting very low levels of the protein. As shown in figure 5.6B, when stimulated with ATP, LPS-primed BMDMs from WL16 rats release lower levels of active IL-1β compared to WKY BMDMs but similar to macrophages from DC rats. Interestingly, BMDMs from LW16 rats produce much higher levels of active IL-1β compared to LEW BMDMs and similar to WL16 macrophages (figure 5.6B). The decreased IL-1β secretion in response to ATP in WL16 macrophages compared to the WKY ones was confirmed by ELISA as well as the increased secretion observed in LW16 macrophages compared to the LEW ones (figure 5.6 C). Mature IL-18 was only slightly decreased in WL16 BMDMs in response to ATP stimulation, however LW16 macrophages exhibited much higher levels of active IL-18 compared to LEW BMDMs and similar to the levels of active IL-18 released by WKY BMDMs (figure 5.6D). Active caspase-1 in response to ATP stimulation, was also much lower in WL16 BMDMs compared to the WKY ones, while LW16 macrophages showed similar levels of active caspase-1 as the LEW ones (figure 5.6 E). Interestingly, macrophages from DC rats exhibit higher active caspase-1 levels compared to WL16, LW16 and LEW macrophages, but much lower than the WKY ones (figure 5.6 E). According to the ELISA results, nephritic glomeruli from WL16 rats show markedly lower levels of active IL-1β compared to WKY glomeruli, while glomeruli from LW16 rats show similar levels of active IL-1β as LEW glomeruli (figure 5.6 F). No statistically significant difference in IL-1β levels was observed between glomeruli from WL16, DC, LW16 and LEW rats. However, when analysed by Western blotting, WL16 glomeruli exhibit similar levels of P2X7 protein, active IL-1β and IL-18 as WKY glomeruli, whereas LW16 glomeruli

resemble the LEW ones, showing a very low P2X7 protein expression and both active IL-1β and IL-18 were not detectable (figure 5.6 G, H and j).

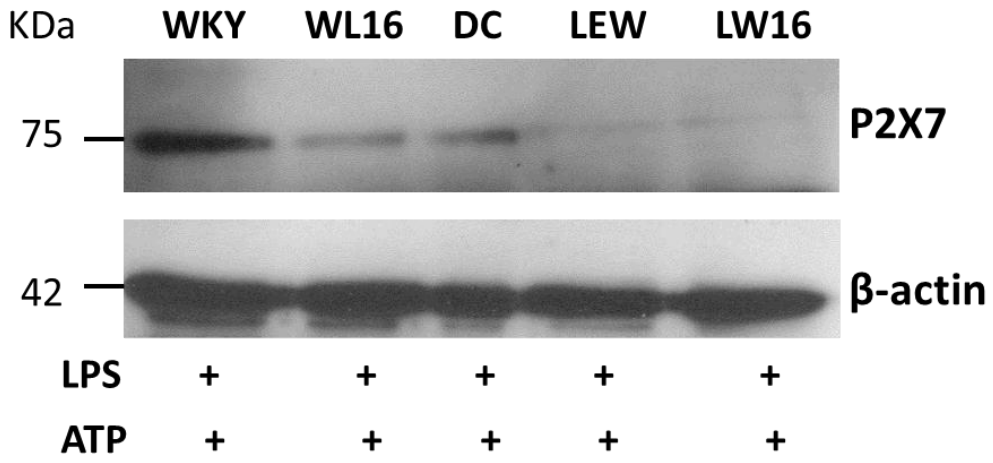

Figure 5.6A P2X7R expression in BMDMs from single and double congenic rat strains.

BMDMs from WKY, WL16, DC, LEW and LW16 rats were plated in six-well plates at a density of 1 x 10^6 cells per well, primed with LPS 1 μg/ml for 5 hours and then stimulated with ATP 5 mM for 30 minutes. Supernatants and cell layers were then collected and analysed by Western blotting. For P2X7 protein detection, a specific anti-P2X7 antibody from Alomone Labs was used. Beta-actin was used as loading control.

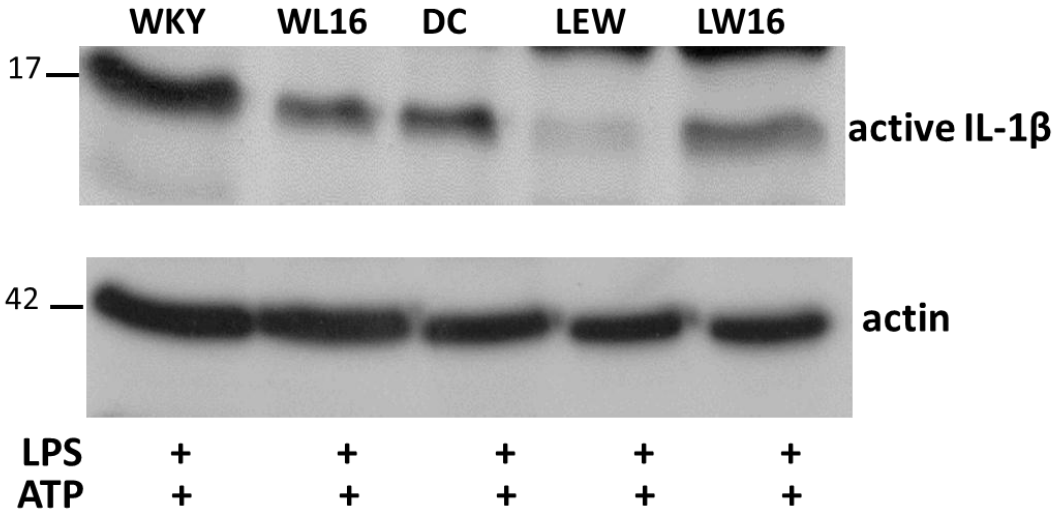

Figure 5.6B IL-1β secretion in response to ATP in LPS primed BMDMs from congenic rat strains.

BMDMs from WKY, WL16, DC, LEW and LW16 rats were plated in six-well plates at a density of 1 x 106 cells per well, primed with LPS 1 μg/ml for 5 hours and then stimulated with ATP 5 mM for 30 minutes. Supernatants and cell layers were then collected and analysed by Western blotting. For active IL-1β detection, a specific anti-cleaved IL-1β antibody from Santa Cruz (USA) was used. Beta-actin was used as loading control.

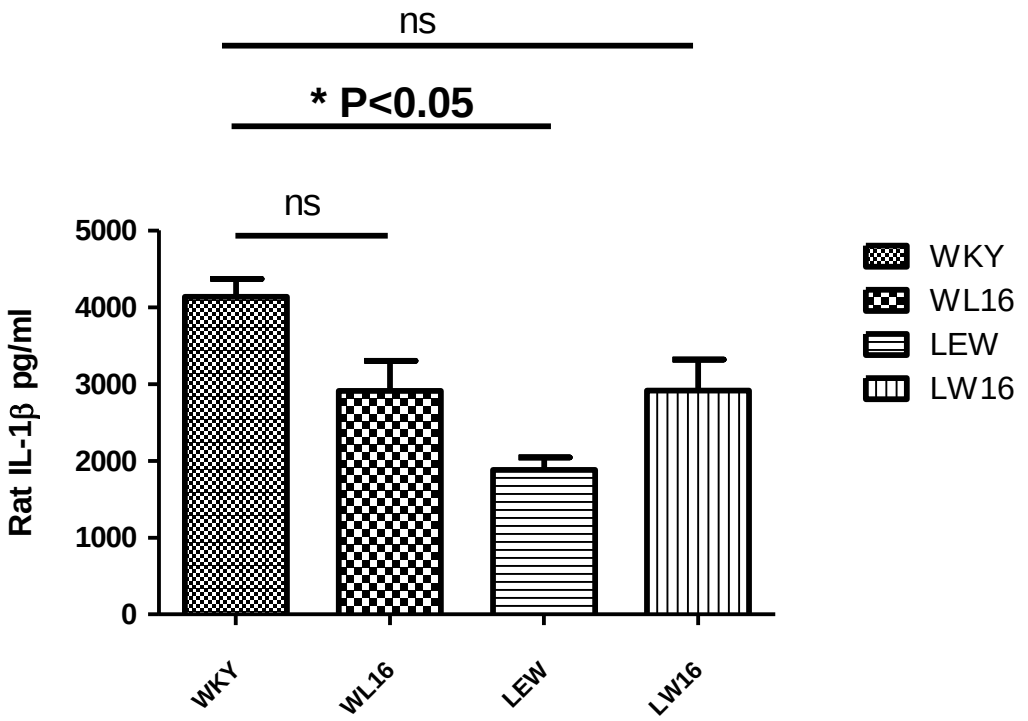

Figure 5.6C Active IL-1β secretion in response to ATP in LPS primed BMDMs from congenic rat strains.

BMDMs from WKY, WL16, LEW and LW16 rats were plated in six-well plates at a density of 1 x 106 cells per well, primed with LPS 1 μg/ml for 5 hours and then stimulated with ATP 5 mM for 30 minutes. Supernatants were then collected and analysed by sandwich ELISA (Rat IL-1β/DuoSet Kit, R&D Systems). Data are representative of three independent experiments.

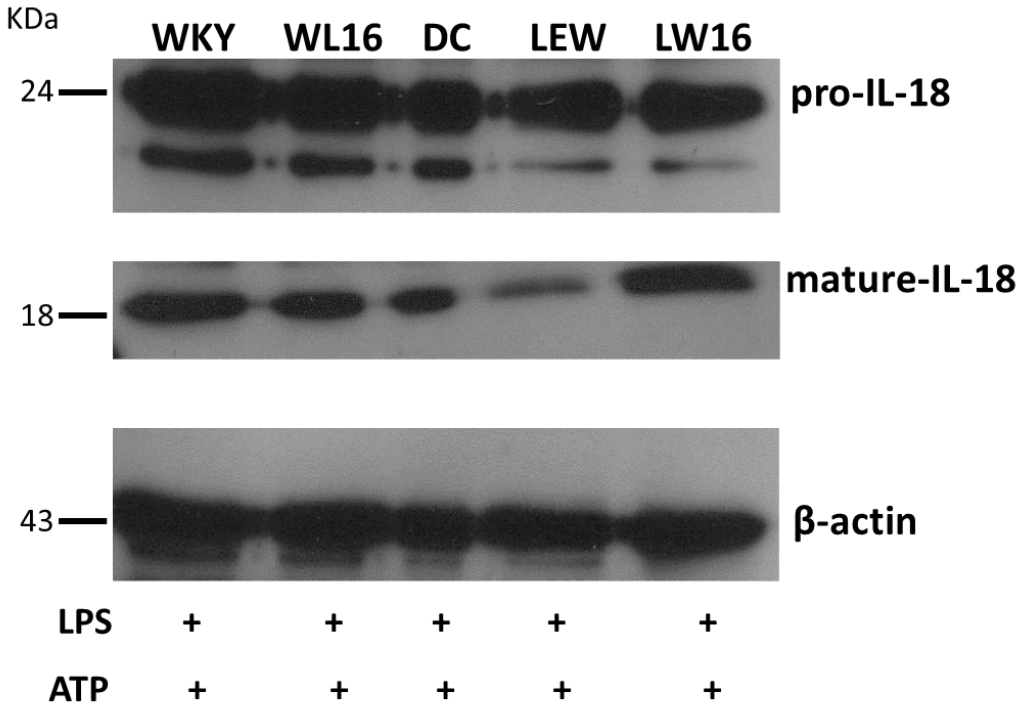

Figure 5.6D IL-18 secretion in BMDMs from congenic rat strains.

BMDMs from WKY, WL16, DC, LEW and LW16 rats were plated in six-well plates at a density of 1 x 10^6 cells per well, primed with LPS 1 μg/ml for 5 hours and then stimulated with ATP 5 mM for 30 minutes. Supernatants and cell layers were then collected and analysed by Western blotting. For pro- and active IL-18 detection, a specific anti IL-18 antibody from Santa Cruz (USA) was used. Beta-actin was used as loading control.

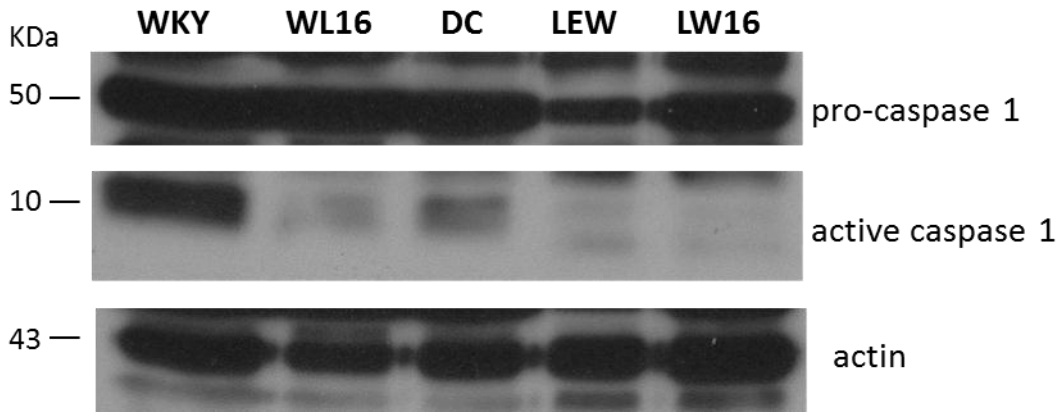

Figure 5.6E Caspase-1 activation in BMDMs from congenic rat strains.

BMDMs from WKY, WL16, DC, LEW and LW16 rats were plated in six-well plates at a density of 1 x 10^6 cells per well, primed with LPS 1 μg/ml for 5 hours and then stimulated with ATP 5 mM for 30 minutes. Supernatants and cell layers were then collected and analysed by Western blotting. For pro- and active caspase-1 detection, a specific anti caspase-1 antibody from Santa Cruz (USA) was used. Beta-actin was used as loading control.

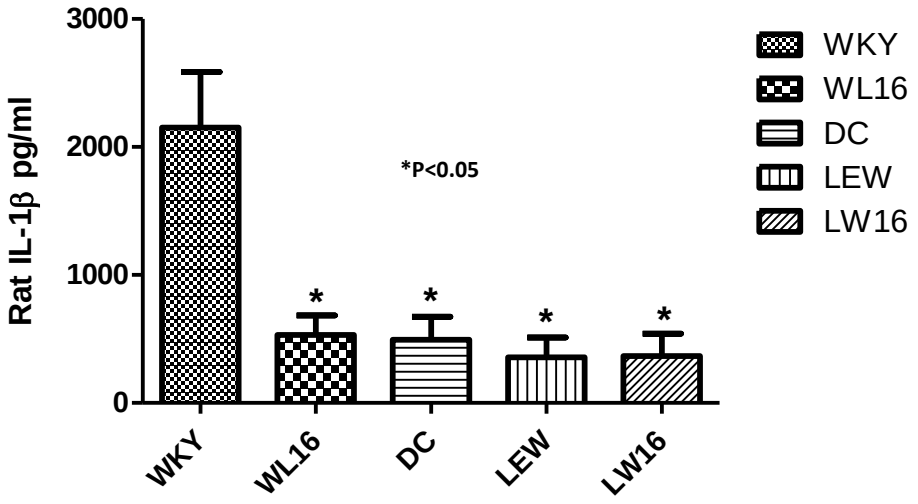

Figure 5.6F IL-1β secretion in cultured nephritic glomeruli from congenic rat strains.

Nephritic glomeruli from WKY, WL16, DC, LEW and LW16 rats were isolated at day 4 from NTS injection and cultured for 72 hours in serum free medium. Supernatants were then collected and analysed by sandwich ELISA (Rat IL-1β/DuoSet from R&D Systems). Data are representative of three independent experiments.

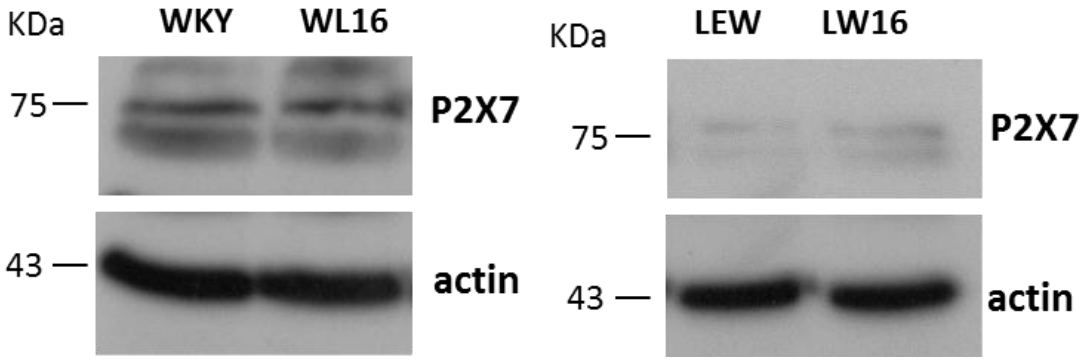

Figure 5.6G P2X7R expression in cultured glomeruli from WKY, WL16, LEW and LW16 rats.

Nephritic glomeruli from WKY, WL16, DC, LEW and LW16 rats were isolated at day 4 from NTS injection and cultured for 72 hours in serum free medium. Supernatants and cell layers were then collected and analysed by Western blotting.

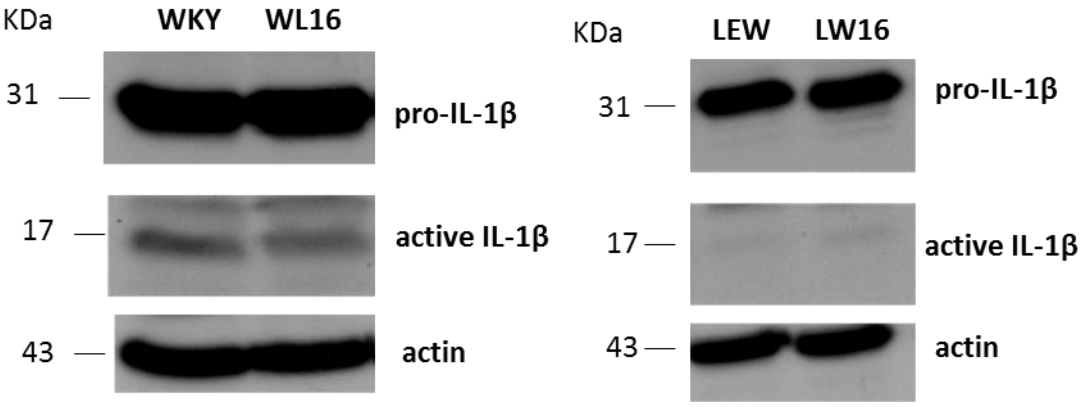

Figure 5.6H IL-1 β secretion in cultured glomeruli from WKY, WL16, LEW and LW16 rats.

Nephritic glomeruli from WKY, WL16, DC, LEW and LW16 rats were isolated at day 4 from NTS injection and cultured for 72 hours in serum free medium. Supernatants and cell layers were then collected and analysed by Western blotting.

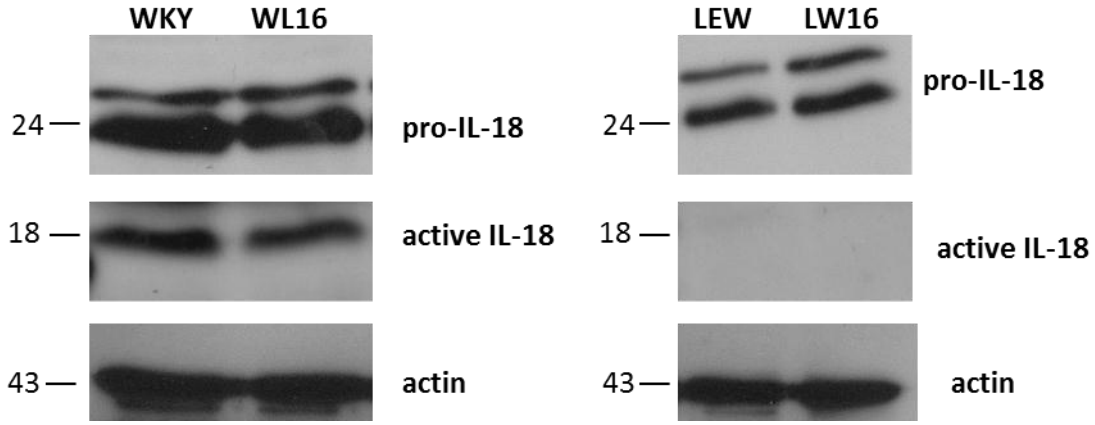

Figure 5.6J IL-18 secretion in cultured nephritic glomeruli from WKY, WL16, LEW and LW16 rats.

Nephritic glomeruli from WKY, WL16, DC, LEW and LW16 rats were isolated at day 4 from NTS injection and cultured for 72 hours in serum free medium. Supernatants and cell layers were then collected and analysed by Western blotting.

5.7 ROLE OF JUND IN THE REGULATION OF THE INFLAMMASOME ACTIVATION

Aims and experimental plan

Within the CRGN2 interval the activator protein-1 (AP-1) transcription factor gene Jund has been recognized as an important potentiator of macrophage activity and it has been shown to be markedly upregulated in both BMDMs and glomeruli from WKY rats (Behmoaras et al., 2008). To assess whether Jund plays a role in the regulation of P2X7R expression and in the activation of the inflammasome, I have first examined the effects of Jund silencing by siRNA on the secretion of active IL-1β, IL-18 and caspase-1 in response to ATP in LPS primed BMDMs from WKY rats. Due to the possibility that a prolonged LPS priming might increase Jund expression and abolish the effects of siRNA treatment, the timing of the priming step was shorted to only one hour so that no new protein synthesis could occur. Although the siRNA approach is usually a very powerful method to assess the role of a protein in many cellular functions, however sometimes, especially when the efficiency of the transfection is not great, it could become difficult to make clear conclusions. Another factor that could limit siRNA-mediated silencing is the half-life of the protein. It might be difficult to effectively silence genes that encode proteins with long half-lives by transient transfection of siRNA. In view of the possibility that Jund might regulate P2X7R expression and the inflammasome activation during the macrophage differentiation process, I have analysed and compared inflammasome-mediated cytokine production in response to ATP stimulation in LPS-primed BMDMs from WT and Jund deficient mice.

Results

Treatment of WKY BMDMs with Jund specific siRNA for 48 hours led to a decreased Jund protein expression as shown in figure 5.7 A. When primed with LPS 1 μg/ml and stimulated with ATP 5 mM for 30 minutes WKY BMDMs treated with Jund siRNA produce similar levels of active IL-1β as cells treated with scrambled siRNA according to the Western blotting results (figure 5.7B, left panel). However when the same samples were analysed by sandwich ELISA, there was a 20% reduction in IL-1β secretion in WKY BMDMs treated with Jund siRNA compared to the ones treated with scrambled siRNA (figure 5.7 B, right panel). JunD siRNA treatment in WKY BMDMs did not affect neither the secretion of active IL-18 (figure 5.7C) nor the activation of caspase-1 (figure 5.7D) in response to ATP. LPS-primed BMDMs from Jund deficient mice show similar levels of active IL-1β and caspase-1 as the WT controls when stimulated with ATP (figures 5.7E and 5.7F). Interestingly, the levels of active IL-18 released by Jund knock-out mice in response to ATP were markedly reduced compared to WT mice (figure 5.7G). No differences in P2X7 protein levels were seen between BMDMs from WT and Jund knock-out mice (figure 5.7H).

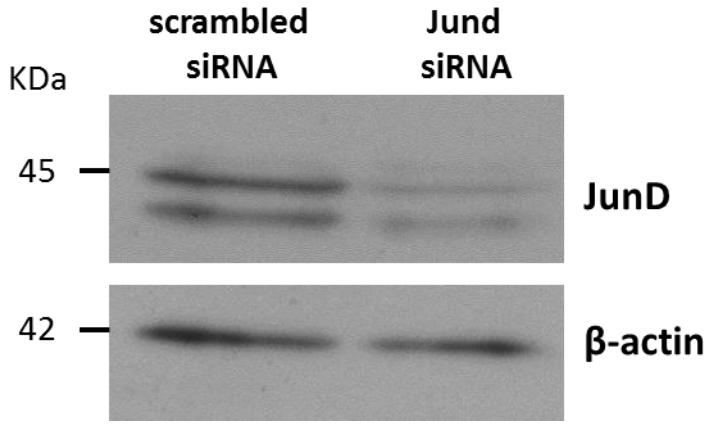

Figure 5.7A Jund specific siRNA treatment decreases Jund protein expression in WKY BMDMs.

WKY BMDMs were plated into six-well plates at a density of 1 x 10^6 cells per well and treated with Jund specific siRNA or a scrambled oligonucleotide for 48 hours before total protein was extracted for Western blotting analysis. For Jund detection a specific anti-Jund antibody from Santa Cruz Biotechnology (USA) was used.

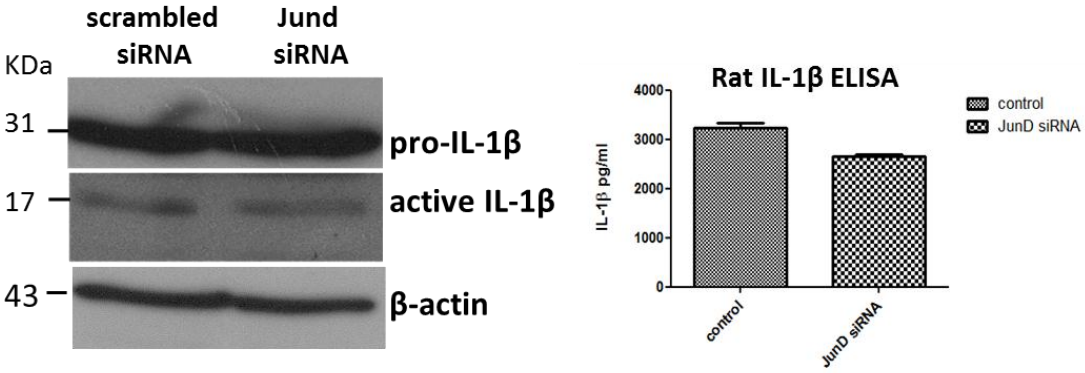

Figure 5.7B Effects of Jund siRNA on IL-1 beta secretion in response to ATP in LPS-primed BMDMs from WKY rats.

WKY BMDMs were treated with scrambled siRNA (control) or specific Jund siRNA. After 48 hours of incubation, macrophages were primed with LPS 1 µg/ml for 1 hour and stimulated with ATP 5 mM for further 30 minutes. Supernatants were then collected and analysed by Western blotting and sandwich ELISA. For detection of both pro- and active IL-1β by western blotting a specific anti IL-1β antibody from New England Biolabs (UK) was used. Sandwich ELISA for detection of Rat IL-1β was conducted using the Rat IL-1β/DuoSet ELISA kit from R&D Systems.

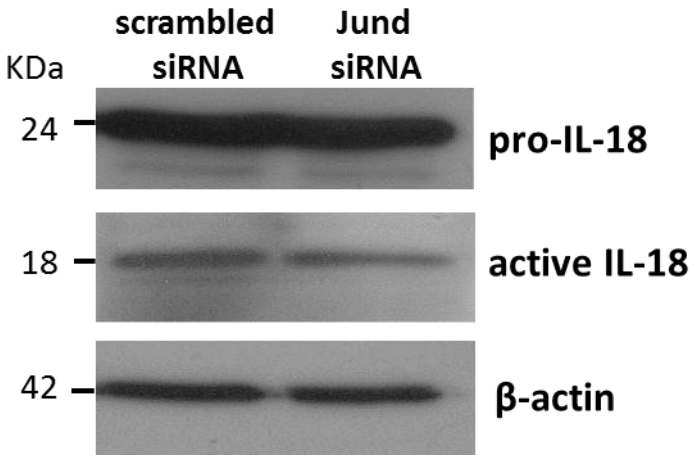

Figure 5.7C Effects of Jund siRNA treatment on IL-18 secretion in response to ATP in LPS primed BMDMS from WKY rats.

WKY BMDMs were treated with scrambled siRNA (control) or specific Jund siRNA. After 48 hours of incubation, macrophages were primed with LPS 1 µg/ml for 1 hour and stimulated with ATP 5 mM for further 30 minutes. Supernatants were then collected and analysed by Western blotting. For detection of both pro- and active IL-18 a specific anti IL-18 antibody from Santa Cruz Biotechnology was used.

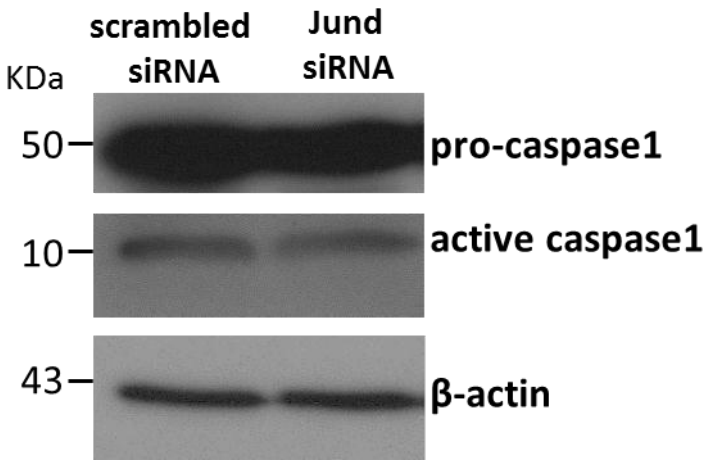

Figure 5.7D Effects of Jund siRNA treatment on caspase-1 activation in response to ATP in LPS primed BMDMS from WKY rats.

WKY BMDMs were treated with scrambled siRNA (control) or specific Jund siRNA. After 48 hours of incubation, macrophages were primed with LPS 1 µg/ml for 1 hour and stimulated with ATP 5 mM for further 30 minutes. Supernatants were then collected and analysed by Western blotting. For detection of both pro- and active caspase-1 by a specific anti IL-18 antibody from Santa Cruz Biotechnology was used.

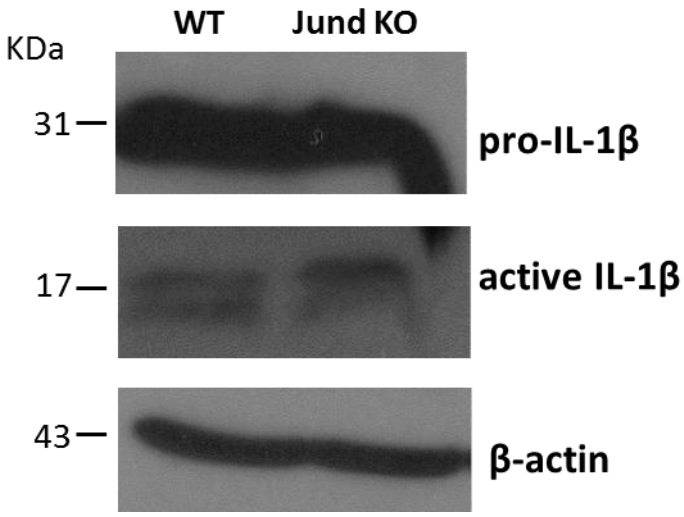

Figure 5.7E IL-1β secretion in response to ATP in LPS primed BMDMs from WT and Jund knock-out mice.

BMDMs from WT and Jund deficient mice were plated in six-well plates at a density of 1 x 10^6 cells per well, primed with LPS 1 μg/ml for 5 hours and then stimulated with ATP 5 mM for 30 minutes. Supernatants and cell layers were then collected and analysed by Western blotting. For pro- and active IL-1β detection, a specific anti-IL-1β antibody from New England Biolabs was used. Beta-actin was used as loading control.

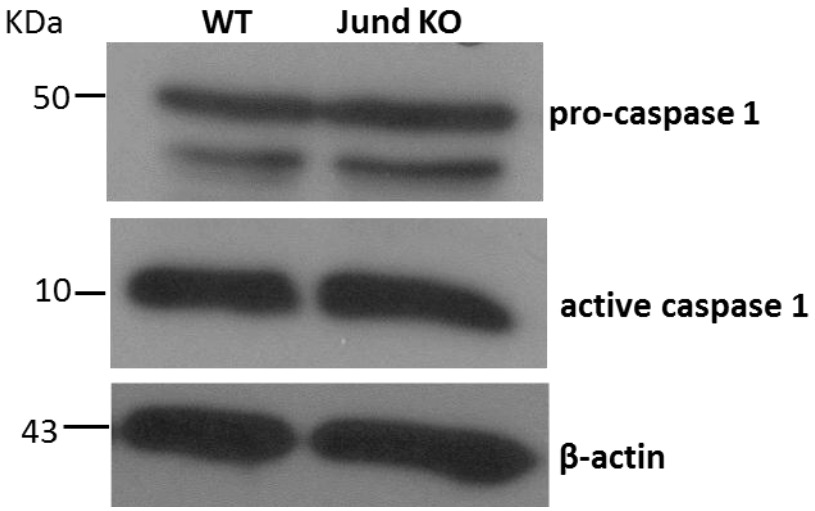

Figure 5.7F Caspase-1 activation in response to ATP in LPS-primed BMDMs from WT and Jund Knock-out mice.

BMDMs from WT and Jund deficient mice were plated in six-well plates at a density of 1 x 10^6 cells per well, primed with LPS 1 μg/ml for 5 hours and then stimulated with ATP 5 mM for 30 minutes. Supernatants and cell layers were then collected and analysed by Western blotting. For pro- and active caspase-1 detection, a specific anti-caspase-1 antibody from Santa Cruz Biotechnology (CA, US) was used. Beta-actin was used as loading control.

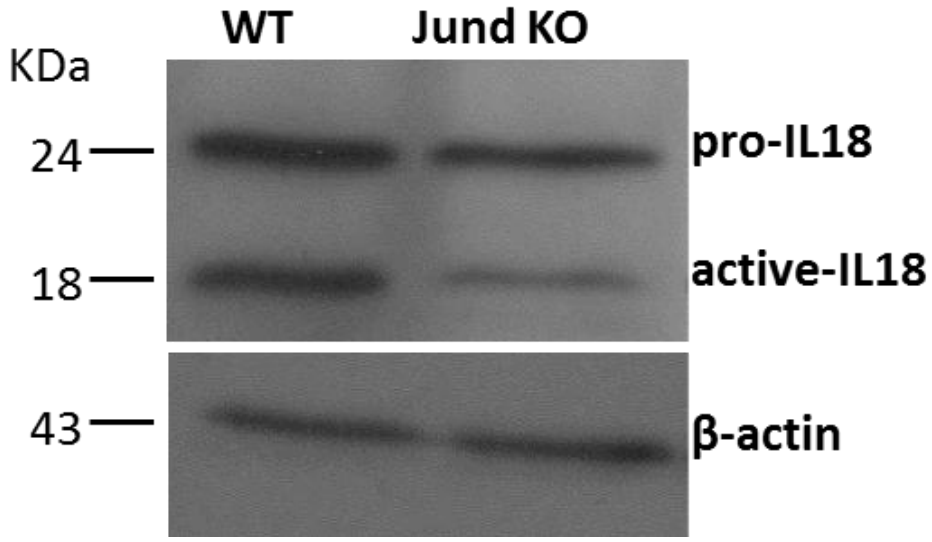

Figure 5.7G IL-18 secretion in response to ATP in LPS primed BMDMs from WT and Jund knock-out mice.

BMDMs from WT and Jund deficient mice were plated in six-well plates at a density of 1 x 10^6 cells per well, primed with LPS 1 µg/ml for 5 hours and then stimulated with ATP 5 mM for 30 minutes. Supernatants and cell layers were then collected and analysed by Western blotting. For pro- and active IL-18 detection, a specific anti-IL-18 antibody from Santa Cruz Biotechnology (CA, US) was used. Beta-actin was used as loading control.

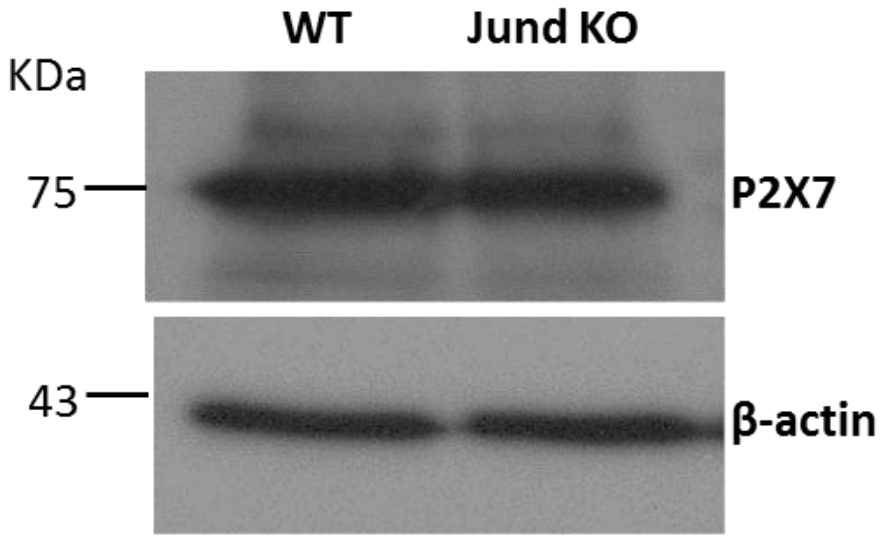

Figure 5.7H P2X7R expression in BMDMs from WT and Jund knock-out mice.

BMDMs from WT and Jund deficient mice were plated in six-well plates at a density of 1 x 10^6 cells per well, primed with LPS 1 µg/ml for 5 hours and then stimulated with ATP 5 mM for 30 minutes. Aliquots of protein (20 µg) from cell lysates were then analysed by Western blotting. For P2X7 protein detection a specific anti-P2X7 antibody from Alomone Labs (Israel) was used. Beta actin was used as loading control.

5.8 DISCUSSION

My studies led me to the following conclusions:

1) WKY BMDMs show a marked upregulation of the majority of the inflammasome-related genes compared to LEW BMDMs.

2) WKY BMDMs show higher P2X7 mRNA and protein levels both under basal conditions and after stimulation with LPS compared to LEW BMDMs.

3) WKY BMDMs release higher levels of both active IL-1β and IL-18 in response to ATP stimulation compared to LEW BMDMs.

4) WKY BMDMs show higher levels of active caspase-1 in response to ATP stimulation compared to LEW BMDMs.

5) The increased secretion of active IL-1β and IL-18 in WKY BMDMs is not due to an increased synthesis of the precursors in response to LPS priming.

6) Caspase-1 inhibition dramatically affects both IL-1β and IL-18 secretion in WKY BMDMs.

7) WKY BMDMs show markedly increased MMP-9 gene expression and enzymatic activity compared to LEW BMDMs.

8) In response to LPS priming, DC BMDMs exhibit lower levels of P2X7 protein compared to WKY BMDMs but higher than LEW macrophages.

9) DC BMDMs release lower levels of both active IL-1β and IL-18 in response to ATP stimulation compared to WKY BMDMs but higher than LEW macrophages.

10) In response to ATP stimulation, DC BMDMs show decreased caspase-1 activation compared to WKY BMDMs but higher than LEW macrophages.

11) In response to ATP treatment, BMDMs from WL16 rats release lower levels of active IL-1β compared to WKY macrophages but higher than LEW BMDMs.

12) In response to ATP stimulation, BMDMs from LW16 rats exhibit higher levels of both active IL-1β and active IL-18 than LEW BMDMs.

13) At day 4 from NTS injection, WKY nephritic glomeruli express higher levels of P2X7 protein than LEW glomeruli.

14) At day 4 from NTS injection, WKY nephritic glomeruli show higher levels of active IL-1β, IL-18, caspase-1 compared to LEW glomeruli.

15) At day 4 from NTS injection, nephritic glomeruli from single and double congenic rat strains express lower levels of P2X7 protein than WKY glomeruli, but higher than LEW glomeruli.

16) At day 4 from NTS injection, cultured nephritic glomeruli from DC rats release lower levels of active IL-1β and active IL-18 than WKY glomeruli but higher compared to LEW ones.

17) At day 4 from NTS injection, nephritic glomeruli from DC rats show lower levels of active caspase-1 than WKY glomeruli but higher compared to LEW glomeruli.

18) According to the ELISA results, cultured nephritic glomeruli from WL16 rats show much lower levels of active IL-1β compared to WKY glomeruli, while glomeruli from LW16 rats release similar levels of active IL-1β as LEW glomeruli.

19) According to the Western blotting results, WL16 glomeruli exhibit similar active IL-1β and IL-18 levels as WKY glomeruli and also show similar P2X7 protein levels. LW16 glomeruli resemble the LEW ones showing very low P2X7 protein levels, whereas active IL-1β and IL-18 were not detectable.

Analysis of inflammasome-related genes expression in WKY, DC and LEW BMDMs

The analysis of the inflammasome-related genes P2X7, IL-18, Pycard and caspase-1 revealed that WKY macrophages, under basal conditions, express

significant higher mRNA levels compared to LEW BMDMs. Interestingly, macrophages from DC rats resemble WKY BMDMs exhibiting even higher P2X7 and caspase-1 mRNA levels. However, when I analysed ASC, pro-caspase-1 and pro-IL-18 protein levels by western blotting, I could not find any differences among macrophages from the three rat strains (data not shown). As previously discussed, under basal conditions, P2X7 protein levels were much higher in WKY macrophages compared to LEW ones, while DC BMDMs, in accordance with the RT-PCR results, showed similar levels as WKY macrophages. In response to LPS stimulation, WKY macrophages exhibit much higher P2X7 protein levels than under basal conditions, while no major changes in protein levels were seen in both DC and LEW ones. The ability of LPS to induce an upregulation of P2X7R is well documented. Previous studies from Humphreys et al. have shown that P2X7 receptor expression in human monocytes is upregulated by several pro-inflammatory stimuli such as LPS, INF-γ and TNF-α (Humphreys & Dubyak, 1998). In their studies however, THP-1 cells were incubated for at least 48 hours and LPS was not used alone but in association with INF-γ. The observation that stimulation with LPS 1 μg/ml for 5 hours induces an upregulation of P2X7 protein only in WKY and not in DC or LEW macrophages suggests an increased sensitivity of WKY BMDMs to LPS pro-inflammatory effects. These data are in accordance with other results which show that WKY BMDMs have a lower threshold for the activation of the inflammasome compared to LEW macrophages. Indeed, WKY macrophages release similar levels of active IL-1β when primed with either LPS 100 ng/ml or 1 μg/ml. On the other hand, LEW macrophages, when primed with LPS 100 ng/ml show similar levels of active IL-1β as when treated with LPS 100 ng/ml alone, indicating that the latter concentration of LPS is not sufficient to induce the inflammasome activation in these cells. Among the inflammasome-related genes analysed were IL-1RN and IL-18BP, which encode the proteins IL-1 receptor antagonist (IL-1Ra) and IL-18 binding protein, physiologic inhibitors of IL-1β and IL-18 respectively. To date,

three forms of IL-1Ra have been identified, one soluble form and two intracellular forms, referred to as sIL-1Ra, icIL-1RaI, and icIL-1RaII, respectively (Burger & Dayer, 1995). The soluble form of IL-1Ra inhibits both IL-1α and IL-1β by competitively binding to IL-1 receptor. IL-1Ra knockout mice exhibit growth retardation after weaning and an increased susceptibility to lethal endotoxemia and collagen-induced arthritis, suggesting that IL-1Ra plays an important role in both health and pathologic conditions (Ma et al., 1998). In humans, the circulating blood levels of sIL-1Ra are low in normal conditions while are significantly increased in several auto-immune and chronic inflammatory diseases such as rheumatoid arthritis and non-perforating Crohn's disease (Firestein et al., 1992), (Gilberts, Greenstein, Katsel, Harpaz, & Greenstein, 1994). The IL-18 binding protein (IL-18BP) is a circulating inhibitor of the proinflammatory cytokine IL-18. It is constitutively expressed in mononuclear cells, and elevated expression is induced by IFN-γ (Hurgin, Novick, & Rubinstein, 2002). IL-18BP binds IL-18 with a high affinity and, at equimolar ratios, inhibits 50–70% of IL-18 activity; at twofold molar excess, IL-18BP neutralises nearly all IL-18 activity (Dinarello, 2001). IL-18BP is constitutively secreted and was isolated in urine of healthy subjects (Dinarello, 2000). Previous studies from He et al. have shown that IL-18BP transgenic mice are functionally and histologically protected against ischemic acute kidney injury (AKI) induced by bilateral renal pedicle clamping (He et al., 2008). On the other hand, studies conducted on patients with active Crohn's disease (CD) have revealed that the levels of IL-18BP transcript and protein are significantly up-regulated in active CD specimens compared with control specimens and that macrophages were the major source of IL-18BP within the intestinal submucosa (Corbaz et al., 2002). These studies highlight the complexity of IL-18/IL-18BP biology and the significance of IL-18BP upregulation is not fully understood yet. My data show that BMDMs from WKY rats express significant higher pro-IL-18 and IL-18BP mRNA levels compared to macrophages from LEW rats under basal conditions. One possible explanation of

these findings is that, even under basal conditions, WKY BMDMs exhibit an hyperactivated phenotype and the increased expression of IL-18BP gene is secondary to the increased pro-IL18 mRNA levels in order to modulate the excessive IL-18 activity that might derive from that. Similarly, IL-1RA mRNA levels are significantly higher in WKY macrophages compared to LEW ones although no differences in pro-IL-1β mRNA and protein levels were seen between macrophages from the two rat strains.

Analysis of inflammasome-mediated cytokine production in WKY, DC and LEW BMDMs

When primed with LPS 1 μg/ml for 5 hours and stimulated with ATP for 30 minutes, WKY macrophages produce significant higher levels of both IL-1β and IL-18 and show much higher levels of active caspase-1 compared to DC and LEW macrophages. Since WKY BMDMs in response to LPS express higher levels of P2X7 mRNA and protein compared to DC and LEW macrophages, it is reasonable to say that the increased IL-1β and IL-18 secretion in WKY BMDMs might be secondary to an increased P2X7R activity. In accordance with this hypothesis, macrophages from DC rats which show intermediate levels of P2X7 protein between WKY and LEW also exhibit intermediate levels of active IL-1β and IL-18 when stimulated with ATP. Since the only difference between WKY and DC rats is in the chromosome 13 and 16 intervals Crgn1 and Crgn2 respectively, it is possible to assume that either Crgn1 or Crgn2 contains one or more genes that are responsible for P2X7R expression regulation in response to LPS. Among the genes included in the Crgn2 interval is Jund, which encodes the activator protein-1 (AP-1) transcription factor Jund. It has been already demonstrated that Jund is a major determinant of macrophage activity and is associated with glomerulonephritis susceptibility. Furthermore, microarray and QRT-PCR

analyses showed that Jund expression is significantly higher in WKY than in LEW glomeruli both at baseline and in NTN-induced glomeruli (Behmoaras et al., 2008). Therefore Jund represented a good candidate for a possible role in the regulation of P2X7R expression and consequent modulation of the inflammasome activation. I have then analysed the effects of Jund siRNA on the secretion of active IL-1β, IL-18 and caspase-1 in response to ATP stimulation in LPS-primed WKY BMDMs but I could not see any major differences, there was only about 20% reduction in IL-1β secretion according to the ELISA results. To further investigate the role of Jund in the regulation of P2X7 protein expression and inflammasome activation I have cultured BMDMs from WT and Jund deficient mice and looked at the inflammasome-related cytokine secretion in response to ATP but WT and Jund knock-out mice exhibit similar levels of active IL-1β, IL-18 and caspase-1 and no differences were seen in the P2X7 protein levels, indicating that other genes but Jund are playing this role. The analysis of inflammasome-related cytokine secretion also revealed that the use of a selective caspase-1 inhibitor (YVAD) dramatically affects both IL-1β and IL-18 secretion in response to ATP in WKY BMDMs suggesting that the production of these cytokines is caspase-1 dependent. However, while IL-18 secretion was completely abolished by the use of the caspase-1 inhibitor, active IL-1β was still detectable in WKY BMDMs indicating that other caspase-1 independent alternative pathways might contribute to the generation of active IL-1β in these cells. Aside from caspase-1, other proteases are indeed capable of cleaving pro-IL1β including bacterial enzymes, trypsin or chymotrypsin and enzymes such as leukocyte elastase and granzyme A (Schonbeck, Mach, & Libby, 1998). Different members of the metalloproteinase (MMP) family, in particular gelatinase A (MMP-2) and gelatinase B (MMP-9) have been shown to be able to generate active IL-1β and are usually overexpressed at sites of inflammation. IL-1β itself, is known to regulate the expression and activation of MMPs, demonstrating a cross-regulation among these two classes of effectors of inflammation (Yoo et

al., 2002). My results show that both MMP-9 mRNA levels and enzymatic activity are increased in WKY BMDMs compared to LEW ones. To evaluate the contribute of MMP-9 in the generation of active IL-1β in WKY macrophages, I have looked at the production of active IL-1β in response to ATP in the presence of the MMP inhibitor Ilomastat (Millipore, UK) by ELISA and the use of the MMP inhibitor led to a reduction of about 20% of IL-1β secretion (data not shown), indicating that the majority of IL-1β secretion in WKY BMDMs is caspase-1 dependent. My data also show that the levels of both IL-1β and IL-18 precursors in response to LPS are the same in WKY and LEW BMDMs. These findings suggest that the increased levels of mature IL-1β and IL-18 in response to ATP seen in WKY macrophages are not a consequence of a dysregulation of the TLR4/NF-kb pathway but is the conversion of the precursors into their active form that is accelerated or more active in WKY BMDMs.

Ex-vivo analysis of the inflammasome activation in nephritic glomeruli from WKY, DC and LEW rats

Ex-vivo incubation of isolated glomeruli from WKY, DC and LEW rats at day 4 from the injection of NTS revealed that WKY nephritic glomeruli, in the absence of any stimuli, show higher levels of active IL-1β, IL-18 and caspase-1 compared to glomeruli from DC and LEW rats. Glomeruli from DC rats exhibit higher levels of active IL-1β, IL-18 and caspase-1 compared to LEW glomeruli but much lower than WKY ones. The analysis of P2X7 protein expression in nephritic glomeruli also revealed that WKY nephritic glomeruli express much higher P2X7 protein levels compared to DC and LEW glomeruli. Glomeruli from DC rats showed intermediate P2X7 protein levels between WKY and LEW glomeruli. These findings are very important because they confirm the important role of the inflammasome-mediated cytokines in the pathogenesis of NTN and they also

show that the grade of inflammasome activation correlates well with the severity of the disease in vivo. Indeed, when injected with NTS, DC rats exhibit an intermediate phenotype between WKY and LEW rats showing a decreased macrophage infiltration and a 34% reduction in the number of glomerular crescents compared to WKY rats. Furthermore, these data confirm the positive correlation between P2X7 protein levels and the grade of inflammasome activation. The analysis of the levels of the inflammasome activation in macrophages and isolated glomeruli from single congenic rat strains is more complicated. According to the IL-1β ELISA's results, glomeruli isolated from WL16 rats show significant lower levels of IL-1β compared to WKY nephritic glomeruli and only slightly higher compared to the ones seen in glomeruli from DC rats. When I analysed the same samples by western blotting, the scenario was completely different with WL16 glomeruli resembling the WKY ones, showing similar levels of active IL-1β, while in LW16 glomeruli active IL-1β was not detectable as in the LEW ones. Likewise, WL16 glomeruli exhibited similar levels of P2X7 proteins and active IL-18 as the WKY ones, while in LW16 and LEW glomeruli active IL-18 was not detectable and P2X7 protein levels were very low. Previous studies from Behmoaras et al. have shown that the introgression of LEW Crgn2 into the WKY recipients reduced glomerular crescents only by 8% (Behmoaras et al., 2010). There seems to be therefore a good correlation between the IL-1β levels detected by western blotting in isolated glomeruli from WL16 rats and the severity of the disease. It is however surprising that the results coming from western blotting and ELISA were so different. One possible explanation could be that by ELISA I have analysed only the secreted component, whereas with western blotting I have also examined the amount of the cytokine that is retained inside the glomeruli and the infiltrating macrophages. I found a poor correlation between ELISA and western blotting results also when I analysed the levels of IL-1β released by BMDMs in response to ATP. According to the ELISA results, macrophages from WL16 rats showed

about 30% reduction compared to WKY ones and about 20% higher IL-1β levels compared to LEW macrophages. Western blotting analysis of the same samples revealed that WL16 BMDMs release lower levels of IL-1β compared to the WKY ones but much higher than LEW macrophages. The two techniques in this case show a similar pattern, however the differences between the levels of IL-1β released by WL16 and LEW macrophages appear to be more dramatic in the western blotting results rather than the ELISA ones. One interesting result that has been confirmed both by ELISA and western blotting is that LW16 macrophages in response to ATP release much higher levels of IL-1β compared to the LEW ones. What is surprising is that the levels of P2X7 protein from LW16 and LEW macrophages are similar. The levels of active IL-18 secreted after stimulation with ATP were also much higher in LW16 BMDMs compared to LEW ones. These findings seem to indicate that the Crgn2 interval contains one or more genes that are able to control both IL-1β and IL-18 secretion in a P2X7 independent way. This hypothesis is also in accordance with the observation that, although BMDMs from LW16 rats exhibit higher levels of both IL-1β and IL-18 compared to LEW ones, active caspase-1 appears to be not increased suggesting that the increased secretion of these cytokines in LW16 macrophages does not involve caspase-1 nor P2X7R. On the other hand, BMDMs from WL16 rats show lower P2X7 protein expression, lower caspase-1 activation and lower levels of active IL-1β and IL-18 compared to WKY macrophages. Although my data clearly show that IL-1β secretion is mainly caspase-1 dependent in macrophages from WKY rats as demonstrated by the observation that its secretion is dramatically reduced with the use of a specific caspase-1 inhibitor, it is possible that other alternative pathways might be switch on in the presence of different inflammatory stimuli. Crgn2 interval might contain one or more genes that control the switch of either the classical or the alternative pathways for IL-1β and IL-18 processing and release.

Key discoveries in this chapter

P2X7R levels as well as the expression of several genes belonging to the Nlrp3-inflammasome pathway are up-regulated in macrophages of the WKY rat, a strain uniquely susceptible to experimental nephrotoxic nephritis. Following P2X7R activation by ATP, WKY BMDMs produce markedly increased levels of active IL-1β, IL-18 and caspase-1 when compared with the NTN-resistant Lewis rat BMDMs. Similar results were obtained analysing isolated nephritic glomeruli from the two rat strains confirming a role for the P2X7-mediated inflammasome activation in the pathogenesis of glomerulonephritis.The analysis of both macrophages and nephritic glomeruli from single and double congenic rats appears to show that the P2X7R-inflammasome axis is at least partly under the genetic control of two previously identified Crgn quantitative trait loci (Crgn1, Crgn2) in the WKY NTN model. In conclusion, these results advocate the critical role of the P2X7R-mediated inflammasome activation in glomerulonephritis, highlighting it as a potential therapeutic target.

CHAPTER SIX-GENERAL DISCUSSION

6.1 DISCUSSION

The existence of plasma membrane receptors for extracellular nucleotides was recognised for the first time in 1978 by Geoff Burnstock. Since then, an incredible progress has been done in the understanding of purinergic receptor functions and their role in many important biological processes. Among the various purinergic receptors, P2X7 appears to be a very complex one, having different functions in different or even the same cells. It is now well established that P2X7R is not a simple ion channel with pore-formation activity but is instead a fundamental mediator of the immune response and is involved in many important cellular activities such as cell cycle regulation. There are still many unanswered questions about its mechanism of action and its exact role in inflammatory diseases. The work presented in this thesis embraces three different aspects of P2X7R activation: 1) pro-inflammatory cytokine production, 2) activation of cell signalling transduction pathways and 3) P2X7R-mediated inflammasome activation and its role in the pathogenesis of crescentic glomerulonephritis. To investigate P2X7R contribution in the secretion of the pro-inflammatory cytokines IL-1β and IL-18, I have compared the levels of these cytokines released in response to ATP in macrophages from WT mice and two different P2X7 deficient mouse lines, the GSK and the Pfizer ones. Similarly, macrophages from WT and P2X7 deficient mice have been used to explore the cell signalling cascade following ATP stimulation and to establish which pathways were selectively activated by P2X7R. Finally, to analyse the role of P2X7-mediated inflammasome activation in the pathogenesis of crescentic glomerulonephritis I have analysed and compared both macrophages and nephritic glomeruli from the glomerulonephritis-susceptible rat strain WKY with

the ones from the resistant rat strain Lewis. In order to establish the contribution of the Crgn1 and Crgn2 loci in the regulation of the NLRP3-inflammasome activation, I have extended the analysis to macrophages and nephritic glomeruli from single and double congenic rat strains.

Analysis of the P2X7-mediated pro-inflammatory cytokine production

P2X7R expression is necessary for the activation of caspase-1 in response to ATP. Macrophages from GSK and Pfizer KO mice do not exhibit any active caspase-1 after treatment with ATP. P2X7R-mediated caspase-1 activation significantly potentiates the release of both IL-1β and IL-18. Compared to BMDMs from Pfizer KO mice, macrophages from WT mice produce significant higher levels of IL-1β in response to ATP, BzATP and LL37 and show much higher levels of active IL-18 in response to ATP. Macrophages from GSK mice behaved differently from the Pfizer ones. Although they do not show any active caspase-1 following ATP stimulation, they release significant higher levels of both IL-1β and IL-18 in response to all the P2X7 agonists tested compared to macrophages from Pfizer mice. When stimulated with LL37, they release similar levels of IL-1β as macrophages from WT mice. Since active caspase-1 was never detectable in these cells in all the experiments conducted, it seems that both IL-1β and IL-18 are secreted through alternative, caspase-1 independent pathways in the GSK BMDMs. One other possibility could be that the Western blot technique may not be sensitive enough to detect low/moderate amount of active caspase-1. One important question that I tried to answer in this study was whether macrophages from GSK mice do effectively lack P2X7R or not. My Western blotting results clearly show that macrophages from GSK mice exhibit a band of the same size as the full length receptor using a specific anti-P2X7 antibody that recognises an epitope localized in a very distal region of the C-terminus of the

receptor. Using specific primers for the normal exon 1 and for the alternative exon 1 of the variant P2X7k, I could demonstrate by PCR that the band detected by Western blotting cannot correspond to the full length receptor, since no amplification was seen in GSK macrophages when primers for the normal exon 1 were used. However, no amplification was seen even when primers for the alternative exon-1 of the variant P2X7k were used. An important limitation of this experiment was the lack of a positive control. Since it has been shown that the P2X7k variant is highly expressed in the spleen of GSK mice, I should have included in the analysis also spleen RNA samples. In this way I could have established whether the lack of alternative exon-1 expression in GSK BMDMs was due to a technical issue or to the possibility that GSK macrophages express another P2X7 isoform with a different exon 1 from the P2X7k variant. The expression of an alternative new P2X7 isoform, if confirmed, appears to be at least in part functional and might explain why GSK BMDMs release much higher levels of active IL-1β and IL-18 compared to Pfizer macrophages, but lower compared to the WT ones.

Cell signalling cascade following P2X7R activation by ATP

Despite the numerous studies that have documented the activation of several signalling pathways in response to ATP stimulation in different cell lines, many questions still remain on P2X7R relative contribution in these processes. In many studies P2X7R involvement was demonstrated with the use of a selective or non-selective P2X7R antagonist which partially or completely abolished the effects seen with ATP treatment. However the use of inhibitors in the study of cell trasnduction pathways could be problematic as many of them require a pretreatment which itself can alter the intracellular signals. Due to the presence

in literature of several studies indicating a role for P2X7R in cell growth and proliferation, my first objective was to establish whether ATP stimulation would differentially activate the MAPK and the mTOR signalling pathways in macrophages from WT and P2X7R deficient mice. The analysis was then extended to all the signalling pathways activated by ATP using a phosphoproteomic approach.

Main findings

P2X7R plays a fundamental role in the activation of the ribosomal pathway, in the organization of actin cytoskeleton and in the regulation of vesicle transport and trafficking. P2X7R also contributes, together with other purinergic receptors to the activation of other important signalling pathways, including MAPK, mTOR, B and T cell receptor signalling pathways, Fcγ receptor mediated phagocytosis, endocytosis, apoptosis, chemokine signalling pathways and many others. One of the most relevant finding that came out from the phosphoproteomics analysis was the observation that ATP stimulation leads to an increased phosphorylation of 15 different peptides within the ribosomal pathway and all of these peptides showed an increased phosphorylation only in macrophages from WT mice, while macrophages from P2X7R deficient mice did not show any increased phosphorylation following ATP treatment. The ribosomal proteins that exhibited an increased phosphorylation were: RLA1, RLA2, RL3, RL5, RL11, RL13, RS 14 and RS15. Ribosomal proteins are essential for ribosome biogenesis, a very complex process consisting of the coordinated synthesis and assembly of four ribosomal RNAs with about 80 ribosomal proteins which in turn interact with more than 150 non-ribosomal proteins and other factors (Robledo et al., 2008). Ribosomal proteins have attracted a lot of interest since the discovery that the pathogenesis of a number of inherited and acquired diseases is linked to

mutations in genes encoding proteins involved in ribosome maturation, assembly, or export. An example is represented by the Diamond Blackfan anemia (DBA), an inherited red cell aplasia caused by mutations in one or several ribosomal proteins (Farrar et al., 2011). Since phosphorylation of ribosomal proteins affects critical steps of protein synthesis, the observation that P2X7R expression is necessary for their phosphorylation to occur, clearly indicates that P2X7R is a key regulator of the translation machinery. Although several studies in literature have documented that ATP induces the activation of the MAPK signalling pathway and this effect was attributed to P2X7R activation, my data show that effectively the MAPK signalling pathway is the most activated one in response to ATP, however this activation involves other purinergic receptors apart from P2X7. Some proteins within the MAPK signalling pathway appear to be more phosphorylated in the macrophages from KO mice than in the ones from WT mice, which might indicate that P2X7R acts as a negative regulator of these proteins. The contribution of P2X7R in the activation of the mTOR signalling pathway appears to be very complex too. Apart from a few proteins such as S6 kinase and Akt which exhibit higher levels of phosphorylation in WT macrophages compared to the KO ones, all the others showed higher levels of phosphorylation in macrophages from P2X7 deficient mice. This is not surprising, considering the many different functions attributed to the mTOR signalling pathway. It is possible that P2X7R might positively regulate some functions and negatively regulate some others within the same pathway.

P2X7-mediated inflammasome activation and its role in the pathogenesis of glomerulonephritis

The analysis of the P2X7-mediated inflammasome activation and its role in the pathogenesis of glomerulonephritis has been conducted using the rat model of NTN. I have first investigated the expression of inflammasome-related genes and the inflammasome-dependent cytokine production in macrophages from WKY and LEW rats and I have then extended my analysis on macrophages from single and double congenic rats. Furthermore, to correlate my in vitro data with the severity of disease I have examined the inflammasome activation in isolated cultured glomeruli from WKY, LEW and congenic rat strains.

Main findings

WKY BMDMs even under basal conditions show an upregulation of the majority of the inflammasome genes including P2X7. Not only the mRNA but also P2X7 protein levels are significantly higher in macrophages from WKY rats compared to the ones from LEW rats. Similarly to what happens with WT and P2X7 deficient mice, WKY macrophages that express higher P2X7 protein levels also show higher caspase-1 activation and release higher levels of both IL-1β and IL-18 compared to LEW macrophages. Caspase-1 inhibition dramatically affects the secretion of active IL-18 but does not abolish completely the release of active IL-1β in WKY macrophages treated with ATP. The increased secretion of mature Il-1β and IL-18 in WKY BMDMs is not due to an increased synthesis of the precursors following LPS priming, since WKY and LEW macrophages exhibit similar levels of both pro-IL-1β and pro-IL-18 in response to LPS. This suggests that it is the processing and release of these two cytokines that is different in macrophages from the two rat strains. Similarly, WKY glomeruli collected four

days after the injection of NTS and cultured for 72 hours in serum-free conditions and in the absence of any pro-inflammatory stimuli exhibit higher levels of P2X7 protein, higher caspase-1 activation and higher levels of both IL-1β and IL-18 compared to glomeruli from LEW rats. The analysis of macrophages and glomeruli from the congenic rat strains appears to be more complex. When injected with NTS, double congenic rats show a 34% reduction in the number of glomerular crescents. DC macrophages, when primed with LPS and stimulated with ATP exhibit lower levels of P2X7 protein, lower caspase-1 activation and lower levels of both IL-1β and IL-18 compared to WKY macrophages indicating a good correlation between P2X7R-mediated inflammasome activation and the severity of disease. This was also confirmed by the analysis of cultured nephritic glomeruli which perfectly resembled the macrophages, showing lower P2X7R expression, lower caspase-1 activation and lower levels of active IL-1β and IL-18 compared to WKY glomeruli. DC rats have Chromosome 13 and Chromosome 16 intervals from the LEW rat introgressed into the WKY genetic background. Thus, in order to study the relative role of chromosome 16 and chromosome 13, I have used the single congenic rat strains WL16 and LW16. Unfortunately I could not use the WL13 rats because no longer available. Interestingly I found that WL16 macrophages express lower levels of P2X7 protein, show attenuated caspase-1 activation, IL-1β and IL-18 production compared to WKY macrophages but similar to DC ones. On the other hand, macrophages from LW16 rats, although they expressed similar levels of both P2X7 protein and active caspase-1 as LEW macrophages, surprisingly release much higher levels of both active IL-1β and IL-18 comparable to the levels of these cytokines in macrophages from WL16 rats. However, this pattern was not completely reproduced in the nephritic glomeruli. Indeed, according to the ELISA results, glomeruli from WL16 rats showed much lower levels of active IL-1β compared to WKY glomeruli, while LW16 glomeruli exhibit the same levels as LEW glomeruli. My Western blotting data on the other hand, reveal that WL16 glomeruli release similar IL-1β and IL-18 levels as WKY

glomeruli, whereas LW16 perfectly resemble the LEW glomeruli. Therefore, there seems to be a poor correlation between macrophages and glomeruli data from single congenic rats. The analysis of BMDMs from single congenic rats seems to indicate that the chromosome 16 interval contains one or more genes that regulate the inflammasome activation and the consequent secretion of both IL-1β and IL-18. WL16 macrophages, indeed, show lower IL-1β and IL-18 levels compared to WKY macrophages, while LW16 exhibit much higher levels of these cytokines than LEW macrophages. However, it still remains unclear whether this regulation is linked to P2X7R expression or not. WL16 macrophages, indeed, exhibit lower P2X7 protein levels compared to the WKY ones and this is associated to attenuated caspase-1 activation and to a lower production of active IL-1β and IL-18. This suggests that whatever is controlling the inflammasome activation within the chromosome 16 interval, is doing it through a down-regulation of P2X7R expression. On the other hand, the observation that LW16 macrophages release more IL-1β and more IL-18 than the LEW ones, although they express similar levels of P2X7R and exhibit the same level of active caspase-1 indicate that the WKY chromosome 16 interval is inducing an increased secretion of both IL-1β and IL-18 in a P2X7R and caspase-1 independent way. It is possible that the genetic background in which chromosome 16 interval is introgressed influences the outcome leading to either the activation of the classical or the alternative pathways for the secretion of active IL-1β and IL-18. The poor correlation between macrophages and nephritic glomeruli from single congenic rats suggests that, although the chromosome 16 interval Crgn2 seems to regulate IL-1β and IL-18 secretion in macrophages, other genes not included in the Crgn2 interval as well as intrinsic renal cells are contributing to the pathogenesis of glomerulonephritis as previously demonstrated by kidney transplant experiments. My data also indicate that JunD is not involved in the regulation of the inflammasome activation. No major effects were seen on the release of active IL-1β and IL-18 using specific siRNA

targeting JunD. Similarly, macrophages from JunD KO mice exhibit similar levels of active IL-1β, caspase-1 and P2X7 protein as the WT mice. Only IL-18 appeared to be decreased in macrophages from JunD deficient mice and the significance of this effect remains unclear.

6.2 CONCLUSIONS

The work presented in this thesis demonstrates for the first time a fundamental role for P2X7R-mediated inflammasome activation in the pathogenesis of Crgn and indicates it as a possible therapeutic target. To my knowledge, to date there is only one published study that has investigated the role of the NLRP3 inflammasome activation in glomerular inflammation. In this study, conducted by Lichtnekert et al., they used a mouse model of heterologous anti-GBM nephritis and concluded that the NLRP3-ASC-caspase-1 axis does not contribute to intrinsic glomerular inflammation via glomerular parenchymal cells. Indeed, they could not demonstrate any pro-IL-1β production upon LPS stimulation and no caspase-1 activation after an additional exposure to ATP nor in mouse glomeruli nor in mesangial cells, glomerular endothelial cells and podocytes but only in renal dendritic cells (Lichtnekert et al., 2011). However, heterologous phase of anti GBM glomerulonephritis used in this study is an acute model of neutrophil mediated glomerular injury with only a minor role for macrophages. In contrast, NTN is a severe model of crescentic glomerulonephritis, strongly macrophage-dependent, with progression to fibrosis and renal failure. Since macrophages accumulation within glomeruli occurs in several models of renal disease, such as in diabetic nephropathy, the results of my macrophages studies could have important implications also for the treatment of other macrophage-dependent renal diseases.

Role of P2X7R-mediated inflammasome activation in other inflammatory conditions

Recently, P2X7R-mediated inflammasome activation has also been implicated in other models of inflammatory diseases such as Chronic Obstructive Pulmonary Disease (COPD), a cigarette smoke-related inflammatory disease of the airways characterised by a progressive and irreversible decline in lung function (Eltom et al., 2011). In their study, Eltom et al. reported attenuated caspase-1 activation, IL-1β release and airway inflammation in P2X7R deficient mice exposed to cigarette smoke compared to the WT controls. Another study conducted by Kolliputi et al. demonstrated a role for P2X7R-mediated inflammasome activation in hyperoxic acute lung injury (Kolliputi et al., 2010). Culturing primary murine alveolar macrophages exposed to hyperoxia, they showed that hyperoxia induces potassium efflux through the P2X7R, leading to inflammasome activation and secretion of proinflammatory cytokines and these effects were completely abolished by the use of oxidized ATP. Furthermore, P2X7R activation has been reported to play an important role in pulmonary fibrosis. Using a murine model of lung fibrosis induced by airway-administered bleomycin and through the quantification of ATP levels in bronchoalveolar lavage fluid from control subjects and patients with idiopathic pulmonary fibrosis, Riteau et al. concluded that ATP released from bleomycin-injured lung cells acts as an endogenous danger signal that engages the P2X7R leading to IL-1β maturation and lung fibrosis (Riteau et al., 2010). Finally, an interesting study from Babelova et al. provides evidence of direct activation of the NLRP3 inflammasome by biglycan, an important component of the extra-cellular matrix, generally released under tissue stress conditions (Babelova et al., 2009). The novelty of this study is represented by the discovery that biglycan, acting as an endogenous danger signal activates the NLRP3 inflammasome by directly interacting with Toll-like and purinergic P2X4 and P2X7 receptors without the costimulatory effect of ATP. The proof for the involvement of both P2X4 and P2X7 in the

biglycan-induced IL-1β secretion was obtained by the use of macrophages from P2X7 deficient mice, P2X7 inhibitors such as KN62 and specific siRNA to knock-down P2X4 gene expression. The interaction between biglycan and P2X7 and P2X4 receptors was confirmed by immunoprecipitation experiments. Using a model of non-infectious inflammatory renal injury (unilateral ureteral obstruction) and a model of LPS-induced sepsis, they show that biglycan deficient mice release lower levels of active caspase-1 and mature IL-1β, resulting in less damage to target organs. Taken together these data suggest a novel mechanism of downstream activation of the NLRP3 inflammasome and confirm the role of internal danger signals as inducers of inflammation. Furthermore, these studies highlight the complexity of the inflammasome activation process and indicate that modulation of P2X7R-mediated inflammasome activation may provide a substantial clinical benefit in a wide range of inflammatory conditions.

6.3 FUTURE DIRECTIONS

The results reported in this thesis suggest that several areas of research on P2X7R role in the pathogenesis of glomerulonephritis are worthy of further investigation.

Identification of genes within the Crgn2 interval that control IL-1β and IL-18 secretion

The analysis conducted on macrophages from single congenic rat strains has demonstrated that the chromosome 16 interval contains one or more genes that control the secretion of both IL-1β and IL-18 in these cells and the identification of this genetic link would be extremely important to better understand the exact mechanisms by which the inflammasome activation is regulated and could potentially reveal new markers of disease and new therapeutic targets. Since the chromosome 16 interval contains many different genes (about 300), identifying the right one is not easy and it all becomes more complicated if it is more than one gene involved. One possible approach would be to select a preliminary panel of genes on the basis of a previously described connection with the inflammasome activation, to silence these genes using specific siRNAs and by microarray analysis examine the expression of inflammasome-related genes.

Contribution of intrinsic renal cells

Both the kidney transplants experiments and my data on nephritic glomeruli from single congenic rats suggest that the severity of glomerulonephritis is the

result of a delicate balance between macrophages and intrinsic renal cells interaction. It would be therefore relevant to analyse the secretion of cytokines that might positively or negatively regulate the inflammasome activation in intrinsic renal cells including mesangial cells and podocytes. One thing to do would be to analyse by ELISA the cytokines released by nephritic glomeruli from WKY, LEW and congenic rats and once identified one or more cytokines that appear to be differentially expressed and well correlate with the severity of the disease, I would stimulate macrophages from the different rat strains with increasing concentrations of the recombinant cytokine identified and examine the effects of this cytokine on the inflammasome activation. Another possible approach would be to isolate mesangial cells from the different rat strains, to stimulate them with LPS and to analyse and compare the levels of cytokines released. Then I would transfer the supernatant from these cells into macrophages cultures and examine the effects on IL-1β and IL-18 secretion in response to ATP. It would be also worthy to analyse the release of the physiologic inhibitors of IL-1β and IL-18, IL-1RA and IL-18bp, in the supernatants of both macrophages and nephritic glomeruli from the different rat strains. The in vitro results will then be applied to in vivo studies to prove the biological relevance of the findings.

Effects of P2X7 inhibition on the phosphorylation of ERK

One important result that emerges from the Western blot analysis of the cell signalling cascade following ATP stimulation in macrophages, is that ATP leads to an increase phosphorylation of ERK only in macrophages from WT mice indicating a clear involvement of P2X7R in this process. Differently from other members of the P2X family, P2X7R is known to be potently inhibited by zinc and copper even at submicromolar concentrations. The molecular basis for this strong functional inhibition is not fully understood yet, although it has been

suggested that these divalent cations inhibit P2X7R directly interacting with specific residues of its ectodomain. To my knowledge, the functional inhibition by zinc and copper in regard of P2X7R mediated cell signalling cascade has never been investigated. The majority of studies available have indeed focused their attention on the effects of these divalent cations on ATP or BzATP evoked currents, failing to analyse their effect on other important aspects of P2X7R functional activity. Therefore it would be relevant to investigate the effects of zinc and copper on P2X7R mediated cell signalling network and in particular to see whether the addition of zinc or copper in the medium is able to prevent ERK phosphorylation in macrophages from WT mice following stimulation with ATP. The findings might provide a fundamental insight into the actions of these divalent cations and the modulation of P2X7R mediated signalling activity.

Analysis of the cell signalling pathways activated in glomerulonephritis

The phosphoproteomic analysis conducted on macrophages from WT and P2X7R deficient mice stimulated with ATP has provided very useful informations about the signalling pathways activated by ATP and the relative contribution of P2X7R in the activation of these pathways. One of the most relevant and novel finding that came out from this analysis is that P2X7R strongly regulates the ribosomal pathway and might therefore have a crucial role in protein synthesis. Functional assays are certainly required to demonstrate P2X7R role in the regulation of the translation process. Quantitative phosphoproteomics could be also applied to the nephritic glomeruli from WKY, LEW and congenic rat strains to examine the cell signalling network activated in response to NTS injection and to discover which signalling pathways are differentially regulated in the different rat strains. This complex analysis could reveal new insights in the pathogenesis of the disease and could help uncover novel potential therapies for glomerulonephritis.

Reference List

Abbracchio, M. P. & Burnstock, G. (1994). Purinoceptors: are there families of P2X and P2Y purinoceptors? *Pharmacol.Ther., 64,* 445-475.

Abbracchio, M. P., Burnstock, G., Boeynaems, J. M., Barnard, E. A., Boyer, J. L., Kennedy, C. et al. (2006). International Union of Pharmacology LVIII: update on the P2Y G protein-coupled nucleotide receptors: from molecular mechanisms and pathophysiology to therapy. *Pharmacol.Rev., 58,* 281-341.

Acosta-Jaquez, H. A., Keller, J. A., Foster, K. G., Ekim, B., Soliman, G. A., Feener, E. P. et al. (2009). Site-specific mTOR phosphorylation promotes mTORC1-mediated signaling and cell growth. *Mol.Cell Biol., 29,* 4308-4324.

Adinolfi, E., Callegari, M. G., Ferrari, D., Bolognesi, C., Minelli, M., Wieckowski, M. R. et al. (2005). Basal activation of the P2X7 ATP receptor elevates mitochondrial calcium and potential, increases cellular ATP levels, and promotes serum-independent growth. *Mol.Biol.Cell, 16,* 3260-3272.

Adinolfi, E., Cirillo, M., Woltersdorf, R., Falzoni, S., Chiozzi, P., Pellegatti, P. et al. (2010). Trophic activity of a naturally occurring truncated isoform of the P2X7 receptor. *FASEB J., 24,* 3393-3404.

Adinolfi, E., Melchiorri, L., Falzoni, S., Chiozzi, P., Morelli, A., Tieghi, A. et al. (2002). P2X7 receptor expression in evolutive and indolent forms of chronic B lymphocytic leukemia. *Blood, 99,* 706-708.

Aga, M., Johnson, C. J., Hart, A. P., Guadarrama, A. G., Suresh, M., Svaren, J. et al. (2002). Modulation of monocyte signaling and pore formation in response to agonists of the nucleotide receptor P2X(7). *J.Leukoc.Biol., 72,* 222-232.

Aganna, E., Martinon, F., Hawkins, P. N., Ross, J. B., Swan, D. C., Booth, D. R. et al. (2002). Association of mutations in the NALP3/CIAS1/PYPAF1 gene with a broad phenotype including recurrent fever, cold sensitivity, sensorineural deafness, and AA amyloidosis. *Arthritis Rheum., 46,* 2445-2452.

Agostini, L., Martinon, F., Burns, K., McDermott, M. F., Hawkins, P. N., & Tschopp, J. (2004). NALP3 forms an IL-1beta-processing inflammasome with increased activity in Muckle-Wells autoinflammatory disorder. *Immunity., 20,* 319-325.

Aitman, T. J., Dong, R., Vyse, T. J., Norsworthy, P. J., Johnson, M. D., Smith, J. et al. (2006). Copy number polymorphism in Fcgr3 predisposes to glomerulonephritis in rats and humans. *Nature, 439,* 851-855.

Alcaraz, L., Baxter, A., Bent, J., Bowers, K., Braddock, M., Cladingboel, D. et al. (2003). Novel P2X7 receptor antagonists. *Bioorg.Med.Chem.Lett., 13,* 4043-4046.

Alzola, E., Perez-Etxebarria, A., Kabre, E., Fogarty, D. J., Metioui, M., Chaib, N. et al. (1998). Activation by P2X7 agonists of two phospholipases A2 (PLA2) in ductal cells of rat submandibular gland. Coupling of the calcium-independent PLA2 with kallikrein secretion. *J.Biol.Chem., 273,* 30208-30217.

Amstrup, J. & Novak, I. (2003). P2X7 receptor activates extracellular signal-regulated kinases ERK1 and ERK2 independently of Ca2+ influx. *Biochem.J., 374,* 51-61.

Armstrong, J. N., Brust, T. B., Lewis, R. G., & MacVicar, B. A. (2002). Activation of presynaptic P2X7-like receptors depresses mossy fiber-CA3 synaptic transmission through p38 mitogen-activated protein kinase. *J.Neurosci., 22,* 5938-5945.

Arulkumaran, N., Unwin, R. J., & Tam, F. W. (2011). A potential therapeutic role for P2X7 receptor (P2X7R) antagonists in the treatment of inflammatory diseases. *Expert.Opin.Investig.Drugs, 20,* 897-915.

Babelova, A., Moreth, K., Tsalastra-Greul, W., Zeng-Brouwers, J., Eickelberg, O., Young, M. F. et al. (2009). Biglycan, a danger signal that activates the NLRP3 inflammasome via toll-like and P2X receptors. *J.Biol.Chem., 284,* 24035-24048.

Bandyopadhyay, J., Lee, J., Lee, J., Lee, J. I., Yu, J. R., Jee, C. et al. (2002). Calcineurin, a calcium/calmodulin-dependent protein phosphatase, is involved in movement, fertility, egg laying, and growth in Caenorhabditis elegans. *Mol.Biol.Cell, 13,* 3281-3293.

Barden, N., Harvey, M., Gagne, B., Shink, E., Tremblay, M., Raymond, C. et al. (2006). Analysis of single nucleotide polymorphisms in genes in the chromosome 12Q24.31 region points to P2RX7 as a susceptibility gene to bipolar affective disorder. *Am.J.Med.Genet.B Neuropsychiatr.Genet., 141B,* 374-382.

Baricordi, O. R., Melchiorri, L., Adinolfi, E., Falzoni, S., Chiozzi, P., Buell, G. et al. (1999). Increased proliferation rate of lymphoid cells transfected with the P2X(7) ATP receptor. *J.Biol.Chem., 274,* 33206-33208.

Bauernfeind, F. G., Horvath, G., Stutz, A., Alnemri, E. S., MacDonald, K., Speert, D. et al. (2009). Cutting edge: NF-kappaB activating pattern recognition and cytokine receptors license NLRP3 inflammasome activation by regulating NLRP3 expression. *J.Immunol., 183,* 787-791.

Baxter, A., Bent, J., Bowers, K., Braddock, M., Brough, S., Fagura, M. et al. (2003). Hit-to-Lead studies: the discovery of potent adamantane amide P2X7 receptor antagonists. *Bioorg.Med.Chem.Lett., 13,* 4047-4050.

Behmoaras, J., Bhangal, G., Smith, J., McDonald, K., Mutch, B., Lai, P. C. et al. (2008). Jund is a determinant of macrophage activation and is associated with glomerulonephritis susceptibility. *Nat.Genet., 40,* 553-559.

Behmoaras, J., Smith, J., D'Souza, Z., Bhangal, G., Chawanasuntoropoj, R., Tam, F. W. et al. (2010). Genetic loci modulate macrophage activity and glomerular damage in experimental glomerulonephritis. *J.Am.Soc.Nephrol., 21,* 1136-1144.

Belkhir, R., Moulonguet-Doleris, L., Hachulla, E., Prinseau, J., Baglin, A., & Hanslik, T. (2007). Treatment of familial Mediterranean fever with anakinra. *Ann.Intern.Med., 146,* 825-826.

Bhat, N. R., Zhang, P., & Bhat, A. N. (1999). Cytokine induction of inducible nitric oxide synthase in an oligodendrocyte cell line: role of p38 mitogen-activated protein kinase activation. *J.Neurochem., 72,* 472-478.

Bianchi, B. R., Lynch, K. J., Touma, E., Niforatos, W., Burgard, E. C., Alexander, K. M. et al. (1999). Pharmacological characterization of recombinant human and rat P2X receptor subtypes. *Eur.J.Pharmacol., 376,* 127-138.

Bianchi, M. E. & Manfredi, A. A. (2009). Immunology. Dangers in and out. *Science, 323,* 1683-1684.

Bianco, F., Ceruti, S., Colombo, A., Fumagalli, M., Ferrari, D., Pizzirani, C. et al. (2006). A role for P2X7 in microglial proliferation. *J.Neurochem., 99,* 745-758.

Black, R. A., Kronheim, S. R., Cantrell, M., Deeley, M. C., March, C. J., Prickett, K. S. et al. (1988). Generation of biologically active interleukin-1 beta by proteolytic cleavage of the inactive precursor. *J.Biol.Chem., 263,* 9437-9442.

Boldt, W., Klapperstuck, M., Buttner, C., Sadtler, S., Schmalzing, G., & Markwardt, F. (2003). Glu496Ala polymorphism of human P2X7 receptor does not affect its electrophysiological phenotype. *Am.J.Physiol Cell Physiol, 284,* C749-C756.

Bours, M. J., Swennen, E. L., Di, V. F., Cronstein, B. N., & Dagnelie, P. C. (2006). Adenosine 5'-triphosphate and adenosine as endogenous signaling molecules in immunity and inflammation. *Pharmacol.Ther., 112,* 358-404.

Bradford, M. D. & Soltoff, S. P. (2002). P2X7 receptors activate protein kinase D and p42/p44 mitogen-activated protein kinase (MAPK) downstream of protein kinase C. *Biochem.J., 366,* 745-755.

Brake, A. J., Wagenbach, M. J., & Julius, D. (1994). New structural motif for ligand-gated ion channels defined by an ionotropic ATP receptor. *Nature, 371,* 519-523.

Brenner, M., Ruzicka, T., Plewig, G., Thomas, P., & Herzer, P. (2009). Targeted treatment of pyoderma gangrenosum in PAPA (pyogenic arthritis, pyoderma gangrenosum and acne) syndrome with the recombinant human interleukin-1 receptor antagonist anakinra. *Br.J.Dermatol., 161,* 1199-1201.

Bryant, C. & Fitzgerald, K. A. (2009). Molecular mechanisms involved in inflammasome activation. *Trends Cell Biol., 19,* 455-464.

Buell, G., Chessell, I. P., Michel, A. D., Collo, G., Salazzo, M., Herren, S. et al. (1998a). Blockade of human P2X7 receptor function with a monoclonal antibody. *Blood, 92,* 3521-3528.

Buell, G. N., Talabot, F., Gos, A., Lorenz, J., Lai, E., Morris, M. A. et al. (1998b). Gene structure and chromosomal localization of the human P2X7 receptor. *Receptors.Channels, 5,* 347-354.

Burckstummer, T., Baumann, C., Bluml, S., Dixit, E., Durnberger, G., Jahn, H. et al. (2009). An orthogonal proteomic-genomic screen identifies AIM2 as a cytoplasmic DNA sensor for the inflammasome. *Nat.Immunol., 10,* 266-272.

Burger, D. & Dayer, J. M. (1995). Inhibitory cytokines and cytokine inhibitors. *Neurology, 45,* S39-S43.

Burnstock, G. (1972). Purinergic nerves. *Pharmacol.Rev., 24,* 509-581.

Burnstock, G. (2006a). Pathophysiology and therapeutic potential of purinergic signaling. *Pharmacol.Rev., 58,* 58-86.

Burnstock, G. (2006b). Purinergic signalling--an overview. *Novartis.Found.Symp., 276,* 26-48.

Burnstock, G., Campbell, G., Satchell, D., & Smythe, A. (1970). Evidence that adenosine triphosphate or a related nucleotide is the transmitter substance released by non-adrenergic inhibitory nerves in the gut. *Br.J.Pharmacol., 40,* 668-688.

Burnstock, G., Fredholm, B. B., North, R. A., & Verkhratsky, A. (2010). The birth and postnatal development of purinergic signalling. *Acta Physiol (Oxf), 199,* 93-147.

Burnstock, G. & Kennedy, C. (1985). Is there a basis for distinguishing two types of P2-purinoceptor? *Gen.Pharmacol., 16,* 433-440.

Burrows, C., Abd, L. N., Lam, S. J., Carpenter, L., Sawicka, K., Tzolovsky, G. et al. (2010). The RNA binding protein Larp1 regulates cell division, apoptosis and cell migration. *Nucleic Acids Res., 38,* 5542-5553.

Cabrini, G., Falzoni, S., Forchap, S. L., Pellegatti, P., Balboni, A., Agostini, P. et al. (2005). A His-155 to Tyr polymorphism confers gain-of-function to the human P2X7 receptor of human leukemic lymphocytes. *J.Immunol., 175,* 82-89.

Cankurtaran-Sayar, S., Sayar, K., & Ugur, M. (2009). P2X7 receptor activates multiple selective dye-permeation pathways in RAW 264.7 and human embryonic kidney 293 cells. *Mol.Pharmacol., 76,* 1323-1332.

Cario-Toumaniantz, C., Loirand, G., Ferrier, L., & Pacaud, P. (1998). Non-genomic inhibition of human P2X7 purinoceptor by 17beta-oestradiol. *J.Physiol, 508 (Pt 3),* 659-666.

Cerretti, D. P., Kozlosky, C. J., Mosley, B., Nelson, N., Van, N. K., Greenstreet, T. A. et al. (1992). Molecular cloning of the interleukin-1 beta converting enzyme. *Science, 256,* 97-100.

Chaumont, S. & Khakh, B. S. (2008). Patch-clamp coordinated spectroscopy shows P2X2 receptor permeability dynamics require cytosolic domain rearrangements but not Panx-1 channels. *Proc.Natl.Acad.Sci.U.S.A, 105,* 12063-12068.

Chavele, K. M., Martinez-Pomares, L., Domin, J., Pemberton, S., Haslam, S. M., Dell, A. et al. (2010). Mannose receptor interacts with Fc receptors and is critical for the development of crescentic glomerulonephritis in mice. *J.Clin.Invest, 120,* 1469-1478.

Cheewatrakoolpong, B., Gilchrest, H., Anthes, J. C., & Greenfeder, S. (2005). Identification and characterization of splice variants of the human P2X7 ATP channel. *Biochem.Biophys.Res.Commun., 332,* 17-27.

Chen, L. & Brosnan, C. F. (2006). Exacerbation of experimental autoimmune encephalomyelitis in P2X7R-/- mice: evidence for loss of apoptotic activity in lymphocytes. *J.Immunol., 176,* 3115-3126.

Chen, Z., Raman, M., Chen, L., Lee, S. F., Gilman, A. G., & Cobb, M. H. (2003). TAO (thousand-and-one amino acid) protein kinases mediate signaling from carbachol to p38 mitogen-activated protein kinase and ternary complex factors. *J.Biol.Chem., 278,* 22278-22283.

Cheng, S. W., Fryer, L. G., Carling, D., & Shepherd, P. R. (2004). Thr2446 is a novel mammalian target of rapamycin (mTOR) phosphorylation site regulated by nutrient status. *J.Biol.Chem., 279,* 15719-15722.

Chessell, I. P., Hatcher, J. P., Bountra, C., Michel, A. D., Hughes, J. P., Green, P. et al. (2005). Disruption of the P2X7 purinoceptor gene abolishes chronic inflammatory and neuropathic pain. *Pain, 114,* 386-396.

Chiang, G. G. & Abraham, R. T. (2004). Determination of the catalytic activities of mTOR and other members of the phosphoinositide-3-kinase-related kinase family. *Methods Mol.Biol., 281,* 125-141.

Chiang, G. G. & Abraham, R. T. (2005). Phosphorylation of mammalian target of rapamycin (mTOR) at Ser-2448 is mediated by p70S6 kinase. *J.Biol.Chem., 280,* 25485-25490.

Chiozzi, P., Sanz, J. M., Ferrari, D., Falzoni, S., Aleotti, A., Buell, G. N. et al. (1997). Spontaneous cell fusion in macrophage cultures expressing high levels of the P2Z/P2X7 receptor. *J.Cell Biol., 138,* 697-706.

Choi, A. M. & Nakahira, K. (2011). Dampening insulin signaling by an NLRP3 'meta-flammasome'. *Nat.Immunol., 12,* 379-380.

Cohen, P. (2002). The origins of protein phosphorylation. *Nat.Cell Biol., 4,* E127-E130.

Coleman, M. L., Marshall, C. J., & Olson, M. F. (2004). RAS and RHO GTPases in G1-phase cell-cycle regulation. *Nat.Rev.Mol.Cell Biol., 5,* 355-366.

Collo, G., Neidhart, S., Kawashima, E., Kosco-Vilbois, M., North, R. A., & Buell, G. (1997). Tissue distribution of the P2X7 receptor. *Neuropharmacology, 36,* 1277-1283.

Conforti-Andreoni, C., Ricciardi-Castagnoli, P., & Mortellaro, A. (2011). The inflammasomes in health and disease: from genetics to molecular mechanisms of autoinflammation and beyond. *Cell Mol.Immunol., 8,* 135-145.

Cook, H. T., Singh, S. J., Wembridge, D. E., Smith, J., Tam, F. W., & Pusey, C. D. (1999). Interleukin-4 ameliorates crescentic glomerulonephritis in Wistar Kyoto rats. *Kidney Int., 55,* 1319-1326.

Corbaz, A., ten, H. T., Herren, S., Graber, P., Schwartsburd, B., Belzer, I. et al. (2002). IL-18-binding protein expression by endothelial cells and macrophages is up-regulated during active Crohn's disease. *J.Immunol., 168,* 3608-3616.

Costa, M., Marchi, M., Cardarelli, F., Roy, A., Beltram, F., Maffei, L. et al. (2006). Dynamic regulation of ERK2 nuclear translocation and mobility in living cells. *J.Cell Sci., 119,* 4952-4963.

Costa-Junior, H. M., Sarmento, V. F., & Coutinho-Silva, R. (2011). C terminus of the P2X7 receptor: treasure hunting. *Purinergic.Signal., 7,* 7-19.

Costanzi, S., Siegel, J., Tikhonova, I. G., & Jacobson, K. A. (2009). Rhodopsin and the others: a historical perspective on structural studies of G protein-coupled receptors. *Curr.Pharm.Des, 15,* 3994-4002.

Couser, W. G. (1999). Glomerulonephritis. *Lancet, 353,* 1509-1515.

Coutinho-Silva, R., Perfettini, J. L., Persechini, P. M., Dautry-Varsat, A., & Ojcius, D. M. (2001). Modulation of P2Z/P2X(7) receptor activity in macrophages infected with Chlamydia psittaci. *Am.J.Physiol Cell Physiol, 280,* C81-C89.

Coutinho-Silva, R., Stahl, L., Raymond, M. N., Jungas, T., Verbeke, P., Burnstock, G. et al. (2003). Inhibition of chlamydial infectious activity due to P2X7R-dependent phospholipase D activation. *Immunity., 19,* 403-412.

Cutillas, P. R. & Vanhaesebroeck, B. (2007). Quantitative profile of five murine core proteomes using label-free functional proteomics. *Mol.Cell Proteomics., 6,* 1560-1573.

De la Fuente van Bentem, Mentzen, W. I., de la Fuente, A., & Hirt, H. (2008). Towards functional phosphoproteomics by mapping differential phosphorylation events in signaling networks. *Proteomics., 8,* 4453-4465.

De, Y., Chen, Q., Schmidt, A. P., Anderson, G. M., Wang, J. M., Wooters, J. et al. (2000). LL-37, the neutrophil granule- and epithelial cell-derived cathelicidin, utilizes formyl peptide receptor-like 1 (FPRL1) as a receptor to chemoattract human peripheral blood neutrophils, monocytes, and T cells. *J.Exp.Med., 192,* 1069-1074.

Denlinger, L. C., Fisette, P. L., Sommer, J. A., Watters, J. J., Prabhu, U., Dubyak, G. R. et al. (2001). Cutting edge: the nucleotide receptor P2X7 contains multiple protein- and lipid-interaction motifs including a potential binding site for bacterial lipopolysaccharide. *J.Immunol., 167,* 1871-1876.

Denlinger, L. C., Shi, L., Guadarrama, A., Schell, K., Green, D., Morrin, A. et al. (2009). Attenuated P2X7 pore function as a risk factor for virus-induced loss of asthma control. *Am.J.Respir.Crit Care Med., 179,* 265-270.

Denlinger, L. C., Sommer, J. A., Parker, K., Gudipaty, L., Fisette, P. L., Watters, J. W. et al. (2003). Mutation of a dibasic amino acid motif within the C terminus of the P2X7 nucleotide receptor results in trafficking defects and impaired function. *J.Immunol., 171,* 1304-1311.

Dennis, P. B., Jaeschke, A., Saitoh, M., Fowler, B., Kozma, S. C., & Thomas, G. (2001). Mammalian TOR: a homeostatic ATP sensor. *Science, 294,* 1102-1105.

Di Virgilio, F. (1995). The P2Z purinoceptor: an intriguing role in immunity, inflammation and cell death. *Immunol.Today, 16,* 524-528.

Dinarello, C. A. (2000). Targeting interleukin 18 with interleukin 18 binding protein. *Ann.Rheum.Dis., 59 Suppl 1,* i17-i20.

Dinarello, C. A. (2001). Novel targets for interleukin 18 binding protein. *Ann.Rheum.Dis., 60 Suppl 3,* iii18-iii24.

Dinarello, C. A. (2004). Unraveling the NALP-3/IL-1beta inflammasome: a big lesson from a small mutation. *Immunity., 20,* 243-244.

Dong, C., Davis, R. J., & Flavell, R. A. (2002). MAP kinases in the immune response. *Annu.Rev.Immunol., 20,* 55-72.

Donnelly-Roberts, D. L. & Jarvis, M. F. (2007). Discovery of P2X7 receptor-selective antagonists offers new insights into P2X7 receptor function and indicates a role in chronic pain states. *Br.J.Pharmacol., 151,* 571-579.

Dostert, C. & Petrilli, V. (2008). [Asbestos triggers inflammation by activating the Nalp3 inflammasome]. *Med.Sci.(Paris), 24,* 916-918.

Drury, A. N. & Szent-Gyorgyi, A. (1929). The physiological activity of adenine compounds with especial reference to their action upon the mammalian heart. *J.Physiol, 68,* 213-237.

Du, W. & Maniatis, T. (1994). The high mobility group protein HMG I(Y) can stimulate or inhibit DNA binding of distinct transcription factor ATF-2 isoforms. *Proc.Natl.Acad.Sci.U.S.A, 91,* 11318-11322.

Dubyak, G. R. (2007). Go it alone no more--P2X7 joins the society of heteromeric ATP-gated receptor channels. *Mol.Pharmacol., 72,* 1402-1405.

Dufner, A. & Thomas, G. (1999). Ribosomal S6 kinase signaling and the control of translation. *Exp.Cell Res., 253,* 100-109.

Durando, M. M., Meier, K. E., & Cook, J. A. (1998). Endotoxin activation of mitogen-activated protein kinase in THP-1 cells; diminished activation following endotoxin desensitization. *J.Leukoc.Biol., 64,* 259-264.

Elssner, A., Duncan, M., Gavrilin, M., & Wewers, M. D. (2004). A novel P2X7 receptor activator, the human cathelicidin-derived peptide LL37, induces IL-1 beta processing and release. *J.Immunol., 172,* 4987-4994.

Eltom, S., Stevenson, C. S., Rastrick, J., Dale, N., Raemdonck, K., Wong, S. et al. (2011). P2X7 receptor and caspase 1 activation are central to airway inflammation observed after exposure to tobacco smoke. *PLoS.One., 6,* e24097.

Erb, L., Liao, Z., Seye, C. I., & Weisman, G. A. (2006). P2 receptors: intracellular signaling. *Pflugers Arch., 452,* 552-562.

Fairbairn, I. P., Stober, C. B., Kumararatne, D. S., & Lammas, D. A. (2001). ATP-mediated killing of intracellular mycobacteria by macrophages

is a P2X(7)-dependent process inducing bacterial death by phagosome-lysosome fusion. *J.Immunol., 167,* 3300-3307.

Fantuzzi, G., Ku, G., Harding, M. W., Livingston, D. J., Sipe, J. D., Kuida, K. et al. (1997). Response to local inflammation of IL-1 beta-converting enzyme- deficient mice. *J.Immunol., 158,* 1818-1824.

Farrar, J. E., Vlachos, A., Atsidaftos, E., Carlson-Donohoe, H., Markello, T. C., Arceci, R. J. et al. (2011). Ribosomal protein gene deletions in Diamond-Blackfan anemia. *Blood*.

Faustin, B., Lartigue, L., Bruey, J. M., Luciano, F., Sergienko, E., Bailly-Maitre, B. et al. (2007). Reconstituted NALP1 inflammasome reveals two-step mechanism of caspase-1 activation. *Mol.Cell, 25,* 713-724.

Feng, Y. H., Li, X., Wang, L., Zhou, L., & Gorodeski, G. I. (2006a). A truncated P2X7 receptor variant (P2X7-j) endogenously expressed in cervical cancer cells antagonizes the full-length P2X7 receptor through hetero-oligomerization. *J.Biol.Chem., 281,* 17228-17237.

Feng, Y. H., Li, X., Zeng, R., & Gorodeski, G. I. (2006b). Endogenously expressed truncated P2X7 receptor lacking the C-terminus is preferentially upregulated in epithelial cancer cells and fails to mediate ligand-induced pore formation and apoptosis. *Nucleosides Nucleotides Nucleic Acids, 25,* 1271-1276.

Fernando, S. L., Saunders, B. M., Sluyter, R., Skarratt, K. K., Goldberg, H., Marks, G. B. et al. (2007). A polymorphism in the P2X7 gene increases susceptibility to extrapulmonary tuberculosis. *Am.J.Respir.Crit Care Med., 175,* 360-366.

Ferrari, D., Chiozzi, P., Falzoni, S., Dal, S. M., Melchiorri, L., Baricordi, O. R. et al. (1997). Extracellular ATP triggers IL-1 beta release by activating the purinergic P2Z receptor of human macrophages. *J.Immunol., 159,* 1451-1458.

Ferrari, D., Chiozzi, P., Falzoni, S., Hanau, S., & Di, V. F. (1997). Purinergic modulation of interleukin-1 beta release from microglial cells stimulated with bacterial endotoxin. *J.Exp.Med., 185,* 579-582.

Ferrari, D., Pizzirani, C., Adinolfi, E., Lemoli, R. M., Curti, A., Idzko, M. et al. (2006). The P2X7 receptor: a key player in IL-1 processing and release. *J.Immunol., 176,* 3877-3883.

Ferrari, D., Stroh, C., & Schulze-Osthoff, K. (1999). P2X7/P2Z purinoreceptor-mediated activation of transcription factor NFAT in microglial cells. *J.Biol.Chem., 274,* 13205-13210.

Ferrari, D., Villalba, M., Chiozzi, P., Falzoni, S., Ricciardi-Castagnoli, P., & Di, V. F. (1996). Mouse microglial cells express a plasma membrane pore gated by extracellular ATP. *J.Immunol., 156,* 1531-1539.

Ferrari, S., Bandi, H. R., Hofsteenge, J., Bussian, B. M., & Thomas, G. (1991). Mitogen-activated 70K S6 kinase. Identification of in vitro 40 S ribosomal S6 phosphorylation sites. *J.Biol.Chem., 266,* 22770-22775.

Fields, R. D. & Burnstock, G. (2006). Purinergic signalling in neuron-glia interactions. *Nat.Rev.Neurosci., 7,* 423-436.

Fingar, D. C., Richardson, C. J., Tee, A. R., Cheatham, L., Tsou, C., & Blenis, J. (2004). mTOR controls cell cycle progression through its cell

growth effectors S6K1 and 4E-BP1/eukaryotic translation initiation factor 4E. *Mol.Cell Biol., 24,* 200-216.

Finlayson, A. E. & Freeman, K. W. (2009). A cell motility screen reveals role for MARCKS-related protein in adherens junction formation and tumorigenesis. *PLoS.One., 4,* e7833.

Firestein, G. S., Berger, A. E., Tracey, D. E., Chosay, J. G., Chapman, D. L., Paine, M. M. et al. (1992). IL-1 receptor antagonist protein production and gene expression in rheumatoid arthritis and osteoarthritis synovium. *J.Immunol., 149,* 1054-1062.

Flotow, H. & Thomas, G. (1992). Substrate recognition determinants of the mitogen-activated 70K S6 kinase from rat liver. *J.Biol.Chem., 267,* 3074-3078.

Friedle, S. A., Curet, M. A., & Watters, J. J. (2010). Recent patents on novel P2X(7) receptor antagonists and their potential for reducing central nervous system inflammation. *Recent Pat CNS.Drug Discov., 5,* 35-45.

Fujinaka, H., Yamamoto, T., Takeya, M., Feng, L., Kawasaki, K., Yaoita, E. et al. (1997). Suppression of anti-glomerular basement membrane nephritis by administration of anti-monocyte chemoattractant protein-1 antibody in WKY rats. *J.Am.Soc.Nephrol., 8,* 1174-1178.

Fuller, S. J., Stokes, L., Skarratt, K. K., Gu, B. J., & Wiley, J. S. (2009). Genetics of the P2X7 receptor and human disease. *Purinergic.Signal., 5,* 257-262.

Gargett, C. E. & Wiley, J. S. (1997). The isoquinoline derivative KN-62 a potent antagonist of the P2Z-receptor of human lymphocytes. *Br.J.Pharmacol., 120,* 1483-1490.

Gilberts, E. C., Greenstein, A. J., Katsel, P., Harpaz, N., & Greenstein, R. J. (1994). Molecular evidence for two forms of Crohn disease. *Proc.Natl.Acad.Sci.U.S.A, 91,* 12721-12724.

Goerdt, S., Politz, O., Schledzewski, K., Birk, R., Gratchev, A., Guillot, P. et al. (1999). Alternative versus classical activation of macrophages. *Pathobiology, 67,* 222-226.

Goncalves, R. G., Gabrich, L., Rosario, A., Jr., Takiya, C. M., Ferreira, M. L., Chiarini, L. B. et al. (2006). The role of purinergic P2X7 receptors in the inflammation and fibrosis of unilateral ureteral obstruction in mice. *Kidney Int., 70,* 1599-1606.

Gonnord, P., Delarasse, C., Auger, R., Benihoud, K., Prigent, M., Cuif, M. H. et al. (2009). Palmitoylation of the P2X7 receptor, an ATP-gated channel, controls its expression and association with lipid rafts. *FASEB J., 23,* 795-805.

Grahames, C. B., Michel, A. D., Chessell, I. P., & Humphrey, P. P. (1999). Pharmacological characterization of ATP- and LPS-induced IL-1beta release in human monocytes. *Br.J.Pharmacol., 127,* 1915-1921.

Gu, B. J., Zhang, W., Worthington, R. A., Sluyter, R., Dao-Ung, P., Petrou, S. et al. (2001). A Glu-496 to Ala polymorphism leads to loss of function of the human P2X7 receptor. *J.Biol.Chem., 276,* 11135-11142.

Gu, Y., Kuida, K., Tsutsui, H., Ku, G., Hsiao, K., Fleming, M. A. et al. (1997). Activation of interferon-gamma inducing factor mediated by interleukin-1beta converting enzyme. *Science, 275,* 206-209.

Guarda, G. & So, A. (2010). Regulation of inflammasome activity. *Immunology, 130,* 329-336.

Guile, S. D., Alcaraz, L., Birkinshaw, T. N., Bowers, K. C., Ebden, M. R., Furber, M. et al. (2009). Antagonists of the P2X(7) receptor. From lead identification to drug development. *J.Med.Chem., 52,* 3123-3141.

Guo, C., Masin, M., Qureshi, O. S., & Murrell-Lagnado, R. D. (2007). Evidence for functional P2X4/P2X7 heteromeric receptors. *Mol.Pharmacol., 72,* 1447-1456.

Gutierrez-Martin, Y., Bustillo, D., Gomez-Villafuertes, R., Sanchez-Nogueiro, J., Torregrosa-Hetland, C., Binz, T. et al. (2011). P2X7 receptors trigger ATP exocytosis and modify secretory vesicle dynamics in neuroblastoma cells. *J.Biol.Chem., 286,* 11370-11381.

Han, G., Ye, M., Jiang, X., Chen, R., Ren, J., Xue, Y. et al. (2009). Comprehensive and reliable phosphorylation site mapping of individual phosphoproteins by combination of multiple stage mass spectrometric analysis with a target-decoy database search. *Anal.Chem., 81,* 5794-5805.

Harada, H., Chan, C. M., Loesch, A., Unwin, R., & Burnstock, G. (2000). Induction of proliferation and apoptotic cell death via P2Y and P2X receptors, respectively, in rat glomerular mesangial cells. *Kidney Int., 57,* 949-958.

Hawkins, P. N., Lachmann, H. J., & McDermott, M. F. (2003). Interleukin-1-receptor antagonist in the Muckle-Wells syndrome. *N.Engl.J.Med., 348,* 2583-2584.

He, Z., Lu, L., Altmann, C., Hoke, T. S., Ljubanovic, D., Jani, A. et al. (2008). Interleukin-18 binding protein transgenic mice are protected against ischemic acute kidney injury. *Am.J.Physiol Renal Physiol, 295,* F1414-F1421.

Hide, I., Tanaka, M., Inoue, A., Nakajima, K., Kohsaka, S., Inoue, K. et al. (2000). Extracellular ATP triggers tumor necrosis factor-alpha release from rat microglia. *J.Neurochem., 75,* 965-972.

Hietakangas, V. & Cohen, S. M. (2007). Re-evaluating AKT regulation: role of TOR complex 2 in tissue growth. *Genes Dev., 21,* 632-637.

Hillman, K. A., Burnstock, G., & Unwin, R. J. (2005). The P2X7 ATP receptor in the kidney: a matter of life or death? *Nephron Exp.Nephrol., 101,* e24-e30.

Hise, A. G., Tomalka, J., Ganesan, S., Patel, K., Hall, B. A., Brown, G. D. et al. (2009). An essential role for the NLRP3 inflammasome in host defense against the human fungal pathogen Candida albicans. *Cell Host.Microbe, 5,* 487-497.

Hoedemaeker, P. J. & Weening, J. J. (1989). Relevance of experimental models for human nephropathology. *Kidney Int., 35,* 1015-1025.

Hoffman, H. M. (2009). Therapy of autoinflammatory syndromes. *J.Allergy Clin.Immunol., 124,* 1129-1138.

Hogquist, K. A., Unanue, E. R., & Chaplin, D. D. (1991). Release of IL-1 from mononuclear phagocytes. *J.Immunol., 147,* 2181-2186.

Honore, P., Donnelly-Roberts, D., Namovic, M. T., Hsieh, G., Zhu, C. Z., Mikusa, J. P. et al. (2006). A-740003 [N-(1-{[(cyanoimino)(5-quinolinylamino)methyl]amino}-2,2-dimethylpropyl)-2-(3,4-dimethoxyphenyl)acetamide], a novel and selective P2X7 receptor antagonist, dose-dependently reduces neuropathic pain in the rat. *J.Pharmacol.Exp.Ther., 319,* 1376-1385.

Hricik, D. E., Chung-Park, M., & Sedor, J. R. (1998). Glomerulonephritis. *N.Engl.J.Med., 339,* 888-899.

Huang, J. & Manning, B. D. (2009). A complex interplay between Akt, TSC2 and the two mTOR complexes. *Biochem.Soc.Trans., 37,* 217-222.

Humphreys, B. D. & Dubyak, G. R. (1998). Modulation of P2X7 nucleotide receptor expression by pro- and anti-inflammatory stimuli in THP-1 monocytes. *J.Leukoc.Biol., 64,* 265-273.

Humphreys, B. D., Virginio, C., Surprenant, A., Rice, J., & Dubyak, G. R. (1998). Isoquinolines as antagonists of the P2X7 nucleotide receptor: high selectivity for the human versus rat receptor homologues. *Mol.Pharmacol., 54,* 22-32.

Hurgin, V., Novick, D., & Rubinstein, M. (2002). The promoter of IL-18 binding protein: activation by an IFN-gamma -induced complex of IFN regulatory factor 1 and CCAAT/enhancer binding protein beta. *Proc.Natl.Acad.Sci.U.S.A, 99,* 16957-16962.

Hutchison, M., Berman, K. S., & Cobb, M. H. (1998). Isolation of TAO1, a protein kinase that activates MEKs in stress-activated protein kinase cascades. *J.Biol.Chem., 273,* 28625-28632.

Hwang, M., Perez, C. A., Moretti, L., & Lu, B. (2008). The mTOR signaling network: insights from its role during embryonic development. *Curr.Med.Chem., 15,* 1192-1208.

Hwang, S. M., Koo, N. Y., Choi, S. Y., Chun, G. S., Kim, J. S., & Park, K. (2009). P2X7 Receptor-mediated Membrane Blebbing in Salivary Epithelial Cells. *Korean J.Physiol Pharmacol., 13,* 175-179.

Inoki, K., Li, Y., Xu, T., & Guan, K. L. (2003). Rheb GTPase is a direct target of TSC2 GAP activity and regulates mTOR signaling. *Genes Dev., 17,* 1829-1834.

Irmler, M., Hertig, S., MacDonald, H. R., Sadoul, R., Becherer, J. D., Proudfoot, A. et al. (1995). Granzyme A is an interleukin 1 beta-converting enzyme. *J.Exp.Med., 181,* 1917-1922.

Isome, M., Fujinaka, H., Adhikary, L. P., Kovalenko, P., El-Shemi, A. G., Yoshida, Y. et al. (2004). Important role for macrophages in induction of crescentic anti-GBM glomerulonephritis in WKY rats. *Nephrol.Dial.Transplant., 19,* 2997-3004.

Jacobson, K. A. & Boeynaems, J. M. (2010). P2Y nucleotide receptors: promise of therapeutic applications. *Drug Discov.Today, 15,* 570-578.

Jacobson, K. A., Jarvis, M. F., & Williams, M. (2002). Purine and pyrimidine (P2) receptors as drug targets. *J.Med.Chem., 45,* 4057-4093.

Jelassi, B., Chantome, A., Alcaraz-Perez, F., Baroja-Mazo, A., Cayuela, M. L., Pelegrin, P. et al. (2011). P2X(7) receptor activation enhances SK3 channels- and cystein cathepsin-dependent cancer cells invasiveness. *Oncogene, 30,* 2108-2122.

Jenkins, H. T., Baker-Wilding, R., & Edwards, T. A. (2009). Structure and RNA binding of the mouse Pumilio-2 Puf domain. *J.Struct.Biol., 167,* 271-276.

Jensen, O. N. (2006). Interpreting the protein language using proteomics. *Nat.Rev.Mol.Cell Biol., 7,* 391-403.

Jiang, L. H., Mackenzie, A. B., North, R. A., & Surprenant, A. (2000). Brilliant blue G selectively blocks ATP-gated rat P2X(7) receptors. *Mol.Pharmacol., 58,* 82-88.

Johansson, J., Gudmundsson, G. H., Rottenberg, M. E., Berndt, K. D., & Agerberth, B. (1998). Conformation-dependent antibacterial activity of the naturally occurring human peptide LL-37. *J.Biol.Chem., 273,* 3718-3724.

Junttila, M. R., Li, S. P., & Westermarck, J. (2008). Phosphatase-mediated crosstalk between MAPK signaling pathways in the regulation of cell survival. *FASEB J., 22,* 954-965.

Kahlenberg, J. M. & Dubyak, G. R. (2004). Mechanisms of caspase-1 activation by P2X7 receptor-mediated K+ release. *Am.J.Physiol Cell Physiol, 286,* C1100-C1108.

Kanneganti, T. D., Lamkanfi, M., Kim, Y. G., Chen, G., Park, J. H., Franchi, L. et al. (2007). Pannexin-1-mediated recognition of bacterial molecules activates the cryopyrin inflammasome independent of Toll-like receptor signaling. *Immunity., 26,* 433-443.

Kapur, V., Majesky, M. W., Li, L. L., Black, R. A., & Musser, J. M. (1993). Cleavage of interleukin 1 beta (IL-1 beta) precursor to produce active IL-1

beta by a conserved extracellular cysteine protease from Streptococcus pyogenes. *Proc.Natl.Acad.Sci.U.S.A, 90,* 7676-7680.

Karkar, A. M., Smith, J., & Pusey, C. D. (2001). Prevention and treatment of experimental crescentic glomerulonephritis by blocking tumour necrosis factor-alpha. *Nephrol.Dial.Transplant., 16,* 518-524.

Kawasaki, K., Yaoita, E., Yamamoto, T., & Kihara, I. (1992). Depletion of CD8 positive cells in nephrotoxic serum nephritis of WKY rats. *Kidney Int., 41,* 1517-1526.

Kawate, T., Michel, J. C., Birdsong, W. T., & Gouaux, E. (2009). Crystal structure of the ATP-gated P2X(4) ion channel in the closed state. *Nature, 460,* 592-598.

Ke, H. Z., Qi, H., Weidema, A. F., Zhang, Q., Panupinthu, N., Crawford, D. T. et al. (2003). Deletion of the P2X7 nucleotide receptor reveals its regulatory roles in bone formation and resorption. *Mol.Endocrinol., 17,* 1356-1367.

Kersse, K., Vanden Berghe, T., Lamkanfi, M., & Vandenabeele, P. (2007). A phylogenetic and functional overview of inflammatory caspases and caspase-1-related CARD-only proteins. *Biochem.Soc.Trans., 35,* 1508-1511.

Khakh, B. S., Bao, X. R., Labarca, C., & Lester, H. A. (1999). Neuronal P2X transmitter-gated cation channels change their ion selectivity in seconds. *Nat.Neurosci., 2,* 322-330.

Khakh, B. S. & North, R. A. (2006). P2X receptors as cell-surface ATP sensors in health and disease. *Nature, 442,* 527-532.

Khaleghpour, K., Pyronnet, S., Gingras, A. C., & Sonenberg, N. (1999). Translational homeostasis: eukaryotic translation initiation factor 4E control of 4E-binding protein 1 and p70 S6 kinase activities. *Mol.Cell Biol., 19,* 4302-4310.

Khare, S., Luc, N., Dorfleutner, A., & Stehlik, C. (2010). Inflammasomes and their activation. *Crit Rev.Immunol., 30,* 463-487.

Kim, J., Kundu, M., Viollet, B., & Guan, K. L. (2011). AMPK and mTOR regulate autophagy through direct phosphorylation of Ulk1. *Nat.Cell Biol., 13,* 132-141.

Kim, M., Jiang, L. H., Wilson, H. L., North, R. A., & Surprenant, A. (2001). Proteomic and functional evidence for a P2X7 receptor signalling complex. *EMBO J., 20,* 6347-6358.

Kingsbury, S. R., Conaghan, P. G., & McDermott, M. F. (2011). The role of the NLRP3 inflammasome in gout. *J.Inflamm.Res., 4,* 39-49.

Klapperstuck, M., Buttner, C., Schmalzing, G., & Markwardt, F. (2001). Functional evidence of distinct ATP activation sites at the human P2X(7) receptor. *J.Physiol, 534,* 25-35.

Kolliputi, N., Shaik, R. S., & Waxman, A. B. (2010). The inflammasome mediates hyperoxia-induced alveolar cell permeability. *J.Immunol., 184,* 5819-5826.

Kondoh, K., Torii, S., & Nishida, E. (2005). Control of MAP kinase signaling to the nucleus. *Chromosoma, 114,* 86-91.

Korcok, J., Raimundo, L. N., Ke, H. Z., Sims, S. M., & Dixon, S. J. (2004). Extracellular nucleotides act through P2X7 receptors to activate NF-kappaB in osteoclasts. *J.Bone Miner.Res., 19,* 642-651.

Kostenko, S., Dumitriu, G., Laegreid, K. J., & Moens, U. (2011). Physiological roles of mitogen-activated-protein-kinase-activated p38-regulated/activated protein kinase. *World J.Biol.Chem., 2,* 73-89.

Kufer, T. A., Fritz, J. H., & Philpott, D. J. (2005). NACHT-LRR proteins (NLRs) in bacterial infection and immunity. *Trends Microbiol., 13,* 381-388.

Kuida, K., Lippke, J. A., Ku, G., Harding, M. W., Livingston, D. J., Su, M. S. et al. (1995). Altered cytokine export and apoptosis in mice deficient in interleukin-1 beta converting enzyme. *Science, 267,* 2000-2003.

Labasi, J. M., Petrushova, N., Donovan, C., McCurdy, S., Lira, P., Payette, M. M. et al. (2002). Absence of the P2X7 receptor alters leukocyte function and attenuates an inflammatory response. *J.Immunol., 168,* 6436-6445.

Lai, P. C., Cook, H. T., Smith, J., Keith, J. C., Jr., Pusey, C. D., & Tam, F. W. (2001). Interleukin-11 attenuates nephrotoxic nephritis in Wistar Kyoto rats. *J.Am.Soc.Nephrol., 12,* 2310-2320.

Laliberte, R. E., Eggler, J., & Gabel, C. A. (1999). ATP treatment of human monocytes promotes caspase-1 maturation and externalization. *J.Biol.Chem., 274,* 36944-36951.

Lan, H. Y. (1998). Therapeutic effects of cytokine blockade in glomerulonephritis. *Nephrol.Dial.Transplant., 13,* 7-9.

Lan, H. Y., Nikolic-Paterson, D. J., Zarama, M., Vannice, J. L., & Atkins, R. C. (1993). Suppression of experimental crescentic glomerulonephritis by the interleukin-1 receptor antagonist. *Kidney Int., 43,* 479-485.

Larrick, J. W., Lee, J., Ma, S., Li, X., Francke, U., Wright, S. C. et al. (1996). Structural, functional analysis and localization of the human CAP18 gene. *FEBS Lett., 398,* 74-80.

Larsen, M. R., Thingholm, T. E., Jensen, O. N., Roepstorff, P., & Jorgensen, T. J. (2005). Highly selective enrichment of phosphorylated peptides from peptide mixtures using titanium dioxide microcolumns. *Mol.Cell Proteomics., 4,* 873-886.

Le Feuvre, R. A., Brough, D., Iwakura, Y., Takeda, K., & Rothwell, N. J. (2002). Priming of macrophages with lipopolysaccharide potentiates P2X7-mediated cell death via a caspase-1-dependent mechanism, independently of cytokine production. *J.Biol.Chem., 277,* 3210-3218.

Lemjabbar, H., Gosset, P., Lechapt-Zalcman, E., Franco-Montoya, M. L., Wallaert, B., Harf, A. et al. (1999). Overexpression of alveolar macrophage gelatinase B (MMP-9) in patients with idiopathic pulmonary fibrosis: effects of steroid and immunosuppressive treatment. *Am.J.Respir.Cell Mol.Biol., 20,* 903-913.

Lenertz, L. Y., Gavala, M. L., Hill, L. M., & Bertics, P. J. (2009). Cell signaling via the P2X(7) nucleotide receptor: linkage to ROS production, gene transcription, and receptor trafficking. *Purinergic.Signal., 5,* 175-187.

Levine, B., Mizushima, N., & Virgin, H. W. (2011). Autophagy in immunity and inflammation. *Nature, 469,* 323-335.

Li, Z., Liang, D., & Chen, L. (2008). Potential therapeutic targets for ATP-gated P2X receptor ion channels. *Assay.Drug Dev.Technol., 6,* 277-284.

Lichtnekert, J., Kulkarni, O. P., Mulay, S. R., Rupanagudi, K. V., Ryu, M., Allam, R. et al. (2011). Anti-GBM glomerulonephritis involves IL-1 but is independent of NLRP3/ASC inflammasome-mediated activation of caspase-1. *PLoS.One., 6,* e26778.

Lindor, N. M., Arsenault, T. M., Solomon, H., Seidman, C. E., & McEvoy, M. T. (1997). A new autosomal dominant disorder of pyogenic sterile arthritis, pyoderma gangrenosum, and acne: PAPA syndrome. *Mayo Clin.Proc., 72,* 611-615.

Liu, X., Surprenant, A., Mao, H. J., Roger, S., Xia, R., Bradley, H. et al. (2008). Identification of key residues coordinating functional inhibition of P2X7 receptors by zinc and copper. *Mol.Pharmacol., 73,* 252-259.

Locovei, S., Scemes, E., Qiu, F., Spray, D. C., & Dahl, G. (2007). Pannexin1 is part of the pore forming unit of the P2X(7) receptor death complex. *FEBS Lett., 581,* 483-488.

Ma, L., Chen, Z., Erdjument-Bromage, H., Tempst, P., & Pandolfi, P. P. (2005). Phosphorylation and functional inactivation of TSC2 by Erk implications for tuberous sclerosis and cancer pathogenesis. *Cell, 121,* 179-193.

Ma, Y., Thornton, S., Boivin, G. P., Hirsh, D., Hirsch, R., & Hirsch, E. (1998). Altered susceptibility to collagen-induced arthritis in transgenic mice with aberrant expression of interleukin-1 receptor antagonist. *Arthritis Rheum., 41,* 1798-1805.

Mackenzie, A. B., Young, M. T., Adinolfi, E., & Surprenant, A. (2005). Pseudoapoptosis induced by brief activation of ATP-gated P2X7 receptors. *J.Biol.Chem., 280,* 33968-33976.

Maelfait, J., Vercammen, E., Janssens, S., Schotte, P., Haegman, M., Magez, S. et al. (2008). Stimulation of Toll-like receptor 3 and 4 induces interleukin-1beta maturation by caspase-8. *J.Exp.Med., 205,* 1967-1973.

Maratou, K., Behmoaras, J., Fewings, C., Srivastava, P., D'Souza, Z., Smith, J. et al. (2011). Characterization of the macrophage transcriptome in glomerulonephritis-susceptible and -resistant rat strains. *Genes Immun., 12,* 78-89.

Markel, P., Shu, P., Ebeling, C., Carlson, G. A., Nagle, D. L., Smutko, J. S. et al. (1997). Theoretical and empirical issues for marker-assisted breeding of congenic mouse strains. *Nat.Genet., 17,* 280-284.

Marques-da-Silva, C., Chaves, M. M., Castro, N. G., Coutinho-Silva, R., & Guimaraes, M. Z. (2011). Colchicine inhibits cationic dye uptake induced by ATP in P2X2 and P2X7 receptor-expressing cells: implications for its therapeutic action. *Br.J.Pharmacol., 163,* 912-926.

Martelli, A. M., Tabellini, G., Ricci, F., Evangelisti, C., Chiarini, F., Bortul, R. et al. (2011). PI3K/AKT/mTORC1 and MEK/ERK signaling in T-cell acute

lymphoblastic leukemia: New options for targeted therapy. *Adv.Enzyme Regul.*

Martinon, F., Burns, K., & Tschopp, J. (2002). The inflammasome: a molecular platform triggering activation of inflammatory caspases and processing of proIL-beta. *Mol.Cell, 10,* 417-426.

Martinon, F., Mayor, A., & Tschopp, J. (2009). The inflammasomes: guardians of the body. *Annu.Rev.Immunol., 27,* 229-265.

Martinon, F., Petrilli, V., Mayor, A., Tardivel, A., & Tschopp, J. (2006). Gout-associated uric acid crystals activate the NALP3 inflammasome. *Nature, 440,* 237-241.

Masin, M., Young, C., Lim, K., Barnes, S. J., Xu, X. J., Marschall, V. et al. (2011). Expression, assembly and function of novel C-terminal truncated variants of the mouse P2X7 receptor: Re-evaluation of P2X7 knockouts. *Br.J.Pharmacol.*

Masters, S. L., Simon, A., Aksentijevich, I., & Kastner, D. L. (2009). Horror autoinflammaticus: the molecular pathophysiology of autoinflammatory disease (*). *Annu.Rev.Immunol., 27,* 621-668.

McKay, M. M. & Morrison, D. K. (2007). Integrating signals from RTKs to ERK/MAPK. *Oncogene, 26,* 3113-3121.

Mehta, V. B., Hart, J., & Wewers, M. D. (2001). ATP-stimulated release of interleukin (IL)-1beta and IL-18 requires priming by lipopolysaccharide and is independent of caspase-1 cleavage. *J.Biol.Chem., 276,* 3820-3826.

Meyuhas, O. & Dreazen, A. (2009). Ribosomal protein S6 kinase from TOP mRNAs to cell size. *Prog.Mol.Biol.Transl.Sci., 90,* 109-153.

Mizutani, H., Schechter, N., Lazarus, G., Black, R. A., & Kupper, T. S. (1991). Rapid and specific conversion of precursor interleukin 1 beta (IL-1 beta) to an active IL-1 species by human mast cell chymase. *J.Exp.Med., 174,* 821-825.

Montoya, A., Beltran, L., Casado, P., Rodriguez-Prados, J. C., & Cutillas, P. R. (2011). Characterization of a TiO enrichment method for label-free quantitative phosphoproteomics. *Methods, 54,* 370-378.

Motadi, L. R., Bhoola, K. D., & Dlamini, Z. (2011). Expression and function of retinoblastoma binding protein 6 (RBBP6) in human lung cancer. *Immunobiology, 216,* 1065-1073.

Mountain, D. J., Singh, M., Menon, B., & Singh, K. (2007). Interleukin-1beta increases expression and activity of matrix metalloproteinase-2 in cardiac microvascular endothelial cells: role of PKCalpha/beta1 and MAPKs. *Am.J.Physiol Cell Physiol, 292,* C867-C875.

Murgia, M., Hanau, S., Pizzo, P., Rippa, M., & Di, V. F. (1993). Oxidized ATP. An irreversible inhibitor of the macrophage purinergic P2Z receptor. *J.Biol.Chem., 268,* 8199-8203.

Murphy, P. A., Simon, P. L., & Willoughby, W. F. (1980). Endogenous pyrogens made by rabbit peritoneal exudate cells are identical with lymphocyte-activating factors made by rabbit alveolar macrophages. *J.Immunol., 124,* 2498-2501.

Nelson, D. W., Gregg, R. J., Kort, M. E., Perez-Medrano, A., Voight, E. A., Wang, Y. et al. (2006). Structure-activity relationship studies on a series of novel, substituted 1-benzyl-5-phenyltetrazole P2X7 antagonists. *J.Med.Chem., 49,* 3659-3666.

Netea, M. G., Nold-Petry, C. A., Nold, M. F., Joosten, L. A., Opitz, B., van der Meer, J. H. et al. (2009). Differential requirement for the activation of the inflammasome for processing and release of IL-1beta in monocytes and macrophages. *Blood, 113,* 2324-2335.

Neven, B., Prieur, A. M., & Quartier dit, M. P. (2008). Cryopyrinopathies: update on pathogenesis and treatment. *Nat.Clin.Pract.Rheumatol., 4,* 481-489.

Ng, D. C., Zhao, T. T., Yeap, Y. Y., Ngoei, K. R., & Bogoyevitch, M. A. (2010). c-Jun N-terminal kinase phosphorylation of stathmin confers protection against cellular stress. *J.Biol.Chem., 285,* 29001-29013.

Nicke, A. (2008). Homotrimeric complexes are the dominant assembly state of native P2X7 subunits. *Biochem.Biophys.Res.Commun., 377,* 803-808.

Nicke, A., Baumert, H. G., Rettinger, J., Eichele, A., Lambrecht, G., Mutschler, E. et al. (1998). P2X1 and P2X3 receptors form stable trimers: a novel structural motif of ligand-gated ion channels. *EMBO J., 17,* 3016-3028.

Nicke, A., Kuan, Y. H., Masin, M., Rettinger, J., Marquez-Klaka, B., Bender, O. et al. (2009). A functional P2X7 splice variant with an alternative transmembrane domain 1 escapes gene inactivation in P2X7 knock-out mice. *J.Biol.Chem., 284,* 25813-25822.

Nikolic-Paterson, D. J. & Atkins, R. C. (2001). The role of macrophages in glomerulonephritis. *Nephrol.Dial.Transplant., 16 Suppl 5,* 3-7.

Noguchi, T., Ishii, K., Fukutomi, H., Naguro, I., Matsuzawa, A., Takeda, K. et al. (2008). Requirement of reactive oxygen species-dependent activation of ASK1-p38 MAPK pathway for extracellular ATP-induced apoptosis in macrophage. *J.Biol.Chem., 283,* 7657-7665.

North, R. A. (2002). Molecular physiology of P2X receptors. *Physiol Rev., 82,* 1013-1067.

O'Neill, L. A. & Bowie, A. G. (2010). Sensing and signaling in antiviral innate immunity. *Curr.Biol., 20,* R328-R333.

Ohlendorff, S. D., Tofteng, C. L., Jensen, J. E., Petersen, S., Civitelli, R., Fenger, M. et al. (2007). Single nucleotide polymorphisms in the P2X7 gene are associated to fracture risk and to effect of estrogen treatment. *Pharmacogenet.Genomics, 17,* 555-567.

Ohori, M. (2008). ERK inhibitors as a potential new therapy for rheumatoid arthritis. *Drug News Perspect., 21,* 245-250.

Oren, Z., Lerman, J. C., Gudmundsson, G. H., Agerberth, B., & Shai, Y. (1999). Structure and organization of the human antimicrobial peptide LL-37 in phospholipid membranes: relevance to the molecular basis for its non-cell-selective activity. *Biochem.J., 341 (Pt 3),* 501-513.

Oyanguren-Desez, O., Rodriguez-Antiguedad, A., Villoslada, P., Domercq, M., Alberdi, E., & Matute, C. (2011). Gain-of-function of P2X7 receptor gene variants in multiple sclerosis. *Cell Calcium, 50,* 468-472.

Panenka, W., Jijon, H., Herx, L. M., Armstrong, J. N., Feighan, D., Wei, T. et al. (2001). P2X7-like receptor activation in astrocytes increases chemokine monocyte chemoattractant protein-1 expression via mitogen-activated protein kinase. *J.Neurosci., 21,* 7135-7142.

Papp, L., Vizi, E. S., & Sperlagh, B. (2007). P2X7 receptor mediated phosphorylation of p38MAP kinase in the hippocampus. *Biochem.Biophys.Res.Commun., 355,* 568-574.

Pawson, T. & Nash, P. (2000). Protein-protein interactions define specificity in signal transduction. *Genes Dev., 14,* 1027-1047.

Pechstein, A., Bacetic, J., Vahedi-Faridi, A., Gromova, K., Sundborger, A., Tomlin, N. et al. (2010). Regulation of synaptic vesicle recycling by complex formation between intersectin 1 and the clathrin adaptor complex AP2. *Proc.Natl.Acad.Sci.U.S.A, 107,* 4206-4211.

Pelegrin, P. (2011). Many ways to dilate the P2X7 receptor pore. *Br.J.Pharmacol., 163,* 908-911.

Pelegrin, P., Barroso-Gutierrez, C., & Surprenant, A. (2008). P2X7 receptor differentially couples to distinct release pathways for IL-1beta in mouse macrophage. *J.Immunol., 180,* 7147-7157.

Pelegrin, P. & Surprenant, A. (2009). The P2X(7) receptor-pannexin connection to dye uptake and IL-1beta release. *Purinergic.Signal., 5,* 129-137.

Perregaux, D. & Gabel, C. A. (1994). Interleukin-1 beta maturation and release in response to ATP and nigericin. Evidence that potassium depletion

mediated by these agents is a necessary and common feature of their activity. *J.Biol.Chem., 269,* 15195-15203.

Perregaux, D. G., Bhavsar, K., Contillo, L., Shi, J., & Gabel, C. A. (2002). Antimicrobial peptides initiate IL-1 beta posttranslational processing: a novel role beyond innate immunity. *J.Immunol., 168,* 3024-3032.

Petrilli, V., Papin, S., Dostert, C., Mayor, A., Martinon, F., & Tschopp, J. (2007). Activation of the NALP3 inflammasome is triggered by low intracellular potassium concentration. *Cell Death.Differ., 14,* 1583-1589.

Pfeiffer, Z. A., Aga, M., Prabhu, U., Watters, J. J., Hall, D. J., & Bertics, P. J. (2004). The nucleotide receptor P2X7 mediates actin reorganization and membrane blebbing in RAW 264.7 macrophages via p38 MAP kinase and Rho. *J.Leukoc.Biol., 75,* 1173-1182.

Piccini, A., Carta, S., Tassi, S., Lasiglie, D., Fossati, G., & Rubartelli, A. (2008). ATP is released by monocytes stimulated with pathogen-sensing receptor ligands and induces IL-1beta and IL-18 secretion in an autocrine way. *Proc.Natl.Acad.Sci.U.S.A, 105,* 8067-8072.

Pinkse, M. W., Uitto, P. M., Hilhorst, M. J., Ooms, B., & Heck, A. J. (2004). Selective isolation at the femtomole level of phosphopeptides from proteolytic digests using 2D-NanoLC-ESI-MS/MS and titanium oxide precolumns. *Anal.Chem., 76,* 3935-3943.

Poeck, H., Bscheider, M., Gross, O., Finger, K., Roth, S., Rebsamen, M. et al. (2010). Recognition of RNA virus by RIG-I results in activation of CARD9 and inflammasome signaling for interleukin 1 beta production. *Nat.Immunol., 11,* 63-69.

Potucek, Y. D., Crain, J. M., & Watters, J. J. (2006). Purinergic receptors modulate MAP kinases and transcription factors that control microglial inflammatory gene expression. *Neurochem.Int., 49,* 204-214.

Qu, Y. & Dubyak, G. R. (2009). P2X7 receptors regulate multiple types of membrane trafficking responses and non-classical secretion pathways. *Purinergic.Signal., 5,* 163-173.

Raman, M., Earnest, S., Zhang, K., Zhao, Y., & Cobb, M. H. (2007). TAO kinases mediate activation of p38 in response to DNA damage. *EMBO J., 26,* 2005-2014.

Ramirez-Valle, F., Braunstein, S., Zavadil, J., Formenti, S. C., & Schneider, R. J. (2008). eIF4GI links nutrient sensing by mTOR to cell proliferation and inhibition of autophagy. *J.Cell Biol., 181,* 293-307.

Rassendren, F., Buell, G. N., Virginio, C., Collo, G., North, R. A., & Surprenant, A. (1997). The permeabilizing ATP receptor, P2X7. Cloning and expression of a human cDNA. *J.Biol.Chem., 272,* 5482-5486.

Riteau, N., Gasse, P., Fauconnier, L., Gombault, A., Couegnat, M., Fick, L. et al. (2010). Extracellular ATP is a danger signal activating P2X7 receptor in lung inflammation and fibrosis. *Am.J.Respir.Crit Care Med., 182,* 774-783.

Roberts, P. J. & Der, C. J. (2007). Targeting the Raf-MEK-ERK mitogen-activated protein kinase cascade for the treatment of cancer. *Oncogene, 26,* 3291-3310.

Robledo, S., Idol, R. A., Crimmins, D. L., Ladenson, J. H., Mason, P. J., & Bessler, M. (2008). The role of human ribosomal proteins in the maturation of rRNA and ribosome production. *RNA., 14,* 1918-1929.

Roger, S., Mei, Z. Z., Baldwin, J. M., Dong, L., Bradley, H., Baldwin, S. A. et al. (2010). Single nucleotide polymorphisms that were identified in affective mood disorders affect ATP-activated P2X7 receptor functions. *J.Psychiatr.Res., 44,* 347-355.

Roux, P. P. & Blenis, J. (2004). ERK and p38 MAPK-activated protein kinases: a family of protein kinases with diverse biological functions. *Microbiol.Mol.Biol.Rev., 68,* 320-344.

Sanna, B., Bueno, O. F., Dai, Y. S., Wilkins, B. J., & Molkentin, J. D. (2005). Direct and indirect interactions between calcineurin-NFAT and MEK1-extracellular signal-regulated kinase 1/2 signaling pathways regulate cardiac gene expression and cellular growth. *Mol.Cell Biol., 25,* 865-878.

Sato, T., Kawachi, H., Morioka, T., Takashima, N., Saeki, T., Oite, T. et al. (1993). Nephrotoxic serum nephritis in nude rats: the roles of host immune reactions in the accelerated type. *Clin.Exp.Immunol., 91,* 131-134.

Scheid, M. P., Parsons, M., & Woodgett, J. R. (2005). Phosphoinositide-dependent phosphorylation of PDK1 regulates nuclear translocation. *Mol.Cell Biol., 25,* 2347-2363.

Schmelzle, K. & White, F. M. (2006). Phosphoproteomic approaches to elucidate cellular signaling networks. *Curr.Opin.Biotechnol., 17,* 406-414.

Schonbeck, U., Mach, F., & Libby, P. (1998). Generation of biologically active IL-1 beta by matrix metalloproteinases: a novel caspase-1-independent pathway of IL-1 beta processing. *J.Immunol., 161,* 3340-3346.

Schroder, K., Muruve, D. A., & Tschopp, J. (2009). Innate immunity: cytoplasmic DNA sensing by the AIM2 inflammasome. *Curr.Biol., 19,* R262-R265.

Schroder, K. & Tschopp, J. (2010). The inflammasomes. *Cell, 140,* 821-832.

Schroder, K., Zhou, R., & Tschopp, J. (2010). The NLRP3 inflammasome: a sensor for metabolic danger? *Science, 327,* 296-300.

Schulze-Lohoff, E., Hugo, C., Rost, S., Arnold, S., Gruber, A., Brune, B. et al. (1998). Extracellular ATP causes apoptosis and necrosis of cultured mesangial cells via P2Z/P2X7 receptors. *Am.J.Physiol, 275,* F962-F971.

Sebolt-Leopold, J. S. (2000). Development of anticancer drugs targeting the MAP kinase pathway. *Oncogene, 19,* 6594-6599.

Sharp, A. J., Polak, P. E., Simonini, V., Lin, S. X., Richardson, J. C., Bongarzone, E. R. et al. (2008). P2x7 deficiency suppresses development of experimental autoimmune encephalomyelitis. *J.Neuroinflammation., 5,* 33.

Sheerin, N. S., Springall, T., Abe, K., & Sacks, S. H. (2001). Protection and injury: the differing roles of complement in the development of glomerular injury. *Eur.J.Immunol., 31,* 1255-1260.

Sim, J. A., Young, M. T., Sung, H. Y., North, R. A., & Surprenant, A. (2004). Reanalysis of P2X7 receptor expression in rodent brain. *J.Neurosci., 24,* 6307-6314.

Skaper, S. D., Debetto, P., & Giusti, P. (2010). The P2X7 purinergic receptor: from physiology to neurological disorders. *FASEB J., 24,* 337-345.

Skeldon, A. & Saleh, M. (2011). The inflammasomes: molecular effectors of host resistance against bacterial, viral, parasitic, and fungal infections. *Front Microbiol., 2,* 15.

Smith, J., Lai, P. C., Behmoaras, J., Roufosse, C., Bhangal, G., McDaid, J. P. et al. (2007). Genes expressed by both mesangial cells and bone marrow-derived cells underlie genetic susceptibility to crescentic glomerulonephritis in the rat. *J.Am.Soc.Nephrol., 18,* 1816-1823.

Solini, A., Chiozzi, P., Morelli, A., Fellin, R., & Di, V. F. (1999). Human primary fibroblasts in vitro express a purinergic P2X7 receptor coupled to ion fluxes, microvesicle formation and IL-6 release. *J.Cell Sci., 112 (Pt 3),* 297-305.

Solle, M., Labasi, J., Perregaux, D. G., Stam, E., Petrushova, N., Koller, B. H. et al. (2001). Altered cytokine production in mice lacking P2X(7) receptors. *J.Biol.Chem., 276,* 125-132.

Soto, F., Garcia-Guzman, M., & Stuhmer, W. (1997). Cloned ligand-gated channels activated by extracellular ATP (P2X receptors). *J.Membr.Biol., 160,* 91-100.

Srinivasula, S. M., Poyet, J. L., Razmara, M., Datta, P., Zhang, Z., & Alnemri, E. S. (2002). The PYRIN-CARD protein ASC is an activating adaptor for caspase-1. *J.Biol.Chem., 277,* 21119-21122.

Stout, R. D., Jiang, C., Matta, B., Tietzel, I., Watkins, S. K., & Suttles, J. (2005). Macrophages sequentially change their functional phenotype in response to changes in microenvironmental influences. *J.Immunol., 175,* 342-349.

Surprenant, A., Rassendren, F., Kawashima, E., North, R. A., & Buell, G. (1996). The cytolytic P2Z receptor for extracellular ATP identified as a P2X receptor (P2X7). *Science, 272,* 735-738.

Takashiba, S., Van Dyke, T. E., Amar, S., Murayama, Y., Soskolne, A. W., & Shapira, L. (1999). Differentiation of monocytes to macrophages primes cells for lipopolysaccharide stimulation via accumulation of cytoplasmic nuclear factor kappaB. *Infect.Immun., 67,* 5573-5578.

Takeuchi, O. & Akira, S. (2010). Pattern recognition receptors and inflammation. *Cell, 140,* 805-820.

Tam, F. W. (2006). Current pharmacotherapy for the treatment of crescentic glomerulonephritis. *Expert.Opin.Investig.Drugs, 15,* 1353-1369.

Tam, F. W., Smith, J., Morel, D., Karkar, A. M., Thompson, E. M., Cook, H. T. et al. (1999). Development of scarring and renal failure in a rat model of crescentic glomerulonephritis. *Nephrol.Dial.Transplant., 14,* 1658-1666.

Tang, W. W., Feng, L., Vannice, J. L., & Wilson, C. B. (1994). Interleukin-1 receptor antagonist ameliorates experimental anti-glomerular basement

membrane antibody-associated glomerulonephritis. *J.Clin.Invest, 93,* 273-279.

Tato, I., Bartrons, R., Ventura, F., & Rosa, J. L. (2011). Amino acids activate mammalian target of rapamycin complex 2 (mTORC2) via PI3K/Akt signaling. *J.Biol.Chem., 286,* 6128-6142.

Taylor, P. R., Martinez-Pomares, L., Stacey, M., Lin, H. H., Brown, G. D., & Gordon, S. (2005). Macrophage receptors and immune recognition. *Annu.Rev.Immunol., 23,* 901-944.

Taylor, S. R., Turner, C. M., Elliott, J. I., McDaid, J., Hewitt, R., Smith, J. et al. (2009). P2X7 deficiency attenuates renal injury in experimental glomerulonephritis. *J.Am.Soc.Nephrol., 20,* 1275-1281.

Turner, C. M., Tam, F. W., Lai, P. C., Tarzi, R. M., Burnstock, G., Pusey, C. D. et al. (2007). Increased expression of the pro-apoptotic ATP-sensitive P2X7 receptor in experimental and human glomerulonephritis. *Nephrol.Dial.Transplant., 22,* 386-395.

Virginio, C., Mackenzie, A., Rassendren, F. A., North, R. A., & Surprenant, A. (1999). Pore dilation of neuronal P2X receptor channels. *Nat.Neurosci., 2,* 315-321.

Vonend, O., Turner, C. M., Chan, C. M., Loesch, A., Dell'Anna, G. C., Srai, K. S. et al. (2004). Glomerular expression of the ATP-sensitive P2X receptor in diabetic and hypertensive rat models. *Kidney Int., 66,* 157-166.

Waite, A. L., Schaner, P., Richards, N., Balci-Peynircioglu, B., Masters, S. L., Brydges, S. D. et al. (2009). Pyrin Modulates the Intracellular Distribution of PSTPIP1. *PLoS.One., 4,* e6147.

Wang, Q., Wang, L., Feng, Y. H., Li, X., Zeng, R., & Gorodeski, G. I. (2004). P2X7 receptor-mediated apoptosis of human cervical epithelial cells. *Am.J.Physiol Cell Physiol, 287,* C1349-C1358.

Wang, S., Miura, M., Jung, Y. K., Zhu, H., Li, E., & Yuan, J. (1998). Murine caspase-11, an ICE-interacting protease, is essential for the activation of ICE. *Cell, 92,* 501-509.

Ward, J. R., West, P. W., Ariaans, M. P., Parker, L. C., Francis, S. E., Crossman, D. C. et al. (2010). Temporal interleukin-1beta secretion from primary human peripheral blood monocytes by P2X7-independent and P2X7-dependent mechanisms. *J.Biol.Chem., 285,* 23147-23158.

West, M. A. & Heagy, W. (2002). Endotoxin tolerance: A review. *Crit Care Med., 30,* S64-S73.

Wewers, M. D. & Sarkar, A. (2009). P2X(7) receptor and macrophage function. *Purinergic.Signal., 5,* 189-195.

Willard, F. S., Willard, M. D., Kimple, A. J., Soundararajan, M., Oestreich, E. A., Li, X. et al. (2009). Regulator of G-protein signaling 14 (RGS14) is a selective H-Ras effector. *PLoS.One., 4,* e4884.

Wise, C. A., Bennett, L. B., Pascual, V., Gillum, J. D., & Bowcock, A. M. (2000). Localization of a gene for familial recurrent arthritis. *Arthritis Rheum., 43,* 2041-2045.

Yokoo, T. & Kitamura, M. (1996). Dual regulation of IL-1 beta-mediated matrix metalloproteinase-9 expression in mesangial cells by NF-kappa B and AP-1. *Am.J.Physiol, 270,* F123-F130.

Yoo, H. G., Shin, B. A., Park, J. S., Lee, K. H., Chay, K. O., Yang, S. Y. et al. (2002). IL-1beta induces MMP-9 via reactive oxygen species and NF-kappaB in murine macrophage RAW 264.7 cells. *Biochem.Biophys.Res.Commun., 298,* 251-256.

Young, M. T. (2010). P2X receptors: dawn of the post-structure era. *Trends Biochem.Sci., 35,* 83-90.

Young, P. R., Hazuda, D. J., & Simon, P. L. (1988). Human interleukin 1 beta is not secreted from hamster fibroblasts when expressed constitutively from a transfected cDNA. *J.Cell Biol., 107,* 447-456.

Yu, J. R. & Leslie, K. S. (2011). Cryopyrin-associated periodic syndrome: an update on diagnosis and treatment response. *Curr.Allergy Asthma Rep., 11,* 12-20.

Zhang, T. & Hong, W. (2001). Ykt6 forms a SNARE complex with syntaxin 5, GS28, and Bet1 and participates in a late stage in endoplasmic reticulum-Golgi transport. *J.Biol.Chem., 276,* 27480-27487.

Zhang, W. & Liu, H. T. (2002). MAPK signal pathways in the regulation of cell proliferation in mammalian cells. *Cell Res., 12,* 9-18.

Zhang, X. & Mosser, D. M. (2008). Macrophage activation by endogenous danger signals. *J.Pathol., 214,* 161-178.

APPENDIX-A

MAIN REAGENTS USED TO STIMULATE MACROPHAGES

REAGENT	SUPPLIER
Adenosine 5’-triphosphate disodium salt solution	Sigma-Aldrich
Lipopolysaccharides from Escherichia coli	Sigma-Aldrich
IL-1β Converting Enzyme (ICE) Inhibitor I, Ac-YVAD-CHO	Calbiochem
LL-37 human	Axxora
CRAMP-18 mouse	Axxora
2’(3’)-O-(4-Benzoylbenzoyl)adenosine 5’-triphosphate triethylammonium salt (BzATP)	Sigma-Aldrich
GM6001 MMP Inhibitor	Millipore

APPENDIX-B

PRIMARY ANTIBODIES USED FOR WESTERN BLOTTING

ANTIBODY	CATALOGUE NUMBER	SUPPLIER
Anti-P2X7 receptor	APR-004	Alomone Labs
Anti-phospho p44/p42	4377	New England BioLabs
Anti-phospho mTOR (Ser 2448)	2971	New England BioLabs
Anti-phospho S6 Ribosomal protein (Ser 235-236)	4848	New England BioLabs
Anti-IL-1β	2021	New England BioLabs
Anti-IL-1β (R-20)	SC-1252	Santa Cruz Biotechology
Anti-IL-18 (H-173)	SC-7954	Santa Cruz Biotechology
Anti-caspase-1 p10 (M-20)	SC-514	Santa Cruz Biotechology

APPENDIX C

BUFFERS AND SOLUTIONS

1.5 M Tris pH 8.8 (1L)

130.8 g Tris base

66.3 g Tris-Hydrochloride

1 M Tris pH 6.8 (1L)

1.72 g Tris base

76.8 Tris-Hydrochloride

10 X Running buffer (1L)

30.3 Tris base

144 g Glycine

10 g SDS

1 X Running Buffer (1L)

900 ml dH_2O

100 ml 10 X Running Buffer

APPENDIX C continued

10 X Transfer Buffer (1L)

30.3 g Tris base

144 g Glycine

1 X Transfer Buffer (2L)

200 ml 10X Transfer buffer

1400 ml dH_2O

400 ml Methanol

10 X TBS (Tris Buffered Saline) pH 7.4

87.7 NaCl

24.3 Tris base

1M HCl

1 X TBST

900 ml dH_2O

100 ml 10 X TBS

1 ml Tween 20